

**IZMIR KATIP CELEBI UNIVERSITY & GEDIZ UNIVERSITY**  
**★ GRADUATE SCHOOL OF SCIENCE ENGINEERING AND TECHNOLOGY**

**3D PAPER BASED ANALYTICAL MICROFLUIDIC CHIP FOR  
EARLIER MOLECULAR DIAGNOSIS OF CERVICAL CANCER AT THE  
POINT OF CARE**

**Ph.D. THESIS**

**Melike KARAKAYA**

**Institute of Science  
Nanotechnology Joint Ph.D Program**

**Thesis Advisor: Prof. Dr. Salih OKUR**

**MAY 2016**

**IZMIR KATIP CELEBI UNIVERSITY & GEDIZ UNIVERSITY**  
**★ GRADUATE SCHOOL OF SCIENCE ENGINEERING AND TECHNOLOGY**

**3D PAPER BASED ANALYTICAL MICROFLUIDIC CHIP FOR  
EARLIER MOLECULAR DIAGNOSIS OF CERVICAL CANCER AT THE  
POINT OF CARE**

**PhD. THESIS**

**Melike KARAKAYA  
(60611206)**

**Institute of Science**

**Nanotechnology Joint Ph.D Program**

**Thesis Advisor: Prof. Dr. Salih OKUR**

**MAY 2016**

**İZMİR KATİP ÇELEBİ ÜNİVERSİTESİ & GEDİZ ÜNİVERSİTESİ**  
**★ FEN BİLİMLERİ ENSTİTÜSÜ**

**SERVİKS KANSERİNİN POC ERKEN MOLEKÜLER TEŞHİSİ İÇİN 3D  
KAĞIT BAZLI ANALİTİK MİKROAKIŞKAN ÇİP**

**DOKTORA TEZİ**

**Melike KARAKAYA**  
**(60611206)**

**Fen Bilimleri Enstitüsü**

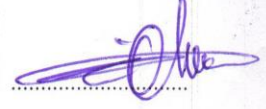
**Nanoteknoloji Ortak Doktora Programı**

**Tez Danışmanı: Prof. Dr. Salih OKUR**

**MAY 2016**

Melike Karakaya, a Ph.D. student of GU Institute of / Graduate School of Science Engineering and Technology student ID 60611206, successfully defended the thesis/dissertation entitled "3D PAPER BASED ANALYTICAL MICROFLUIDIC CHIP FOR EARLIER MOLECULAR DIAGNOSIS OF CERVICAL CANCER AT THE POINT OF CARE", which she prepared after fulfilling the requirements specified in the associated legislations, before the jury whose signatures are below.

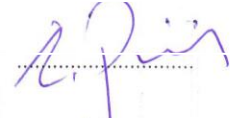
Thesis Advisor : **Prof. Dr. Salih OKUR**  
Izmir Katip Celebi University



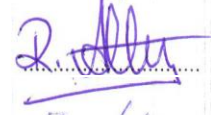
Jury Members : **Prof. Dr. Mehmet Emin Şengün ÖZSÖZ**  
Gediz University



**Prof. Dr. İbrahim Pirim**  
Izmir Katip Celebi University



**Yrd. Doç. Dr. Ramazan ATALAY**  
Gediz University



**Doç. Dr. M.Özgür SEYDİBEYOĞLU**  
Izmir Katip Celebi University



**Yrd. Doç. Dr. Uğur TÜRKAN**  
Gediz University



Date of Submission : 25 April 2016

*To my family,*



## ACKNOWLEDGEMENT

First, I would like to thank my supervisor Prof. Salih Okur for his support and help throughout my Ph.D.'s studies. I am extremely grateful to Prof. Catherrine M. Klapperich to allow me to work in her lab at Boston University, and her support for my thesis studies. I would like to thank Prof. Richard M. Crooks and his Post-Doc Josephine C. Cunningham especially for their collobration and help in fabrication of device and all their support during the experiments.

My deepest appreciation goes to my dear sister, PhD Student Smeyra Gkalp. I would like to thank her for the nights that we stayed together in the labs, for her invaluable help during the writing stage of this thesis, and overall for his patience and moral support. Without her, this thesis would not have been possible.

I would like to thank my thesis committee members Prof. Dr. Mehmet E. Ő. zsz and Do. Dr. Őerafettin Demi for their help and advice on the technical details of my research and the mentoring of my thesis.

I am grateful to my dear mother and father, without their support, I would not be here today. I also thank my dear sister Fulya, my brother Fatih, and the newest members of our family, my dear nephews Enes and Emir, for their constant love and support.

Special thanks to the members of Center for Future Technologies in Cancer Care at Boston University, for their hospitality during the last year of my Ph.D.'s studies. In particular, I thank Prof. Jacqueline C. Linnes for being a mentor, and helping me with my orientation to life in the USA.

Finally I thank Engin Er for his help with graphene synthesis and its analysis. He is always very kind and helpful, has never lost connection and has always provided his support and friendship.

Last but not least, I would like to thank The Scientific and Technological Research Council of Turkey (TUBITAK) to awarded me with 2214/A Research Fellowship Programme for International Researches grant to perform a research in Boston University. I also would like to thank to Scientific Research Project Council of Izmir Katip Celebi University for supporting my 2014-1-TEZ-48 numbered Ph.D. thesis.

May 2016

Melike KARAKAYA  
(Ph.D.)



## TABLE OF CONTENTS

	<u>Page</u>
<b>ACKNOWLEDGEMENT</b> .....	vii
<b>TABLE OF CONTENTS</b> .....	ix
<b>ABBREVIATIONS</b> .....	xii
<b>LIST OF TABLES</b> .....	xiii
<b>LIST OF FIGURES</b> .....	xiv
<b>SUMMARY</b> .....	xix
<b>ÖZET</b> .....	xx
<b>1. CHAPTER: INTRODUCTION</b> .....	<b>1</b>
1.1 HPV and Detection Types.....	2
1.1.1 POC technology for cervical cancer .....	4
1.1.2 Microfluidic Technology for HPV.....	6
1.2 Microfluidic Technologies for Bioanalytical Research .....	8
1.2.1 Paper Microfluidic Devices for POC Applications .....	9
1.3 Proposed Solution Synopsis of Dissertation .....	10
<b>2. CHAPTER: COMBINED HPV 16&amp;18 TYPES AMPLIFICATION</b> .....	<b>12</b>
2.1 Introduction .....	12
2.1.1 Real-time polymerase chain reaction.....	12
2.1.2 Gel electrophoresis.....	16
2.2 Experimental .....	17
2.2.1 Biological fragments.....	18
2.2.2 Cell culture and transcription assay .....	19
2.2.3 Chemicals and materials .....	20
2.2.4 Devices and materials .....	21
2.3 Result and Discussion .....	23
2.3.1 Effects of MgCl <sub>2</sub> and dntps optimization on combined HPV amplification .....	23
2.3.2 Primer-probe testing and concentration optimization.....	26
2.3.3 Effects of DMSO optimization to minimize secondary structures .....	30
2.3.4 Time and temperature adjustment for multiplex PCR amplification.....	31
2.3.5 Cloned DNA and agaros - acrylamide gel confirmation .....	36
2.3.6 Dilution test for combined HPV16, 18 & RNaseP for optimal conditions	41
2.4 Summary and Future Works .....	44
<b>3. CHAPTER: FABRICATION OF PAPER TIP EXTRACTION SUPPORT MATERIAL AND DEVELOPING SINGLE STEP EXTRACTION BUFFER</b> <b>45</b>	
3.1 Introduction .....	46
3.1.1 Extraction of DNA.....	46
3.1.2 Solid phase extraction .....	47
3.1.3 Paper based extraction .....	48
3.2 Experimental .....	50
3.2.1 Making paper extraction supports.....	51
3.2.2 Cell lysis and DNA extraction in tips .....	53
3.3 Result and Discussion .....	57
3.3.1 Setting the proper flow time for paper based single step DNA extraction	58
3.3.2 Elution buffer and stability test for capturing more DNA .....	68
3.3.3 Guanidinium thiocyanate and alcohol effect .....	72



3.4 Summary and Future Works .....	78
<b>4. CHAPTER: OPTIMIZATION AND CHARACTERIZATION OF ELECTROCHEMICAL DETECTION.....</b>	<b>79</b>
4.1 Introduction .....	79
4.1.1 Electrical detection technologies .....	82
4.1.2 Magnetic detection technologies.....	84
4.1.3 Novel paper analytical devices .....	84
4.2 Experimental .....	86
4.2.1 Chemicals and materials .....	87
4.2.2 Instrumentation .....	88
4.2.3 Modification of citrate-capped AgNPs with biotinylated HPV primers and DNA.....	89
4.2.4 Modification of DNA with magnetic bead and Ag bonded primers for analysis of patient samples.....	94
4.2.5 Anodic stripping voltammetry measurements using the conventional electrochemical setup.....	97
4.3 Result and Discussion .....	97
4.3.1 Choosing proper reference electrode .....	99
4.3.2 Electrochemical characterization of AgNPs detection with conventional cell.....	100
4.3.3 Ag/AgCl reference electrode for different concentrations of $\text{KMnO}_4$ ....	101
4.3.4 Preconditioning time optimization.....	104
4.3.5 Preconditioning voltage optimization.....	106
4.3.6 Detection of AgNPs in the presence of borate chloride.....	108
4.3.7 Confirmation of model analyte and analyzes result of silver nanoparticles .....	110
4.3.8 Confirmation results of DNA modified with magnetic bead and Ag bonded primers for detection of patient samples .....	117
4.3.9 Optimization types of labeled primers modification for detection of patient samples.....	119
4.4 Summary and Future Works .....	126
<b>5. CHAPTER: PAPER ANALYTICAL MICROFLUIDIC CHIP FABRICATION .....</b>	<b>127</b>
5.1 Introduction .....	127
5.1.1 Paper device introduction .....	127
5.1.2 Wax patterning of paper microfluidic devices.....	129
5.1.3 Hollow channels of paper microfluidic devices.....	131
5.1.4 Electrodes of paper microfluidic devices.....	132
5.2 Experimental .....	133
5.2.1 Chemicals, materials and instruments.....	133
5.2.2 Paper electrochemical device fabrication .....	134
5.2.3 Carbon ink preparation for stencil printing.....	136
5.2.4 $\text{KMnO}_4$ and blue dye loading onto the paper device .....	138
5.2.5 Preparation of patient sample for detection onto paper device.....	138
5.3 Result and Discussion .....	139
5.3.1 Assembling paper device to achieve final product .....	139
5.3.2 Working principle of the device .....	141
5.3.3 Novel modification method for patient sample detection on paper device .....	143
5.3.4 Testing the efficiency of designed paper analytical device .....	144

5.4 Summary and Future Works .....	150
<b>6. CHAPTER: PENCIL LEAD GRAPHITE ELECTRODE AND GRAPHEN ELECTRODE BASED PAPER DEVICE IN HPV DETECTION .....</b>	<b>151</b>
6.1 Introduction .....	151
6.1.1 Graphene synthesis to use in electrochemistry .....	151
6.1.2 Pencil lead electrodes in electrochemical detection.....	153
6.1.3 Graphene interaction with DNA in electrochemistry .....	154
6.2 Experimental .....	155
6.2.1 Chemicals and instruments .....	155
6.2.2 Synthesis of graphene .....	155
6.2.3 Preparation of the graphene-nafion and modification on glassy carbon electrode .....	156
6.2.4 Modification of pencil lead electrode with graphene, graphene-nafion, graphene oxide and graphite .....	156
6.3 Result and Discussion .....	157
6.3.1 Characterization of synthesized DNA .....	157
6.3.2 Pencil lead electrode included paper device fabrication.....	160
6.3.3 Electrochemical results comparison of HPV model analyte on the surface of pencil lead, graphene, graphene oxide, graphene-nafion and graphite .....	161
6.4 Summary and Future Works .....	166
<b>APPENDIX 1 .....</b>	<b>170</b>
<b>REFERENCES.....</b>	<b>Error! Bookmark not defined.</b>
<b>CURRICULUM VITAE.....</b>	<b>195</b>

## ABBREVIATIONS

<b>2D</b>	: Two Dimensional
<b>3D</b>	: Three Dimensional
<b>HPV</b>	: Human Papilloma Viruses
<b>POC</b>	: Point of care
<b>dsDNA</b>	: Double Stranded DNA
<b>PCR</b>	: Polymer chain reactions (PCR)
<b>LR-HPV</b>	: Low risk types
<b>PrHR-HPV</b>	: High risk types
<b>PDMS</b>	: Polydimethylsiloxane
<b>mTAS</b>	: Total micro analysis systems
<b>ELISA</b>	: Enzyme-Linked ImmunoSorbent Assay
<b>DNTPs</b>	: Deoxynucleotide triphosphates
<b>EDTA</b>	: Etilendiamin tetraasetik asit
<b>TAE</b>	: Tris-Acetate-EDTA
<b>Cy-5</b>	: Cyanine5
<b>FAM</b>	: Fluorescein
<b>TBE</b>	: Tris-Borate-EDTA
<b>APS</b>	: Ammonium persulfate
<b>TEMED</b>	: Tetramethylenediamine
<b>RnaseP</b>	: Ribonuclease P
<b>DMSO</b>	: Dimethyl sulfoxide
<b>Ldr</b>	: Ladder
<b>FISH</b>	: Fluorescence in Situ Hybridization
<b>T-RFLP</b>	: Terminal Restriction Fragment Length Polymorphism
<b>SDS</b>	: Sodium dodecyl sulfate
<b>qPCR</b>	: Quantitative PCR
<b>SPE</b>	: Solid phase extraction
<b>LOD</b>	: Limit of detection
<b>CHR</b>	: Chromatography
<b>GuSCN</b>	: Guanidinium thiocyanate
<b>RTPCR</b>	: Real time PCR
<b>PAD</b>	: Paper analytical device
<b>AgNPs</b>	: Silver nanoparticle
<b>ASV</b>	: Anodic stripping voltammetry
<b>PTFE</b>	: Polytetrafluoroethylene
<b>PBS</b>	: Phosphate Buffer Solution
<b>S</b>	: Thiol
<b>Bio</b>	: Biotin
<b>Rev</b>	: Reverse
<b>Fwd</b>	: Forward
<b>GR/NFN</b>	: Graphene-Nafion
<b>GCE</b>	: Glassy Carbon Electrode
<b>ABS</b>	: Acidic Buffer Solution
<b>GO</b>	: Graphene Oxide
<b>GR</b>	: Graphene
<b>Gre</b>	: Graphene

## LIST OF TABLES

	<u>Page</u>
<b>Table 2.1</b> : The primers and E7 gene sequences of HPV16 and 18.....	
<b>Table 2.2</b> : The last denaturation, extension and reading time and temperature for maximum amplification of each DNA types.....	
<b>Table 2.3</b> : Optimal reagents concentrations for combined HPV 16,18 and RNaseP amplification via TaqMan reaction setup.....	
<b>Table 3.1</b> : The LOD of HPV 16 AND 18 in the literature.....	
<b>Table 3.2</b> : Flow time results of DNA for several flow time range paper tips.....	59
<b>Table 3.3</b> : Flow times.....	64
<b>Table 3.4</b> : 2 minutes flow time tips in DNA extraction.....	67
<b>Table 3.5</b> : The flow rates of tips.....	68
<b>Table 3.7</b> : Comparison of 35% butanol, 50% butanol and 50% isopropanol.....	74
<b>Table 3.8</b> : Paper tips flow rates which is used for the last adjusted conditions.....	76
<b>Table 4.1</b> : Comparison of Biosensor Technologies for HPV Diagnostics (Tasoglu et al., 2015) .....	80
<b>Table 4.2</b> : Modified DNA sequence.....	94
<b>Table 4.3</b> : Potential Range of the Processes.....	99
<b>Table 4.4</b> : KMnO4 Concentrations for 100 nM, 100 $\mu$ M, 10 $\mu$ M and 1 $\mu$ M.....	102
<b>Table 4.5</b> : Preconditioning timr peak current results.....	103
<b>Table 4.6</b> : AgNPs voltage optimization for -0.4V and -0.3V.....	105
<b>Table 4.7</b> : Borate and PBSCl medium peak current results.....	107
<b>Table 4.8</b> : 10 $\mu$ M and 100 $\mu$ M amounts of ds-DNA have been used for various concentrations of single-step hybridization of model analyte .....	120
<b>Table 5.1</b> : Charge values of patient samples for 104, 105 and 106 cp/mL DNA amounts compared to concentrations of AgNPs from 530fM to 2.65pM.....	146
<b>Table 6.1</b> : GCE and Pencil Electrode results for AgNPs...161	
<b>Table 6.2</b> : Charge values of each type modified pencil electrodes for comparison.....	164

## LIST OF FIGURES

	<u>Page</u>
<b>Figure 2.1</b> : Real-time PCR working principle .....	15
<b>Figure 2.2</b> : Applied Biosystem 7500 Fast Real-Time PCR System and Molecular Imager VersaDoc™ MP 4000 System.....	21
<b>Figure 2.3</b> : Thermo Scientific NanoDrop ND-2000c .....	22
<b>Figure 2.4</b> : BioRad PowerPac Basic Power Supply and Thermo Fisher automatic propipetter OWL gel boxes.....	22
<b>Figure 2.5</b> : HPV 18 for 1,5mM, 3,5mM 1,5mM, 3,5mM MgCl <sub>2</sub> .....	24
<b>Figure 2.6</b> : HPV 16 for 1,5Mm and 4mM MgCl <sub>2</sub> .....	25
<b>Figure 2.7</b> : HPV 16, 18&RNaseP 1,5mM and 4mM MgCl <sub>2</sub> from 10 <sup>10</sup> to 10 <sup>8</sup> copies of DNA.....	25
<b>Figure 2.8</b> : HPV 16, 18&RNaseP 3,5mM MgCl <sub>2</sub> 10 <sup>11</sup> to 10 <sup>8</sup> copies of DNA .....	25
<b>Figure 2.9</b> : 10 <sup>10</sup> copies per mL HPV types for 10,5 and 2.5 uM primer concentrations .....	27
<b>Figure 2.10</b> : Confirmation of 10 <sup>10</sup> copies per mL HPV types for 10,5 and 2.5 uM primer concentrations.....	28
<b>Figure 2.11</b> : a,b,c,d 10 <sup>10</sup> copies/mL HPV16,18 and RNaseP for combined HPV .	28
<b>Figure 2.12</b> : RNaseP HPV16 10 <sup>7</sup> HPV18 10 <sup>10</sup> to RNaseP HPV16 10 <sup>2</sup> HPV18 10 <sup>5</sup> .....	29
<b>Figure 2.13</b> : HPV 16 amplification result for 1,5mM MgCl <sub>2</sub> &1mM DMSO, for only 1,5mM MgCl <sub>2</sub> and for 4mM MgCl <sub>2</sub> &1mM DMSO .....	30
<b>Figure 2.14</b> : Combined amplification results of HPV 16, 18 & RNaseP for only 1,5mM MgCl <sub>2</sub> , for 1,5mM MgCl <sub>2</sub> &1mM DMSO, and for 4mM MgCl <sub>2</sub> from left higher one to right lower.....	31
<b>Figure 2.15</b> : HPV 16 and RNaseP for 10 <sup>10</sup> , 10 <sup>9</sup> , 10 <sup>8</sup> cp/mL DNA because 10 <sup>7</sup> , 10 <sup>6</sup> , 10 <sup>5</sup> could not show 20 cycle (hpv 18 did not show because its).....	33
<b>Figure 2.16</b> : 54°C Temperature annealing (extension) for DNA from 10 <sup>9</sup> to 10 <sup>4</sup> cp/mL amounts of combined HPV16,18 and RNaseP.....	33
<b>Figure 2.17</b> : 52°C Temperature annealing (extension) for DNA from 10 <sup>9</sup> to 10 <sup>4</sup> cp/MI amounts of combined HPV16,18 and RNaseP.....	34
<b>Figure 2.18</b> : 55°C 30s annealing time, 45s denaturation and 1 min. 60°C reading time for 10 <sup>10</sup> to 10 <sup>5</sup> cp/mL combined HPV DNA .....	34
<b>Figure 2.19</b> : 60°C 30s annealing time, 15s denaturation and 1 min. 60°C reading time for 10 <sup>11</sup> to 10 <sup>7</sup> cp/mL combined HPV DNA.....	34
<b>Figure 2.20</b> : Separately amplification of HPV 16 and HPV 18 from 10 <sup>11</sup> to 10 <sup>7</sup> cp/mL concentrations at 55°C annealing and 1.5 min reading time.....	35
<b>Figure 2.21</b> : Combined form of HPV amplification from 10 <sup>9</sup> to 10 <sup>4</sup> cp/mL concentrations at 55°C annealing and 1.5 min reading time .....	35
<b>Figure 2.22</b> : 10 <sup>11</sup> copies/mL HPV16 DNA with negative template control .....	38
<b>Figure 2.23</b> : HPV16,18&Rnasep cloning with blue dye .....	38
<b>Figure 2.24</b> : HPV16, 18&Rnasep cloning and gel extraction .....	39
<b>Figure 2.25</b> : HPV18 Midi prep digest after gel extract with 100bp Ldr and 1 kB Ldr for HPV18-1x4, HPV18-2x4 .....	39
<b>Figure 2.26</b> : HPV16 and 18 calibrations .....	39
<b>Figure 2.27</b> : RNaseP PCR product .....	40

<b>Figure 2.28</b> : PCR amplification plot for $10^7$ cp/mL of RNaseP & HPV 16 and $10^{10}$ cp/mL HPV18 .....	41
<b>Figure 2.29</b> : PCR amplification plot of HPV 16 and 18 for $10^{11}$ to $10^7$ cp/mL DNA .....	42
<b>Figure 2.30</b> : Combined form of HPV amplification from $10^7$ to $10^2$ cp/mL concentrations .....	42
<b>Figure 2.31</b> : Combined form of HPV amplification from $10^9$ to $10^4$ cp/mL concentrations .....	42
<b>Figure 3.1</b> : Preparation of paper extraction support material using 3MM CHR paper as following the steps cutting triangles, rolling and placing into 200uL pipette tips respectively .....	52
<b>Figure 3.2</b> : Real images of paper extraction support material after fabrication into the pipette tips in the use of nucleic acid extraction .....	52
<b>Figure 3.3</b> : Simple pressure manifold for using in determination of flow rates of the paper tips in order to use in lysis and extraction of HPV DNA prior to detection .....	52
<b>Figure 3.4</b> : Preparation of single step buffer which contains guanidinium thiocyanate (GuSCN), sodium chloride (NaCl), isopropanol and glycogen co-precipitant to lyse and extract HPV on paper extraction support material .....	54
<b>Figure 3.5</b> : The working principle of paper based extraction platform .....	56
<b>Figure 3.6</b> : The multiplex pressure manifold is used for pushing the single-step extraction buffer from the paper-based tips. ....	56
<b>Figure 3.7</b> : Serial dilutions of combined HPV DNA from $10^9$ to $10^4$ cp/mL have been prepared as using the standard HPV16, 18&RNaseP and mixed with the single step extraction matrix and extracted from the tips while the rest of the samples flow through. ....	59
<b>Figure 3.8</b> : PCR results of HPV 16 for $10^9$ and $10^5$ cp/mL DNA paper extraction as comparison of flow through, precipitation control and paper tips with the standards .....	60
<b>Figure 3.9</b> : <b>a.</b> Dilutions of stocks to the Ct value from PCR <b>b.</b> Dilution of cell lysed compare to DNA copy number <b>c.</b> Number of cell input compare to DNA copy number <b>d.</b> Column Graphic of Number of cell input compare to DNA copy number .....	61
<b>Figure 3.10</b> : PCR amplification result of $10^9$ cp/mL of HPV 16,18 and RNaseP DNA for paper extraction as comparison of standards with paper tips, flow through and precipitation control from left to right. ....	63
<b>Figure 3.11</b> : PCR amplification result of $10^4$ cp/mL of HPV 16,18 and RNaseP DNA for paper extraction as comparison of standards with paper tips, flow through and precipitation control from left to right. ....	63
<b>Figure 3.12</b> : <b>a.</b> Ct values versus dilution <b>b.</b> HPV copy number versus starting concentration <b>c.</b> DNA copy numbers compare to Number of cell input <b>d.</b> Extraction and amplification of DNA versus Viable cells.....	65
<b>Figure 3.13</b> : PCR amplification result of $10^9$ cp/mL of HPV 16, 18 and RNaseP DNA as comparison of standards with paper tips, flow through and precipitation control from left to right. ....	66
<b>Figure 3.14</b> : PCR amplification result of $10^5$ cp/mL of HPV 16, 18 and RNaseP DNA as comparison of standards with paper tips, flow through and precipitation control from left to right. ....	66

<b>Figure 3.15</b> : Ct values versus dilution <b>b.</b> HPV copy number versus starting concentration <b>c.</b> DNA copy numbers compare to Number of cell input <b>d.</b> Extraction and amplification of DNA versus Viable cells.....	68
<b>Figure 3.16</b> : <b>a.</b> Ct values versus dilution, <b>b.</b> HPV copy number versus starting concentration for Tip-, <b>c.</b> HPV copy number versus starting concentration for Tip-1, <b>d.</b> HPV copy number versus starting concentration for Tip-2 .....	70
<b>Figure 3.17</b> : <b>a.</b> Ct values versus dilution of 100uL elution buffer used extraction <b>b.</b> HPV copy number versus starting concentration <b>c.</b> HPV copy number versus starting concentration .....	72
<b>Figure 3.18</b> : Alcohol and GuSCN test for the Extraction results .....	73
<b>Figure 3.19</b> : Extraction solution components Nanodrop spectra of direct solutions	73
<b>Figure 3.20</b> : Comparison of 35% butanol, 50% butanol and 50% isopropanol .....	74
<b>Figure 3.21</b> : The PCR amplification graphic of %50 isopropanol .....	75
<b>Figure 3.22</b> : <b>a,b.</b> Calibration curve of Extracted DNA for Ct values and copy numbers versus concentrations of HPV 16 and 18 <b>c,d.</b> HPV copy number versus starting concentration for last conditions .....	77
<b>Figure 4.1</b> : <b>a.</b> Cervical cancer distribution around the world: Cervical cancer cases per 100 000 people based on data from the International Association of Cancer Registries, 2012. High incidence is observed in Africa and SouthAmerica (Ferlay et al., 2015). <b>b.</b> Worldwide HPV prevalence: Estimate for HPV prevalence by country based on data compiled by the Institut Catala` d'Oncologi (ICO) Information Centre on HPV and Cancer, updated 2014 (Bruni et al., 2014). .....	79
<b>Figure 4.2</b> : Model anayte preperation figure .....	90
<b>Figure 4.3</b> : 4 days precipitation process for AgNps bonded DNA .....	90
<b>Figure 4.4</b> : Reduction of the volume of AgNPs-DNA .....	91
<b>Figure 4.5</b> : Confirmation of AgNPs Bonded DNA .....	92
<b>Figure 4.6</b> : Binding of Magnetic Micro Beads .....	94
<b>Figure 4.7</b> : Modification of DNA with Magnetic Bead and Ag Bonded Primers for Analysis of Patient Samples.....	96
<b>Figure 4.8</b> : Conventional Electrochemical Cell Setup. 3 different reference electrodes have been used during experiments such as Mercury, Wire Ag and Ag/AgCl. It has also used different working electrodes such as Graphite Pencil, Glassy Carbon and Graphene electrode. ....	99
<b>Figure 4.9</b> : Electrochemical results, obtained using a conventional electrochemical cell.....	101
<b>Figure 4.10</b> : KMnO <sub>4</sub> Concentrations sensitivity results .....	102
<b>Figure 4.11</b> : The peak current results of KMnO <sub>4</sub> concentrations for 3.53pM AgNPs .....	103
<b>Figure 4.12</b> : Time optimization peak current results .....	105
<b>Figure 4.13</b> : Sensitivity results of time optimization.....	105
<b>Figure 4.14</b> : Peak Current results of voltage changes.....	107
<b>Figure 4.15</b> : Comparing -0.4 V and -0.3V preconditioning voltage.....	107
<b>Figure 4.16</b> : Sensitivity results of -0.4 V and -0.3V preconditioning voltage.....	108
<b>Figure 4.17</b> : Borate medium peak current results .....	109
<b>Figure 4.18</b> : Sensitivity results PBSCl medium .....	109
<b>Figure 4.19</b> : Electron Microscope analyze results of AgNPs which were purchased from from Ted Pella (Redding, CA) .....	110

<b>Figure 4.20</b> : UV-Visible Spectrometer and mass concentration results of AgNPs which were purchased from Ted Pella (Redding, CA) .....	110
<b>Figure 4.21</b> : UV -Vis spectra showing the formation of the AgNP/biotin/streptavidin/magnetic microbead model analyte.....	111
<b>Figure 4.22</b> : Confirmation of AgNPs bonded DNA decrease adsorption of DNA coated AgNpS .....	112
<b>Figure 4.23</b> : Comparing the model liquid and its magnetic bead suspension analyte differences .....	112
<b>Figure 4.24</b> : Supernatant of model analyte model analyte in borate medium .....	113
<b>Figure 4.25</b> : Confirmation of AgNPs removing from the environment via washing .....	114
<b>Figure 4.26</b> : Model analyte formation compared to Ag-DNA solution.....	114
<b>Figure 4.27</b> : DNA modification with reagents .....	115
<b>Figure 4.28</b> : Borate effect in preparation of model analyte .....	116
<b>Figure 4.29</b> : PBS medium effect in AgNPs modification with DNA.....	116
<b>Figure 4.30</b> : Two thiol included DNA modification with AgNPS in PBS medium .....	116
<b>Figure 4.31</b> : DNA hybridization confirmation with reagents labeled primers .....	117
<b>Figure 4.32</b> : DNA modifications with the primers have also been proved with Nano-Drop DNA analyser .....	118
<b>Figure 4.33</b> : Absorbance measurements have been done in the DNA detection range as a proof of hybridization of AgNPs-Primer with DS-DNA.....	119
<b>Figure 4.34</b> : ASV result of first modification type which has been done with two step hybridization resulted analyte.....	120
<b>Figure 4.35</b> : ASV result of one step hybridization used model analyte .....	121
<b>Figure 4.36</b> : 10 $\mu$ M ds-DNA hybridized model analyte.....	122
<b>Figure 4.37</b> : 100 $\mu$ M ds-DNA used model analyte.....	122
<b>Figure 4.38</b> : 100 $\mu$ M model analyte which is prepared as using 200 $\mu$ L AgNPs-primer.....	123
<b>Figure 4.39</b> : Comparison of 100 $\mu$ M 200 $\mu$ L AgNPs-Primer, 100 $\mu$ M 100 $\mu$ L AgNPs-Primer, 10 $\mu$ M 200 $\mu$ L AgNPs-Primer and 10 $\mu$ M 100 $\mu$ L AgNPs-Primer for 2.65pM model analyte .....	124
<b>Figure 4.40</b> : Comparison of using double side and one side thiol labeled primers and their several concentration values in 636fM model analyte.....	125
<b>Figure 4.41</b> : 100uM S-primer-S used model analyte sensitivity and ASV result..	125
<b>Figure 5.1</b> : Paper wax pattern and stencil design and dimensions Prof Crooks Lab collaborative work for HPV detection .....	135
<b>Figure 5.2</b> : SolidWork detailed design of paper device and stencil for using in laser cutter system. This figure includes only target cutting areas of paper, polymer sheet and plate.....	136
<b>Figure 5.3</b> : Stencil placing onto device and printed line .....	137
<b>Figure 5.4</b> : Electrical contacts of carbon paste printed electrode .....	138
<b>Figure 5.5</b> : Dispensing on Blue dye and KMnO <sub>4</sub> onto the paper device locations	138
<b>Figure 5.6</b> : Layer by layer composition of paper device and formed last production images from top .....	140
<b>Figure 5.7</b> : Folding of the device for assembling in 3D form as aligning hollow channels, electrode surfaces and movable slip layer.....	141
<b>Figure 5.8</b> : Working principle of paper device from lateral section display for describing electrodes, hollow channel and preconcentration steps.....	142



<b>Figure 5.9</b> : Preparation of the model anlyte with novel method .....	143
<b>Figure 5.10</b> : Standard and patient sample DNA ASV peak for same concentration and copies.....	144
<b>Figure 5.11</b> : $10^4$ cp/mL standard DNA ASV graphic and calibration curve compared to several dilutions of AgNPs .....	145
<b>Figure 5.12</b> : $10^4$ cp/mL patient sample DNA ASV graphic and calibration curve compared to several dilutions of AgNPs .....	146
<b>Figure 5.13</b> : $10^6$ cp/mL patient sample DNA ASV graphic and calibration curve compared to several dilutions of AgNPs .....	146
<b>Figure 5.14</b> : $10^5$ cp/mL patient sample DNA ASV graphic and calibration curve compared to several dilutions of AgNPs .....	147
<b>Figure 5.15</b> : Saturation of the model analyte for $10^4, 10^5$ and $10^6$ cp/MI DNA.....	148
<b>Figure 5.16</b> : AgNPs labeled HPV 18 primer hybridization with HPV 16 DNA resulted model analyte ASV plots.....	149
<b>Figure 5.17</b> : Specificity conformation of model analyte as comparing different primers hybridized patient DNA.....	149
<b>Figure 6.1</b> : GO (A) and GR (B) FTIR .....	158
<b>Figure 6.2</b> : TGA curves of GO (A) and GR (B).....	159
<b>Figure 6.3</b> : TEM images of GO (A) and GR (B) nanosheets. ....	159
<b>Figure 6.4</b> : Pencil Lead electrode in paper microfluidic chip fabrication .....	160
<b>Figure 6.5</b> : Electrical contacts of pencil lead electrodes.....	160
<b>Figure 6.6</b> : Comparison of Glassy Carbon electrode, Pencil electrode and Graphene electrode .....	161
<b>Figure 6.7</b> : GRE 1.21 modified pencil lead electrode ASV result and calibration curve.....	163
<b>Figure 6.8</b> : GRE 1.9 modified pencil lead electrode ASV result and calibration curve.....	163
<b>Figure 6.9</b> : GRO modified pencil lead electrode ASV result and calibration curve .....	164
<b>Figure 6.10</b> : Graphene-Nafion modified pencil lead electrode ASV result and calibration curve.....	164

# **3D PAPER BASED ANALYTICAL MICROFLUIDIC CHIP FOR EARLIER MOLECULAR DIAGNOSIS OF CERVICAL CANCER AT THE POINT OF CARE**

## **SUMMARY**

In this study, a point of care (POC) paper based analytical microfluidic chip is developed for extraction, non-enzymatic amplification, and detection of combined human papillomavirus (HPV) 18&16, the etiological agent of cervical cancer. This device includes both paper extraction support material and paper based detection tool.

As a result of this thesis, we obtained a novel point of care extraction and detection tool for earlier molecular diagnosis of cervical cancer. A special modification technique has been used to allow non-enzymatic amplification in our analytical detection chip by using magnetic micro beads and silver nanoparticles labeled primers. The low cost point of care device allows doctors to diagnose, advise, and treat the patients all within the same visit, and the entire process can be completed in less than 30 minutes for low limit of detection (LOD) value of HPV. It is a beneficial tool for detection of HPV positive patients in both low resource settings and developed countries.

Herein, also an extraction tool and its chemical single step buffer have been developed for combined HPV form. Their flow rates and times were adjusted in order to use in microfluidic chip prior to detection. Principally, cervical cells lysed to extract HPV for releasing DNA via paper support material. Then, DNA has been modified with thiol labeled silver nanoparticles and streptavidin coated magnetic microbeads for amplification, and detection of the target analyte. All of the steps are optimized, and designed in order to achieve paper microfluidic device. Finally, a paper based microfluidic detection platform was fabricated using wax printer and hollow channels in its design. Microfluidic paper analytic chip had also fabricated as included stencil printed, pencil lead, graphene, and graphene oxide modified electrodes forms. Then, the paper device assembled its 3D form as folding it.

Traditionally, microfluidic devices require enzymes for amplification and detection of HPV DNA in polymerase chain reaction (PCR). There is not wholly integrated non-enzymatic paper based point of care detection tool reported in the literature for earlier detection of cervical cancer which is very critical for the developed countries.

**Keywords:** Microfluidics, Point of Care (POC) Devices, Paper analytical chip, Human Papilloma Virus (HPV), Cervical Cancer, Molecular diagnosis

# SERVİKS KANSERİNİN POC ERKEN MOLEKÜLER TEŞHİSİ İÇİN 3D KAĞIT BAZLI ANALİTİK MİKROAKIŞKAN ÇİP

## ÖZET

Bu çalışmada, serviks kanserinin etiyolojik ajanı insan papiloma virüsü (HPV) 18 ve 16'nın ekstraksiyonu, enzimsiz amplifikasyonu ve teşhisi için nokta analizlerinde (POC) kullanılan kağıt tabanlı analitik mikroakışkan çip geliştirilmiştir.

Bu tez çalışmasının sonucu olarak serviks kanserinin moleküler düzeyde erken teşhisini sağlayacak yeni bir nokta analiz (POC) ekstraksiyon ve teşhis cihazı elde edilmiştir. Analitik tayin çipinde enzimsiz amplifikasyona olanak veren, manyetik mikrobuncuk ve gümüş nano parçacıklı primerler aracılığı ile özel bir modifikasyon tekniği kullanılmıştır. Bu düşük maliyetli POC cihaz 30 dakika içerisinde HPV DNA sını çok düşük tayin değerlerini teşhis ederek, doktorun hastasını aynı ziyarette hem teşhis edip hem de tavsiye ve tedavisine başlamasını sağlamaktadır. Bu cihaz HPV nin gelişmiş ve gelişmekte olan ülkelerde kolayca tayininin yapılabilmesi için çok büyük bir avantaj sağlamaktadır.

Burada, ayrıca kombine HPV formu için bir ekstraksiyon malzemesi ve onun kimyasal tek basamak kullanımlı tampon çözeltisi geliştirilmiştir. Bu ekstraksiyon malzemesinin mikroakışkan çipde kullanımı için tayin öncesinde akış hızları ve zamanları ayarlanmıştır. Prensipte olarak bu kağıt ekstraksiyon malzemesi serviks hücrelerinin lizisi ile HPV ekstraksiyonu sonucu DNA salınımını sağlamaktadır. Elde edilen bu DNA, hedef analitin amplifikasyonu ve teşhisi için, tiyol bağlı gümüş nano parçacıklar ve streptavidin kaplı manyetik mikro buncuklarla modifiye edilmiştir. Kağıt tabanlı mikroakışkan cihazı elde etmek için uygulanan tüm aşamaların dizaynı yapılmış ve optimizasyonu gerçekleştirilmiştir. Son olarak wax yazıcı ve boşluk kanallar kullanılarak dizayn edilen kağıt tabanlı mikroakışkan tayin platformunun üretimi yapılmıştır. Mikroakışkan kağıt tabanlı analitik çip üretiminde kalıpla basılmış grafit elektrot, kalem ucu grafit elektrot ile grafen ve grafenoksit modifiye elektrot formları kullanılmıştır. Son olarak da kağıt cihaz 3 boyutlu formuna ulaştırılmak için katlanarak birleştirilmiştir.

Geleneksel olarak, mikroakışkan cihazlar HPV DNA sını, polimer zincir reaksiyonu ile amplifikasyonu ve tayini için, enzim gerektirmektedir. Şu ana kadar literatürde, gelişmekte olan ve gelişmiş ülkeler için kritik rol oynayan serviks kanserinin erken teşhisi için, ekstraksiyon ve tayin ünitesinin tamamını içeren enzimsiz kağıt tabanlı bir POC cihaz rapor edilmemiştir.

**Anahtar Kelimeler:** Mikroakışkan, Nokta analiz cihazları (POC), Kağıt tabanlı analitik çip, İnsan Papiloma Virüsü (HPV), Serviks Kanseri, Moleküler teşhis

## **1. CHAPTER: INTRODUCTION**

Cervical Cancer is the second most common cancer among women worldwide which is ended with the mortality especially for the people between 25-65 years old. It requires dozen of cellular differentiation for progression of the cancer from dysplasia to invasive carcinoma. Till it has been learnt that HPV (Human Papilloma Viruses) carry oncogenous which includes fundamental mutations, it has been accepted as a most common risk factor for cervical cancer. The definition of HPV quantity survey is totally based on viral nucleic acid detection.

A a point of care (POC) device has been developed for global health applications during this work. The earlier detection of cervical cancer will be getting easier with the developed fast, cheap, portable, and non-error microfluidic device which detects the HPV.

The purpose of this study is to provide a cheap, portable, sensitive, and low time sample answered microfluidic device as POC (point of care) technologies which can early detect and define the cervical cancer by extraction and amplification of nucleic acid biomarkers from viruses. Also, the device is optimized and applied for the real patient samples.

The first, single use, rapid, and cheap POC microfluidic device has been developed with paper based platform and wax printing technology which has a low pressure and non-enzymatic features. There are not any requirements like clean room and other expensive techniques for this method. It can be use very simply and forward the aqua through the paper support material.

The extractions of DNA from viruses for detection of cancer have been done with the provided device. The real time polymer chain reactions (PCR) have been applied for control experiments and optimization-validation parameters of the device. The novel

device is also tested on the patient samples, and results were validated with several characterization techniques.

### **1.1 HPV and Detection Types**

HPV (Human papilloma viruses) have been classified according to their oncogenic risk potential as low risk types (LR-HPV), probably high risk types (PrHR-HPV), and high risk types (HR-HPV) after it has been proved that the etiological connection of cervical cancer (Leto et al., 2011).

HPV infections have very high percent viral clearance. For examples, after 12 month period from the infection the %70 of these cases and after 18 month period up to %80 of these cases have been determined as HPV-DNA (Baseman and Koutsky, 2005; Bierman et al., 1998). By the way, cervical cancer which is related to HPV is the second most common cancer (Baseman and Koutsky, 2005). It has been suspected that every year 500.000 people catch newly to the cervical cancer among women worldwide and most of them are resulted with the mortality (Hoory et al., 2008).

Pap-Smear and HPV-DNA tests are very important for earlier detection of cervical cancer, because HR-HPV infections have approximately 10 years latent period from beginning to cervical cancer progress (P syrri and DiMaio, 2008).

Cervical cancer is the second most common cancer among women worldwide which is ended mortality and kills 270,000 women per year (Ferlay et al., 2010). Approximately %85 of these cases in developing countries, which have limited resources for screening (Ferlay et al., 2010). When diagnosed early and accurately cervical cancer has high cure rate thus underscoring the value of early detection.

Current HPV detection method is the Pap-Smear for which the turnaround times in weeks and requires highly trained pathologists for screening. It is not suitable for developing countries which have limited resources for screening. In addition to that it causes delays for the developed countries such as the U.S., because the traditional test requires samples need to be sent to an outside of the center for analysis. Hence, there is a significant need to develop a low cost, robust detection tool for cervical cancer.

Human Papilloma virus has up to 170 agents and more than 40 of them are typically transmitted through sexual contact (Control and Prevention, 2007). HPV 16 and HPV18 types are the etiological agent of cervical cancer and the case status are up to %70 (Schiffman et al., 2007).

HPV DNA viruses effectuate mucous membranes or keratinocytes of the skin. Qiagen Digene HC2 test also has been used for detection of HPV DNA, and it has been picked out that the test is more effective than Pap-Smear method. Furthermore, FDA (Food and Drug Administration) also approved using HPV DNA test (Roche cobas HPV) as a detection tool of first-line cervical cancer upon the Pap-Smear.

It seems that detection of HPV DNA has higher sensitivity and specificity compared to the pap-smear. Besides, these tests also require highly trained personals, intensive needs for resource, and turnaround times in days according to the how far the center from there. These limitations block usage of them for POC in low-resource setting areas and lead researchers for new usable technologies.

The interest to the Rapid and selective detection technologies which can integrate easily is continued to increase recently (Liu et al., 2012a; Pai et al., 2012). Microfluidic devices are very good and potential choices for developing the global health and controlling the epidemics (Huang et al., 2013). These devices have so much advantages like low cost, more power yield, having complex functions on a single chip, employs minimal sample preparation more sensitively, portable, robust and fast for field tests (Sia and Kricka, 2008). These amazing unique features are customized this microfluidic devices for portable point of care systems (Marie Dupuy et al., 2005; Toner and Irimia, 2005).

It has been verify that there is a significant need to develop a single use devices which can control itself for the global world according to the results of joint approaches (Yager et al., 2006). These devices should be simple, reliable, and also suitable to the main ambient temperature, robust and portable (Mabey et al., 2004). Nowadays, we have a huge literature about the new devices which can do very complex biological manipulations and not require any limitation or lab support (Curtis et al., 2012; LaBarre et al., 2011). For example, La Barre and his friends did an isothermal amplification by

using CaO as a heat source (LaBarre et al., 2010). Also, Wang and his friends placed the hand usable eggbeater into the centrifuge for isolate the whole blood plasma (Wong et al., 2008). In addition to this it has been known that there are a lot of paper based microfluidics which can be used for bioanalysis (Abe et al., 2008; Chow et al., 2008).

The nucleic acid based experiments have been successfully performed recently because of accurate analysis and velocity (Brinkmann, 1998; Sidransky, 1997). Normally, standard tube based PCR can be completed approximately 30 minutes (Boel et al., 2005). However, temperature control steps, highly trained analysts and clean lab environment requirements and limitations make the technique complicated. Therefore, single use low-cost platform devices are significant need for providing amplification and extraction at low temperatures as a very charming option. This combined systems are very efficient for low cost diagnosis (Faulstich et al., 2009; Goldmeyer et al., 2008).

The significant need for getting over these limitations to provide POC is translating the processes such as miniaturize the restrictions. The faster and special featured devices allow doctors to diagnose, advise, and treat the asymptomatic patients as well as HPV16 and 18 could be screened more closely in the same visit. A POC microfluidic chip to detect HPV could increase access to screening and early detection for patients, especially in low resource settings where a follow up visit is difficult to achieve, improving their quality of life and reducing mortality from late detection.

### **1.1.1 POC technology for cervical cancer**

Pap Smear is a traditional method to detect cervical cancer based on looking at cervical smear samples under microscope for determination of the cells if look normal or abnormal by trained pathologists. This method takes the turnaround time in weeks, and its sensitivity is quite low as 53%, although it has a high specificity as %96.3 (Ying et al., 2014). This qualitative method is also not suitable for developing countries because of its trained pathologists, proper lab platform, and sample sending processes which take long times.

Visual inspection with acetic acid method is more suitable detection method of the cervical cancer in developing countries. It is not required any microscope for

visualization. This method depends on applying 5% acetic acid on to the cervix and observing if pre-cancerous cells which have more intracellular proteins turn white while the normal do not have any changes in their color. It is more sensitive compared to Pap-smear test and more close to POC technology because of the testing time is much lower. However, it has low specificity, because it can be diagnose a patient with the disease, and it is still based on cytology (Goel et al., 2005; Hegde et al., 2015).

Detection of HPV with cytology has limitations, so that most of researchers have been focused on molecular diagnosis of cervical cancer. Furthermore, HPV DNA test is more sensitive (>96%),and specific (>90%) (Ying et al., 2014). However, molecular diagnostic tools require some special equipment for providing pressure fluid driven, optical instrumentation and cyclic thermal control unit. Thus, it becomes an expensive process with its required instrumentations for a disposable sample-to-answer nucleic acid test. First HPV test (Qiagen Digene Hybrid Capture II (HC2) is based on chemiluminescent detection of RNA probes which hybridized target DNA performed during 6 hours in a lab with plate reader. According to Sankaranarayanan et al., patients who were screened with the Digene HPV test had reduced incidence of advanced cancers and mortality over time compared to cytology or VIA (Sankaranarayanan et al., 2009). A lower cost version of the Digene test – care HPV – was developed by PATH and Qiagen (takes ~2 hours and requires benchtop space) because of its complication of high cost, and the need for sophisticated laboratory equipment.

After 1999's FDA was approved another nucleic acid based diagnostic test called Roche cobas HPV test in 2014. The main idea of the test was providing genotype information for HPV16 and 18 while detecting other 12 high-risk types as amplifying the target DNA with polymerase chain reaction (PCR) by using cobas 4800 system which is not suitable for POC.

Our device can do sample extraction, amplification and detection less than 30 minutes with low cost and disposable platform for HPV16 and 18 DNA at the POC. This molecular test for cervical samples solved the limitations of cytological detections. The novel POC platform eliminates the trained personnel need and output more quantitative results compared to Pap smear and VIA. It also eliminates the need for PCR



thermocycling and enzymes which are required for other molecular diagnostics. Single step extraction based and non-enzymatic analytical paper device is provided faster results than PCR as well as the other enzymatic techniques. Our device will be simple to use and portable, allowing it to be applied in low-resource settings in order to reach a larger pool of patients who may otherwise not get diagnosed due to insufficient resources and personnel.

### **1.1.2 Microfluidic Technology for HPV**

Cancer is the one of the major reason of mortality. Earlier diagnosis of cancer has a high cure rate, and it is a very important factor for treatment (Miller, 2012).

The detection of nucleic acid biomarkers which are gotten from the target analyte is a considerable approach for cancer diagnosis. A large data series which are obtained from transcriptomic studies shows that various biomolecular pieces of cancer cells samples compared to the normal cells are resulted in exploration of protein biomarkers (Bohunicky and Mousa, 2011; Tothill, 2009). These proteins which are not include cells have been found as a high concentrations into the nucleic acids expedite the early cancer diagnosis (Barden et al., 2003; Rosen et al., 2005; Rosen and Stone, 2006; Tothill, 2009).

One of the most important problems of the science and engineering world today is to provide technologies for the people who are in developing countries (Chin et al., 2013). Thus, there is a significant need to develop low cost, robust, sensitive, specific, user friendly and rapid detection tools for biomolecular POC diagnosis (Mabey et al., 2004). These mentioned platforms which are developed for diagnosis are thermoplastic single use microfluidic devices include integrated micro-solid phase columns (Bhattacharyya and Klapperich, 2006; Mahalanabis et al., 2009). Generally, these complex laboratory detection processes have been miniaturized with this new integrated technologies by using microfluidic devices. Also, it has been provided earlier diagnosis with POC devices as using nanoparticles (Chin et al., 2011). These smart microfluidic devices provide advantages for decreasing clinical problems (McCalla et al., 2012).

Microfluidic technologies are the systems which include micrometer level channels inside it, and they are usable for micro volume level liquids (Whitesides, 2006). Rapidly progressive technology in interdisciplinary fields have been caused a lot of inventions which are like revolution. Rapid and commercial prototyping methods for microfluidic devices include these; cast polydimethylsiloxane (PDMS) (Duffy et al., 1998; Thorsen et al., 2002), laser ablation (Brivio et al., 2002; McNeely et al., 1999), stereo lithography (Bertsch et al., 2003), micro dust blast (Brivio et al., 2002), hot embossment (Folch et al., 1999), micro spinning (Friedrich and Vasile, 1996) and lamination (Bartholomeusz et al., 2005; Yuen and Goral, 2010). PDMS casting which is generally named soft lithography is become as a most common prototyping process for the laboratories, because it is simple and reproducible in record time (Duffy et al., 1998; Jo et al., 2000; Xia and Whitesides, 1998). Recently, it has been done so much new creative itinerary for fabrication of microfluidics in order to reduce the time and cost (Tan et al., 2001).

Conveying cancer treatment outside the special centers and providing cures at homecare or local clinics are going to decrease the health cost significantly. Patients should cover a distance for getting treatment from the cancer centers in generally. There are not enough facilities in developing countries for diagnosis and cure of the cancer. Also, surgical treatments have huge infection risks, and there are not enough surgeons for treatment of the patients quite a lot area. It should probably be better follow-up the patients from their own home during the chemotherapy (Chin et al., 2011).

Cancer technology centers develop prototype devices which can provide innovative point of care (POC) methods for following up patients from their home, earlier diagnosis, treatment and browsing (Byrnes et al., 2013). These integrated interdisciplinary teams which include engineers, doctors, public health specialists and technology transfer specialists develop primary nonconventional future technologies in that centers. POC devices are very important for these studies which can be used for diagnosis and also browsing of the patients during the medicine treatment. The diagnosis can be done in very short minutes from the viruses directly via nucleic acids extraction as providing portable-low cost microfluidic devices provided non enzymatic or non-electrical power (Mahalanabis et al., 2009).

All researches are focused on providing and designing microfluidic total micro analysis systems (mTAS) for carrying all sample analysis in order to the POC point as input-output systems. Thereby, the needing for carrying and storage has been eliminated and the possibility of giving the results to the patients tried to be reduced (Chin et al., 2013; Lee et al., 2008).

## **1.2 Microfluidic Technologies for Bioanalytical Research**

Bioanalytical microfluidic sensors which can perform separation, purification and detection steps sequentially have been become one of the most focusing areas in the literature (Ohno et al., 2008). Glass and PDMS integrated fabrication method has been preferred because of several reasons for many years. Elastic structure of PDMS allows soft lithography fabrication techniques for flow rate controllable micro channels and pumps (Anderson et al., 2000). Also, the transparency features of glass and PDMS enable to use of different spectroscopic method such as fluorescence (Hofmann et al., 2002; Zhang et al., 2012), and chemiluminescence (Amatatongchai et al., 2007; Suh et al., 2014).

According to the literature, there are lots of different approaches for bioanalytical microfluidic applications which are integrated for obtaining both extraction and detection of the microbeads bonded analyte. Baeumner et al. provided a microfluidic chip for cholera toxin subunit B (CTB) which can detect electrochemically via fluorescence (Bunyakul et al., 2015). The main idea was using liposomes and magnetic microbeads specific to CTB. Hence, there is a significant need to modify these liposomes with thiol groups and conjugate magnetic micro beads with antigen-antibodies for increasing the yield of fluorescence of desired analyte.

Furthermore, a multiplexed microfluidic biosensor has been engineered by Mirasoli et al. which can detects various parvovirus B19 DNA via chemiluminescence (Mirasoli et al., 2013). The main goal for this study was covalently attaching the complementary DNA probes of each genotype on to the three different glass slide of micro channels. Then, this biotinylated targets were introduced to the device, and avidin-modified HRP added and detected.

The main logic for designing microfluidic device is to carry out all analysis process inside the same platform from input to output of the diagnosis. In addition to this, microfluidic applications platform should be more quantitative and sensitive.

Ji et al performed a microfluidic integrated platform as an example of this logic (Ji et al., 2013). The device separated, enriched, and detected the peptides with reverse phase liquid chromatography (RPLC), droplet microfluidics and electrospray ionization mass spectrometry methods ESI-MS/MS. The RPLC separated peptides were transformed into the droplets of analyte with the connected end of RPLC-microfluidic device. Then, the analyte was detected into the ESI-MS/MS. However, these devices needs to be simple and requires minimal instrumentations from input sample to output signal processes for real use as home-based applications. Thus, point of care devices have been developed by the researchers recently for simple and rapid diagnosis platforms (Weaver et al., 2014).

### **1.2.1 Paper Microfluidic Devices for POC Applications**

Eventhough PDMS and glass microfluidic platforms are very popular and usable for application of bio-sensor, they have limitations for POC technologies. These are the a few of limitations of PDMS; photolithography requirements for mold production, scale-up production difficulty and high absorption properties of the proteins on to the micro channel walls (Sharma et al., 2011). These restrictions inspired to researchers for new featured platforms for POC microfluidic devices. Cellulose paper is the most important invention for microfluidic POC technology recently.

There were a few research for the development of the first glucose meter in 1970 (Clarke and Foster, 2012), nitrocellulose lateral-flow pregnancy test in 1980's (Davies et al., 2007), and some commercially available tests (Yetisen et al., 2013), as cellulosic paper microfluidics until Whiteside's group revolutionized the area in 2007 by providing a three-dimensional paper analytical devices (Duffy et al., 1998; Martinez et al., 2008). Cellulose papers are biodegradable, biocompatible, filter like, easily modifiable, scale-up, flexible and inexpensive. These features provide advantages to the cellulose paper for bioanalytical POC applications (Hu et al., 2014; Then and Garnier, 2013).

Pollock et al. produced an integrated 3D paper based micro analytical device which can spontaneously detect drug-induced liver damage markers in human blood (Pollock et al., 2012). The device loaded with the sample for plasma separation such as filtering red blood cells away from the sample and route only blood plasma to the channels. Then, the preloaded reagents contacted with the filtered sample in sequence resulted in specific color changes to each reaction. Color changes compared to the read guide for quantitative analysis of the samples.

The literature also shows that other paper microfluidic examples such as bacterial DNA *E. coli* extraction and lysing included origami device for molecular paper based diagnosis (Govindarajan et al., 2012), and 3D multiple valve controlled lateral flow device for reagent introduction of rabbit IgG detection via Enzyme-Linked ImmunoSorbent Assay ELISA (Gerbers et al., 2014).

Indeed paper based microfluidic devices are directly corresponded to point of care diagnostic technologies with their outstanding properties such as portable, low cost, robust and rapid features. It can be designed and integrated with the systems for single-use bioanalytical platforms of variety of targets in personalized healthcare. This interdisciplinary area will provide simple and sensitive suitable diagnosis platforms to the developing countries and facilitate rapid and low cost diagnosis for developed countries.

### **1.3 Proposed Solution Synopsis of Dissertation**

The proposed solution is to develop a paper based analytical microfluidic chip that allows extraction, non-enzymatic amplification and detection of combined HPV16 and 18 types in order to diagnose cervical cancer. The disposable paper based POC analytical device package includes both three steps for molecular diagnostics.

Recently, researchers have focused on low cost and portable paper molecular diagnostics as inspiring from lateral flow pregnancy test strips (Martinez et al., 2009; Rohrman et al., 2012). Paper based platforms do not require pumps and vacuum for driving fluid flow because of capillary effects. Modification effect to the amplification of target detection nucleic acids eliminates enzymatic amplification and PCR.

Modifying nucleic acids with silver nanoparticles and magnetic microbeads for non-enzymatic amplification eliminates the need for thermal cycler and some of enzymatic needs completely. In addition to that paper is an ideal material with its outstanding properties such as inexpensive and wicking features which make it necessary for lateral flow detection.

Prof. Klapperich Lab has a huge experience for preparation of nucleic acid samples (Byrnes et al., 2013; Cao et al., 2012; Huang et al., 2013). Prof. Crooks group has a lot experiences in paper based non enzymatic amplification and detection devices (Renault et al., 2014; Scida et al., 2014). Prof Klapperich from Boston University has a collaboration with Prof. Crooks from Texas University. We are all confident that each molecular diagnostic step can be performed in paper, combined with analytical and non-enzymatic detection device.

A low-cost POC test for HPV would enhance screening coverage and enable early detection, resulting in improved treatment outcomes and prevention of further transmission. The proposed solution is using low-cost paper modules with novel modification method for non-enzymatic amplification, extraction and detection in a disposable POC device.

Our proposed paper analytic microfluidic device for HPV 16 and 18 tests can be detected cervical cancer at the POC. This device resulted in validated proof-of-concept device suitable for future development activities including clinical testing. Consequently, this work will develop a rapid platform for molecular diagnostics that can be adapted to the other diseases by altering the primers in the modification step for analytical detection.

## **2. CHAPTER: COMBINED HPV 16&18 TYPES AMPLIFICATION**

Human papilloma viruses cause different kinds of anogenital lesions, however only high risk genotypes induce cancer (Munoz et al., 1992; Poletti et al., 1998). HPV16 and HPV18 are the most common types which causes cervical cancer (Bosch et al., 1995).

HPV 18 &16 DNA can be found together or alone in the samples. Our purpose is to extract and detect these two common high risk types with paper based analytical microfluidic chip. The method should extract both two types together and detect them specifically. The paper based developed device can do quantitative detection of HPV DNA sequences. Thus, a TaqMan based real time assay protocol is developed and optimized for cervical smear samples to detect real time amplification of HPV E7 genes in order to compare extracted samples with non-extracted quantified DNA standards. Samples also were processed with Qiagen DNeasy Blood and Tissue kit as a positive control. Once the limit of detection is established for the paper supports, the extracted DNA directly modified for electroanalytical detection.

In this chapter, a real time PCR based assay reported for detection and quantitation control steps of HPV DNA sequences for both HPV16&18 types in positive and negative control samples according to the detection limits in the literature.

### **2.1 Introduction**

#### **2.1.1 Real-time polymerase chain reaction**

Real-time PCR is based on polymerase chain reaction which quantitatively shows the amplification of a target DNA. There are two methods for real time PCR detection. One of them is nonspecific and the other one is sequence specific. First one can intercalate with any double stranded DNA with non-specific fluorescent dyes. The other one can detect specific DNA probes labeled fluorescent after hybridization of the complementary sequence.

Kary Mullis developed a PCR technology that amplifies a few copies of DNA sequence for various applications such as functional analysis, diagnosis of diseases and

identification of genes in molecular biology in 1983 (Henson and French, 1993; Lee et al., 1990; Mullis et al., 1990).

DNA is melted and replicated enzymatically with thermal cycling method as heating and cooling the sample respectively through a defined series of temperature steps. The short DNA fragments called primers are the key components for the repeated amplifications of target sequences. Generally PCR applications require heat-stable DNA polymerase as Taqman polymerase. The enzyme assembles on single-stranded DNA template with the nucleotides and by the help of the primers that initiate the DNA synthesis.

First, DNA is melted for separating the double helix DNA physically. Then, the DNA strands are templated as decreasing the temperature for amplification of target DNA selectively via using polymerase and primers.

Real-time PCR is relied on a thermal cycler to illuminate each sample by a beam of light and detect the fluorescence emitted. The PCR technology contains series of temperature changes. These cycles consist of three stages. First one is around 95 °C and it allows the separation of the nucleic acids. Second temperature is around 50-60 °C that allows the primers for binding with DNA template (Lasky et al., 1992; Lee et al., 1990; Scorza et al., 1995). Third one is between 68 - 72 °C and it enables to polymerization via enzyme (Erlich et al., 1991). The fluorescence is measured during short temperature phase lasting only a few seconds in each cycle.

Real time PCR detects only the DNA that is complementary of the fluorescent reporter probes. Thus, there is a significant increase of specificity in the use of reporter probe. It also enables to use the technique in the presence of different DNA medium. Also, fluorescent probes allow monitoring several targets as using different-colored labels for multiplex assays. The method consists of a DNA-based probe with a fluorescent reporter. Quencher is very close to the reporter, so it prevents the detection before polymerization. After TaqMan, polymerase breaks the reporter that it allows emission of fluorescence. Fluorescence is detected and measured in a real-time PCR machine, and its geometric increase which is corresponding to exponential increase of the product is used to determine the quantification cycle in each reaction.



The target DNA strand is amplified by PCR. Generally, fragments between 0.1 to 10 kbp DNA can be amplified by PCR. Basically, a PCR set up has some components. A DNA template includes the target gene for amplification, two primers of complementary ends of the strand, Taq polymerase enzyme at approximately 70 °C temperature, dNTPs (nucleotides) to synthesize a new strand DNA, buffer solution for providing optimum chemical environment of polymerase,  $Mg^{2+}$  and potassium ions for mutagenesis (Erlich et al., 1991; Lasky et al., 1992; Scorza et al., 1995).

Commonly, PCR includes repeatable temperature changes called cycles. These series are approximately between 20 to 40 cycles which consist of 2 to 3 discrete temperature steps. Generally, cycle begins with high temperature step and follows by a middle hold one and ended extension. The temperatures and their length depend on different kinds of parameters such as enzyme features, ions and dNTPs (deoxynucleotide triphosphates) concentrations and the melting temperature of the primers (Hadidi et al., 1995; Yang et al., 1992)

Temperature steps are totally applied for six different periods. The first one is called as initialization step which required for hot-start PCR (Powledge, 2004). The temperature for this step is 94-98 °C and time is 1-9 minutes length. The second one is denaturation for separation of DNA at 94-98 °C for 20-30 seconds. The third one is annealing step. Temperature is decreased to 50-65 °C for 20-40 seconds for binding primers to the target complementary single stranded DNA. The temperature is very important for correct binding of primers to the template. Furthermore, efficiency and specificity are affected by the annealing temperature in PCR and an incorrect annealing temperature can cause an error. The other step is extension which depends on the enzyme temperature for maximum activity. It is commonly between 75-80 °C for TaqMan polymerase (Dieffenbach et al., 1993; Innis et al., 2012). The DNA polymerase forms a new strand by the help of the dNTPs. Extension time depends on the length of DNA fragment.

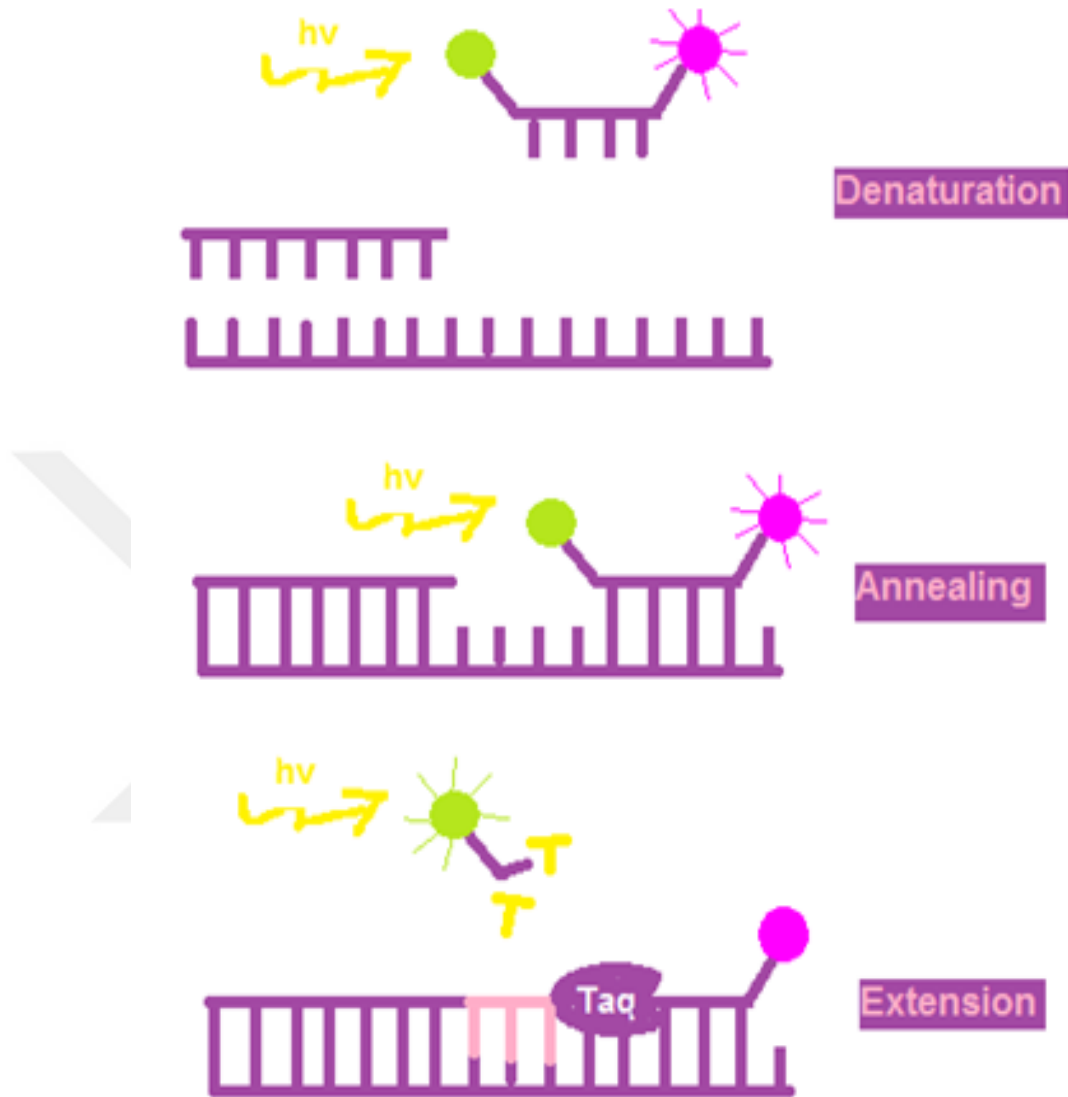


**Figure 2.1 :** Real-time PCR working principle

All of the parameters that mentioned above such as temperatures, time length and cycle are depend on various parameter optimizations such as melting point of primers, enzyme features, concentrations of dNTPs and ions and multiplex assays (Hadidi et al., 1995; Innis et al., 2012; Weising et al., 1994)

PCR reaction can be confirmed if it amplified the expected DNA fragment or not via gel electrophoresis. It can show size separation. The resulted DNA product runs on the gel with known size DNA fragments contained DNA ladder for comparison.

### 2.1.2 Gel electrophoresis

Macromolecules such as proteins and DNA-RNA fragments separate and analyze according to their size and charge values via gel electrophoresis to use in biochemistry, clinical chemistry, and molecular biology (Kryndushkin et al., 2003).

The separation of the nucleic acids is provided by applying an electrical field. The molecules that are charged negatively move through a matrix of agarose according to their length. Shorter molecules migrate faster and easily through the pores of gel matrix (Maniatis et al., 1982). Gel is used for moving the charged particles during electrophoresis in an electrical field as sieving medium. Also, post electrophoresis stain can be applied to the gel (Berg et al., 2002). Gel electrophoresis method is generally used for analytical applications after amplification of DNA by PCR.

Basically, molecules can be moved using an electrical field through a gel such as agar or polyacrylamide by electrophoresis as processing the molecules based on their size. The negative charge of the electrical field pushes the molecules from one end of the gel through the other positive charge end which pulls the molecules.

Casted gel material includes well for dispensing the molecules. Then the gel tray placed in a chamber for applying electrophoresis method via connected power source. Species that are positively charged migrate towards the cathode which is negatively charged. If the species are negatively charged they migrate towards the positively charged anode (Robyt and White, 1990).

Gel consists of a crosslinked polymer. These polymer types are classified and used relied on their composition and porosity according to the specific weight and composition of the analyte. Acrylamide gel is usually used for separating small nucleic acids. It has high resolving power for small fragments such as 5-500 bp DNA. However, agarose gel is used for separating larger nucleic acids such as over a few hundred bases. Agarose gels and polyacrylamide gels run in different configuration. Agarose gels run horizontally while polyacrylamide gels run vertically. The casting and polymerization methods of each gel also different. Agarose gel casts thermally as polyacrylamide gel polymerizes in chemically.

The natural structure of agarose gel consists of polysaccharide polymer which is extracted from seaweed. It is proper for protein electrophoresis which is larger than 200kDa even though it does not have a uniform pore size (Smisek and Hoagland, 1989). Principally, agarose gel dissolves in the electrophoresis buffer between %0.7 to %2 from large to small fragments respectively (Lewis, 2001).

Polyacrylamide gel provides uniform pore size for separating fragment size from 5 to 2000 kDa.

Pore size arrange with different concentrations of both acrylamide and bis-acrylamide. The percentage of gel depends on the size of proteins and changes from %6 to %15 according to the wished probe in the sample (Schägger, 2006).

Electrophoresis consists of carrying current through the gel and it is provided by the ions in the buffer. The buffer also maintains the pH level at constant value relatively. Tris-Acetate-EDTA (etilendiamin tetraasetik asit) and Tris-Borate-EDTA are the most common buffer types for nucleic acids. TAE (Tris-Acetate-EDTA) has the lowest buffering capacity but provides the best resolution for larger DNA which means a lower voltage and more time, but a better product (Brody and Kern, 2004).

Staining processes should be applied to the molecules into gel to make them visible after electrophoresis is completed. Generally ethidium bromide is used to visualize DNA. Other methods may also be used to visualize the separation of the mixture's components on the gel. Photograph of gel is taken via Gel Doc systems.

## **2.2 Experimental**

Cervical smear samples can include two types of HPV 18 and 16 together or separate. Our device can detect both of them so it is required to optimize the concentration of primers, reagents (MgCl, dNTPs), temperature and reaction time. Different dilutions of each reagent and solution are tested to determine the proper concentration for optimal saturation of both samples and maximum amplification of each. The Taq-Man polymerase amplification assay for HPV 16, HPV 18, and RnaseP are tested and evaluated on real-time PCR, nanodrop and via acrylamide gel- agarose gel method.

The sample preparation step is also very important for optimization of extraction, detection and amplification parts.

HPV DNA stocks have been prepared by cloning the E7 genes for HPV 16 and HPV 18 using the Pgem-T Easy Vector system. After that, they confirmed using GeneWiz, Inc.

These plasmids have been used as the HPV DNA standards for TaqMan PCR optimization. We optimized the HPV DNA both in separated and combined forms to be sure if the conditions and reagents work properly to use of comparing patient sample.

The method applied and optimized for HPV16 first before HPV18 ,since HPV16 is the most common genotype.

Extraction performance will be evaluated in the presence of Rox reference dyes on an Applied Biosystems 7500 real-time thermal cyclers.

### **2.2.1 Biological fragments**

The E7 genes of HPV 16 and 18 fragments which are the high risk types of the cervical cancer used as standards of experiments for comparison and confirmation of extraction and cloning experiments via amplification of each. Thus, they were purchased from Integrated DNA Technologies.

The primers and probes of HPV 16&18 and RNaseP and its primers and probes were used for PCR Taq-Man amplification of the target DNA and combined form of HPV types. These primers and probes were also purchased from Integrated DNA Technologies. All probes were purchased as labeled with Cy-5 (Cyanine5) and FAM (Fluorescein) fluorophore.

Taqman primers for HPV 16 and 18 have been previously published and used for positive control and confirmation experiments. The primers and E7 gene sequences of HPV16 and 18 are listed in Table 2.1.

HPV 16 E7 gene	5'-GGT TAC AAT ATT GTA ATG GGC TCT GTC CGG TTC TGC TTG TCC AGC TGG ACC ATC TAT TTC ATC CTC CTC CTC TGA GCT -3'
HPV 18 E7 gene	5'-ATG TCA CGA GCA ATT AAG CGA CTC AGA GGA AGA AAA CGA TGA AAT AGA TGG AGT TAA TCA TCA ACA TTT ACC AGC CCG ACG AGC CGA ACC ACA ACG TCA CAC AAT GTT GTG TAT GTG TTG TAA GTG TGA AGC CAG AA -3'
HPV 16 Forward Primer	5'-AGC TCA GAG GAG GAG GAT GAA -3'
HPV 16 Reverse Primer	5'-GGT TAC AAT ATT GTA ATG GGC TC-3'
HPV 16 Probe	5'-CCA GCT GGA CAA GCA GAA CCG G-3'
HPV 18 Forward Primer	5'- ATG TCA CGA GCA ATT AAG C-3'
HPV 18 Reverse Primer	5'-TTC TGG CTT CAC ACT TAC AAC A-3'
HPV 18 Probe	5'-CAT CAA CAT TTA CCA GCC CG-3'

**Table 2.1.** The primers and E7 gene sequences of HPV16 and 18

### 2.2.2 Cell culture and transcription assay

The HPV DNA stocks are prepared as cloning E7 genes for each HPV 16 and 18 types into two respective plasmids using the pGEM-T Easy Vector system (Promega, Madison, WI). The sequences have been confirmed using GeneWiz, Inc (Cambridge, MA). These plasmids were used as the DNA standards for extraction optimization and

comparison to the PCR gold standard in order to make sure the reagents and conditions are working properly before using DNA purified from cervical smear samples (A.1; Cloning procedure).

### **2.2.3 Chemicals and materials**

The efficiency and specificity of the Taq-Man reaction were optimized by altering the concentration of primers, reagents ( $MgCl_2$ , dNTPs), temperature and reaction time. Serial dilutions of each reagent were tested to determine the optimal concentration for maximum amplification.

TaqMan buffer was used for dilution and storage. TaqMan polymerase were used as an enzyme for biological catalyst. They both purchased from Invitrogen.  $MgCl_2$  was purchased from Sigma-Aldrich and used for promoting the DNA interactions. Thus, Mg was entered in the protein for join and created forces making the polymerase stronger and capable to join dNTPs, however a high concentration of Mg can play a role of antagonist in the PCR. Nuclease free water was used for re-suspending the probes which were purchased from Applied-Biosystems. Rox reference dye was purchased from Qiagen and used as a passive reference, which is used to normalize real-time PCR reactions. dNTPs were used for building blocks of nucleic acids and purchased from Thermo Fisher Scientific. Finally, 96 well PCR plates were purchased from Applied Biosystems.

The cloned plasmids and amplified DNA fragments were analyzed with acrylamide and agarose gel for confirmation experiments. When acrylamide dissolved in water, it took place in slow, spontaneous auto polymerization . Bis-acrylamide is the most frequently used cross linking agent for polyacrylamide gels. Rnase-Free water is used for obtaining target volume. Tris-Borate-EDTA (TBE) Buffer is commonly used in nucleic acid electrophoresis for providing effective under slightly basic conditions, which keeps DNA deprotonated , water-soluble, and protected from degradation , ammonium persulfate (APS). It is a source of free radicals, and it is often used as an initiator for gel formation. Tetramethylenediamine (TEMED) stabilize free radicals, and improves polymerization, ultrapure agarose. dsDNA runs faster with Tris-acetate-EDTA (TAE) Buffer. EtBr Ethidium bromide is an intercalating agent commonly used as a

fluorescent tag (nucleic acid stain).Ficoll blue is a gel loading dye for molecular biology, DNA ladder markers are used it to accurately determine both sizes and quantities of DNA samples on a gel. All above mentioned chemicals were purchased from Sigma-Aldrich.

#### 2.2.4 Devices and materials

Applied Biosystem 7500 Fast Real-Time PCR System was used for optimization and confirmation experiments via amplification of HPV 16&18 DNA and RnaseP (Figure 2.2). The concentrations of fragments were analyzed, and confirmed for comparison of PCR by Thermo Scientific NanoDrop ND-2000c (Figure 2.3). The sizes and amounts of fragments were analyzed, and confirmed with Agarose and Acrylamide Gel Electrophoresis. Thermo Fisher automatic propipetter and micro-pipets were used during experiments. Gels were placed in OWL gel boxes, and electrophoresis performed using BioRad PowerPac Basic Power Supply (Figure 2.4). Gel images were taken with Molecular Imager VersaDoc™ MP 4000 System (Figure 2.2).



**Figure 2.2 :** Applied Biosystem 7500 Fast Real-Time PCR System and Molecular Imager VersaDoc™ MP 4000 System





**Figure 2.3 :** Thermo Scientific NanoDrop ND-2000c

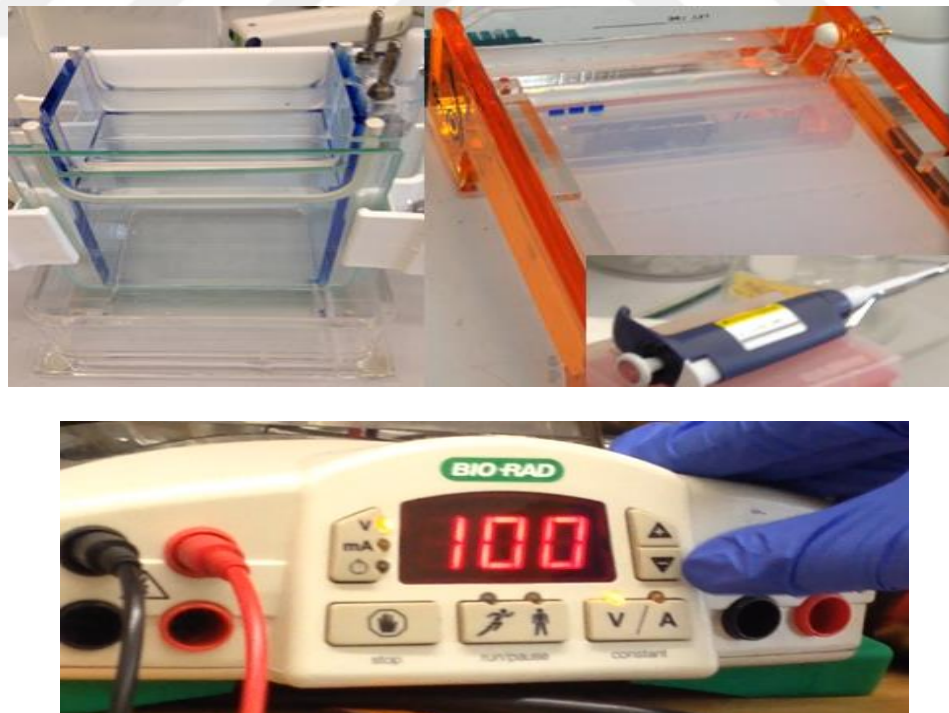


**Figure 2.4 :** BioRad PowerPac Basic Power Supply and Thermo Fisher automatic propipetter OWL gel boxes

## **2.3 Result and Discussion**

PCR optimization is very important to improve the DNA amplification performance and minimize failure by applying various techniques. The PCR amplification method is extremely sensitive. Therefore, many standard procedures obtained during the setup of PCR reactions such as using filter tips, wearing gloves, using clean cabinets or divided rooms etc. In addition to this,  $MgCl_2$ , dNTPs, primers concentrations and denaturation, annealing, extension times with cycling conditions are optimized for the efficiency and specificity of TaqMan PCR reaction.

The amplification of multiple targets by PCR in one experiment is called Multiplex PCR technique that is used widely. More than one sequence can be amplified in a multiplex assay by using multiple templates and several primers in the same reaction tube mixture. This method has considerable advantages such as saving time and effort. It has also some disadvantages like cross hybridization of primers and mis-priming. Thus, designing specific primer sets is a key to carry out successful multiplex reaction. It has been designed primers and probes for multiplex PCR amplification of HPV 16,18 and RNaseP. The optimization parameters of TaqMan PCR reaction set up has been setup for multiplex form. And, the primer concentrations were defined for combined form of each target sequences.

This part consists of TaqMan PCR reagents concentrations and times optimization of combined HPV 16, 18&RNaseP, cloned DNA results and their PCR-Gel confirmations, and application of the optimized parameters for patient samples.

### **2.3.1 Effects of $MgCl_2$ and dntps optimization on combined HPV amplification**

Magnesium is very strong, and it is required agent of Real-Time PCR as a co-factor for thermostable DNA polymerase. Determination of the optimum concentration is very critic, and it is provided for the success of the PCR reaction with magnesium-dependent Taq polymerase enzyme (Markoulatos et al., 2002).

$Mg^{++}$  binds to the alpha phosphate group of dntp during replication. The dNTP's gets broken down to dnmp's to form phosphodiester and  $Mg^{++}$  helps in the removal of beta and gamma Phosphate from dntp.  $Mg^{2+}$  in the PCR mixture stabilizes dsDNA and raises

the  $T_m$ . Therefore,  $Mg^{2+}$  concentration is required for controlling the specificity of the reaction.

Actually,  $Mg^{++}$  plays dual role in PCR as forming complexes with DNA and also promotes DNA interactions. PCR yield depends on the concentration of  $Mg^{++}$  for lots of cases. In point of fact, if the reaction setup includes a few  $Mg^{2+}$  ions, it results in a low yield of PCR product because primers fail to anneal to the target DNA. In addition to this, if it has too many  $Mg^{2+}$  ions, it increases the yield of non-specific products and promotes misincorporation. Besides that, the base pairing becomes too strong and the amplicon fails to denature completely for high concentrations of  $Mg^{++}$ . (Ellsworth et al., 1993; Williams, 1988)

Hence, high  $Mg^{++}$  increases Taq, but less  $Mg^{++}$  decreases Taq's activity as well as increases its specificity. The challenge is knowing how much to use it. Therefore, various concentrations of  $MgCl_2$  are used in the PCR reaction to determine the optimal  $MgCl_2$  concentration for only HPV 16, only HPV 18 and combined form of HPV 16, 18 & RNaseP. It has been tested 4 different concentration of  $MgCl_2$  such as 1,5mM, 3,5mM, 4mM and 1,5mM, 3,5mM. The results showed below for both combined and separate form of HPV types (Figure 2.5, Figure 2.6, Figure 2.7).

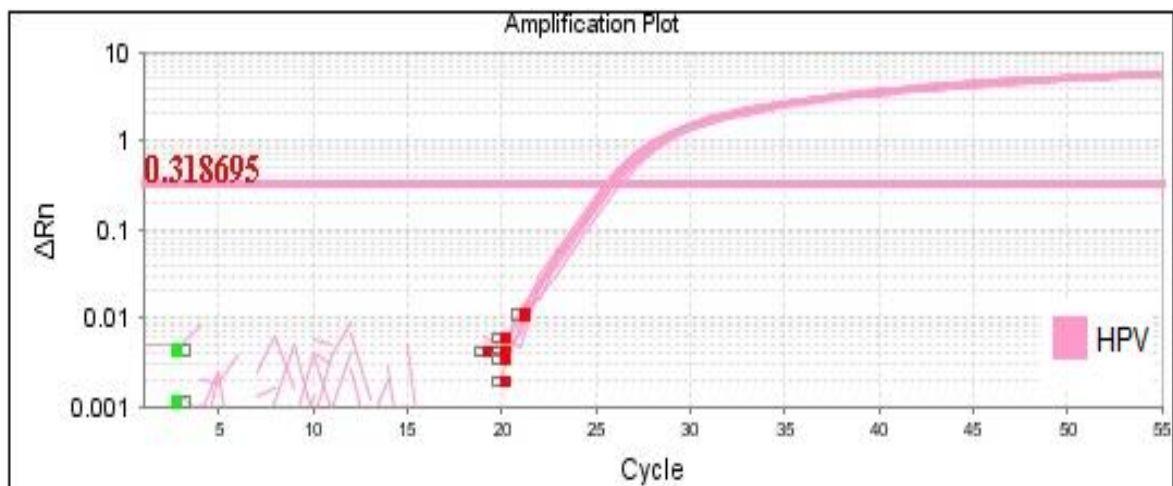


**Figure 2.5 :** HPV 18 for 1,5mM, 3,5mM 1,5mM, 3,5mM  $MgCl_2$

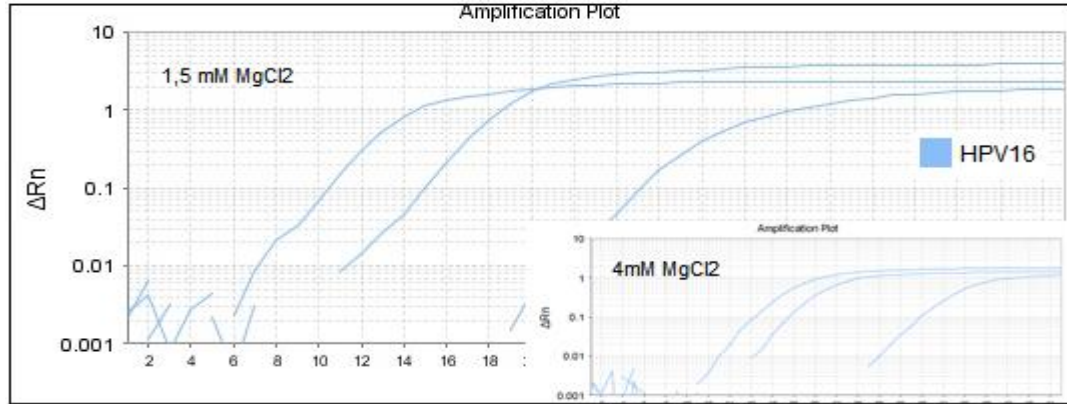


**Figure 2.6 :** HPV 16 for 1,5Mm and 4mM MgCl<sub>2</sub>

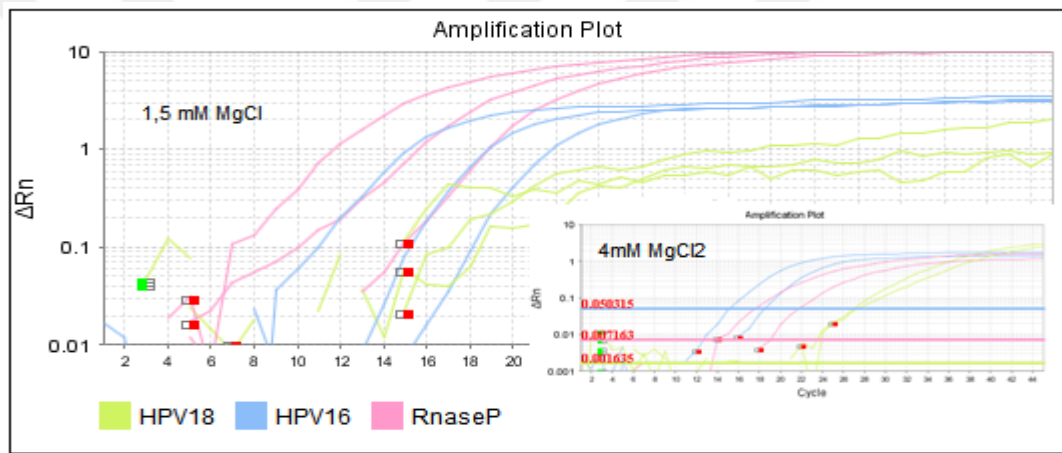


**Figure 2.7 :** HPV 16, 18&RNaseP 1,5mM and 4mM MgCl<sub>2</sub> from 10<sup>10</sup> to 10<sup>8</sup> copies of DNA

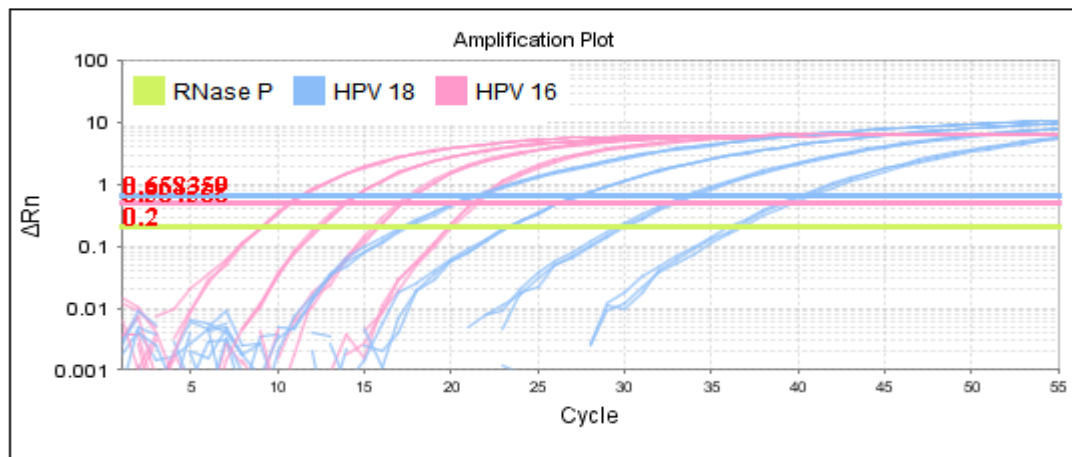


**Figure 2.8 :** HPV 16, 18&RNaseP 3,5mM MgCl<sub>2</sub> 10<sup>11</sup> to 10<sup>8</sup> copies of DNA

The results show that using 1,5mM, 3,5mM MgCl<sub>2</sub> for HPV 18 in the PCR reaction setup did not have a significant difference according to the amplification plot (Figure 2.9). Thus, HPV 16 amplification tested for 10<sup>10</sup> to 10<sup>8</sup> copies of DNA for 1.5 and 4Mm MgCl<sub>2</sub>. The data for 1,5mM MgCl<sub>2</sub> on Figure 8 did not saturated straightly for concentrations of HPV 16. Whereas, the PCR reaction which took place in the presence of 4mM MgCl<sub>2</sub> gave better saturation for 10<sup>10</sup> to 10<sup>8</sup> copies of HPV 16 DNA (Figure 2.10). Then, 1.5 and 4Mm MgCl<sub>2</sub> concentrations had been applied for combined HPV 16, 18&RNaseP as you can see in Figure 13. The PCR amplification results which are for 10<sup>10</sup> to 10<sup>8</sup> copies of combined DNA form was proofed that 1,5mM MgCl<sub>2</sub> is inconvenient concentration because of disorderly saturation. 4Mm MgCl<sub>2</sub> gave more ordered peaks and straight saturation compared to the 1,5mM MgCl<sub>2</sub> in the same condition even though it's amplification cycle began late than 1,5mM MgCl<sub>2</sub> (Figure 2.11). Finally, combined form of 10<sup>11</sup> to 10<sup>8</sup> copies of HPV 16, 18&RNaseP DNA is amplified in the presence of 3,5mM MgCl<sub>2</sub> included PCR reaction setup for achieving the proper optimal medium (Figure 2.8). It has been decided to use 3,5mM for all experiments.

### **2.3.2 Primer-probe testing and concentration optimization**

All primer pairs should work at the same annealing temperature during the PCR reaction , so that the primer pairs have to be optimized. However, it is required that multiple primer sets to produce varying sizes of amplicons which are specific to different DNA sequences. Multiplex PCR gave additional information as targeting multiple sequences with a single test run.

Successful multiplex reaction requires designing of specific primer sets. The essential primer design parameters for high yielded specific amplification described in this part. First, the length of the primers should be in the range of 18-22 bases for designing. Second, T<sub>m</sub> variation values of the primers arranges between 3°-5° C as almost similar preferably between 55°C-60°C. Higher T<sub>m</sub> is recommended for high GC content primers. Also, the specificity of designed primers should be taken in consideration. Finally, the primer dimerization should be checked because it leads to unspecific amplification.

After designing the primers for multiplex PCR reaction as considering designing parameters, the concentrations of the primers arranged, because higher concentrations of primers can have different effects. Raising the primers concentration is resulted in the creation of primer-dimers or leads to non-specific primer binding. Therefore, raising the primer concentration does not cause an increase in the effective product whereas the low primer concentration generally ensures cleaner product, and lower background.

Several experiments had been done for controlling the designed primers such as single and multiplex form of each HPV 16, 18&RNaseP by the Real time PCR in order to decide, and test the proper as well as correcting forms of primers and cloneDNA types. Then, it has been decided to use primers which were presented in Table 1. Here in, the optimized concentration results of combined HPV types were explained with their PCR plots. First, several dilutions of primers such as 10 uM, 5uM and 2.5 uM concentrations were tested for combined HPV types from  $10^{10}$  to  $10^5$  dilutions for each DNA. After that, it was confirmed on PCR (Figure 2.9 & 2.10). Also, DNA dilutions were changed for arranging the optimal amplification on PCR. While the RNaseP and HPV 16 were added from  $10^7$  to  $10^2$ , HPV18 were added from  $10^{10}$  to  $10^5$  (Figure 2.12). Then,  $10^{10}$  copies/mL combined HPV16,18 and RNaseP PCR amplification plot (Figure 2.11.a). It compared with the single form of HPV18 (Figure 2.11.c), only HPV16&18 (Figure 2.11.b), and RNaseP& HPV18 (Figure 2.11.d).

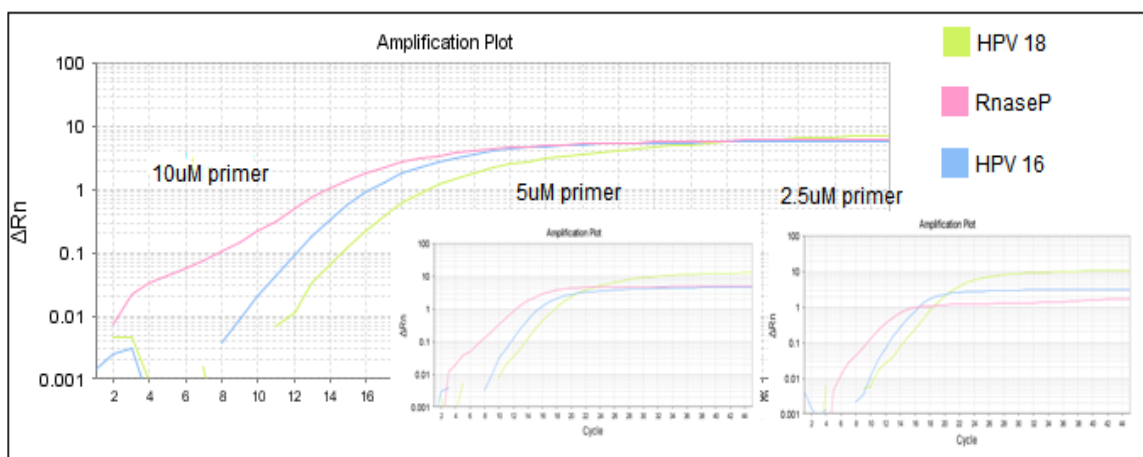


**Figure 2.9 :**  $10^{10}$  copies per mL HPV types for 10,5 and 2.5 uM primer concentrations



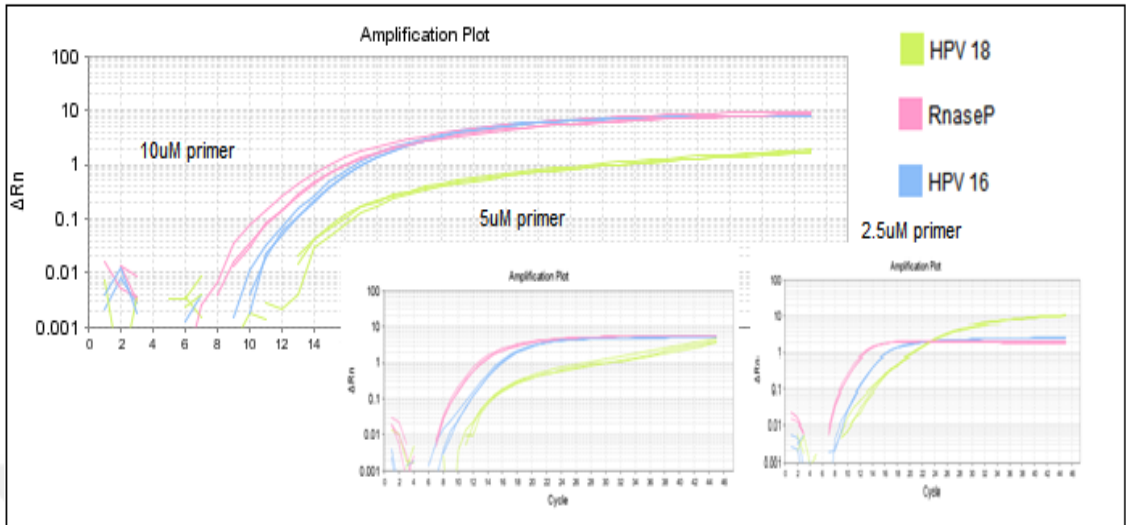


**Figure 2.10 :** Confirmation of  $10^{10}$  copies per mL HPV types for 10,5 and 2.5 uM primer concentrations

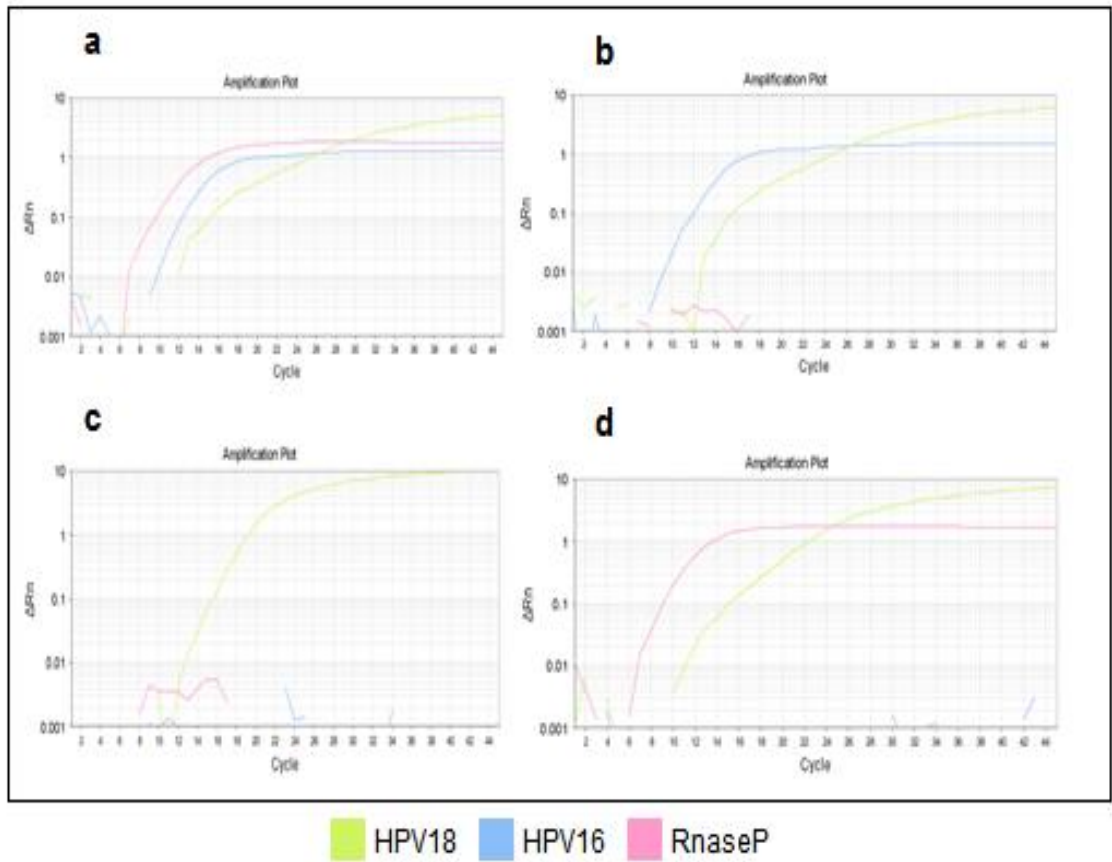


**Figure 2.11 : a,b,c,d**  $10^{10}$  copies/mL HPV16,18 and RNaseP for combined HPV

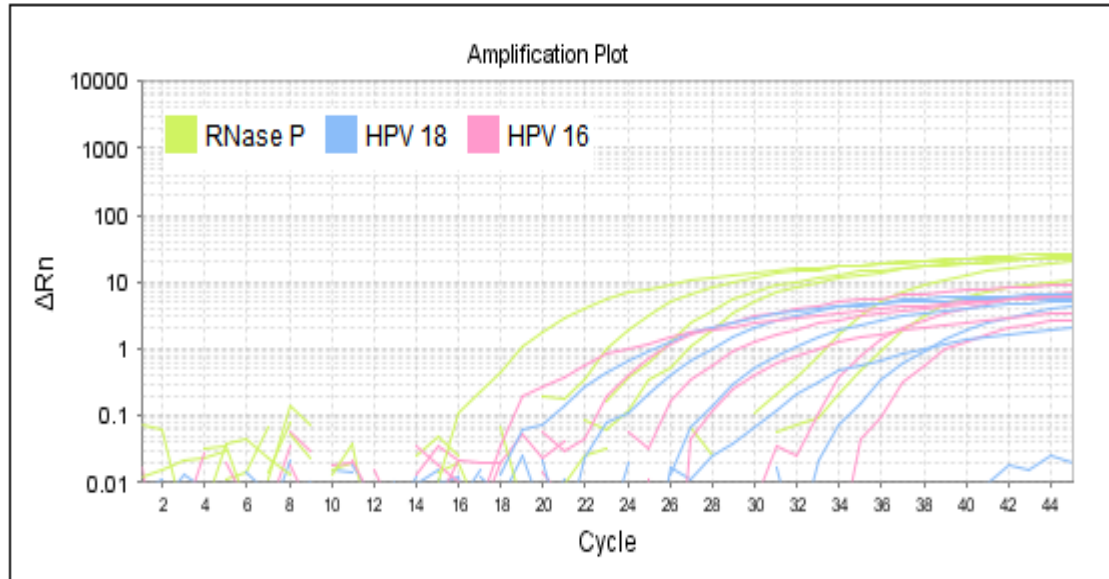


**Figure 2.12 :** RNaseP HPV16  $10^7$  HPV18  $10^{10}$  to RNaseP HPV16  $10^2$  HPV18  $10^5$

All the results were shown above for the optimized concentrations of each HPV primer types. Figure 2.9& 2.10 show that the concentration of HPV 16 and RNaseP primers should be equal at the amount of 2.5uM for optimal saturation. These results also show that HPV 18 could not be saturated together at the same amount of primer. The concentration of HPV primer selected as 10uM for optimum PCR amplification and proper saturation of combined form.

Also, the effect of RNaseP and HPV16 to the HPV18 had been detected as shown in Figure 2.11 for deciding optimal conditions. Finally, dilutions of DNA types were changed in order to understand if the inconvenience HPV 18 plot into the combined form was because of the primer effect or not (Figure 2.12). These results never gave single point saturation because of the multiplex PCR environment. It has been decided to use the same amount of combined HPV form. In addition to this, 2.5uM HPV 16 and RNaseP and 10uM HPV18 were selected as proper primer concentrations. The rest of optimal saturation point for the combined form had been decided to arrange with the temperature arrangement.



### 2.3.3 Effects of DMSO optimization to minimize secondary structures

DMSO (Dimethyl sulfoxide) can be used for inhibiting secondary structures of DNA and also the primers in the PCR reaction (Chakrabarti and Schutt, 2001). It destabilizes double helix structure. It is useful in templates with high GC content (Simon et al., 2009). The increased hydrogen bonds cause more difficulty for denaturing, and resulted to form more readable intermolecular structures for competing with primer annealing (Chakrabarti and Schutt, 2001). Therefore, the addition of DMSO can increase the specificities and yields of PCR. However, it can lead to increase mutation rates to the priming region as a consideration.

Thus, optimization of DMSO in the PCR reaction setup plays a significant role to understand if it can eliminate secondary structures or not. It is undesirable especially for multiplex PCR because of the secondary structures in the DNA result in knotting and folding of DNA primers or template which leads to decreased product yield. 1mM of DMSO was used with two different concentration of MgCl<sub>2</sub> (1,5mM & 4mM) for obtaining the best result with HPV 16, 18 & RNaseP and their combined forms from 10<sup>9</sup> to 10<sup>7</sup> copies per mL (Figure 2.13& 2.14 ).

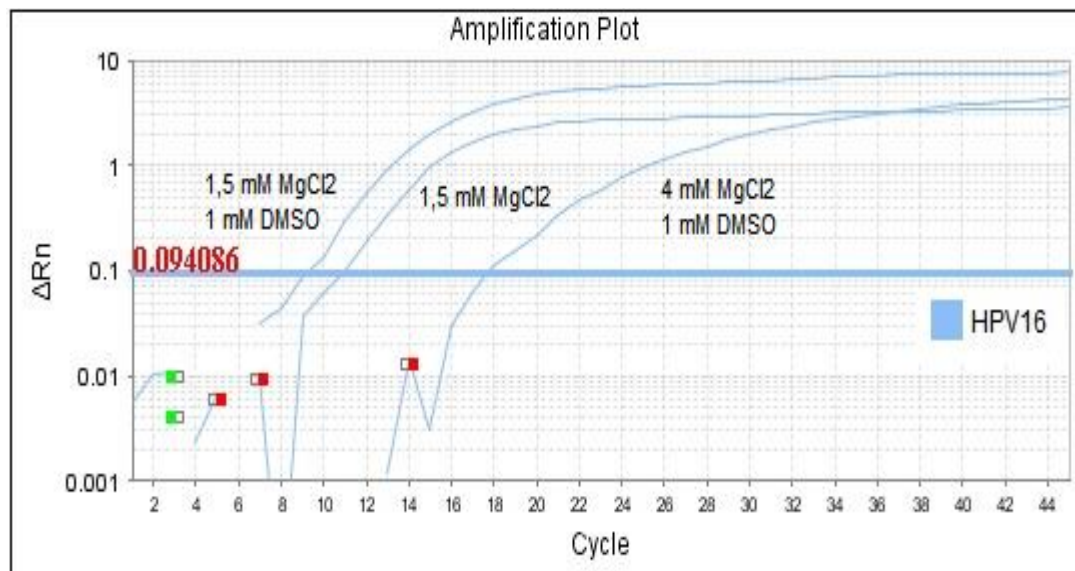


**Figure 2.13 :** HPV 16 amplification result for 1,5mM MgCl<sub>2</sub>&1mM DMSO, for only 1,5mM MgCl<sub>2</sub> and for 4mM MgCl<sub>2</sub>&1mM DMSO

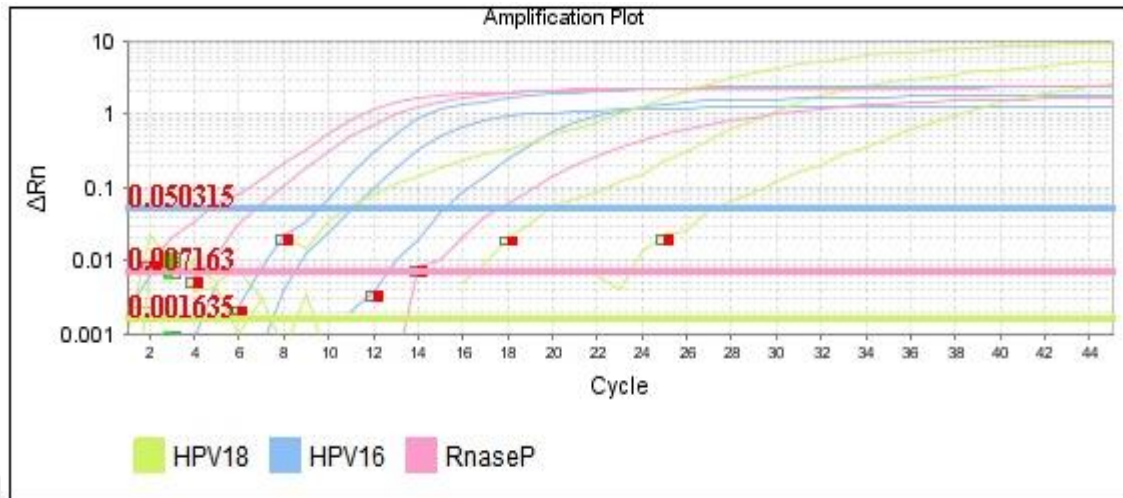


**Figure 2.14 :** Combined amplification results of HPV 16, 18 & RNaseP for only 1,5mM MgCl<sub>2</sub>, for 1,5mM MgCl<sub>2</sub>&1mM DMSO, and for 4mM MgCl<sub>2</sub> from left higher one to right lower.

The results show that using 1mM DMSO caused to increase the yield of HPV 16 for 1,5mM MgCl<sub>2</sub> region. However, adding 1mM DMSO into the 4mM MgCl<sub>2</sub> was decreased the yield of HPV 16 amplification. Also, the amplification yield of HPV 16 was very close to each other for both 1,5mM MgCl<sub>2</sub> and 1,5mM MgCl<sub>2</sub>&1mM DMSO medium, while it was very lower for 4mM MgCl<sub>2</sub> (Figure 2.13). Although, DMSO was contributed to increase the yield of HPV16, and it had not have the same effect for combined HPV 16, 18 & RNaseP (Figure 2.14). When 1,5mM MgCl<sub>2</sub> was used without DMSO, it reached the maximum efficiency compared to the 1,5mM MgCl<sub>2</sub>&1mM DMSO for multiplex form of HPV. 4mM MgCl<sub>2</sub> medium had minimum yield for combined HPV form and especially for HPV 18 (Figure 2.14). Therefore, DMSO was not used for Real-Time PCR reaction setup for combined HPV 16, 18&RNaseP form.

### 2.3.4 Time and temperature adjustment for multiplex PCR amplification

The annealing temperature determines the specificity of the primer annealing to the complementary DNA sequences during a polymerase chain reaction. Specific primer annealing is required for successful DNA amplification. Multiplex PCR amplification also needs optimal conditions in order to prevent nonspecific annealing. Due to the wrong temperature and extension time primers, it can anneal with the non-complementary sequences.

The specific and nonspecific annealing of the primer molecules maintenance is very important to carry on successfully PCR amplification. Annealing of primer molecules largely depends on annealing temperature. The optimal primer annealing temperature is dependent on several reasons such as the base, primer concentration, and ionic reaction environment.

Annealing temperatures for each of the primer sets optimized for multiplex PCR for achieving the successful amplification results of combined HPV form. Extension time is arranged for larger PCR products. The number of cycles had been increased because of the low amount of template DNA.

Thus, arranging the optimal temperature, time and cycle of PCR is very significant for preventing nonspecific annealing of the primers. The optimal conditions also cause to increase the PCR amplification amount of DNA. The multiplex form also requires very specific working parameters such as time, and temperature because of the different DNA and primer environment. According to these reasons, different time conditions and temperatures are tested for combined HPV 16, 18&RNaseP as multiplex DNA form. Some of them have been shown only below to present how the conditions affect the annealing, and increasing of the combined HPV DNA forms.

The number of cycle has a significant role for getting higher amplification results from the lowest concentrations as low as  $10^4$  mM of multiplex forms. It has been proved with Figure 2.15 as using 20 number of cycle. And, it was getting lower amounts such as from  $10^9$  to  $10^7$ . Variable annealing temperatures such as 52°C, 54°C and 55°C had been tested as annealing temperatures for 30 seconds period together with 95°C initial denaturation during 10 minutes. It is denatured at 95°C denatures for 30 seconds, and it has been read at 60°C for 1.5 minutes (Figure 2.16, 2.17, 2.21).  $10^9$  to  $10^4$  mM DNA concentrations were used during the changing of annealing temperature experiment. In addition to this, 55°C and 60°C annealing temperatures were tested in 1 minute annealing time condition for different denaturation times such as 45 seconds, and 15 seconds respectively (Figure 2.18, 2.19). These results are also compared with Figure 2.16 which has 55°C annealing temperature for 30 seconds and 95°C denaturation temperature for 30 seconds. The initial 95°C denaturation and 60°C reading

temperatures had been pegged for 10 minutes, and 1 minute respectively for Figure 2.18, 2.19 and 2.20. Figure 2.19 and 2.20. It also showed that the amplification results of HPV DNA types were affected different because of the non-combined form conditions during cycling in the various temperature medium. Finally, 95°C initial denaturation for 10 minutes, 30 seconds 95°C denaturation time and 30 seconds 55°C annealing temperature conditions used, and compared with the 60°C reading time for 1 minutes and 1.5 minutes conditions. The resulted 1.5 reading time showed in Figure 2.20.

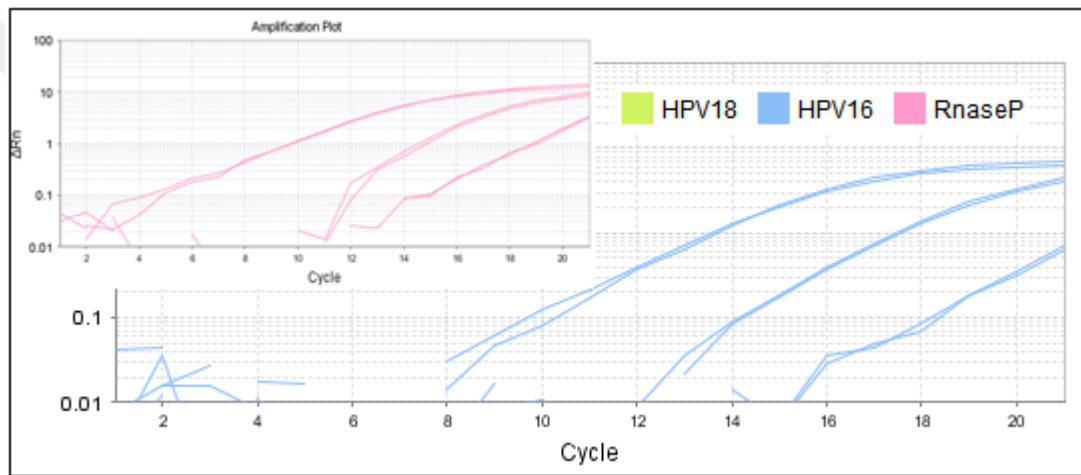


**Figure 2.15 :** HPV 16 and RNaseP for  $10^{10}$ ,  $10^9$ ,  $10^8$  cp/mL DNA because  $10^7$ ,  $10^6$ ,  $10^5$  could not show 20 cycle (hpv 18 did not show because its)

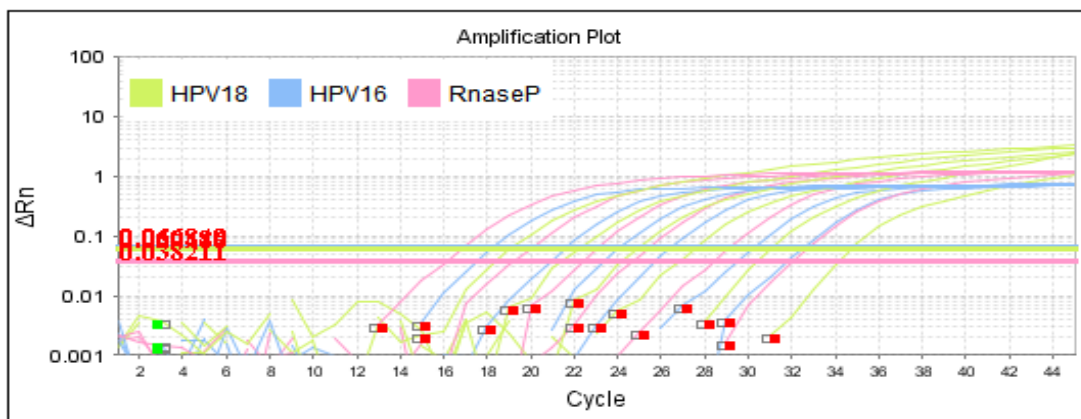


**Figure 2.16 :** 54°C Temperature annealing (extension) for DNA from  $10^9$  to  $10^4$  cp/mL amounts of combined HPV16,18 and RNaseP

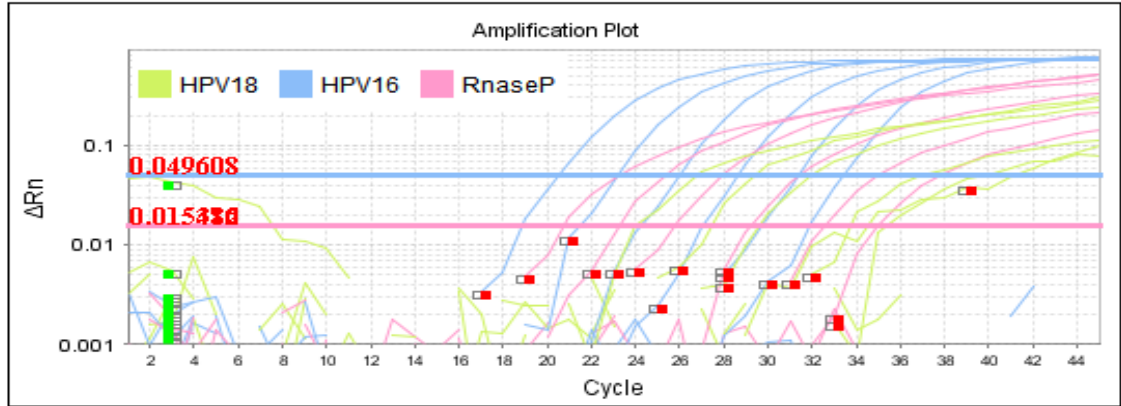


**Figure 2.17** : 52°C Temperature annealing (extension) for DNA from  $10^9$  to  $10^4$ cp/ml amounts of combined HPV16,18 and RNaseP

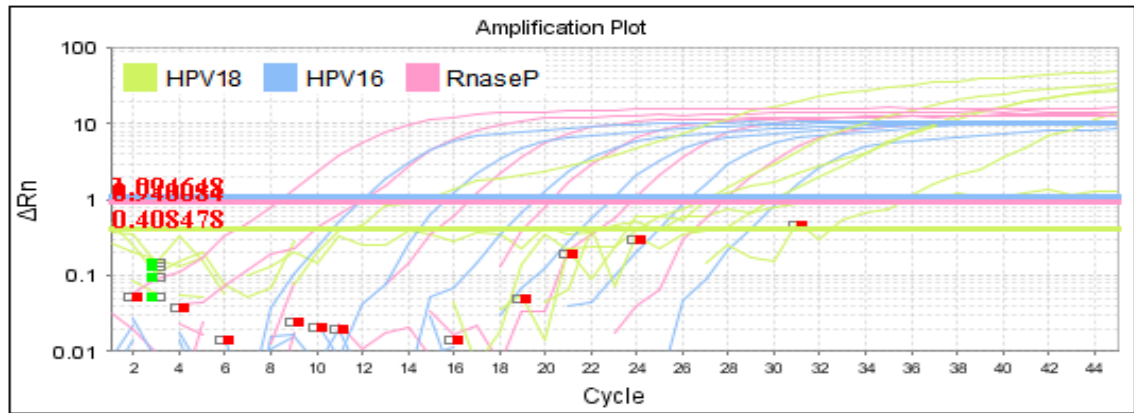


**Figure 2.18** : 55°C 30s annealing time, 45s denaturation and 1 min. 60°C reading time for  $10^{10}$  to  $10^5$ cp/mL combined HPV DNA

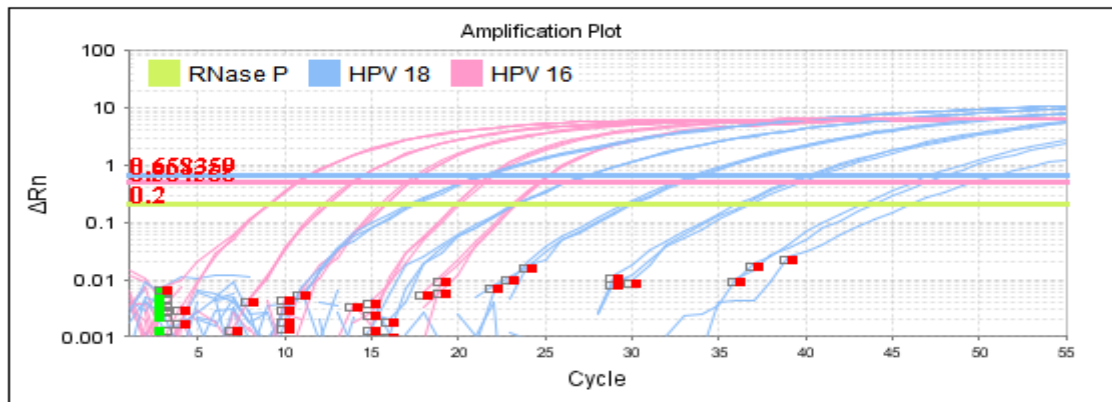


**Figure 2.19** : 60°C 30s annealing time, 15s denaturation and 1 min. 60°C reading time for  $10^{11}$  to  $10^7$ cp/mL combined HPV DNA

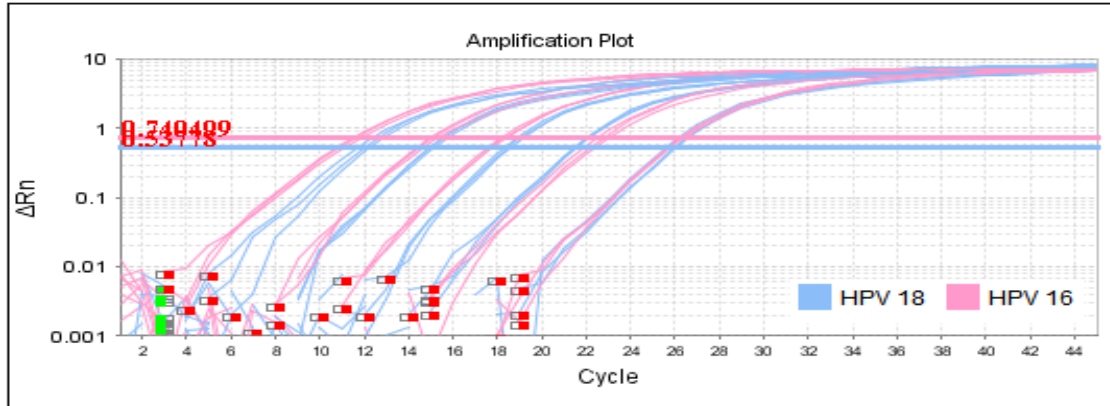


**Figure 2.20 :** Separately amplification of HPV 16 and HPV 18 from  $10^{11}$  to  $10^7$  cp/mL concentrations at 55°C annealing and 1.5 min reading time

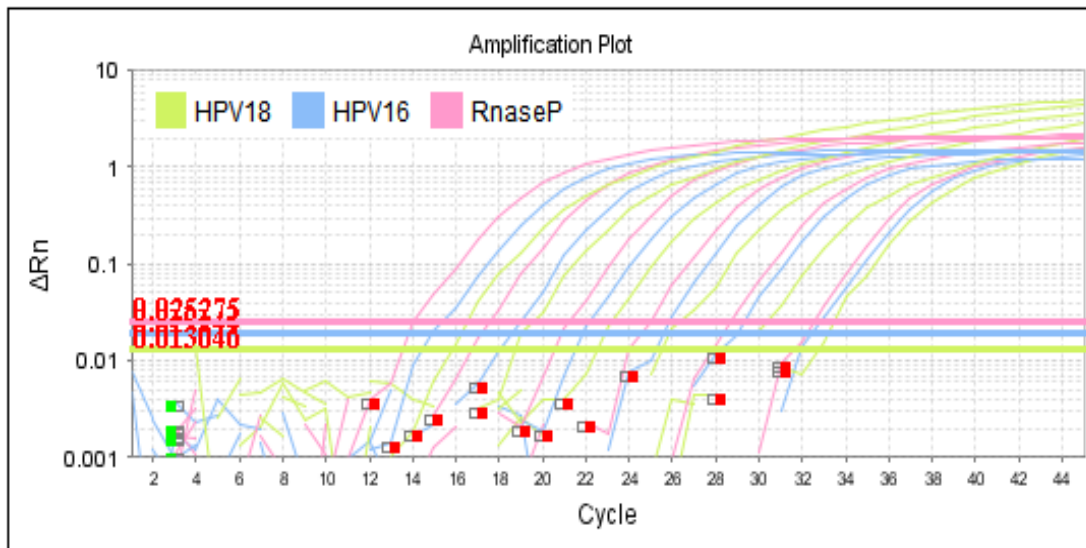


**Figure 2.21 :** Combined form of HPV amplification from  $10^9$  to  $10^4$  cp/mL concentrations at 55°C annealing and 1.5 min reading time

Briefly, the number of cycle should be about 45 for the multiplex combined HPV DNA form. The lower DNA concentrations such as  $10^7$ ,  $10^6$ ,  $10^5$ , and  $10^4$  cp/mL had not been amplified as using only 20 cycles (Figure 2.15). Also, 52°C and 54°C annealing temperatures did not saturate as expected compared to the 55°C for the concentrations of combined HPV16, 18&RnaseP from  $10^9$  to  $10^4$  cp/mL in same denaturation and reading time in temperature conditions (Figure 2.16, 2.17, 2.21). In addition to this, the annealing time is increased from 30 seconds to 1 minute for 55°C and 60°C with 45 seconds, and 15 seconds denaturation time respectively. 1 minute at 60°C same reading

time did not give a smooth saturation point especially for HPV18 (Figure 2.18, 2.19). Another important point is that using the same annealing time with the combined and separate form of HPV 16 and 18 resulted in giving extremely different cycling and amplification results which are shown in Figure 20 and 21. It is the significant proof of multiplex PCR amplification complication. Table 2.2 shows the last denaturation, the extension and reading time as well as the temperature for maximum amplification of each DNA types. The performance was evaluated in the presence of Rox reference dye on an Applied Biosystems 7500 real-time thermal cycle. The resulted PCR amplification plot is shown in Figure 31 for the concentrations of combined HPV from  $10^9$  to  $10^4$  mM.

Phsn PCR Reaction Conditions	Condition	Temperature	Time
Cycle	Initial denature	95	10 (min)
	denature	95	30 (s)
Cycles = 45	extension	55	30 (s)
	read	60	1.5 (min)
	Store	4	$\infty$

**Table 2.2.** The last denaturation, extension and reading time and temperature for maximum amplification of each DNA types.

### 2.3.5 Cloned DNA and agaros - acrylamide gel confirmation

The etiological agent of cervical cancer is E7 gene for HPV 16 and 18 which were used for TaqMan optimization and all confirmation and comparing experiments. They were listed in Table 2.1. These E7 genes have been cloned for preparing HPV DNA stocks



using Pgem-T Easy Vector system (Appendix 1) They are confirmed by using GeneWiz, Inc. These plasmids have been optimized separately and combined form of it to make sure the conditions and reagents work properly for comparing to the patient sample.

The reaction quality, and the yield of PCR products can be analyzed with gel electrophoresis as a standard method. PCR amplifications products are generally range up to 10kb however majority are about at 1kb which can be most effective for Polyacrylamide Gel Electrophoresis Analysis.

The Polyacrylamide Gel Electrophoresis and Agarose Gel analysis are preferred according to their purification need for the size range from 400 to 1000 bases. Agarose is more suitable for purification. The size of the product reveals with the electrophoresis. It also shows the quantity of the predicted band and nonspecific amplification products.

The amount of cross-linker is very important for giving optimal pore sizes according to the desired DNA size while the polyacrylamide gel are prepared. Ethidium bromide is often used for staining. It has been used both agarose and polyacrylamide gel during the cloning of HPV types and PCR confirmation steps. These are the amount of chemicals and polymeric materials for the both types of gel below.

%10 acrylamide gel had been prepared as using 4mL %30 acrylamide, 5.6mL milipore water, 2.4mL 5xTBE. After that, 200 $\mu$ L APS and 10 $\mu$ L TEMED were added and mixed by inverting 5 times. The gel are polymerized in 10 minutes. After that, 1xTBE buffer added to the reservoirs and DNA added to the wells as diluting 5:1 with ficoll blue dyes. Finally, the ladder is added to the well, and the gel run at 100V for 2 hours. The gel should be stained with 3 $\mu$ L SybrGreen in 30mL of TBE buffer for 30 minutes before imaging on Versadoc gel imager.

%2 agarose gel used for the experiments, and prepared using 2g agarose per 100mL 1xTAE buffer as microwaving 1.5 minutes with the shaking periodically. The bottle was cooled, and 6 $\mu$ L ethidium bromide was added and mixed. The mixture was poured without bubble into the gel box and waited about 30 minutes for polymerization. After polymerization the DNA, ladder was filled to the wells in the ratio of 5:1 ficoll. All the



gel was covered as pouring 1xTAE buffer and run at 100V for 1 hour. The results are taken via Versadoc gel imager system.

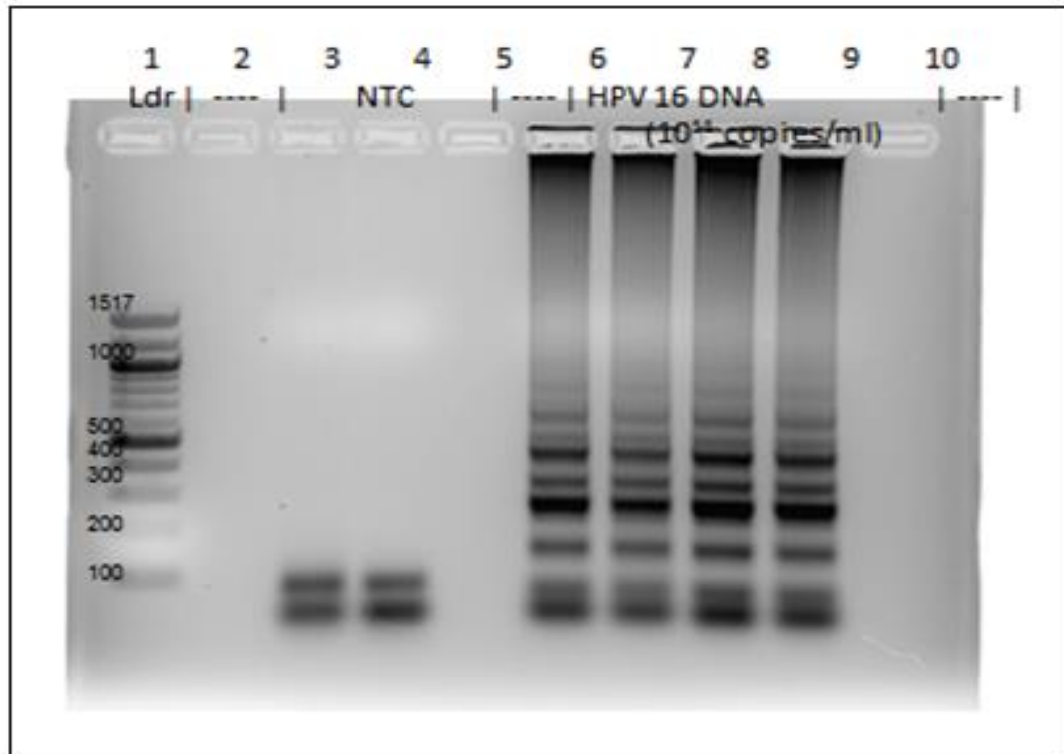


**Figure 2.22 :** 10<sup>11</sup> copies/mL HPV16 DNA with negative template control

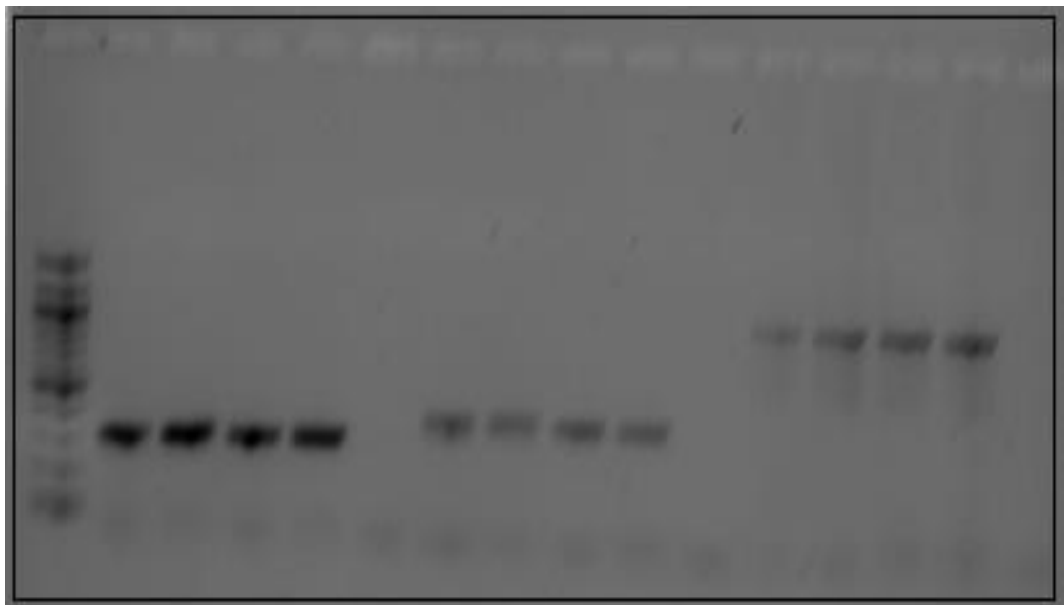


**Figure 2.23 :** HPV16,18&Rnasep cloning with blue dye

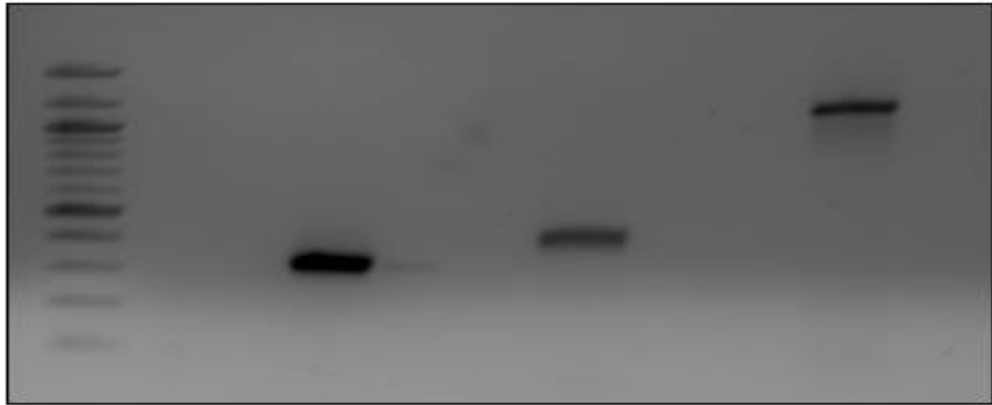


**Figure 2.24 :** HPV16, 18&Rnasep cloning and gel extraction

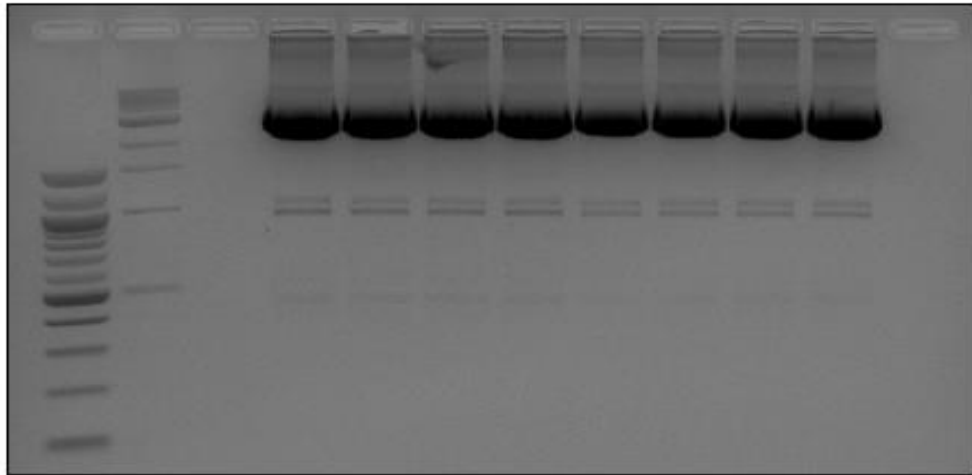


**Figure 2.25 :** HPV18 Midi prep digest after gel extract with 100bp Ldr and 1 kB Ldr for HPV18-1x4, HPV18-2x4

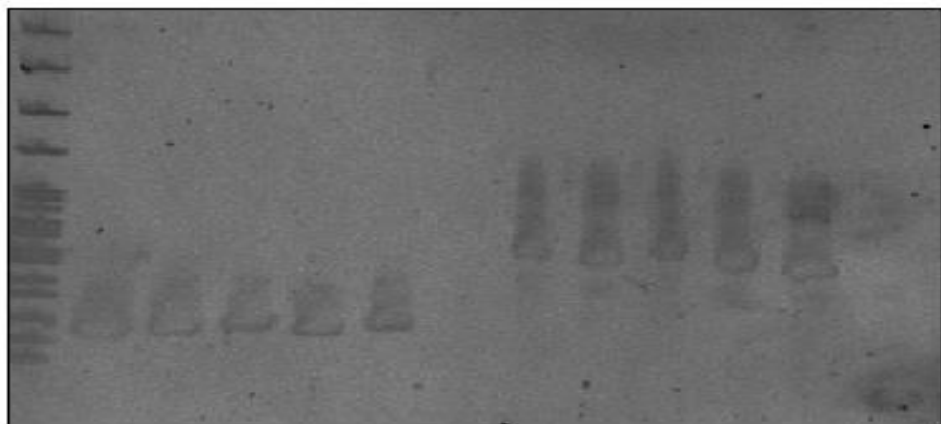


**Figure 2.26 :** HPV16 and 18 calibrations



**Figure 2.27 : RNaseP PCR product**

The ladder and comparison form of DNA was run on the same gel as a result of the higher yield with the single strong band of correct sizes. Identities were confirmed with the restriction enzyme. All unexpected bands were identified as running without substrate as a control reaction.  $Mg^{++}$  amount also has been adjusted according to these results for preventing primer-dimer. In addition to this, multiple bands were detected for the PCR products for eliminating them, and the hybridization temperature was arranged as raising it. Furthermore, the identified incorrect amplification was eliminated in order to reduce the primer concentrations. The target bands had been cut and purified very well.

The gel result of  $10^{11}$  copies/mL HPV16 DNA with negative template control showed in Figure 2.22 HPV16, 18&Rnasep cloning image with blue dye and the extraction of them were presented by Figure 2.23 and 2.24. After that, sHPV18 Midi prep digested after gel extraction with 100bp Ldr (Ladder) which is shown in Figure 2.25. 1 kB (kilobyte) Ldr for HPV18-1x4, HPV18-2x4. HPV16, 18 and RNaseP PCR product calibration confirmed with Figure 2.26 and 2.27.

### 2.3.6 Dilution test for combined HPV16, 18 & RNaseP for optimal conditions

RNaseP the minimum detection limits were determined from the literature after finishing all the optimization parameters for detection of combined HPV16,18. According to Y.Xu et.al. Anal. Chem. in 2014 the detection limit of HPV 16 is 10 kilobyte and the detection limit of HPV 18 is  $10^2$  cp/ $\mu$ l (Xu et al., 2014). They are all separated to form of HPV. Regarding to C.P. Chan et. Al. ICO in 2014 the combined detection limit of HPV 16 and HPV 18 are  $10^3$  cp/ $\mu$ L (Chung et al., 2015). These information clarified the target aim a direction for determination of HPV types. It is important because they have been used for all the future experiments such as extraction and detection of patient samples. The detection limits should be preferred as their single form, because patient samples have unknown HPV types. The HPV 16 and 18 should be detected at least 10cp/ul ( $10^4$ cp/mL).

The dilution tests have been done for combined and separated form of HPV 16,18, and RNaseP. From  $10^{11}$  to  $10^2$  for determine the target DNA copies in the literature, they are all showed below in Figure 2.28, 2.29, and 2.30 All of the tests have been carried out with the DNA and primers of HPV16, 18 and RNaseP which were shown in Table 2.1 as using all optimized reagents in Table 2.3 with the time controlling steps in Table 2.2. It has been achieved the minimum determined limit  $10^4$ cp/mL DNA for combined HPV form in Figure 2.31.

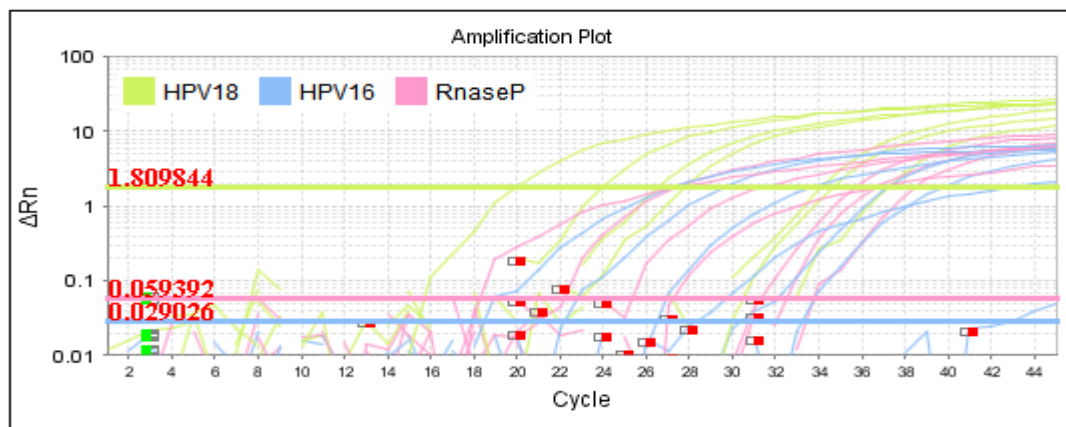


**Figure 2.28 :** PCR amplification plot for  $10^7$ cp/mL of RNaseP & HPV 16 and  $10^{10}$ cp/mL HPV18

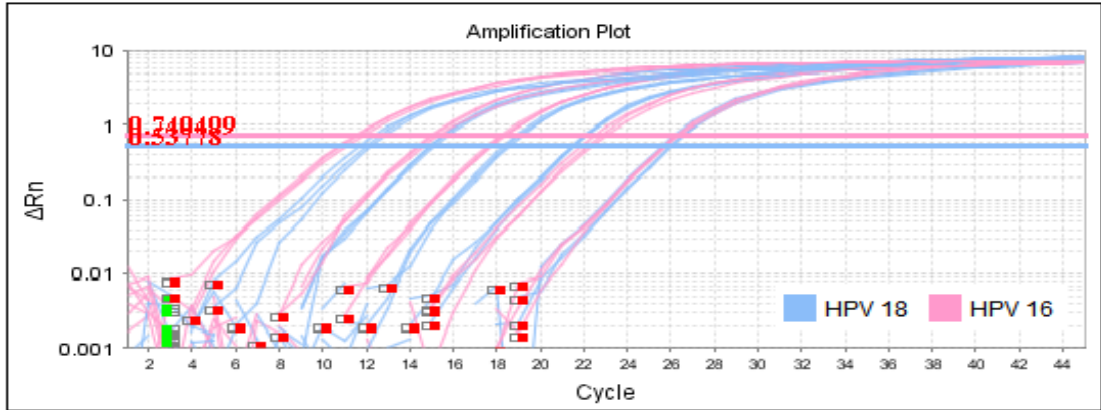


**Figure 2.29** : PCR amplification plot of HPV 16 and 18 for  $10^{11}$  to  $10^7$ cp/mL DNA

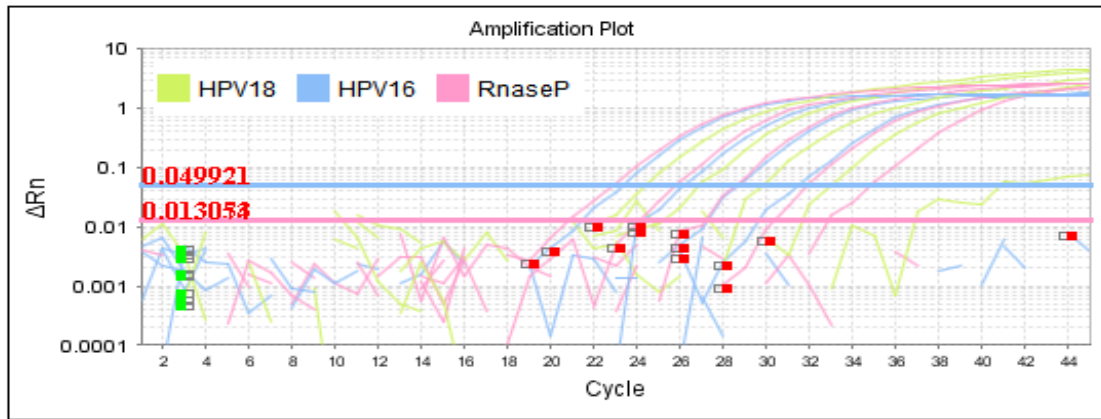


**Figure 2.30** : Combined form of HPV amplification from  $10^7$  to  $10^2$ cp/mL concentrations

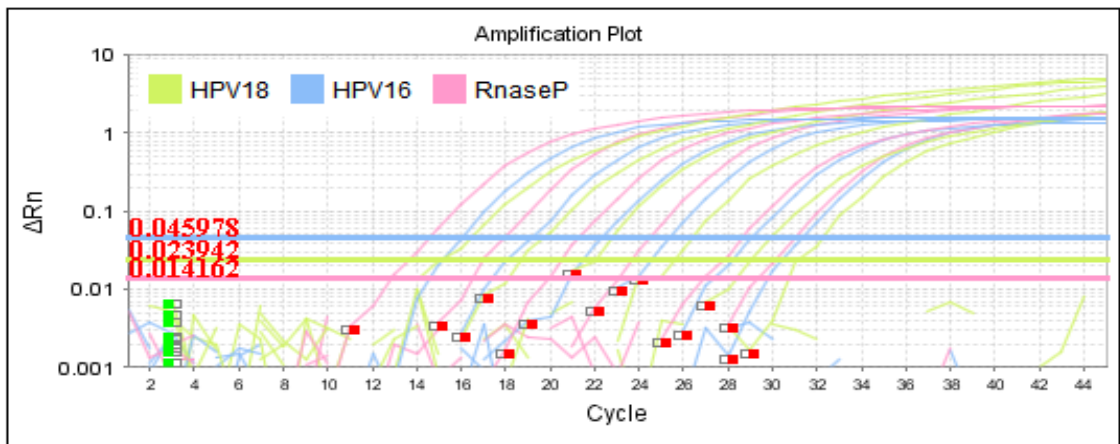


**Figure 2.31** : Combined form of HPV amplification from  $10^9$  to  $10^4$  cp/mL concentrations

<b>Reagent</b>	<b>Final concentration</b>	<b>Actual Rxn (25ul Vol)</b>
<b>Nuclease-free H<sub>2</sub>O</b>	----	10.375
<b>10x TaqMan Buffer</b>	1 X	2.5
<b>MgCl<sub>2</sub>(50mM)</b>	3.5 mM	1.75
<b>dNTPs (10mM)</b>	200 uM	0.5
<b>HPV16 uF primer(0.25uM)</b>	200 nM	0.5
<b>HPV16 R Primer(0.25uM)</b>	200 nM	0.5
<b>HPV16 Probe (0.25uM)</b>	200 nM	0.5
<b>HPV18 F primer(10uM)</b>	200 nM	0.5
<b>HPV18 R Primer(10uM)</b>	200 nM	0.5
<b>HPV18 Probe (10uM)</b>	200 nM	0.5
<b>RNaseP F primer(0.25uM)</b>	200 nM	0.5
<b>RNaseP R Primer(0.25uM)</b>	200 nM	0.5
<b>RNaseP Probe (0.25uM)</b>	200nM	0.5
<b>ROX reference Dye (1/10x)</b>	0.1X	0.25
<b>Taq Polymerase (5U/ul)</b>	0.025 U/ul	0.125
<b>Total</b>	0	20
<b>DNA template</b>	Conc.	H <sub>2</sub> O (ul)
<b>gDNA (0.5 ng/ul)</b>	0.5 ng/ul	0
<b>H<sub>2</sub>O only</b>	0	5

**Table 2.3.** Optimal reagents concentrations for combined HPV 16,18 and RNaseP amplification via TaqMan reaction setup

## 2.4 Summary and Future Works

DNA primers for HPV16 and 18 have been investigated and published previously. It has been developed an optimal assay. And, it is used as a starting point. The E7 genes which are used in the experiment, for HPV 16 and HPV 18 , are listed in Table 2.1.

HPV DNA stocks have been prepared by cloning the E7 genes for HPV 16 and HPV 18 using the Pgem-T Easy Vector system and they confirmed using GeneWiz, Inc.

These plasmids have been used as the HPV DNA standards for TaqMan optimization. The separately and combined form of HPV DNA is optimized to make sure the conditions and reagents work properly for comparing to the patient sample.

The efficiency, and specificity of the TaqMan reaction were optimized by variety concentration of MgCl<sub>2</sub>, dNTPs, and primers (Zhang et al., 2005). Serial dilutions of each reagent were tested in order to determine the optimal concentration for maximum amplification. Table 2.2 shows the last decided concentrations of the reagents, and the primers.

Temperature and reaction time are also optimized for the specificity and efficiency of the TaqMan reaction. Table 2.3 shows the last denaturation, extension and reading time and temperature for maximum amplification of each DNA types. The performance was evaluated in the presence of Rox reference dye on an Applied Biosystems 7500 real-time thermal cycle.

The validation of the PCR reaction has been done with Agarose Gel method. It is required 1.5 g of ultrapure agarose, and 100 mL of 1x TAE buffer for a larger agarose gel. The gel was microwaved for 2 minutes until solution seems clear. After flask is cooled to touch, 5 µL Ethidium Bromide has been added directly into flask. The gel was poured into the tray avoiding bubbles. It has been polymerized at room temperature for 30 minutes.

NEB 100bp ladder and DNA loading Dye with Ficoll at 1:5 ratios were added into the appropriate lane which is covered 1xTAE buffer. Then, the leads were attached, and connected to power supply. It was run for approximately one hour under 100 V. Quantity One system was used for imaging the gel.

### **3. CHAPTER: FABRICATION OF PAPER TIP EXTRACTION SUPPORT MATERIAL AND DEVELOPING SINGLE STEP EXTRACTION BUFFER**

Human Papilloma Virus types 16 and 18 are the main risk factors of cervical cancer. As known before, it can be cure highly in the early stages. The Pap smear test is one of the most common methods for detection of cervical cancer . Unfortunately, it has low sensitivity and specificity. The Pap smear test is also required highly trained pathologists and proper laboratory environment. Thus, it is highly requirement to develop inexpensive, robust screening tool which improves the detection quantity and quality of HPV.

The low cost POC device should be done the extraction part cheaper and easily for lysis and purification of DNA. There are so many researches for sample in, answer out microfluidic systems which eliminate sample storage and later date results (Chin et al., 2013; Lee et al., 2008; Niemz et al., 2011). Although, these systems have impressive capabilities, and they may not be applicable to all settings. Most of them require upstream instrumentation and sample preparation which are extremely inconvenience and expensive. The requirements of those methods are generally include additional downstream purifications.

The ideal POC sample preparation technology should be able to purify DNA without permanent instrumentation, temperature sensitive reagents, trained operators and electricity (Niemz et al., 2011; Puren et al., 2010; Yager et al., 2008). In this sense, microfluidic paper extraction support material alternative to the solid phase extraction techniques for DNA purification. It has been used for a fully integrated nucleic acid detection system which combines the extraction, amplification and detection steps. The simple paper-based extraction support material requires only chromatography paper, pipette tips, a pressure manifold. Herein, first, fabrication of the extraction support material had been done. The flow rates of the paper tips have been determined. Then, the paper support filters cells from HPV sample followed by elution to the DNA types for using in the detection platform of the paper analytical device. The eluted DNA types were tested on qPCR to determine the LOD of HPV16, 18 and RnaseP. Finally the optimized extraction process applied to the patient samples and controlled with the real



time PCR and gel electrophoresis method. The paper based detection platform also was explained in the device fabrication chapter. The entire process with the paper based sample to detection performs in less than 1 hour.

### **3.1 Introduction**

#### **3.1.1 Extraction of DNA**

DNA extraction is the separation of deoxyribonucleic acid from the viruses or cells. Diagnosis of diseases, and genetic disorders depend on the detection of the DNA which is released from the related bacteria or viruses. There are several methods for DNA extraction in the literature. Some of them are presented below as a predicting that they are not limited only with these techniques.

One of the extraction methods for bacteria is Fluorescence in Situ Hybridization (FISH). It is a molecular technique for identification of specific bacterial groups. Terminal Restriction Fragment Length Polymorphism (T-RFLP) is another method which can quantify patterns in bacteria-plankton communities. Sequencing also can be given as an extraction method example. It is used for comparison of existing sequence as sequencing portions or whole genomes (Green and Sambrook).

Basic DNA extraction consists of six steps which are described here. First, the virus or cells which contain the target nucleic acid are lysed. The breaking open process is often done by sonicating or bead beating the sample. Heated phenol uses while vortexing the sample for lysing the cellular walls and viral capsids. The breaking down process continues with removing the lipid membranes as adding SDS (sodium dodecyl sulfate) detergent. The cellular and DNA associated proteins precipitated as adding protease enzyme. The yield of the precipitation are increased with the addition of ammonium or sodium acetate salt. The proteins are drawn off from the remained organic phase via centrifugation of the phenol-chloroform mixed sample. After that DNA at the interface is precipitated and centrifuged in the medium of cold ethanol or isopropanol because DNA is insoluble in the alcohol. It can easily come out of solution now. The alcohol also provides a washing ability to remove the previously added salt. The resulted DNA is washed with the alcohol again for recovery. The dried alcohol off pellet re-suspended

with the Tris or TE buffer. Finally the presence of DNA is confirmed with several methods such as qPCR (quantitative PCR) and gel electrophoresing. During the extraction some instruments use for lysing, separating phases and precipitation such as bead beater and centrifuge (Green and Sambrook).

### **3.1.2 Solid phase extraction**

Solid phase extraction (SPE) provides a proper surface for the nucleic acids which obtain from lysed samples to bind. The remained salt and proteins simply remove from the environment with the washing steps. Then, the bonded DNA can be eluted with very small volume. Most of approaches include silica solid phases for nucleic acid binding. They all provide high affinity binding conditions in a single step as lyse cells and denature proteins. SPE techniques use homogeneous solutions in the extended different liquid extraction techniques which are more compatible with automation and miniaturization. The commercially available SPE solutions currently are not compatible for POC technology directly (Dineva et al., 2007).

There are various of solid phases such as packed beds of silica particles (Hagan et al., 2008; Tian et al., 2000) patterned silicon surfaces (Cady et al., 2003), organic polymer monoliths with immobilized silica particles (Bhattacharyya and Klapperich, 2006; Bhattacharyya and Klapperich, 2008; Chatterjee et al., 2010; Mahalanabis et al., 2009), sol-gels and sol-gel immobilized silica beads (Bienvenue et al., 2006; Breadmore et al., 2003; Wolfe et al., 2002; Wu et al., 2006) and functionalized surfaces (Wen et al., 2006; Wen et al., 2007) for purification of nucleic acids with the microfluidics. The organic porous monoliths seem like that it has more benefit for in-situ fabrication because of the feature of most compatible and inexpensive. However, these processes show limited compatibility with unprocessed samples in contrast to the aims of POC sample preparation technology such as minimization of infrastructural and operator requirements while maintaining a clinically relevant limit of detection in finger prick compatible volumes of samples.

SPE adaption to the POC technology also has some other challenges such as arranging the binding capacity of the target analyte on the surface of the solid phase as increasing the scales for effective capturing capacity which fully related to increase of the fluidic

resistance of the system. The main idea of POC device is to minimize the solid phase geometry, transmissivity, operating pressure, sample volume, and assay run time. Then the POC can be compatible with the low pressure SPE process.

The large amount of DNA is a huge problem for adaption of SPE as a POC device. The outnumber nucleic acids in biological samples reduces capturing efficiency and by the way it dramatically reduce the extraction efficiency of microfluidic SPE systems (Breadmore et al., 2003; Hagan et al., 2008; Wen et al., 2006; Wu et al., 2006). The problem of many SPE techniques can be solved by using proteinase K enzyme for digestion of denatured proteins after lysis of the samples. However, it causes additional incubation steps which raise the complexity and the cost of the technologies. An alternative developed by Wen et al. (Wen et al., 2007) to capture hydrophobic proteins from the sample followed by downstream tetra-methyl ortho-silicate grafted organic polymer monolith as capturing DNA using two column system. These upgrades still could not improve effectively for whole capacity of the system. Thus, another approach built up by Cao (Cao et al., 2006) and Hagan (Hagan et al., 2008; Hagan et al., 2009) which explains the pH dependent capture of DNA with the using of chitosan solid phase displayed for increasing the compatibility of the samples. This method also includes limitations because of the stabilization and storage of samples. The high pH conditions required for elution have been shown to rapidly degrade RNA through hydrolysis (Komiya et al., 1999).

According to those limitations in SPE, a novel method developed in our laboratory for the nucleic acids extraction from whole sample compatible in the room temperature ambient with non-enzymatic and low pressure needs. This solid phase extraction process provides alcohol precipitation of DNA with the help of glycogen carrier particles for increasing the effect of hydrodynamic radius of precipitated nucleic acids aggregates. This platform provides the nucleic acids to store at room temperature.

### **3.1.3 Paper based extraction**

POC devices would provide both enhanced sensitivity and faster turn-around-time to improve sample detection and treatment. There is not developed any disposable paper-

based devices for analytical HPV detection which combine the extraction, amplification and detection steps required for integrated nucleic acid detection system.

Polymer solid phase extraction materials have been developed as point of care sample preparation in the literature for the extraction and purification of DNA (Kulinski et al., 2009; Wolfe et al., 2002). The Klapperich Lab also developed a DNA purification SPE method as described in previous title (Byrnes et al., 2013). However, the fabrication of this micro solid phase extraction column has some requirements which are make the process more cost and inconvenient because of the requirements such as extensive polymer chemistry expertise to enable the precise control over porosity and flow-rates necessary to ensure nucleic acid capture.

Govindarajan et al. used a paper based method for lysis of E.coli as using syringe based extraction after the isolation process of DNA (Govindarajan et al., 2012). The paper based device have been previously used by Rohrman et al. for only amplification of HIV-1 RNA but the extraction of the nucleic acid have been carried out via traditional bench top methods (Rohrman and Richards-Kortum, 2012).

The paper devices generally have been used in the literature for amplification and detection of nucleic acids. Thus, there is a significant need to develop a low cost simple fabricated extraction tool which is connected to the detection tool. This extraction support material utilizes rapid prototyping method requires only chromatography paper, pipette tips and a pressure manifold. Our lab has also developed a chemistry-based method for a single-step lysis and glycogen precipitation of nucleic acids onto paper supports. The single-step extraction buffer includes both a lysis and a purification buffer.

The detection limit is very important parameter for extracting the proper amount of DNA from paper support material with the help of the single step chemistry based method which requires no centrifuge, and no enzyme during the process. It can be completed in less than 30 minutes. The following paper based detection method depends on electrochemical detection. Therefore, LOD (limit of detection) limits should be determined from the literature according to this (Table 3.1).

<b>Electrochemical Limit of Detection</b>	HPV-16	0.22 nM	57
	HPV-16	18 nM	58
	HPV-16	4 nM	60
	HPV-18	0.17 nM	57
	HPV-16	0.49 nM	63

**Table 3.1.** The LOD of HPV 16 AND 18 in the literature

Approaching to detection limits from copies amount are also should be determined. According to Y.Xu et.al. Anal. Chem. in 2014, the detection limit of HPV 16 is 10 cp/ul and the detection limit of HPV 18 is 102 cp/uL. They are all for separate form of HPV. According to C.P. Chan et. Al. ICO in 2014, the combined detection limit of HPV 16 and HPV 18 are  $10^3$  cp/uL.

### 3.2 Experimental

Here in, it has been presented the development of DNA extraction requiring only chromatography paper, pipette tips, and a simple pressure manifold that can be assembled in minutes. The DNA extraction technique is compatible with both downstream PCR amplification of DNA. Many laboratories do not have the equipment or expertise to perform polymer synthesis needed for many DNA purification process. It has been developed a paper based sample preparation platform that greatly simplifies DNA extraction process for HPV.

HPV is the etiological agent of cervical cancer. It is e known that most common cancer risk types of HPV are 16 and 18. They can both found together or separately in the sample. The provided detection device has been designed according to the combined and separate form of HPV16 and HPV18. Thus, it is a requirement to extract both HPV DNA types from the real patient samples. The quantity of HPV 16, 18 and RnaseP are determined with real time PCR and gel method after extraction. All parameters are

controlled for cloned known DNA concentrations for comparison of patient sample extraction.

The paper extraction support material was fabricated and their flow rates were determined as using a simple pressure manifold. Then, the proper tips had been chosen according to the most extracted DNA yield and minimum time for POC application.

The single step lysis and purification buffer which had been developed in our laboratory is optimized, and developed for combined HPV extraction. The resulted extracted DNA amounts were tested for tip extractions, tube extraction and flows through. The resulted DNA amounts were compared with the commercial Qiagen extraction kit for patient samples. All results are quantified with qPCR, gel and Nanodrop.

### **3.2.1 Making paper extraction supports**

In this part, paper extraction support material is used which had been developed in our lab to lyse and extract DNA from HPV. It takes approximately 20 hours to assemble polymer extraction support material. It takes only 10 minutes to assemble a paper extraction support material, this method were adapted to lyse, and extract DNA from cervical cells using a flow-through paper reaction matrix developed in our lab. The paper-based nucleic acid extraction setup that utilizes rapid prototyping methods requires only chromatography paper, pipette tips, a compressing rod, and simple pressure manifolds.

First, 3MM CHR (chromatography) paper was cut into triangles, rolled and placed into 200uL pipette tips. The paper supports were then compressed into the pipette tips using a 0.0055cm steel rod (Figure 3.1, 3.2). To determine flow rates of paper supports, pipette tips were placed in a pressure manifold built in-house and 300μL of 70% ethanol was pushed through the paper supports at 20 psi (Figure 3.3) (Linnes et al., 2014).

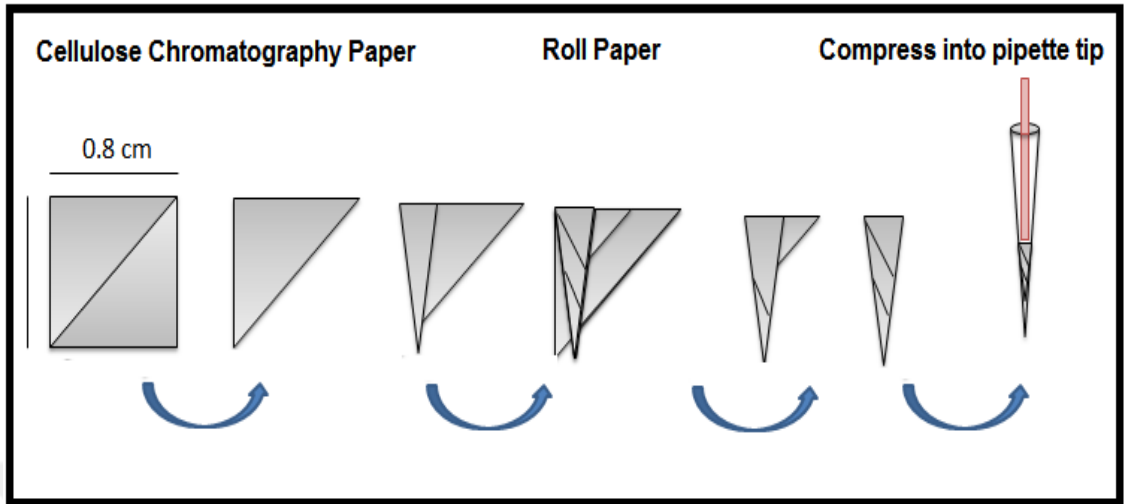


**Figure 3.1 :** Preparation of paper extraction support material using 3MM CHR paper as following the steps cutting triangles, rolling and placing into 200uL pipette tips respectively



**Figure 3.2 :** Real images of paper extraction support material after fabrication into the pipette tips in the use of nucleic acid extraction



**Figure 3.3 :** Simple pressure manifold for using in determination of flow rates of the paper tips in order to use in lysis and extraction of HPV DNA prior to detection

### 3.2.2 Cell lysis and DNA extraction in tips

The chemistry-based recipe has been also developed based on the Boom et al. method for single-step lysis and glycogen precipitation of nucleic acids onto paper supports. The single-step extraction buffer includes both a lysis and a purification buffer (Boom et al., 1990). Serial dilutions of combined HPV DNA from  $10^9$  to  $10^4$ cp/mL have been prepared as using the standard HPV16, 18&RNaseP which were purchased from Integrated DNA Technologies. After that, they cloned as described in previous chapter. Patient samples provided from Beth Israel Deaconess Medical Center. These samples are extracted after finishing the single step extraction buffer optimization. Also, all patient samples extracted with the commercial Qiagen DNeasy Blood&Tissue kit for comparison of the provided single step extraction recipe.

After setting up the pressure manifold by rinsing with Thermo Scientific DNA away and RNA away Surface Decontaminant then wiping them down with %70 ethanol, 20 $\mu$ l of samples were added to the 380 $\mu$ l of optimized chemical lysis, extraction and precipitation matrix containing 5.5M guanidinium thiocyanate (GuSCN), 5M sodium chloride (NaCl), 50% isopropanol (all from Sigma Aldrich, St. Louis, MO) and 15.8  $\mu$ g/ $\mu$ l glycogen co-precipitant (Life Technologies, Grand Island, NY) (Figure 3.4).

Flow rates tested paper based pipette tips (2-3 minutes extraction time tips used for capturing max DNA) were inserted to the pressure manifold and 200 $\mu$ l of each sample added to the paper tips which were set up labeled tubes to collect flow through beneath each tip. 20 psi pressure was applied for the extraction as measuring the flow rates. The glycogen and DNA co-precipitated onto the paper support, while the rest of the sample is flowed through. The flow through collected from the paper tip samples and other 200  $\mu$ l of the samples, and they were ethanol precipitated for controls. The tubes were centrifuged for 10 minutes at 13,000 rpm, 4°C for tube and flow through precipitation. Then, the pellets washed with 300 $\mu$ l %70 and 300  $\mu$ l %100 ethanol as centrifuging each time for 5 minutes at 13,000 rpm, 4°C. Finally, the supernatant was removed and the tubes were inverted to dry the pellet for 15 minutes.

While the flow through and tube precipitation controls had been preparing with the centrifuge washing steps the paper tips also washed on the pressure manifold with 300 $\mu$ l



%70 and 300  $\mu$ l %100 ethanol. Lastly, the tips were allowed to dry under the pressure for 10 minutes and captured DNA was eluted from the paper extraction supports by using 50 $\mu$ l tris-EDTA (TE) buffer. The resulted tube precipitation, flow through and paper tip DNA were quantified on Thermo Scientific NanoDrop ND-2000c , and also Applied Biosystem 7500 Fast Real-Time PCR System for serial dilutions of recovery.

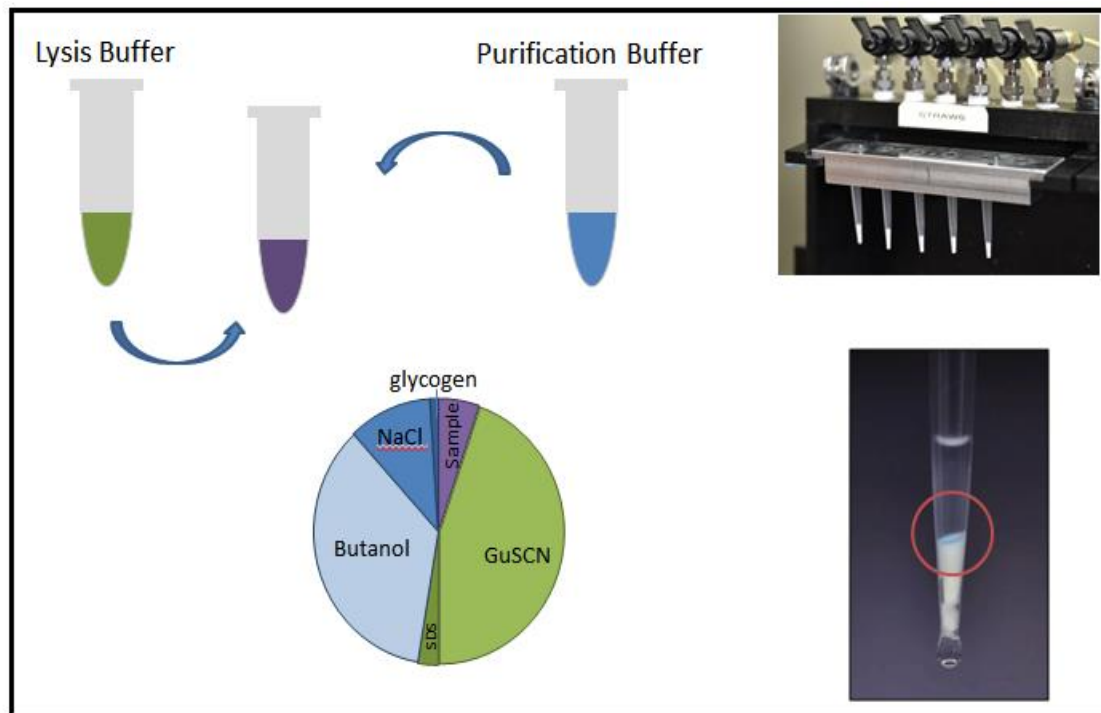


**Figure 3.4 :** Preparation of single step buffer which contains guanidinium thiocyanate (GuSCN), sodium chloride (NaCl), isopropanol and glycogen co-precipitant to lyse and extract HPV on paper extraction support material

The working principle of paper based extraction platform was summarized in Figure 3.5 . As you can see in Figure 3.6, the multiplex pressure manifold is used for pushing the single-step extraction buffer from the paper-based tips. First, the single step chemistry based combined lysis and purification buffer has been lysed the cells. Then, glycogen precipitation has been occurred on to the paper support material. The precipitation still had some of residual protein, and cell pieces, so that it has been rinsed with ethanol. Finally, the precipitated DNA has been eluted from the paper tips with the TE buffer.

The single step extraction buffer specialty is depend on the unique effect of the chemicals in the combined buffer. Guanidinium thiocyanate (GuSCN) is used to lyse the cells and virus particles in RNA and DNA extractions. It also has additional function that prevents activity of RNase enzymes and DNase enzymes by denaturing them. Otherwise, these enzymes can give damage the extract. GuSCN is a chaotropic agent which disrupts the hydrogen bond network between water molecules. The agent weakened the hydrophobic effect caused an effect on the stability of the native states of proteins, macromolecules and nucleic acids in the solution. The amount of order in the structure of a protein also formed by water molecules simply have been reduced with a chaotropic agent which may cause its denaturation (Mason et al., 2003; Shimomura et al., 1978).

Conversely, an antichaotropic agent increases the hydrophobic effects in an aqueous solution. Ammonium sulphate can be given as an example of antichaotropic salts that precipitate substances from the impure mixture. Undesired proteins can be removed from solution during in protein purification processes with these salts. NaCl is used to further break down cell components and then draw off the DNA associated proteins as making it non soluble. Salt neutralizes the charge on the nucleic acid backbone, and it causes the DNA to become less hydrophilic and fall out of solution (Gruenwedel and Hsu, 1969).

Alcohol is trapping the water and facilitates  $\text{Na}^+$  to interact with the  $\text{PO}_3^-$ , and then precipitate DNA as making it a little bit soluble. Because DNA is less soluble in isopropanol, isopropanol allows precipitation of larger species and lower concentrations of nucleic acids. DNA is polar because of its phosphate backbone which is highly charged. According to the principle of 'like dissolves like' DNA is soluble in water that is polar too. The high polarity feature of water makes electrostatic forces between charged particles. They are considerably lower in aqueous solution. This mechanism prevents the forming of negatively charged phosphate groups on a DNA backbone with positive ions are present in solution because of the weak net electrostatic force. Ethanol is less polar than water so adding enough ethanol causes the electrical attraction between phosphate groups and any positive ions present in solution becomes strong enough to form stable ionic bonds and DNA precipitation (Sambrook et al.,

1989). Glycogen is an inert carrier of nucleic acids to enhance the recovery. It is a preferred co-precipitant for solutions containing oligonucleotides or low concentrations of DNA or RNA, as it does not add exogenous nucleic acids like other co-precipitants, such as yeast RNA or tRNA. Glycogen, a highly purified branched chain carbohydrate, is insoluble in ethanol, and isopropanol. It forms a precipitate that traps nucleic acids. Upon centrifugation, the insoluble glycogen/nucleic acid precipitate forms a visible pellet that simplifies downstream sample processing.

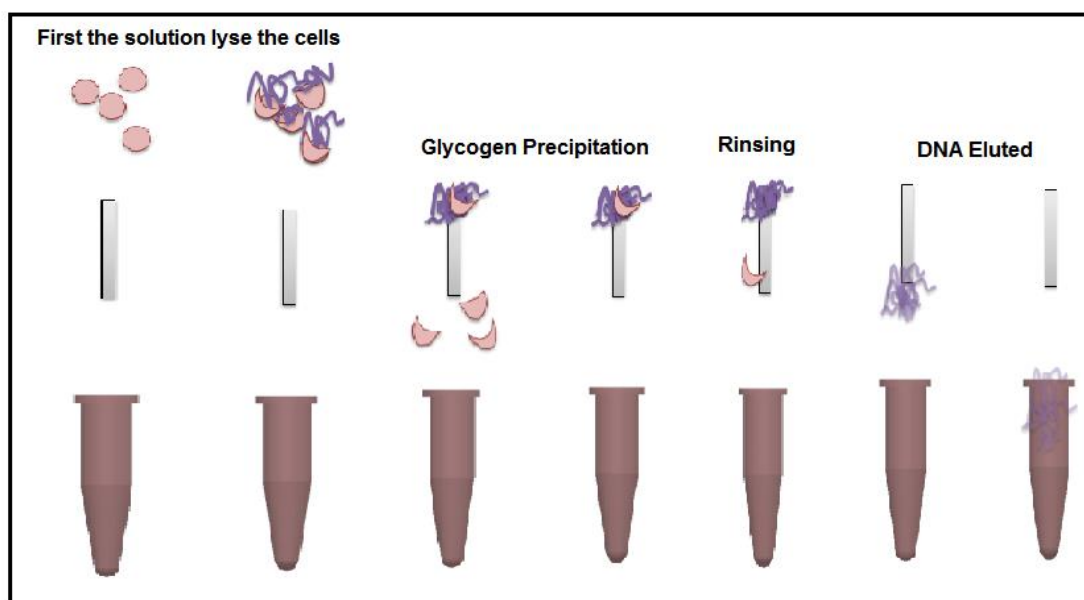


**Figure 3.5 :** The working principle of paper based extraction platform

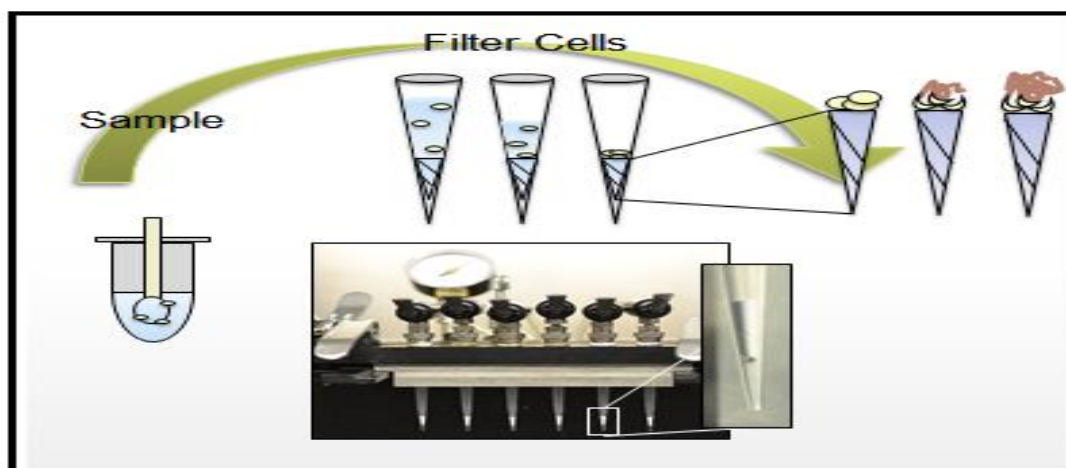


**Figure 3.6 :** The multiplex pressure manifold is used for pushing the single-step extraction buffer from the paper-based tips.

### 3.3 Result and Discussion

Sample preparation of a biological sample before analyzing is very important and unavoidable step. It consists of multiple steps such as cell culture, concentration, nucleic acid extraction, purification etc. This part focused on sample concentration and purification for point-of-care diagnostics of cervical cancer. The increasing of target concentration in a fixed sample volume is the main idea. There are so many methods have been presented to increase and purify the number of analytes in clinical samples. These methods have advantages and limitations. The extraction support material should have the ability to work with whole sample as giving good resolution on the other hand it should reduce the high cost, low throughput, complicated procedures, incompatibility with many types of biosensors and the requirement to work with diluted samples.

To overcome some of these issues, it has been developed an extraction support material and chemistry based lysis and purification for single step extraction of nucleic acids. The concentration process is to purify and concentrate the sample at the same time, while maintaining physiological electrolyte concentrations had been successfully done with this method. The device provides inexpensive, rapid, robust and simple way for point of care diagnosis of sample in low resource settings.

Herein, optimal assay had been arranged and prepared for single step extraction of combined HPV 16, 18&RNaseP from the paper based extraction support material as considering the literature based detection limits on Table 4. The HPV 18 and 16 DNA normally are used in detection with their magnetic bead and silver modified states form. Thus, they need to capture from the paper support material according to the lowest levels in the literature.

Y.Xu et. Al. Chem. 2014 presented the LOD value of HPV 16 as 10 copies/uL and HPV18 102 copies/uL. C.P. Chan et. Al. ICO 2014 presented the combined HPV 16-HPV 18 LOD as  $10^3$  copies/uL (Snyder et al., 2014; Xu et al., 2014). The minimum capturing amounts were defined with the results of experiments in this part considering this LOD value as copy form of DNA using qPCR and Nanodrop. The proper flow rates of the paper support material also were shown here. The possible concentration effects of the chemicals which were used in the single step extraction buffer to the DNA

recovery also determined and showed in this part with their graphical analysis results of PCR amplification and Nanodrop plots.

### **3.3.1 Setting the proper flow time for paper based single step DNA extraction**

The yield of the extraction has been determined for combined HPV DNA form as preparing several dilutions included LOD values in the literature. It has been used  $10^7$ cp/ $\mu$ L to  $10^1$ cp/ $\mu$ L HPV DNA for achieving the best capturing amount. They were all added into the tube which includes extraction matrix in the proper volume presented experimental section before. The PCR yield of the extraction support material and chemical matrix are tested and compared with their flow through and precipitation control after applying the method as described in the Figure 3.7. It is related to the presented details in experimental section.

The paper based DNA extraction efficiency are optimized from the co-precipitated glycogen and DNA as applying the PCR amplification. The resulted captured amount and standard DNA is compared to the resulted plots for both HPV 16 and HPV 18. It is needed to capture with our paper based extraction support material combined form of HPV from the patient sample, because these types can be presented in the sample together or separate.

The optimized PCR amplification conditions which had been previously shown in Table 2.1, 2.2 and Table 2.3 at Chapter 2 were used during the adjustment of extraction.

In this part, the PCR amplification results of the extracted DNA and their analysis were showed. The analysis had been done for starting concentrations and viable HPV DNA versus to the PCR copy numbers. We optimized the efficiency of DNA extraction to achieve the best capture of DNA. The plots in these slides are only for HPV 16 and RNaseP. The row PCR graphic also showed before the analysis plots in Figure 3.8 for HPV16. These plots in Figure 3.9 are determined to the efficiency of the paper tips which have different flow times to ensure proper flow times. The minimum flow times for maximum efficiency are important parameters for a point of care device.

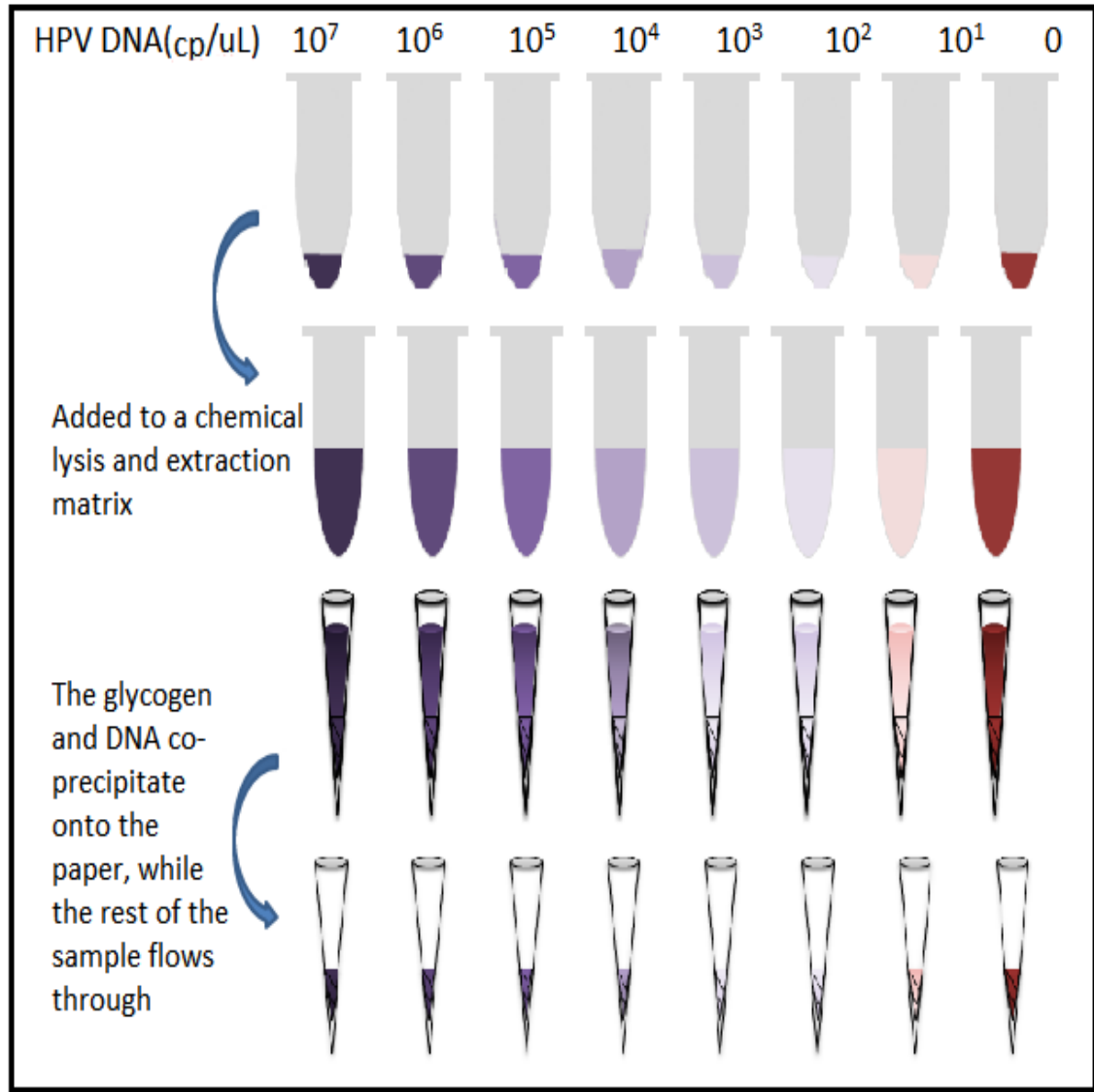


**Figure 3.7 :** Serial dilutions of combined HPV DNA from  $10^9$  to  $10^4$ cp/mL have been prepared as using the standard HPV16, 18&RNaseP and mixed with the single step extraction matrix and extracted from the tips while the rest of the samples flow through.

There were several flow times. They are tested approximately from 1 minutes to 6 minutes interval. The time controlling steps in Table 3.2 shows that 4 and 5-minute flow times are too long for the extraction. These are not suitable extraction times for a point of care device. As such, we continue to use the tips which have shorter flow times.

<b>Dilution</b>	10 <sup>9</sup>	10 <sup>7</sup>	10 <sup>5</sup>	0
<b>Paper tips time with ETHANOL</b>	1 min 31 sec	4 min	1 min 9 sec	5 min 20 sec
<b>Extraction time of DNA</b>	16 min 25 sec	35-40 min did not continue	13 min 30 sec	27 min 51 sec

**Table 3.2.** Flow time results of DNA for several flow time range paper tips

The PCR data below is belong to HPV 16 for 10<sup>9</sup> and 10<sup>5</sup> cp/mL DNA paper extractions. The results are for the standards, paper tip extracted, flow through and precipitation control DNA from left to the right side. The precipitation control values overlay with the paper tip extracted DNA plots. The lower amplification plots are for flow through values as expected.

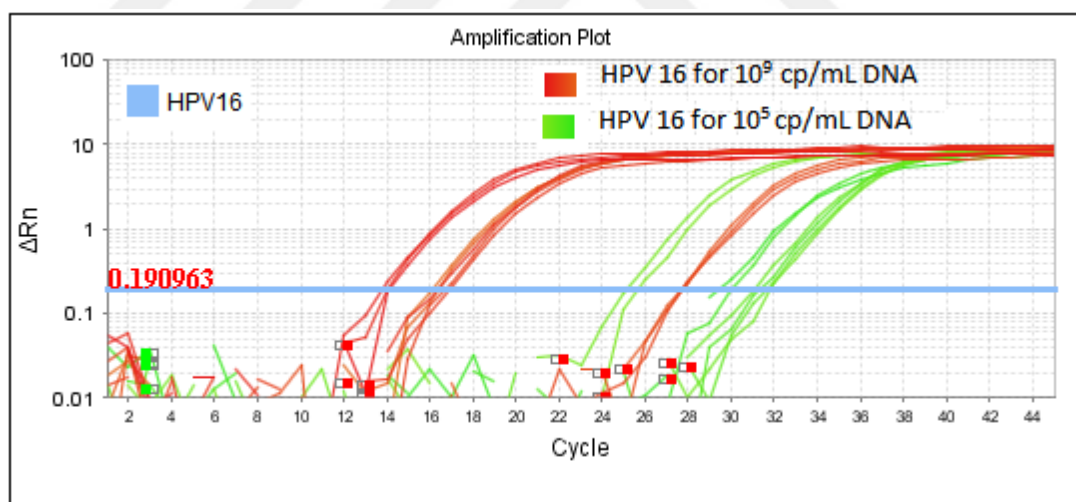


**Figure 3.8 :** PCR results of HPV 16 for 10<sup>9</sup> and 10<sup>5</sup> cp/mL DNA paper extraction as comparison of flow through, precipitation control and paper tips with the standards

The PCR data were analyzed, and their Ct values and Quantities were calculated according to the standard DNA amounts from the imported amplification results. Then, the results compared with the started dilutions of lysed cells from stocks versus copy number of DNA. A number of viable input cells versus are extracted, and amplified DNA copies. They are all shown below as a graphic in Figure 3.9 a, b, c and d.

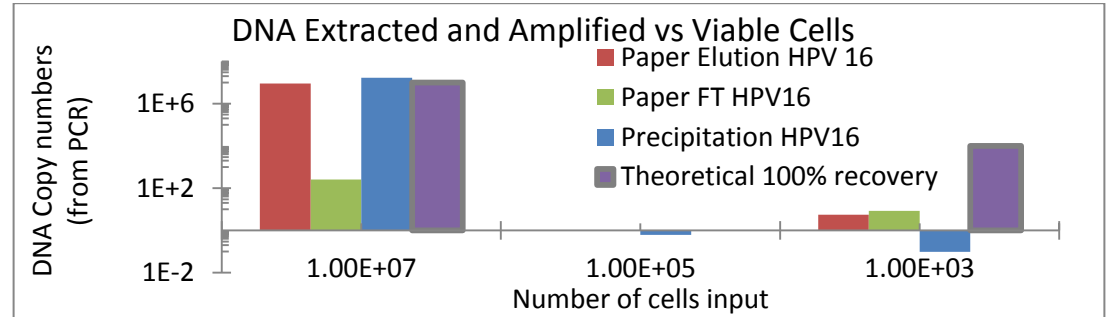
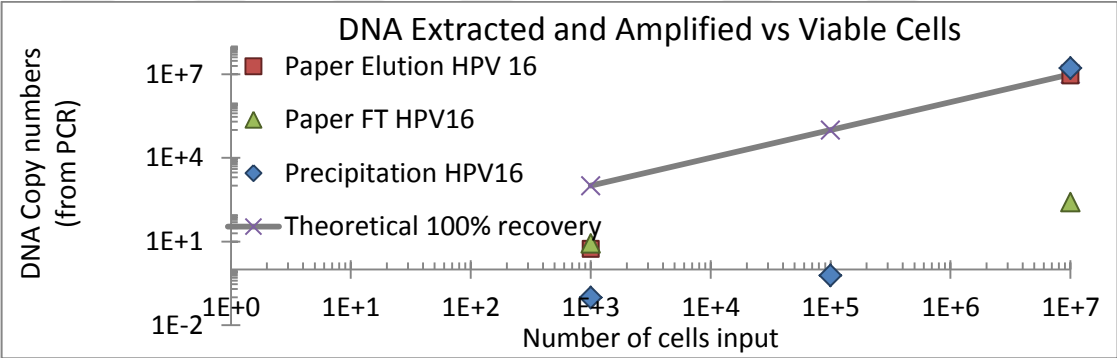
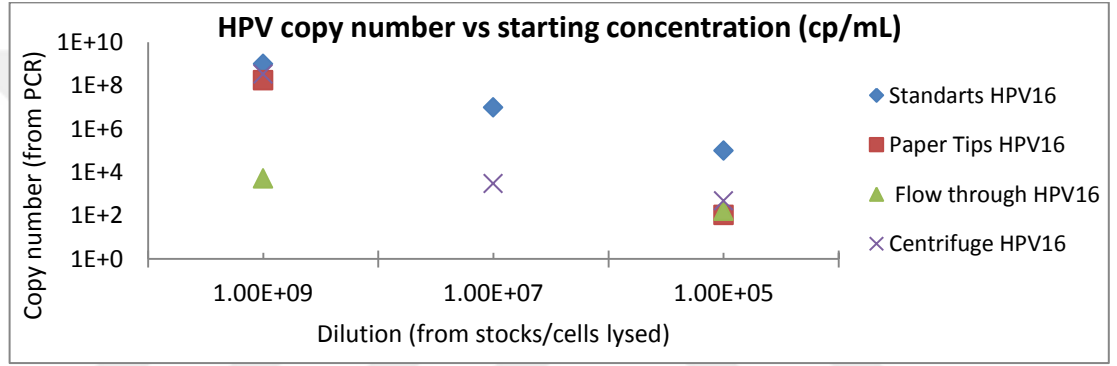
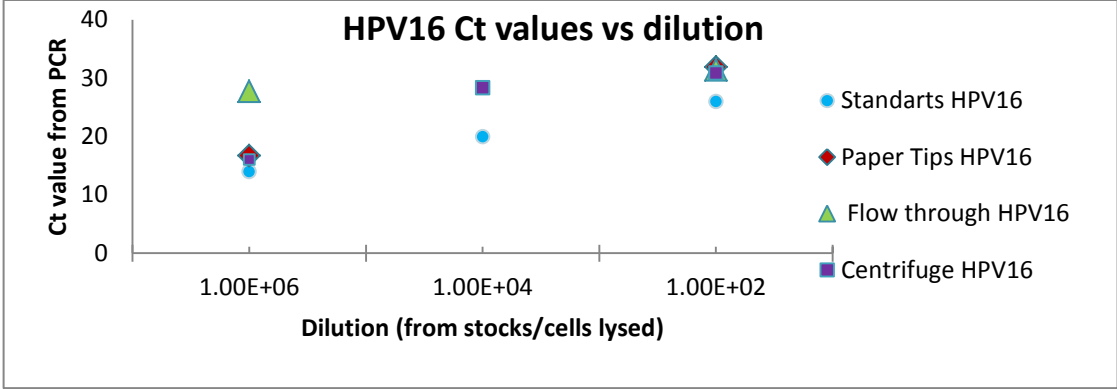


**Figure 3.9 :** a. Dilutions of stocks to the Ct value from PCR b. Dilution of cell lysed compare to DNA copy number c. Number of cell input compare to DNA copy number d. Column Graphic of Number of cell input compare to DNA copy number



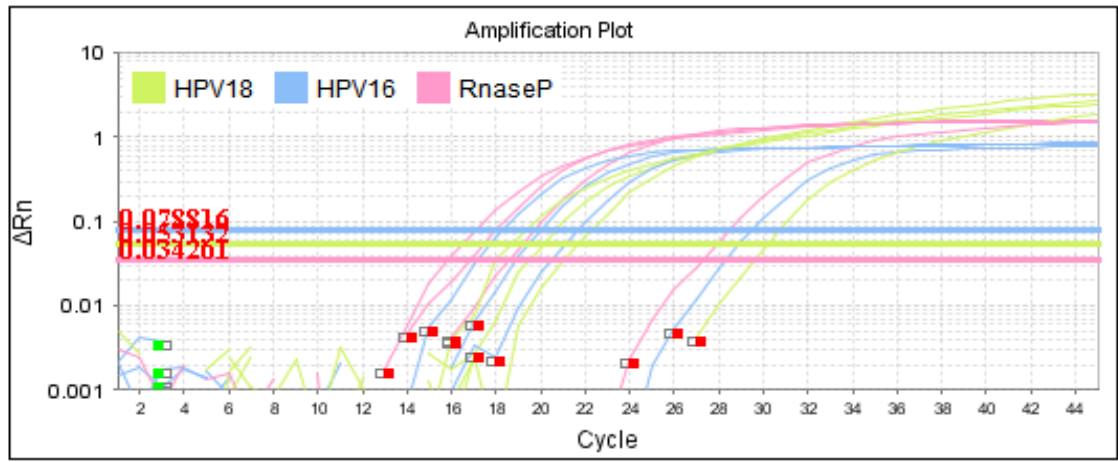
The plots that have been shown for only HPV16 type of DNA. It have also been drawn the plots for HPV18 and RnaseP too. They had not been showed in here, because they were so closed with each other.

These results demonstrate some clues to continue the optimal conditions for the high yield extraction of DNA. The PCR analyze plots of HPV 16 for  $10^9$ cp/mL DNA presented high efficiency for the recovery of the sample from paper tips compared to the standards. The paper tip is extracted DNA. Also, they have approximately same amplification value with the precipitation control. The flow through amount which belongs to non-captured part of DNA from the paper tips were also very lower amounts compared to the extracted DNA as expected. However, PCR analyze plots of HPV 16 for  $10^5$  cp/mL showed very closer recover with flow through, paper tip extracted DNA, and precipitation control according to the analyzed plots. The same value of flow through DNA with the paper tip extracted plots had been thought us if the results are because of the 22 seconds differences of the flow times between  $10^9$ cp/mL DNA and  $10^5$ cp/mL or the single step extraction buffer. The other plots which belong to  $10^7$ cp/mL DNA were also inspected for figure out the problem. The precipitation control and standard DNA amplification graphics show that not only flow times of the tips, but also the chemical extraction matrix should be arranged in the following.

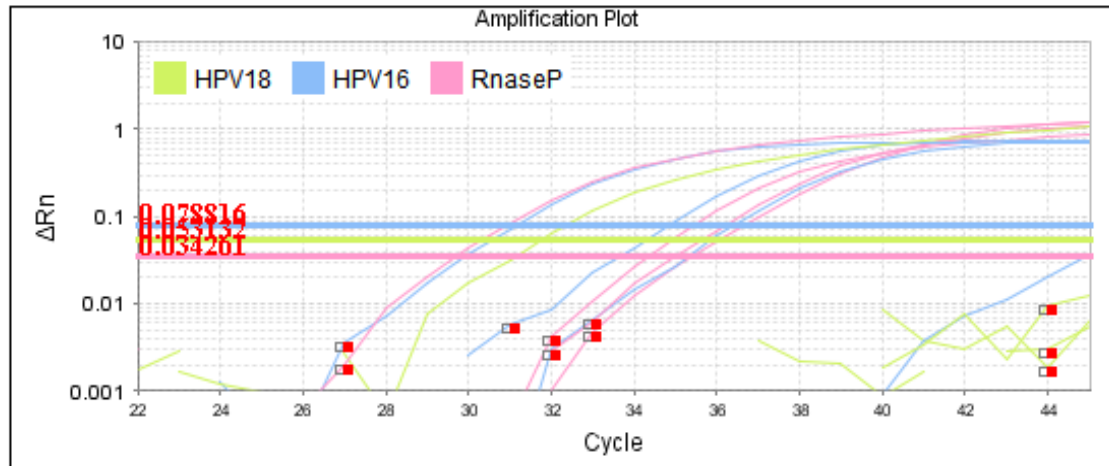
Another issue, the amplification of flow through and paper tip extracted DNA values could not been showed in the graphics for  $10^7$ cp/mL DNA because of the usage of higher flow times tip such as 4 minutes had not been allowed the passing of all liquids from paper tips during more than 40 minutes and blocked. Thus, only the effect of single step extraction matrix can be determined according to the related graphics of it.

The plots below are for the paper tips which have nearly 1 minute flow times (Table 3.3). The results had been shown for both HPV 16 and 18. First the PCR amplification results presented as row data below for  $10^9$ cp/mL and  $10^4$ cp/mL of HPV DNA in Figure 3.10 and 3.11. The extracted paper tips, flow through and precipitation controls were compared with the standards in these graphics. The PCR results are analyzed for all HPV types. The RNaseP data had not been showed here because the results very closed

with HPV 16 analyze plots. Also, RNaseP is only used because of the control of HPV DNA amplification on PCR.

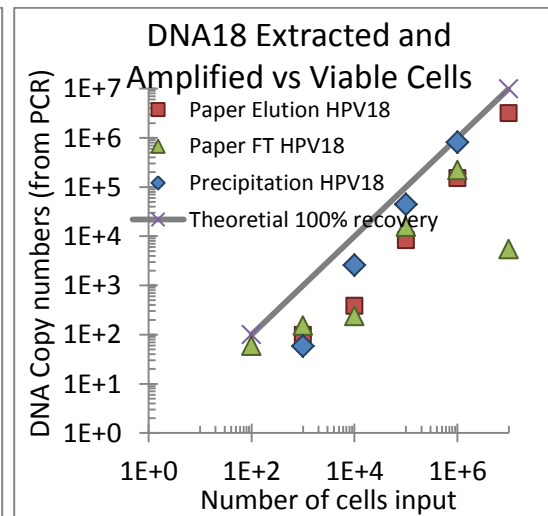
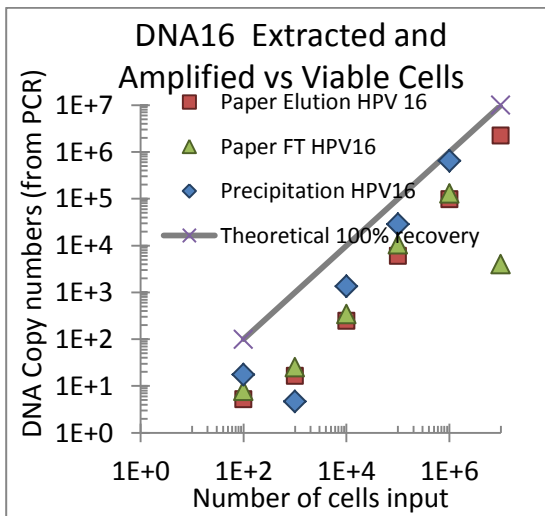
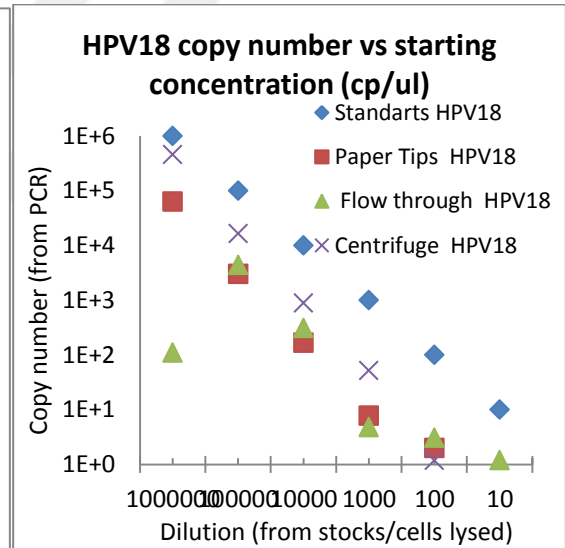
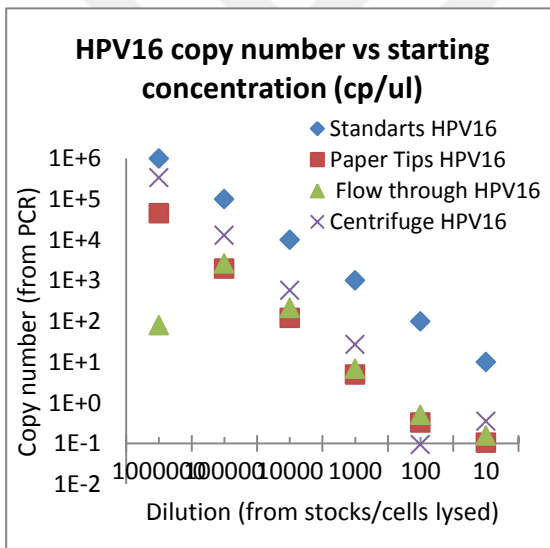
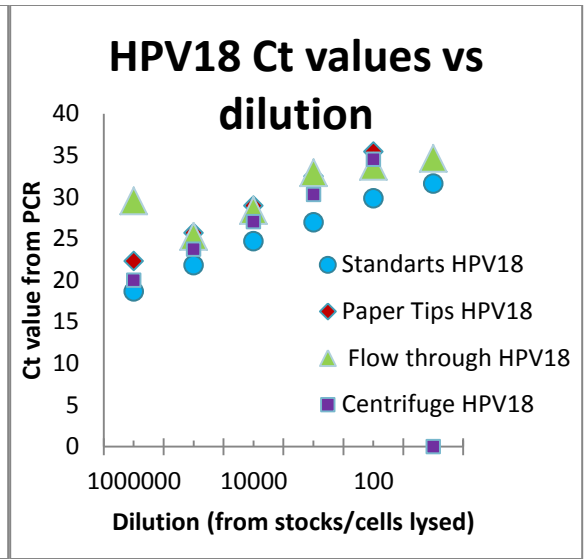
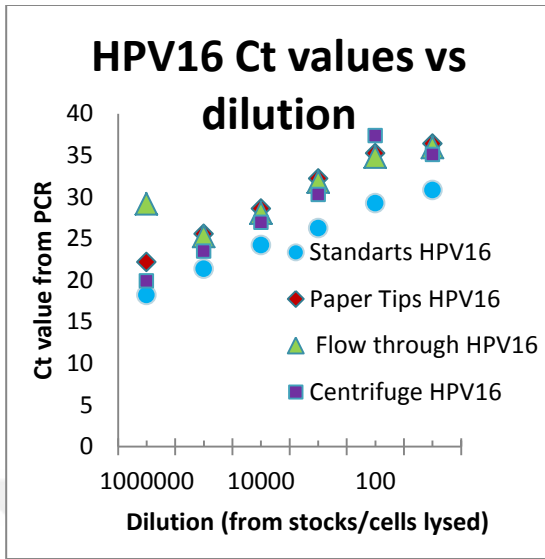


**Figure 3.10 :** PCR amplification result of  $10^9$  cp/mL of HPV 16,18 and RNaseP DNA for paper extraction as comparison of standards with paper tips, flow through and precipitation control from left to right.



**Figure 3.11 :** PCR amplification result of  $10^4$  cp/mL of HPV 16,18 and RNaseP DNA for paper extraction as comparison of standards with paper tips, flow through and precipitation control from left to right.

The PCR amplification results for  $10^9$  and  $10^4$  cp/mL DNA gave us some idea to the adjustment of the extraction parameters but we need to see the analyze results from  $10^9$  to  $10^4$  cp/mL DNA to get more information and decide the proper conditions for extraction setup. The results are evaluated, and compared with the previous conditions in order to achieve the best capturing of the DNA from paper support material.



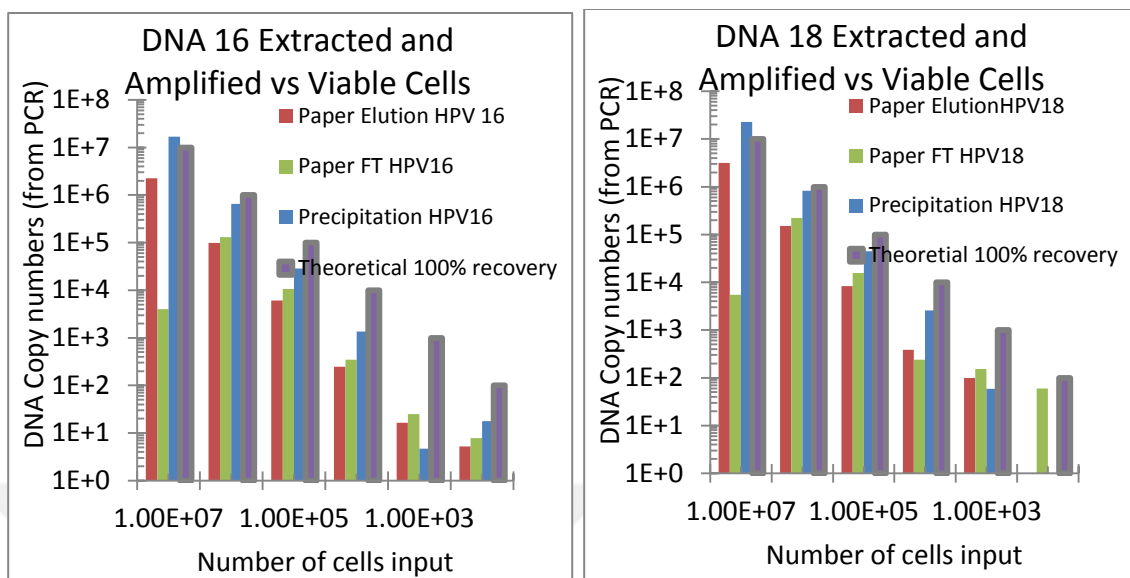


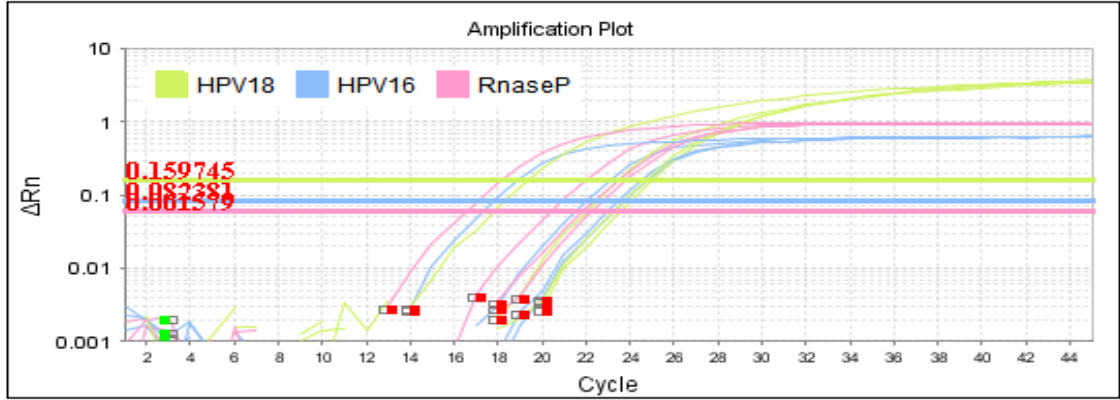
**Figure 3.12 :** a. Ct values versus dilution b. HPV copy number versus starting concentration c. DNA copy numbers compare to Number of cell input d. Extraction and amplification of DNA versus Viable cells

It can be seen from the results that it is not necessary to choose the tips which have 1 minute flow time, because the recovery for the minimum dilutions of DNA are much lower than the standards (Figure 3.12 a,b,c,d). Although, the amount of the paper extracted DNA is very close to precipitation controls, and standards for  $10^9$  cp/mL DNA. Other copies of DNA till  $10^4$  cp/mL were closed to flow through results.

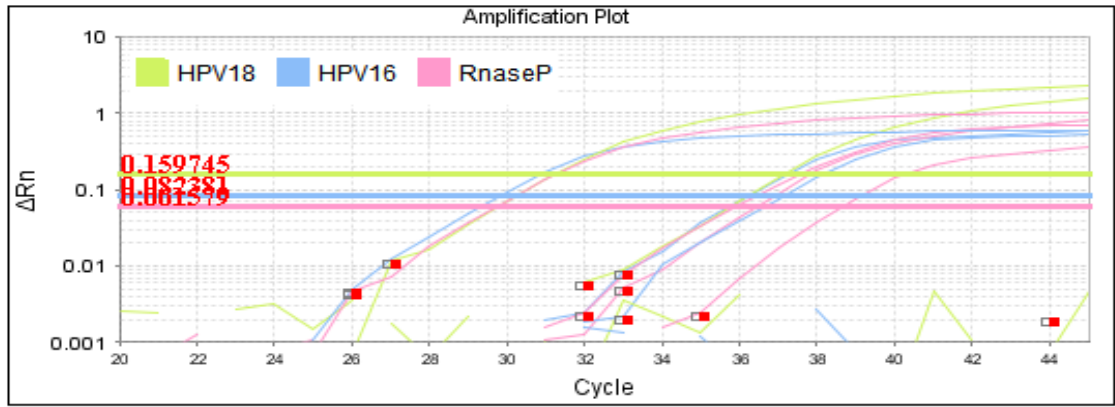
Dilution	$10^9$	$10^8$	$10^7$	$10^6$	$10^5$	$10^4$	0
Paper tips time with Ethanol	1:05	1:13	1:16	1:19	1:32	1:38	1:01
Extraction time of DNA	5:20	4:26	8:41	8:07	8:31	7:31	3:25

**Table 3.3.** Flow times

Thus, it has been decided to use the tips which have nearly 2 minutes flow times (Table 3.4). Then, the PCR amplification results were showed for the new tips, and their analyses values were presented.

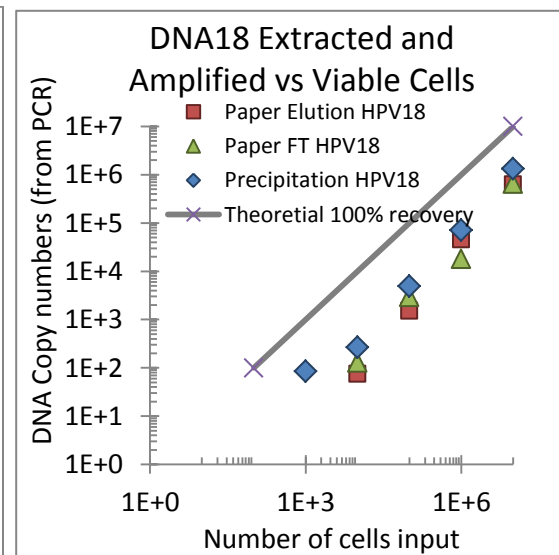
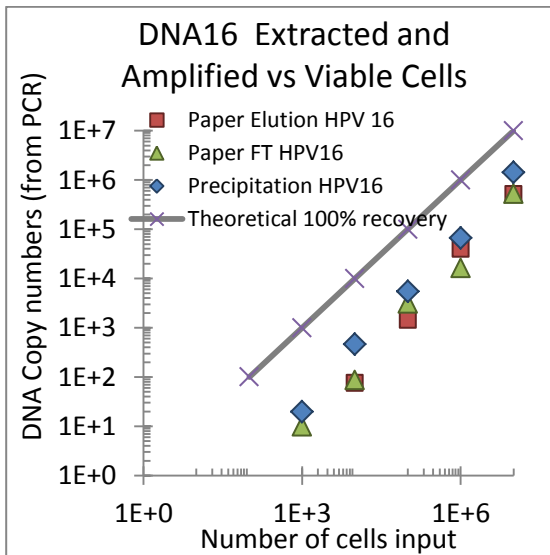
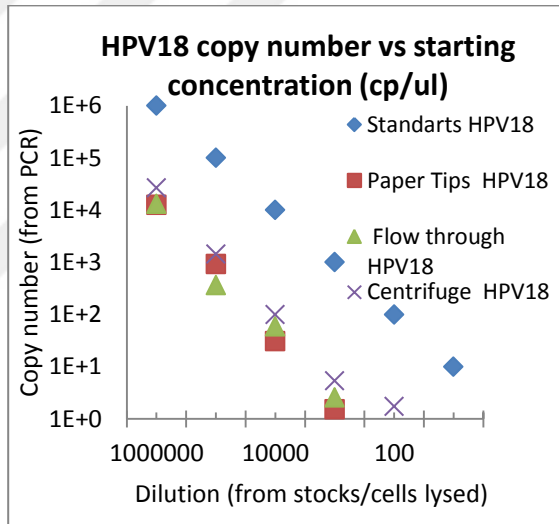
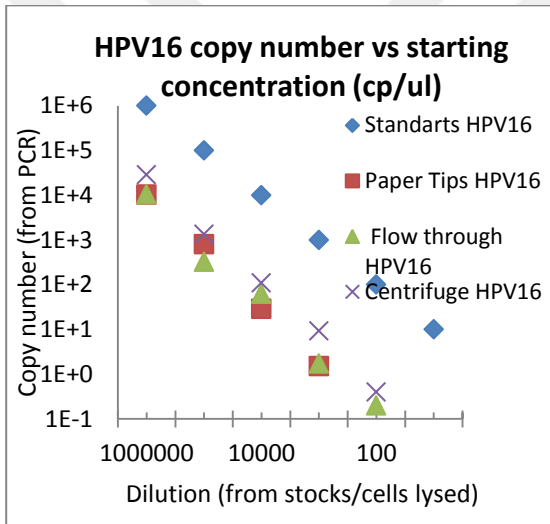
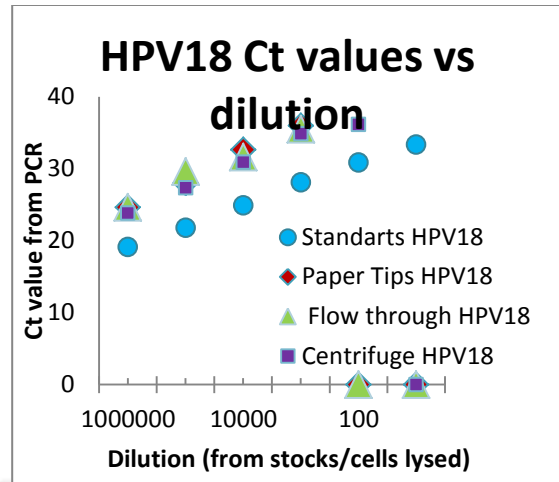
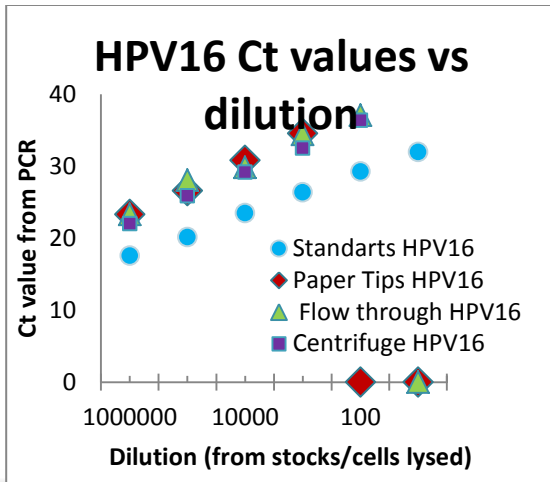


**Figure 3.13 :** PCR amplification result of  $10^9$  cp/mL of HPV 16, 18 and RNaseP DNA as comparison of standards with paper tips, flow through and precipitation control from left to right.



**Figure 3.14 :** PCR amplification result of  $10^5$  cp/mL of HPV 16, 18 and RNaseP DNA as comparison of standards with paper tips, flow through and precipitation control from left to right.

The Figure 3.12 and 3.13 show that the flow through value is almost same with paper tips extracted DNA and precipitation control on PCR. As we can see below in the analyze results, the amount of the capturing DNA did not change significantly as expected, when the 2 minutes flow times tips have been chosen.



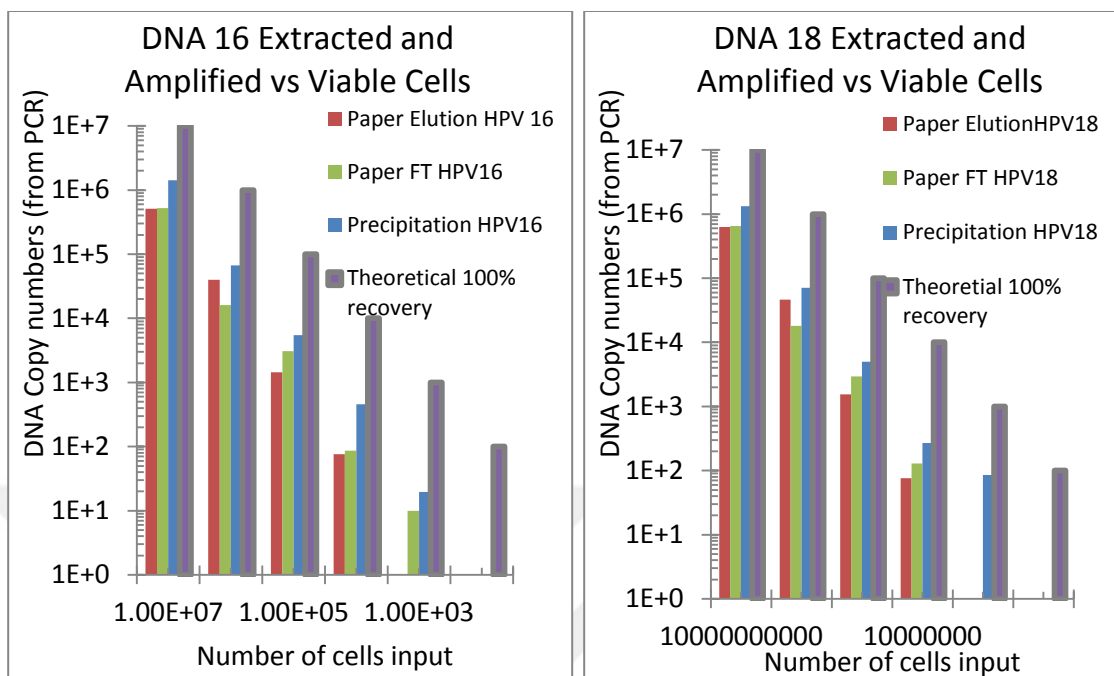


**Figure 3.15 :** Ct values versus dilution **b.** HPV copy number versus starting concentration **c.** DNA copy numbers compare to Number of cell input **d.** Extraction and amplification of DNA versus Viable cells

Figure 3.15 shows that the chemical single step extraction buffer is not good enough for capturing the DNA. The precipitation control also shows this reality to us because there is not any amplification DNA amount for  $10^4$  cp/mL sample. Instead of 2 minutes flow time tips were used for the extraction experimen. Tthe flows through value were almost equal to the centrifuge control precipitated DNA amount for all dilutions.

Dilution	$10^9$	$10^8$	$10^7$	$10^6$	$10^5$	$10^4$	0
Paper tips time with Ethanol	2:10	2:12	2:13	2:16	2:26	2:35	2:49
Extraction time of DNA	10:48	10:37	14:53	14:23	17:05	22:18	23:15

**Table 3.4.** 2 minutes flow time tips in DNA extraction

### 3.3.2 Elution buffer and stability test for capturing more DNA

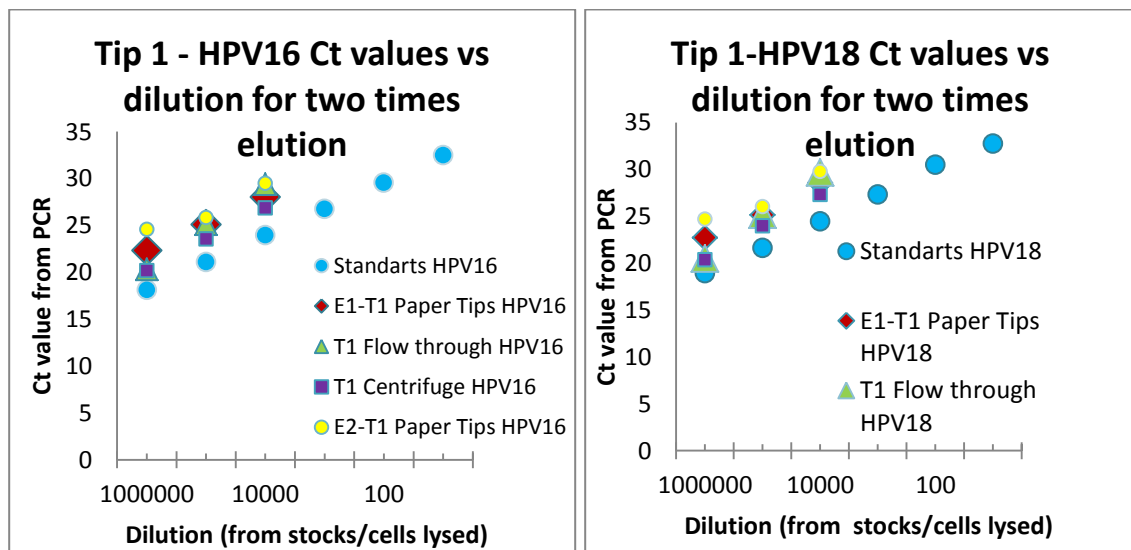
Accordingly, it has been decided to increase the elution buffer volume. First, 50 mL elution buffer is added after the extraction, and washing steps for getting the capturing

extracted DNA to the tube from the paper tips. Then, another 50mL elution buffer is added into the paper tips for getting the rest of the extracted DNA if it exists. The experiments had been done with two different tubes as using 50 microliter buffer for each tube. The red and yellow points in the plots show the results of the captured DNA amount for paper tips in Figure 3.16.

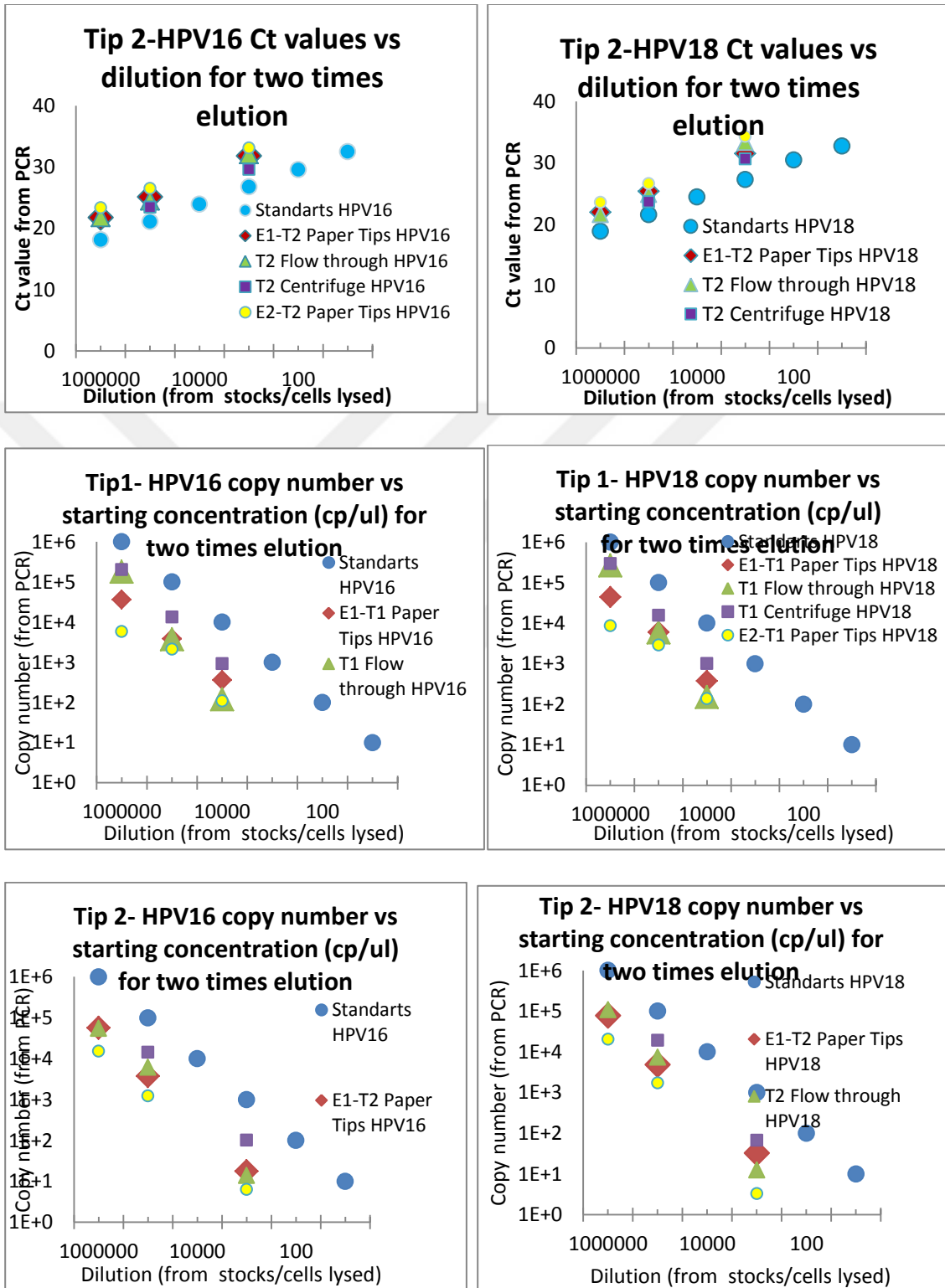
In this experiment, two tips for each dilutions are tried to understand the stability of the extraction (Figure 3.16). It has also been done confirmation experiments for stability of paper extraction. It has been tried to choose same flow time measured tips to maintain correct comparison. The flow rates of tips which were used for this experiment were presented on Table 3.5.  $10^9$  to  $10^6$  cp/mL dilutions of samples had been used for evaluation of stability and more elution solution effects. This experiment had been done for combined HPV forms and the results presented only for HPV16 and HPV 18.

Dilution	$10^9$ tip-1	$10^9$ tip-2	$10^8$ tip-1	$10^8$ tip-2	$10^7$ tip-1	$10^6$ tip-2	0 tip-1	0 tip-2
Paper tips time with Ethanol	1:55	2:00	1:55	2:00	2:03	3:11	1:37	1:26
Extraction time of DNA	11:45	7:57	13:43	17:03	3:22	20:16	2:52	5:36

**Table 3.5.** The flow rates of tips

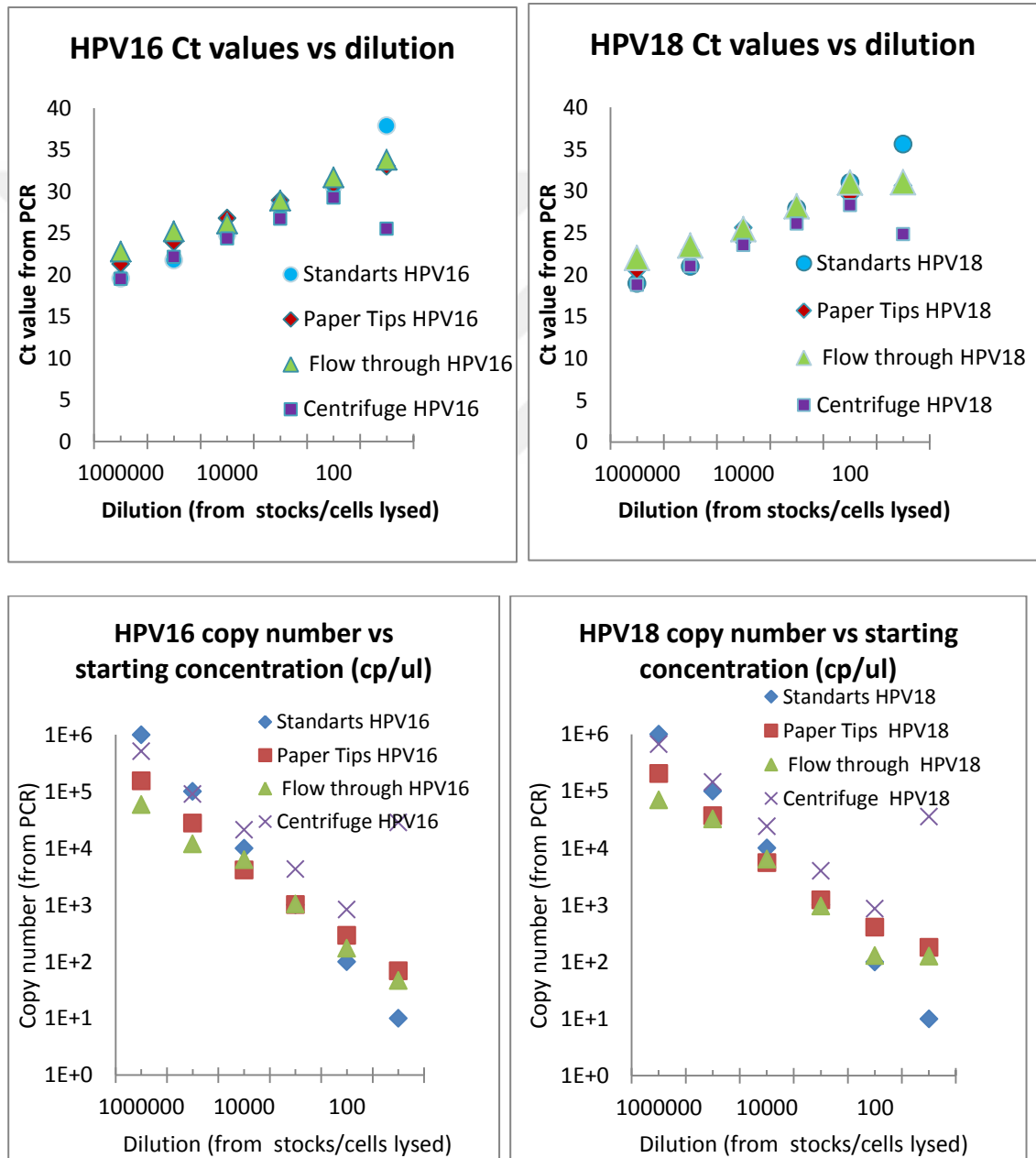






**Figure 3.16 : a.** Ct values versus dilution, **b.** HPV copy number versus starting concentration for Tip-, **c.** HPV copy number versus starting concentration for Tip-1, **d.** HPV copy number versus starting concentration for Tip-2

The analyses of the PCR amplification results of 2<sup>nd</sup> elution cause more captured amount of DNA from the paper tips. The captured DNA value of the 1<sup>st</sup> elution was almost same with the 2<sup>nd</sup> elution. It is also very characteristic result for the minimum dilutions. Thus, the elution solution had been combined as 100 microliter to see if the dilutions affect the results or not (Figure 3.17).



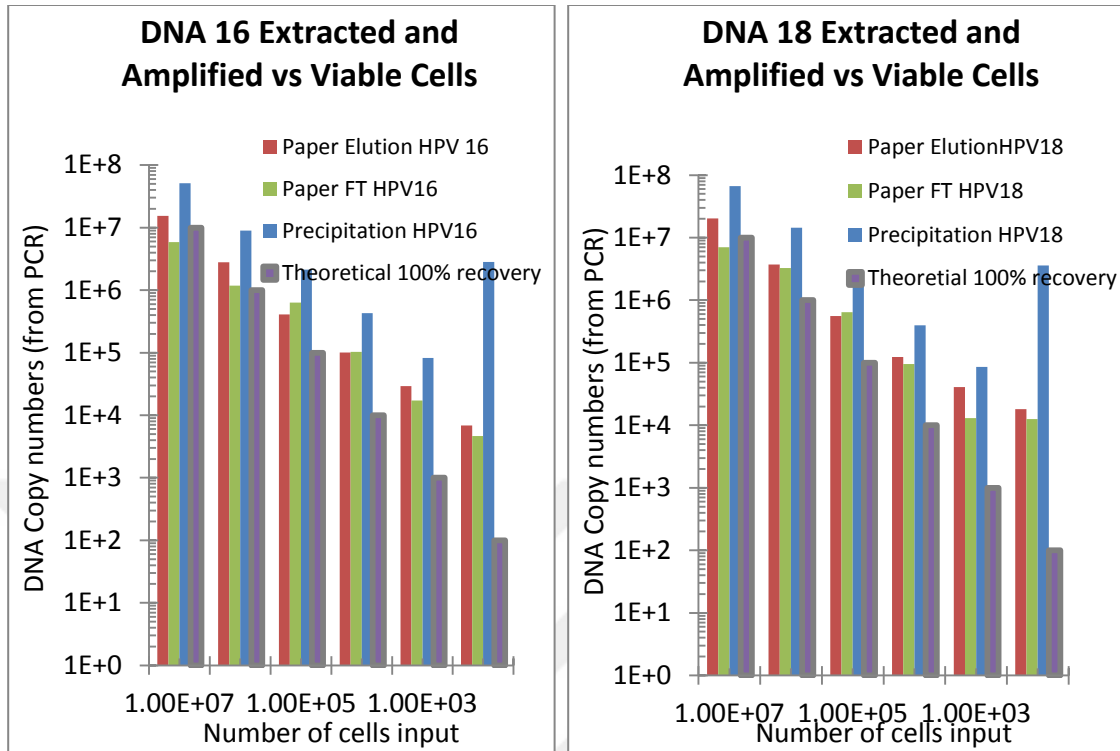


**Figure 3.17 :** a. Ct values versus dilution of 100uL elution buffer used extraction b. HPV copy number versus starting concentration c. HPV copy number versus starting concentration

After the amplification, it can be seen that there was some problem about the results. The flow through and paper elution results are almost same and close with the centrifuge control (Figure 3.17). It means that the DNA amount is much more than the standards. It can be because of the drying step.

### 3.3.3 Guanidinium thiocyanate and alcohol effect

The residual alcohol can affect the results as giving nonspecific amplification. The extracted DNA was tested on the Nanodrop machine to understand if the eluted DNA includes alcohol or not (Figure 3.18).

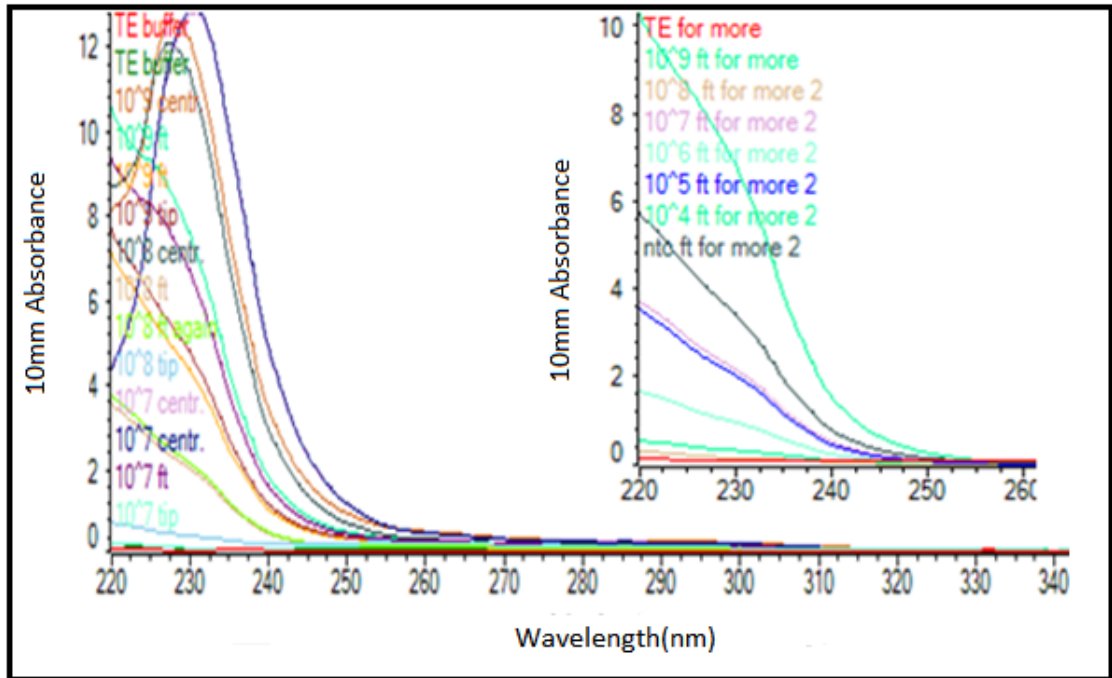


**Figure 3.18 :** Alcohol and GuSCN test for the Extraction results

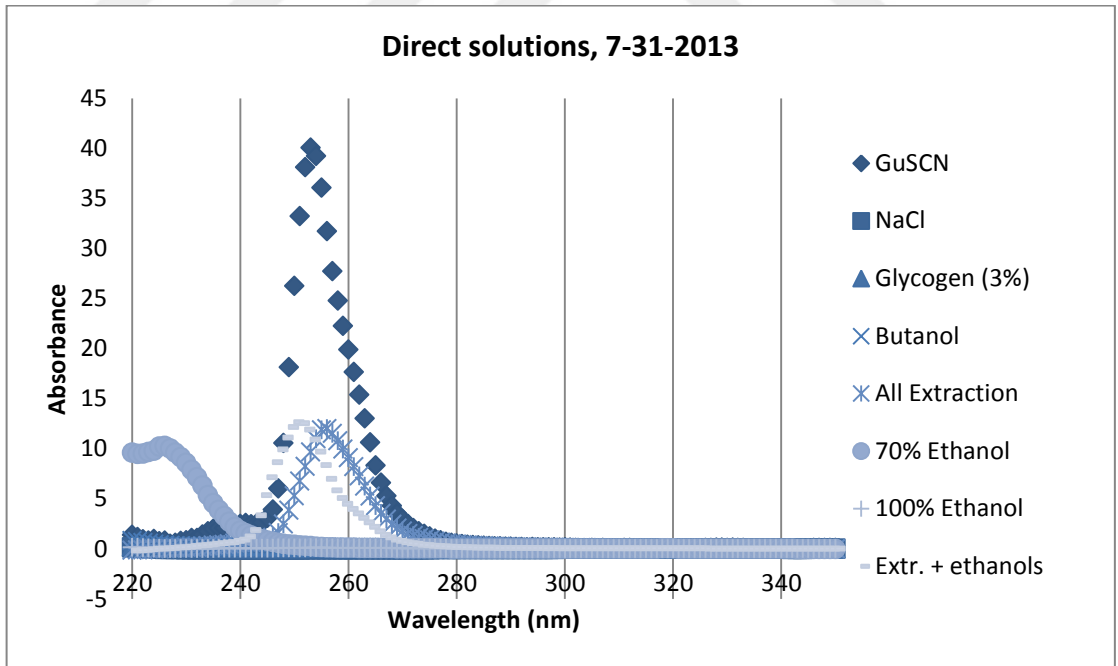


**Figure 3.19 :** Extraction solution components Nanodrop spectra of direct solutions  
 GuSCN has an absorbance peak at ~250 nm in solution and through paper and 70%, ethanol has an absorbance peak at ~230 nm in solution. Solutions with extraction buffer

also had peaks ~255 nm and with extraction, buffer + ethanol had peaks ~250 nm. It is appear that the samples are contaminated with GuSCN, and ethanol (Figure 3.19).

When the results have been compared with elution solution, TE buffer, it has been seen that the sample includes alcohol. They affect the results of the amplification. So it has been tried more drying time for avoiding the alcohol. The other point is that elution solution should be in lower volume for stability. Also, the point of care devices requires minimal sample preparation. In the future test washing methods and paper setups will be arranged to ensure removal of initial extraction solution.

Because we need to increase the precipitation of DNA in lower elution solution, we tried different percentage of isopropanol and butanol (Figure 3.20). It has been tried 50% butanol, 35% butanol and 50% isopropanol instead of 35% butanol for optimization of extraction. Their tube control steps had been done in PCR for comparing the amplification of captured DNA amounts in the medium of different alcohol types and concentrations.

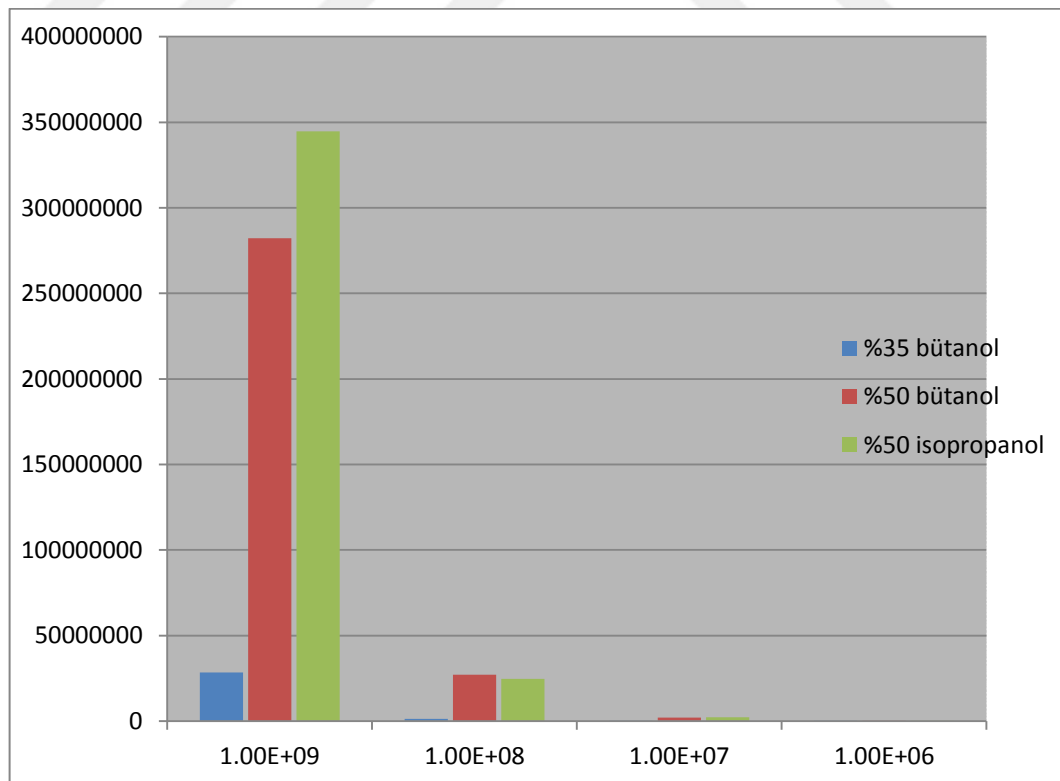
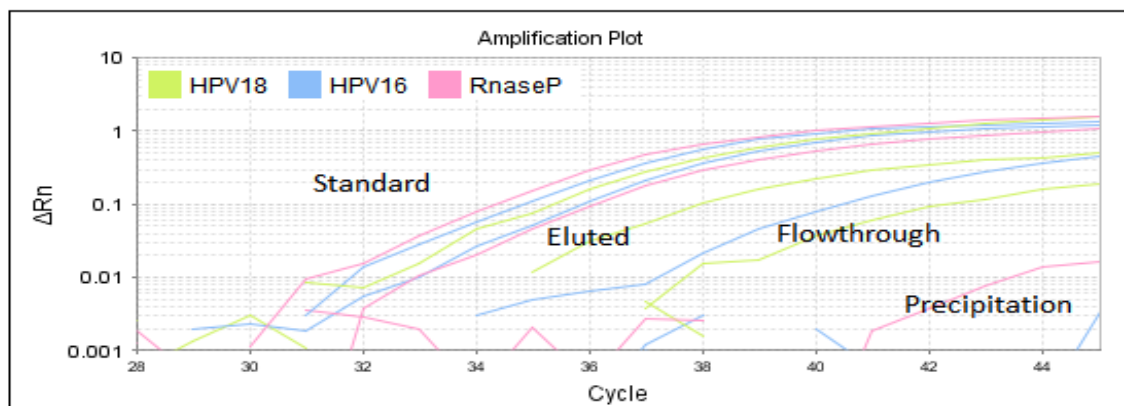


**Figure 3.20** : Comparison of 35% butanol, 50% butanol and 50% isopropanol

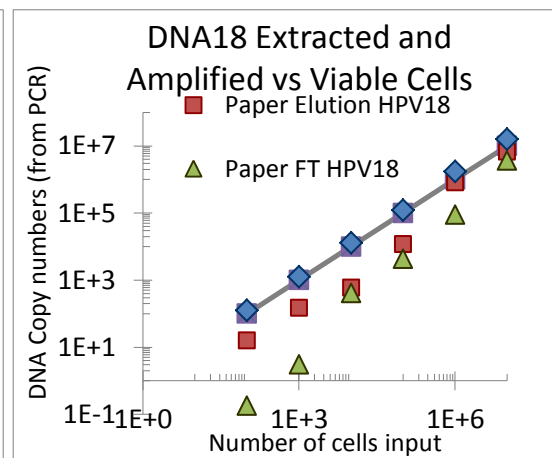
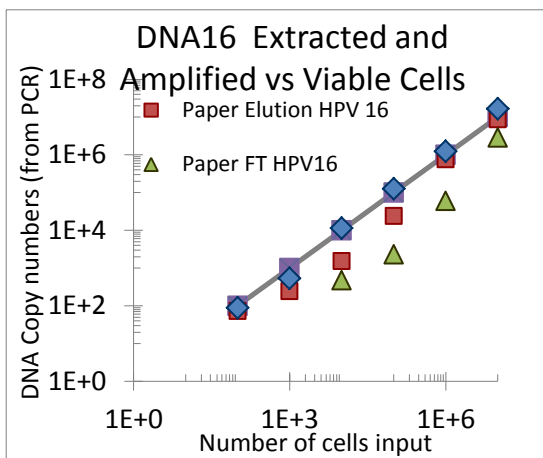
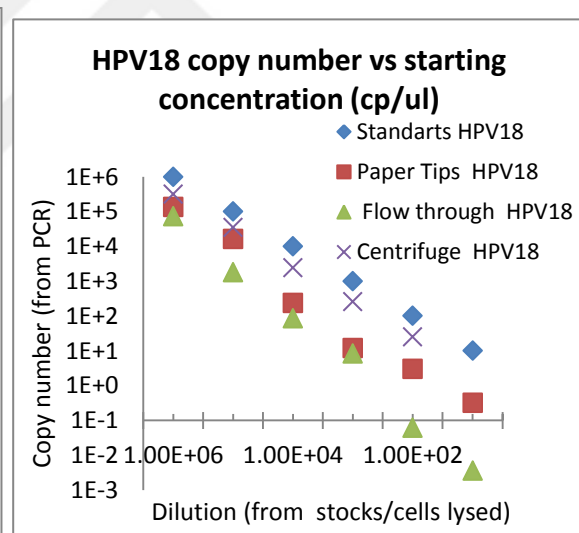
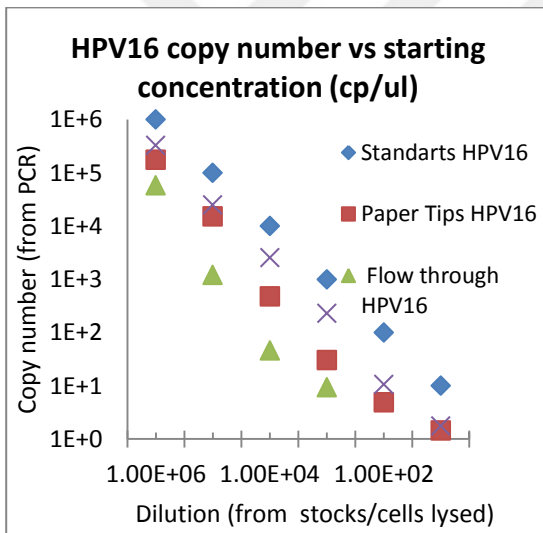
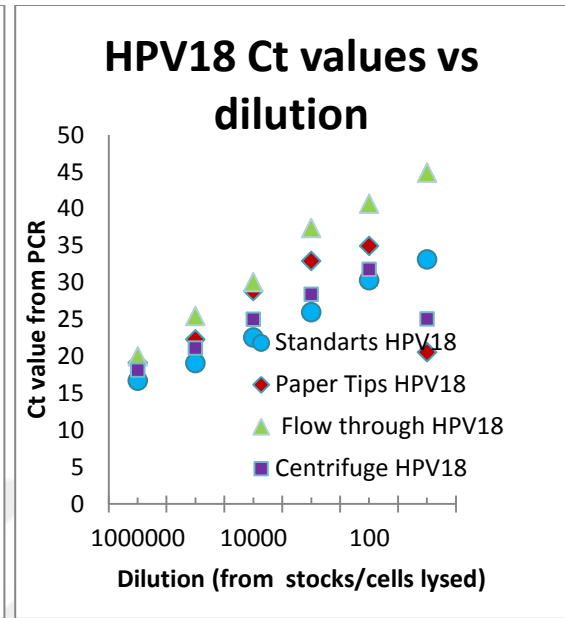
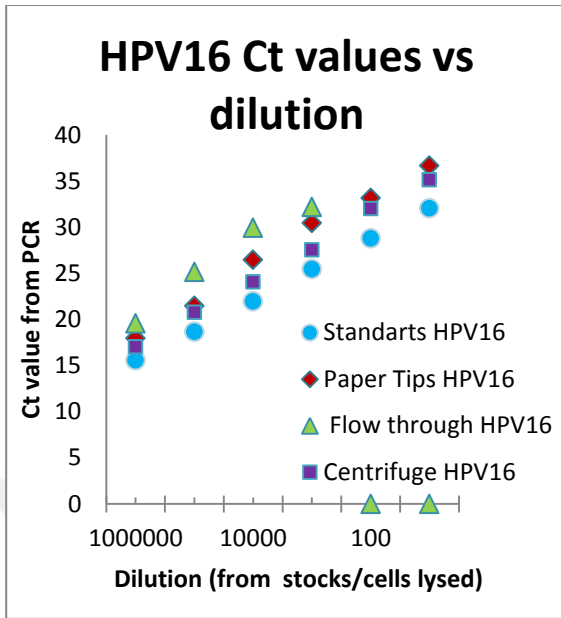
Dilutions	%35 butanol	%50 butanol	%50 isopropanol
1.00E+09	28532782	282302080	344724928
	26690006	319124544	411714528
	33347554	364615392	479480064
1.00E+08	1332617.875	27241658	24744304
	1425716.625	31279256	32471240
	2138292.25	35574068	35519884
1.00E+07	109958.1875	2095945.375	2267697.25
	99879.3125	2964000.75	2331143.25
	169308.3125	2574067.5	2777385.75
1.00E+06	9195.672852	316683.3438	201909.3125
	5378.727051	218511.5156	178292.9219
	10903.40625	305202.7188	237577.0469

**Table 3.7.** Comparison of 35% butanol, 50% butanol and 50% isopropanol

%50 butanol and %50 isopropanol gave 10 fold better recoveries for precipitate the DNA (Table 3.7). As a next step the extraction experiment has been tried with the %50 isopropanol for more drying time (Figure 3.20). Also, 50 $\mu$ L elution buffer used instead of 100 $\mu$ L as same as the beginning protocol. The PCR amplification graphic has been showed first in Figure 3.21 before the analyses plots.



**Figure 3.21 :** The PCR amplification graphic of %50 isopropanol



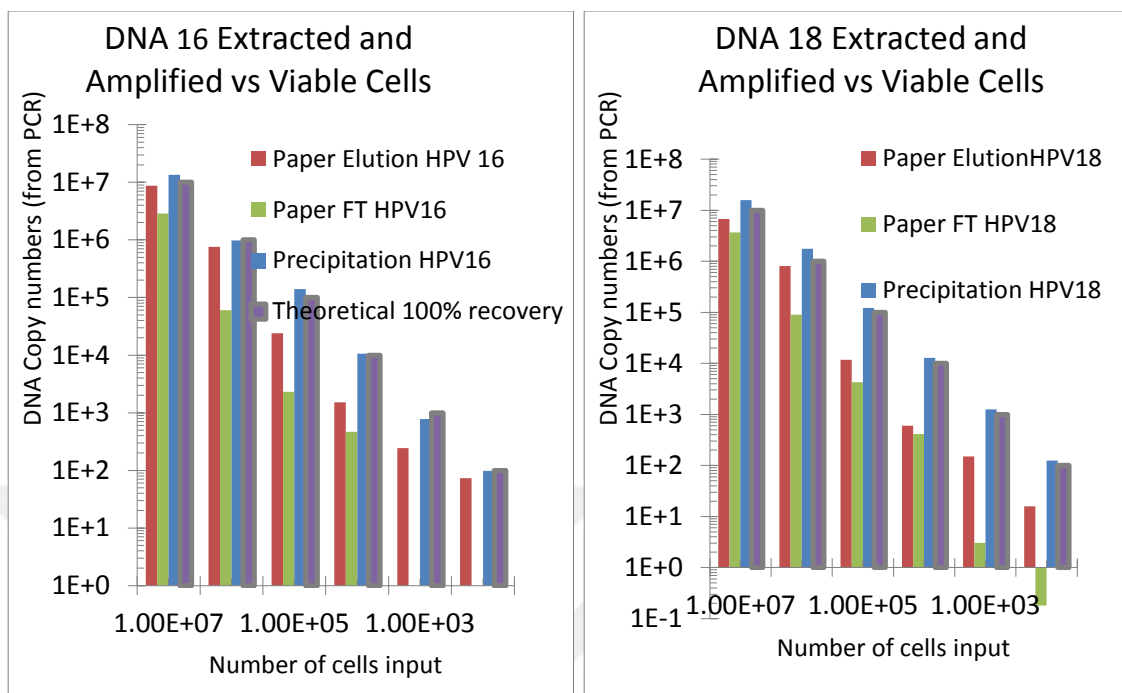


**Figure 3.22 : a,b.** Calibration curve of Extracted DNA for Ct values and copy numbers versus concentrations of HPV 16 and 18 **c,d.** HPV copy number versus starting concentration for last conditions

Dilution	10 <sup>6</sup>	10 <sup>5</sup>	10 <sup>4</sup>	10 <sup>3</sup>	10 <sup>2</sup>	10 <sup>1</sup>	0
Paper tips time with Ethanol	1:43	1:50	2:07	2:10	2:15	2:14	2:28
Extraction time of DNA	4:49	5:44	6:54	7:30	7:55	8:15	10:42

**Table 3.8.** Paper tips flow rates which is used for the last adjusted conditions

The results show that it is achieved 10<sup>1</sup>cp/μL DNA dilutions to extract with the paper tips for both combined HPV 16 and 18. The last optimization parameters can be used for patient sample in these conditions.

This protocol has been extended to extract DNA from whole patient samples and after the optimization step it was adapted for the extraction and precipitation of patient samples in paper matrices. Samples were also processed with the Qiagen DNeasy and Tissue kit as the positive control.



### 3.4 Summary and Future Works

Sample preparation step is very important for microfluidic chip fabrication. Traditional methods require expensive instrumentation as centrifugation, extraction and concentration of DNA to achieve proper low detection limits. The rapid prototype must include an on-chip extraction part. The Klapperich Laboratory has a method for lysis, extraction and precipitation of DNA in a single step. The combined solution has been optimized for HPV DNA and tested on paper pipet tip column. Before the solution flowed through the column, fabrication of paper tips had been done according to described protocol.

Cervical cells have been lysed to release HPV DNA for downstream amplification and detection. The optimal amount of chemical lysis, extraction and precipitation matrix has been arranged as 5.5 M guanidinium thiocyanate, 5 M sodium chloride, 15.8  $\mu\text{g}/\mu\text{l}$  glycogen and 50% isopropanol. For capturing max DNA, it has been decided to use the tips which have nearly 2-3 minutes extraction time.

Lysis&extraction buffer efficiency had been quantified by PCR and drawn the plots of each types of HPV DNA to reach the more precipitation of it for minimum detection limit of the nucleic acids. At least  $10^1\text{cp}/\mu\text{L}$  DNA had been precipitated for combined HPV16,18 and RNaseP as been expected.

In conclusion, it has been demonstrated an on-board paper tip nucleic acid extraction platform for HPV DNA. The optimization and comparing steps had been done successfully. Then it can be continue as the detection step of the DNA without enzymatic amplification via analytical detection in hallow-channels.

For each steps of the device, it is needed to be controlled via PCR for comparing and doing the positive control of the workouts.

## 4. CHAPTER: OPTIMIZATION AND CHARACTERIZATION OF ELECTROCHEMICAL DETECTION

### 4.1 Introduction

HPV viruses are common factor for cervical cancer which is resulted deaths in woman worldwide (Bedford, 2009; Parkin and Bray, 2006; Qiao et al., 2008; Sankaranarayanan et al., 2009). Approximately 270 000 women per year die of cervical cancer who are live in developing countries (Cuzick et al., 2008; Cuzick et al., 2012). According to the Illustration 4.1 the incidence rates range is up to 87.3 per 100 000 in South Eastern Africa and less than 33.4 per 100 000 in Latin America (Cuzick et al., 2008; Schiffman and Castle, 2005).

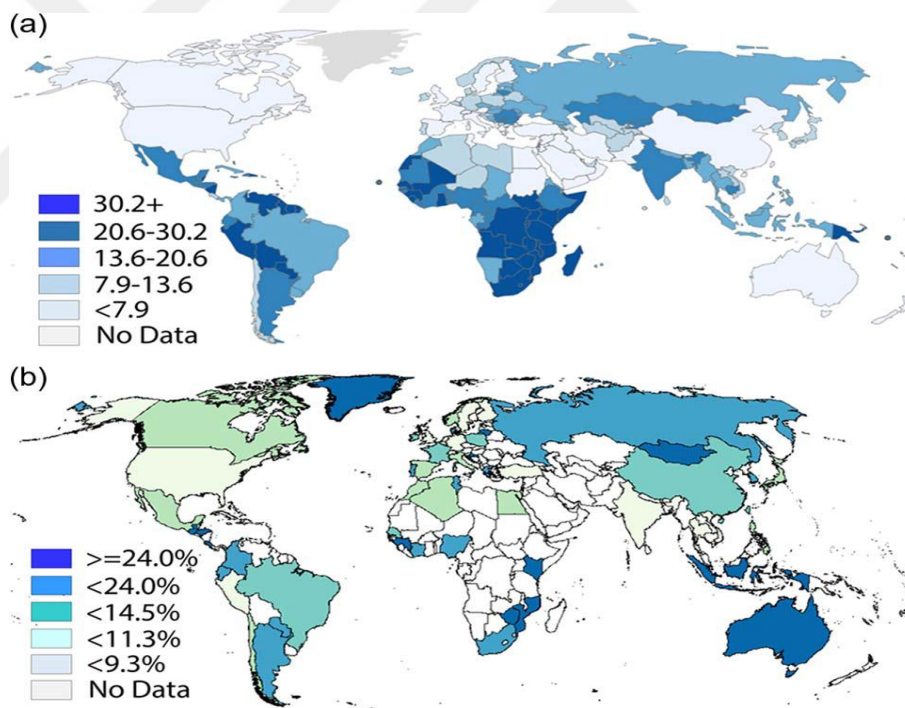


**Figure 4.1 :** **a.** Cervical cancer distribution around the world: Cervical cancer cases per 100 000 people based on data from the International Association of Cancer Registries, 2012. High incidence is observed in Africa and South America (Ferlay et al., 2015). **b.** Worldwide HPV prevalence: Estimate for HPV prevalence by country based on data compiled by the Institut Catala` d'Oncologi (ICO) Information Centre on HPV and Cancer, updated 2014 (Bruni et al., 2014).

The early detection of cervical cancer has high cure rate and can be easily detect from Human Papilloma Viruses compared to the traditional diagnosis methods (Ostrowska et al., 2010; Saslow et al., 2012). Thus detection of HPV presence and degree in the clinical samples has a significant role for cervical cancer (Schiffman and Castle, 2005). Existing cervical cancer screening procedures change in developed and developing countries. Although the developed countries uses molecular probes for screening the cancer, the developing countries uses cytological tests which has low specificity and sensitivity (Arney and Bennett, 2010; Devegowda et al., 2014). These standard screening techniques are limited because of its requirements for both developed and developing countries such as large population, turn-around time in weeks and limited resources (Magrath et al., 2013). Therefore, there is a significant need to improve the quality of cervical cancer screening in developing and resource-limited countries with inexpensive, robust screening techniques (Crow, 2012; Parkin and Bray, 2006).

HPV is not only a risk factor for cervical cancer but also it also been implicated in oropharynx, vagina, anus, and penis cancer(Crow, 2012; Parkin and Bray, 2006). Hence, the developed techniques can also be used for diagnostic of for these other cancers caused by HPV. HPV virus has more than 100 different genotypes and its mucosal types are divided into high-risk (HR) and low-risk HPV (De Villiers et al., 2004; Huang et al., 2004). According to the biological origins and oncogenic potential HPV-16/18 are the most common HR-HPV types which cause cervical cancers in women (Hwang and Shroyer, 2011).

HPV detection give nanotechnology and microfluidics hope to develop bio sensing platforms for ultrasensitive detection. The Table 4.1 shows the applied platforms for HPV diagnostics. As seen from the table HPV biosensor platforms contains different detection area such as magnetic, optical, acoustic, mass and electrical based. These mentioned HPV detection platforms have generally been used in clinical sample diagnostic for monitoring the nucleic acids of it. Target amplification methods are commonly used to produce millions of target HPV nucleic acid amplicons such as PCR, RTPCR and LAMP (Loop-mediated isothermal amplification) in these platforms. In addition to this antibody-antigen interactions and nucleic acid hybridizations have also

been applied for HPV diagnostics, primarily by sensing infected cells and specific HPV capture nucleic acid probes are immobilized.

Detection Method	Biomarker	LOD	Reference
Fluorescence	HPV-16, HPV-18, HPV-45 (Biotinylated DNA strands)	$10^3$ copies $\mu\text{L}^{-1}$	[23]
	Biotinylated HPV DNA strands	20 pM	[24]
	HPV-16 HPV-18 (DNA strands)	0.17 nM 0.78 nM	[25]
	HPV-16 HPV-18 (DNA strands)	70 pM 60 pM	[26]
	HPV DNA strands	1 fM	[28]
	Biotinylated HPV DNA strands	25 pM	[30]
	HPV-16 (DNA strands)	0.7 copies per cell	[32]
	HPV-6b (DNA strands)	< 33 copies $\mu\text{L}^{-1}$	[36]
	HPV-6, HPV-11, and HPV-16, HPV-18 (DNA strands)	10 copies $\mu\text{L}^{-1}$ 102 copies $\mu\text{L}^{-1}$	[34]
	HPV 16 oligonucleotide	0.1 $\mu\text{M}$	[41]
	HPV 16 sequence SiHa cell line	$10^{-6}$ $\mu\text{M}$ 20 cells $\mu\text{L}^{-1}$	[44]
	On-chip nucleic acid extraction	5 cells $\mu\text{L}^{-1}$	[46]
	Molecular beacon-based oligonucleotide detection (HIV presented, HPV not given)	10 nM	[47]
Nanoparticle-based optical	HPV-6, HPV-11, HPV-16, HPV-18 (DNA strands)	50 nM	[51]
	HPV-16, HPV-18 (Biotinylated DNA strands)	30 pM	[52]
	HPV-16, HPV-18 (DNA strands)	0.14 nM	[53]
	HPV DNA strands	50 pM	[54]
Electrochemical	HPV-16 HPV-18 HPV-45 (DNA strands)	0.22 nM 0.17 nM 0.11 nM	[57]
	HPV-16 (DNA strands)	18 nM	[58]
	HPV DNA strands	3.8 nM	[59]
	HPV-16 (DNA strands)	4 nM	[60]
	HPV-6 (DNA strands)	30 pM	[61]
	HPV-16 (antibody)	0.49 nM	[63]
Magnetic	HPV-39 (Biotinylated DNA strands)	10 pM	[64]
Mass	HPV-58 (DNA strands)	100 copies (0.8 pg/mL)	[71]
Surface acoustic wave	HPV-18 (DNA strands)	1.21 fg/mL	[73]
	HPV-18 (DNA strands)	1 fg/mL	[74]

**Table 4.1.** Comparison of Biosensor Technologies for HPV Diagnostics (Tasoglu et al., 2015).

#### 4.1.1 Electrical detection technologies

HPV genotypes also have been detected with electrochemical technologies. HPV-16, HPV-18, and HPV-45 DNA sequences were detected with developed Gold electrode sensor arrays (Civit et al., 2012). Horseradish peroxidase enzymes had been used with thiolated capture probe DNA for hybridization of target DNA between gold electrodes in a sandwich assay to carry out the detection. Horseradish peroxidase enzymes catalyzed the oxidation of tetramethylbenzidine substrate on the sensor area after the addition of tetramethylbenzidine for detection with electrodes using cyclic voltammetry. HPV-16, HPV-18, and HPV-45 multiplex form of HPV genotypes were quantitative detected with this biosensor on the surface of the electrode as functionalization of different thiolated DNA probes. The LOD of each HPV DNA were presented as 220, 170 and 110 pM respectively for HPV-16, HPV-18, and HPV-45.

HPV 16 DNA also was analyzed with an electrochemical biosensor at least 18 nM concentrations (Campos-Ferreira et al., 2013). The main idea of the sensor was to immobilize capture probe DNA as modifying the electrode surface with an electrodeposited cysteine film. Methylene blue was introduced on the surface after hybridization of target DNA with the immobilized probe. The detection of target DNA was carried out with the probe causes the methylene blue signal to decrease as a result of the strong affinity to free guanine on the probe DNA. The reduced methylene blue signal was sensed with a differential pulse voltammetry method.

In another study also had been done and the LOD value of HPV measured as 3.8 nM (Nasirizadeh et al., 2011). The main idea of the study was covering gold electrode surface with probe DNA and observing the hybridization of hematoxylin labeled target DNA. Hematoxylin has more affinity for binding to the double stranded DNA than to single stranded DNA. Therefore, electrode surface can easily detect the presence of complementary DNA with voltammetry.

Another electrochemical method had been developed as a usage of biosensors for detecting HPV-16 DNA with the help of the anthraquinone labeled pyrrolidinyl peptide nucleic acid (Jampasa et al., 2014). A chitosan-modified screen-printed carbon electrode was used for immobilization of a Qterminated capture probe DNA. The

redox-active anthraquinone label had been placed close to the electrode surface before hybridization of target DNA with the probe for high electron transfer to the electrode surface. The hybridization provides a greater rigidity to the double stranded DNA than the probe thus electrochemical signal was reduced as separating anthraquinone from the electrode surface. Therefore, the detection limit of HPV-16 DNA had been reduced down to 4nM.

An electrochemical detection technology was used for detection of target HPV DNA as applying an electrical displacement assay (Liepold et al., 2008). Direct measurements of the target DNA were done in sample tubes via fabricated dipstick-type microelectrode arrays. An exact complementary sequence of target DNA which is longer than the probe DNA hybridized with ferrocene-modified detection DNA after functionalization gold electrodes with probe DNA. Therefore, target DNA released the detection DNA after hybridization on it when the sensor was dipped inside the sample. Eventually, the electrochemical signal of target HPV-6 DNA was decreased and measured down to 30 pM.

The presence of HPV-16 gene E6 had been detected previously with a developed electrochemical sensor (Campos-Ferreira et al., 2013). The graphite based pencil biosensor consists in an oligonucleotide capture probe on the electrode. The electrochemical changes were recorded when the hybridization of E6 gene was occurred. The voltammetry results enable a LOD of 15 $\mu$ M.

There were also new types immune sensors were used for detection of antibody presence to detect low viral loads via DNA avoiding the amplification steps (Piro et al., 2011). This sensor has an interdigitated electrode surface which is covered with an electrolyzed polyaniline multiwalled carbon nanotube film for detection of HPV-16 (Dai Tran et al., 2011). HPV-16 was measured down to 0.49 nM as a result of reduced the electrical signal of the aptamer due to steric hindrance of immuno-reaction between an immobilized antigen aptamer HPV-16-L1 on the surface and an antibody of HPV-16 present in the sample. Also poly(HNQ-co-HNQA) conjugated copolymer used to detect conjugation of grafted HPV-16-L1 to anti-HPV antibody (Piro et al., 2011). Voltammetric analyses gave the result in the presence of anti-HPV according to HPV-

16-L1: anti-HPV conjugation changes the rate of cation exchange between the copolymer and the solution.

#### **4.1.2 Magnetic detection technologies**

HPV detection has been also done with using magnetic nanoparticle labels. There were several examples in the literature. HPV DNA had been analyzed pM using a giant magnetoresistive biosensor as low as 10 pM concentrations (Xu et al., 2008). First, the surface of the chip had been immobilized with capture probe DNA. Then, top of the capture probe had been incubated with biotinylated target DNA. After that, streptavidin coated magnetic particles were bonded to the surface of the chip. Electrical resistance of the sensor had been detected with highly sensitive giant magnetoresistive sensors which changes even binding a single magnetic particle to target DNA (Rife et al., 2003). Another magnetic based approach had been provided which shows the impedance changes to analyze different HPV genotypes such as HPV-16 and HPV-18 target DNA. Target DNA was measured by sensing the presence of the magnetic label via the giant magnetoimpedance based biosensor (Yang et al., 2010).

HPV-16 DNA isolation had been done with combining the specific HPV 16 which conjugated to biotinylated DNA capture probes to superparamagnetic beads to the PCR for detection (Peeters et al., 2012). Two different methods had been evaluated for the maximum efficiency as tuning the probe density as binding magnetic beads to the capture probes before and after the hybridization with target DNA.

#### **4.1.3 Novel paper analytical devices**

Novel paper analytical device (PAD) which provides quantitative electrochemical HPV 16&18 detection and non-enzymatic amplification of the signal has been developed by assembling the paper material as folding it (Dungchai et al., 2009; Liu and Crooks, 2011; Noiphung et al., 2013; Santhiago et al., 2013). These diagnostic tool presents advance functionality for low-cost detection significantly without requirement of complex materials and resources. For instance, the new device consists of hollow channels for improving the sample flow through in it with its unique features (Glavan et al., 2013; Renault et al., 2013). Hollow channels provide a proper area in contrast to

cellulose papers to flow of micrometer size magnetic microbeads through the target detection location which the electrodes included. There are also other labels for modifying the DNA and its primers to allow the electrochemical detection. Here in approximately 20 nm diameter scale Ag nanoparticles (AgNPs) were used beside magnetic micro beads. This paper device also contains a fluid switch which has been made from paper for providing signal amplification with the help of the modified  $\text{KMnO}_4$  (Liu et al., 2013a; Martinez et al., 2009). All these mentioned functions had been integrated to one chip to create a quantitative, low cost, paper-only detection tool for HPV diagnosis as low as 10 copies per  $\mu\text{L}$  DNA and 530 fM of AgNP labels.

Paper based microfluidic chips solves the healthcare accessibility problems in developing countries which has low resource settings with their effective solutions and low cost features as giving conventional medical information to individuals (Anand et al., 2011). In addition to this, working on Paper device development redound so many large areas improvement, accordingly, although some limitations of adapting the large scale scientific and engineering techniques to them (Gubala et al., 2011; Martinez et al., 2009; Maxwell et al., 2013). The large scale uses of paper based tools resulted in so many development of their features even though some specific applications of paper based devices have some requirements which causes challenges. During the progress of PAD so many revaluations had been occurred such as detection strategies that provide quantitative information, lowered LOD, lower cost, increased sensitivity and dynamic range, , robust recognition probes, reduced non- specific amplification, simplified user interfaces, and reduced analysis time superior manufacturability. Although there are so many features which can be work on it for a novel well done paper device, quantitation and yield of low LOD gets the big part to focus on for a user friendly platform which is determined from World Health Organization.

Several chemical forms should use for simple and robust amplifications to achieve the low LODs on paper based devices (Hu et al., 2014). The literature also has amplification methods which can subsequently be released instantaneously to achieve gain after storing the charge as supercapacitors on paper (Ge et al., 2013a). The nanoporous gold amplification platform has been also provided to capture electroactive molecule functionalized DNA (Lu et al., 2012). In addition to these researches gold



nanoparticles have been used for electroless deposition amplification as catalysts (Dungchai et al., 2010; Liu et al., 2010). Also, malarial biomarkers have been detected via ELISA reagents which were dried and stored on a two-dimensional paper network that automated the ELISA steps (Ramachandran et al., 2014). Copper oxide nanoparticles were also importantly been used to activate fluorescence from quantum dots (Ge et al., 2013b). It has been also designed a timed-colorimetry assay to achieve detection limits for enzymes in the femtomolar range based on the differences in flow rates in the presence and absence of an enzyme by Phillips and co-workers (Lewis et al., 2013). There were different more amplification methods have been reported which can only amplify special targets and in addition to all these approaches they includes complicated processes which are not suitable for point of care applications of paper based devices (Ruecha et al., 2014; Wu et al., 2014).

A novel paper based microfluidic chip provided here which is simple, sensitive and robust for analytical detection of Human Papilloma Virus 16 and 18 types. HPV DNA are been modified with silver nanoparticle (AgNP) labels and magnetic microbeads as a unique methods basically. These labels provides two simple pre-concentration steps on the working electrode on-going spontaneous oxidation of these labels in the presence of potassium permanganate ( $\text{KMnO}_4$ ) (Dequaire et al., 2000; Liu et al., 2007). The  $\text{KMnO}_4$  used as oxidizing agent and dispersed on to the movable piece of the paper device then slipped subsequent to label sending into the channel at a specific time and location. The  $\text{Ag}^+$  nanoparticles of magnetic field deposited target DNA are be electrodeposited on the working electrode as zero-valent (Ellerbee et al., 2009). Then, Ag layer which is been pre-concentrated on the electrode as second time is be oxidized with anodic stripping voltammetry (ASV) (Nie et al., 2010). AgNPs labeled target DNA is be detected sensitively approximately only in 5 minutes at 530 fM level after the extraction step which takes 10 minutes.

## **4.2 Experimental**

In this part an electroanalytical paper based microfluidic chip presents for POC application of Human Papilloma Virus in order to diagnose Cervical Cancer. This

device can detect the HPV DNA quantitatively at the concentrations as low as 530fM. Two common high cancer risk types of HPV 16 and 18 can be detected by this novel paper diagnostic tool.

The target DNA calls model analyte is labeled with magnetic micro beads and silver nanoparticles (AgNPs) to provide non-enzymatic amplification which improves stability and response time of device. Preconcentration of AgNPs on the surface of the working electrode is provided by magnetic beads further improves sensitivity. Paper device features is improved with the hollow channels which can also allow the use of magnetic beads for increases the flow rate in the device. In addition to these features, a paper part which designed movable as a switch of chip provides target proper reaction for detection of model analyte.

To ensure optimized performance, the basic principles have been tested using a conventional electrochemical cell prior to translate the approach to the paper based microfluidic device (Scida et al., 2014). There were 3 optimization parameters. One of them was oxidation of AgNPs by  $\text{MnO}_4^-$ , the other one was detection limits for low concentrations, and the last one was presence of a high concentration of  $\text{Cl}^-$  and  $\text{PO}_4^{3-}$  in the buffer solution. It has been also optimized different kind of electrode surfaces.

Before anything else it is really important to find out how AgNPs labels and Magnetic Beads can be bonded to real patient samples for providing analytical detection of these labels. Thus, the modification theories and their results have been worked with details. A novel modification method has been developed for detection of real patient sample DNA HPV 16 and 18 on paper analytical device at the POC.

#### **4.2.1 Chemicals and materials**

Potassium Permanganate, sodium phosphate dibasic, sodium phosphate monobasic, NaCl, NaOH, micro centrifuge tubes, biotin (5-fluorescein) conjugate and microtiter plates (Corning 3650), were purchased from Sigma-Aldrich. AlexaFluor-647/streptavidin conjugate was purchased from Life Technologies (Grand Island, NY). Streptavidin-coated magnetic microbeads (2.9  $\mu\text{m}$  in diameter) were obtained from Bangs Laboratories (Fishers, IN). Citrate-capped AgNPs, nominally 20 nm in diameter,

were from Ted Pella (Redding, CA). They were modified with biotinylated DNA following a protocol by Alivisatos and co-workers (Sönnichsen et al., 2005). Details are provided in the section 4.3.7.

The preparation of the AgNP/biotin/streptavidin/magnetic microbead model analyte, and conjugation of streptavidin-coated magnetic microbeads with biotin-modified fluorescein, are described in sections 4.2.3 and 4.2.4, respectively. E7 gene of HPV 16 and 18 DNA, biotinylated and thiol labeled form of DNA and biotinylated and thiol labeled primers were purchased from IDT Technologies and diluted concentration of 100.0  $\mu$ M. A 1.0 M stock phosphate buffer solution was prepared by dissolving the appropriate amount of sodium phosphate monobasic and sodium phosphate dibasic in 0.5 L of deionized water and adjusting to the desired pH with NaOH. Erioglucine disodium salt (blue dye) was obtained from Acros Organics. All solutions were prepared with RNase free water (Qiagen).

#### **4.2.2 Instrumentation**

All electrochemical measurements were performed using a bipotentiostat (700E, CH Instruments). A polytetrafluoroethylene (PTFE) electrochemical cell was used for conventional electrochemical measurements. These experiments were performed using a glassy carbon working electrode (1.0 mm diameter), Ag/AgCl reference electrode (KCl = 1 M), Ag wire reference electrode, Hg mercury reference electrode and Pt wire counter electrode (CH Instruments).

The citrate-capped AgNPs was characterized and its diameter and size statistic (JFOL 1010 Transmission Electron Microscope), mass concentration (Thermo Fisher X Series 2 1cp-ms) and spectral properties (Agilent 8453 UV-Visible Spectrometer) presented in Figure . The modification of AgNPs with biotinylated DNA was carried out using microtiter plates and these were analyzed for fluorescence using UV-vis measurements were made with a spectrometer using a quartz cell ( $l = 10$  mm, 50  $\mu$ L). Micro Centrifuge (Thermo Scientific) was used in the synthesis of biotinylated AgNPs. Mixing of all solutions was performed with a Mini Vortexer). Vacuum centrifugation was achieved with a Thermo Savant DNA120 SpeedVac Concentrator.

### **4.2.3 Modification of citrate-capped AgNPs with biotinylated HPV primers and DNA**

Citrate capped AgNPs are used for labeling the target HPV gene to allow analytical detection of it. It has been used previously several methods for binding standard thiol ended DNA to citrate capped AgNPs in the literature. Even though modifying target DNA with thiol molecules provide linking citrate included particles, it has complications for using the procedure on the patient samples directly. It has been generally chosen previously in the literature hybridization of target DNA. Unfortunately, using AgNPs together with magnetic microbeads in the detection part have been required special labeling procedure for real patient samples.

Thus, a novel method had been provided here for binding citrate capped Ag nanoparticles with HPV E7 gene of patient sample DNA. The procedure was showed below for only standard DNA. Patient DNA which is relied on primer modification explained in details at Chapter 5. However, primer modification with AgNPs and magnetic microbeads has also been done by the same method below before labeling target DNA.

532uL RNase free water is added on to the 5'-S-HPV16-E7-Bio-3' standard DNA for preparing 100 uL DNA solution. 10 uL of a 100.0  $\mu$ M biotin- HPV standard DNA/thiol solution or HPV DNA primer/thiol solution is added into the 600uL of 0.75 nM citrate-capped AgNPs stock solution in 25 °C and mixture was vortexed at level 3 during 24 hours.

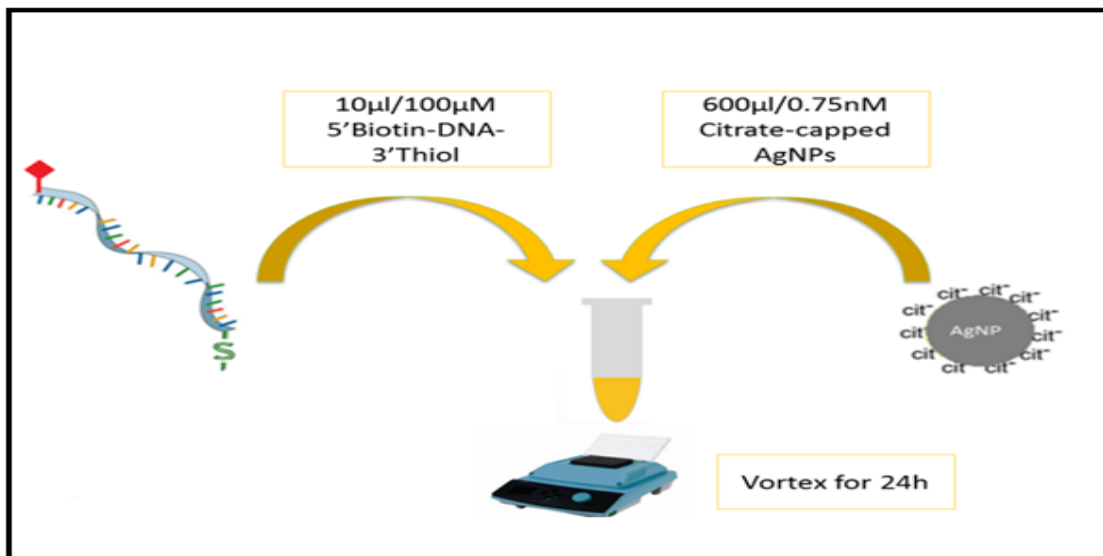


**Figure 4.2 :** Model analyte preparation figure

After this step, the salt concentration of the solution was slowly increased to 70.0 mM NaCl and 7.0 mM. It has been increased by adding 2.5  $\mu$ L of 5.0 M NaCl and 25.0  $\mu$ L of 50.0 mM PBS (phosphate buffer solution) for 4 days straight. It has been continued to vortex salt added solution during 4 days in 25  $^{\circ}$ C at level 3.

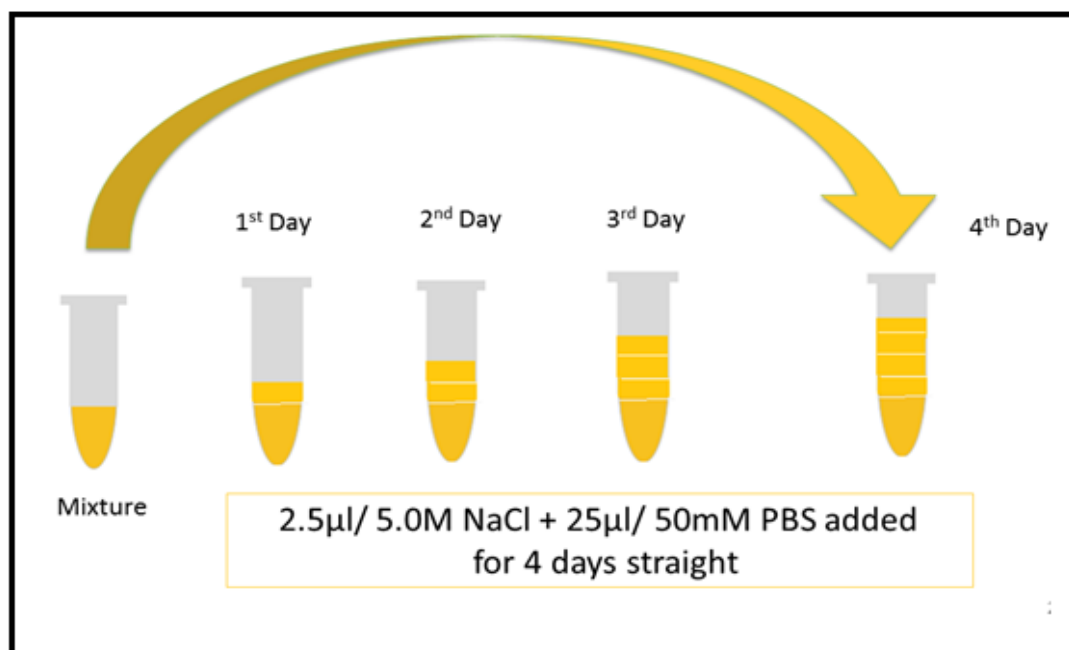


**Figure 4.3 :** 4 days precipitation process for AgNps bonded DNA

After 4 days the volume of the solution is slowly reduced to 250  $\mu$ L by putting it into the vacuum centrifuge machine. Temperature of centrifuge is adjusted to 40  $^{\circ}$ C for 3h. Then, tube is removed from vacuum. The resulted solution is centrifuged 20 min at 16000 g-(RCF) in room temperature. The supernatant is removed and it washed 3 times by a buffer which contains 540  $\mu$ L, 100mM NaCl and 60 $\mu$ L, 10mM phosphate buffer. The total amount of buffer is 600 $\mu$ L for each washing step. Washing procedure is followed by removing the supernatant and adding phosphate buffer solution for each time. Borate chloride also was used as an electrolyte medium. Model analyte modification with AgNPs and magnetic microbeads also had been done in the presence of borate chloride in order to compare effects of medium with phosphate buffer solution.

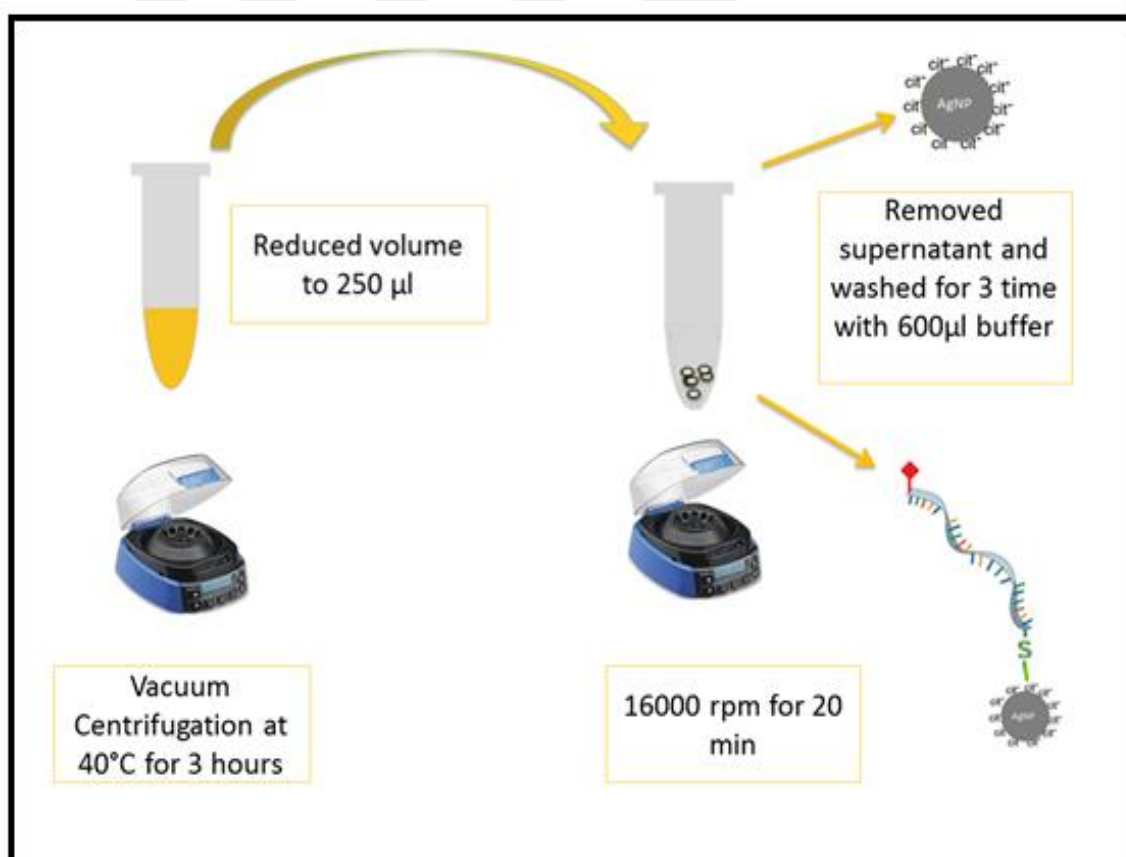


**Figure 4.4 :** Reduction of the volume of AgNPs-DNA

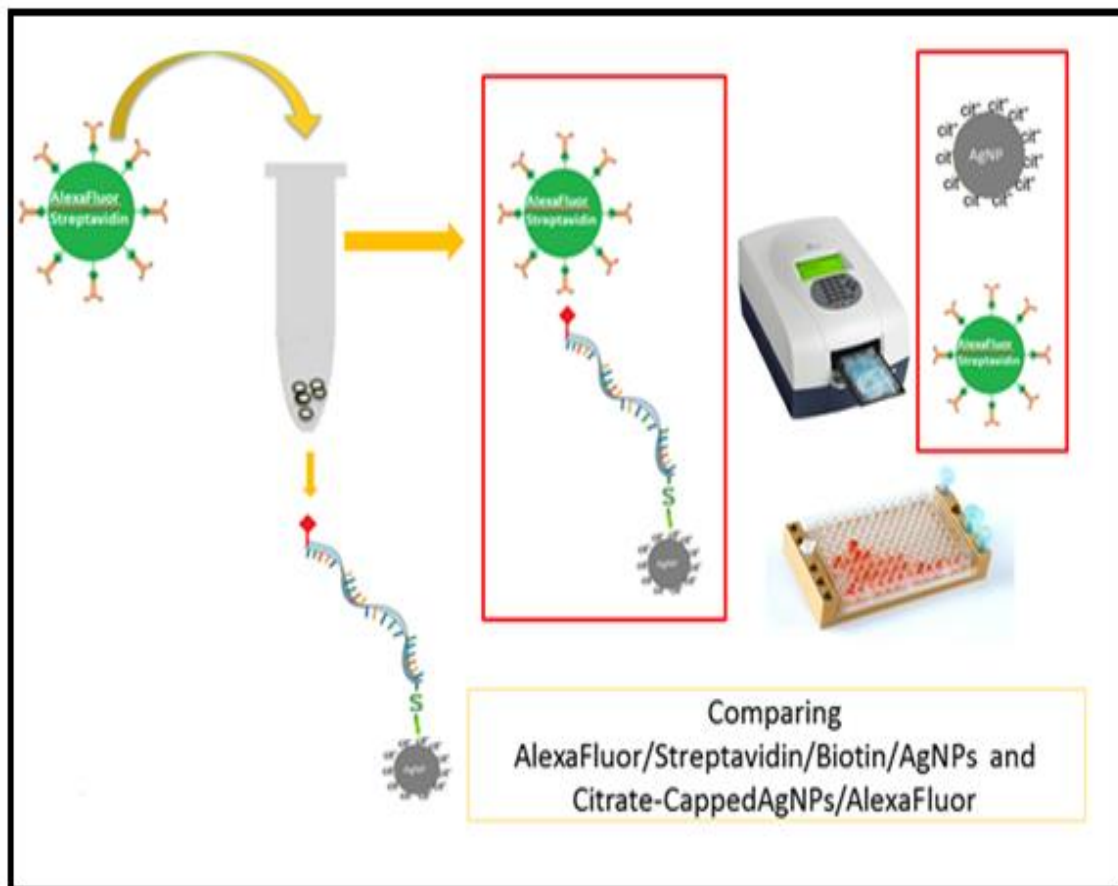


**Figure 4.5 :** Confirmation of AgNPs Bonded DNA

The Bio-DNA-S-Ag is confirmed by Alexa Flour Streptavidin Conjugate fluorescence. The Alexa Flour-647/streptavidin conjugate is prepared by adding 0.5 mL (500uL) adding purchased PBS onto the 1 mg (50.0  $\mu\text{g}/\text{mL}$  final concentration). Save at in 4 ° C. (it should be 2 mg per mL). Take 195(200 uL) biotin-Ag and add 5uL alexa dye. At the same time take 195 uL Ag stock solutions and add 5 uL dyes. Vortex both tubes at level 3 for 30 min in the room temperature. Then the prepared solution is tested by a microplate reader. AlexaFluor-647/streptavidin/biotin/AgNP solution was washed three times with the washing procedure which had been described in previous step.

Also, a control experiment was performed with original concentration which used in the synthesis of biotinylated AgNPs. 600.0  $\mu\text{L}$  of 0.75 nM citrate-capped AgNPs were incubated with the AlexaFluor-647/streptavidin conjugate (50.0  $\mu\text{g}/\text{mL}$  final concentration) at 25 °C for 30 min while vortexing at level 3. Test and control aliquots

from each experiment were placed in a microtiter plate and their fluorescence was read using a microplate reader ( $\lambda_{ex} = 652 \text{ nm}$ ,  $\lambda_{em} = 688 \text{ nm}$ ). The fluorescence recorded for the test experiment was 87% higher than that of the control experiment, (data not shown), confirming biotinylation of the AgNPs. Preparation of the AgNPs modified biotinylated HPV DNA and biotin labeled HPV primer with streptavidin/magnetic microbeads

After we obtained the biotinylated AgNPs I added streptavidin coated magnetic microbeads onto it to complete the model analyte. The magnetic microbeads are used for increasing the concentration of the model analyte on the surface of the electrode. 100  $\mu\text{L}$  of 1.15 pM, 2.90  $\mu\text{m}$  in diameter stock solution of streptavidin-coated magnetic microbeads was placed in a micro centrifuge tube and a magnet was held on a side wall against the tube for 30 s.

After that, the supernatant was removed. Microbeads were washed three times with 50.0  $\mu\text{L}$  of 10.0 mM phosphate buffer. All washing procedure was applied as placing the magnet on tube's wall side for 30 s and followed removing the supernatant. Washing steps of the magnetic microbeads were repeated 3 times.

Finally, resulted washed microbeads were re-suspended in 200.0  $\mu\text{L}$  of the previously synthesized biotinylated AgNPs solution to achieve model analyte. This step was carried out as incubating the AgNPs and magnetic microbeads at 25  $^{\circ}\text{C}$  for 30 min while vortexing at level 3. Then, resulted modified sample washed three times with 100.0  $\mu\text{L}$  of 10.0 mM phosphate buffer (pH 7.4) containing 100.0 mM NaCl. After removing the magnetic microbeads via magnetic separation the supernatant was analyzed with UV-Vis spectra.

The peak at 400 belongs to individual AgNPs and the plasmon excitation at 510 nm belongs to agglomerated AgNPs. The absorption of the DNA coating the AgNPs were showed with band at 260 nm. The decrease of absorbance peak at 400 and 510 nm is proof of the successful attachment of the AgNPs to the magnetic microbeads.



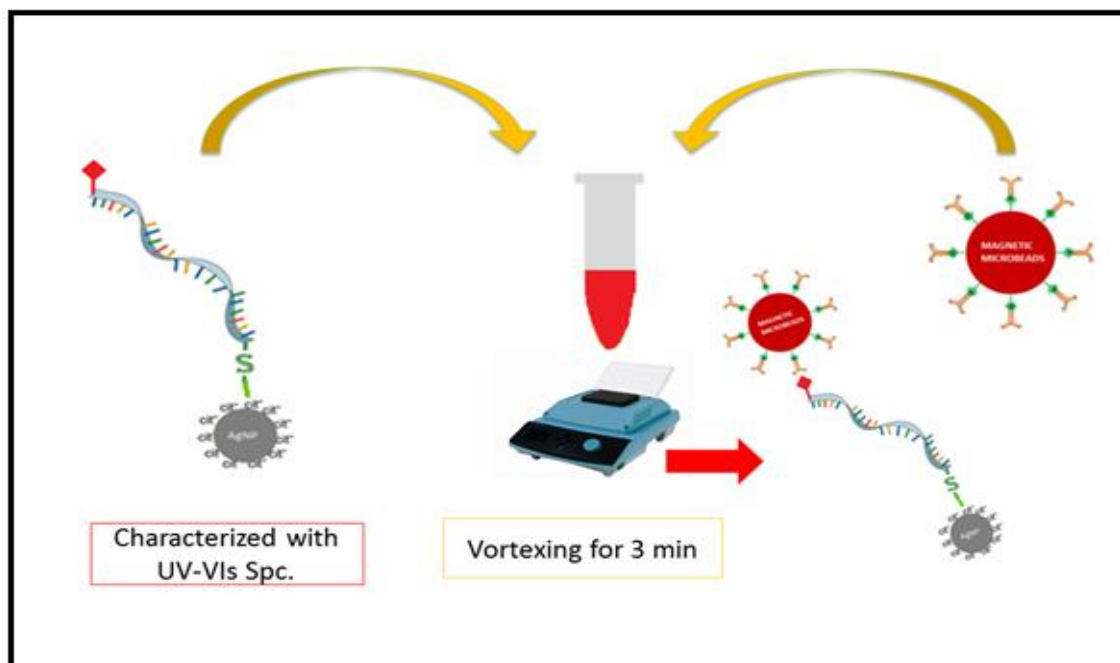


**Figure 4.6 :** Binding of Magnetic Micro Beads

After synthesizing the AgNP/biotin/streptavidin/magnetic microbeads model analyte, the AgNP concentration in the model analyte solution was calculated by adding 125.0  $\mu\text{L}$  of PBCl, 50.0  $\mu\text{L}$  of 187.0  $\mu\text{M}$   $\text{KMnO}_4$ , 3.0  $\mu\text{L}$  of model analyte, and 47.0 ml of deionized water to the conventional electrochemical setup.

#### 4.2.4 Modification of DNA with magnetic bead and Ag bonded primers for analysis of patient samples

DS DNA modified with primers after labeling biotin and thiol ended primers with AgNPs and magnetic beads. Model analyte preparation and confirmation had first been tested using standard single strength biotin and thiol labeled DNA. Then labeled standard DNA directly modified with AgNPs and magnetic microbeads. As known apparently, labeling patient DNA after extraction from real samples has a significant role to prepare analyte for analysis in microfluidic device.

The list of the modified primers and standard DNA which were labeled with biotin and thiol has also been showed below in Table 4.2 .HPV 16 and 18 DNAs were previously purchased from IDT for the other experiments. Herein, primers of these DNA's which

are labeled with specific reagents is showed according to special features of the novel method. Thus, primer sequences were different than the previously given one in part 2.2.1. The new method does not need enzyme for amplification of analyte thus probe is not a requirement for this experiment. Forward and reverse primers generally bind to the opposite strengths of DNA during enzymatic amplifications, contrary to that it has been needed two specific primers which can both bind to same strength of DNA's both ends. One of is which ended 5' should be biotin labeled primer and the other one should be labeled with thiol from its 3' end.

<b>DNA abbreviation</b>	<b>DNA sequence</b>
<b>HPV 18-bio</b>	5'- TGT TGT AAG TGT GAA GCC AGA A/3Bio/-3'
<b>HPV 18-S</b>	5'-/5ThioMC6-D/ATG TCA CGA GCA ATT AAG C-3'
<b>HPV18</b>	5'-ATG TCA CGA GCA ATT AAG CGA CTC AGA GGA AGA AAA CGA TGA AAT AGA TGG AGT TAA TCA TCA ACA TTT ACC AGC CCG ACG AGC CGA ACC ACA ACG TCA CAC AAT GTT GTG TAT GTG TTG TAA GTG TGA AGC CAG AA-3'
<b>HPV16 bio-S</b>	5'-/5ThioMC6-D/AGC TCA GAG GAG GAG GAT GAA ATA GAT GGT CCA GCT GGA CAA GCA GAA CCG GAC AGA GCC CAT TAC AAT ATT GTA ACC /3Bio/-3' -3'
<b>HPV16 –bio-rev</b>	5'- GAGA CCC ATT ACA ATA TTG TAA CC/3Bio/-3'
<b>HPV16 –s-fwd</b>	5'- /5ThioMC6-D/ AGC TCA GAG GAG GAG GAT GAA -3'
<b>S-primer-S</b>	5'- /5ThioMC6-D/ AGC TCA GAG GAG GAG GAT GAA /3ThioMC3-D/-3'

**Table 4.2.** Modified DNA sequence

Different binding methods and different concentrations had been used for experiments with patient sample DNA. DS DNA and primers molarity and volumes were changed to catch optimal parameters. Two different kinds of thiol labeled primers also tested which were bonded from one end and two ends. Labeling primers with AgNPs and magnetic microbeads were relied on the same procedure except using various oligonucleotide concentrations which were described in previous parts 4.2.3 and 4.2.4. The distinguishing feature of this method are bonding amplification and detection suppliers such as AgNPs and magnetic beads with primers, and also purifying the target DNA via hybridization. Previously studies in the literature include modification with Magnetic beads for hybridization of target DNA. However, hybridized DNA also should be labeled with thiol which requires more steps included specific methods. Thus, labeling primers first and combining them together for hybridization followed by removing remains was applied as a preferable and novel method for HPV detection.

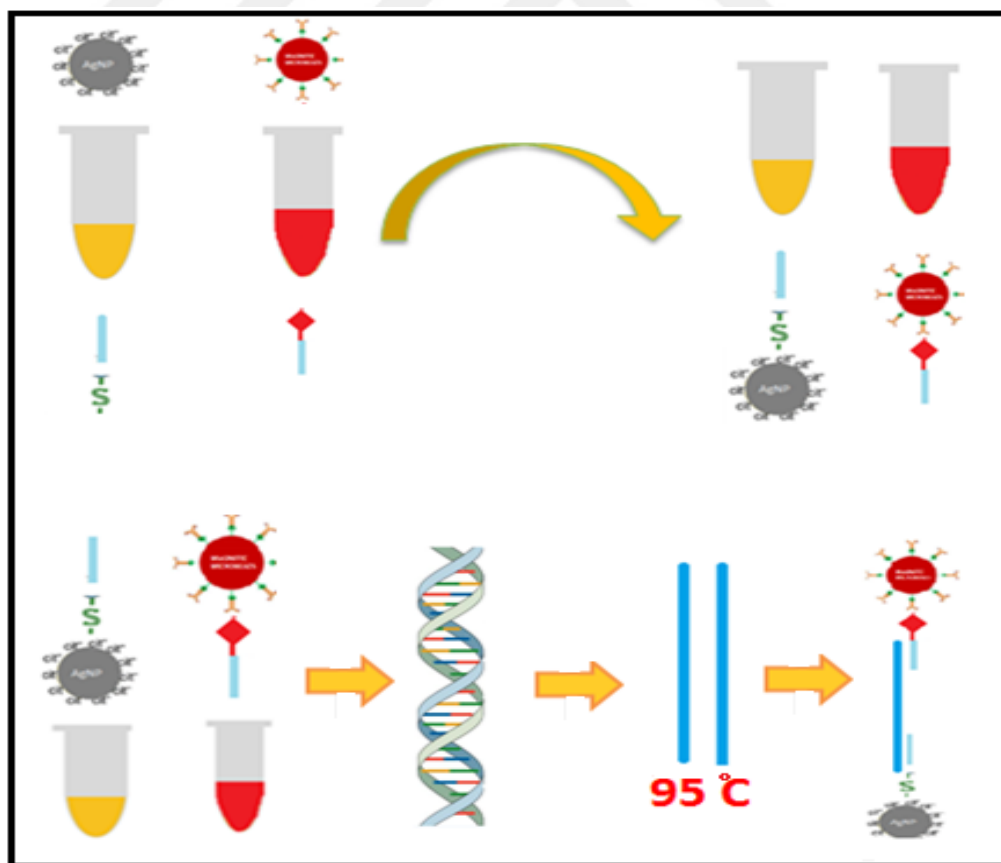


**Figure 4.7 :** Modification of DNA with Magnetic Bead and Ag Bonded Primers for Analysis of Patient Samples

The novel method was described in Figure 4.7. First, changeable various concentrations of specific primers, which are thiol and biotin labelled, were modified with AgNPs and magnetic microbeads (Table 4.2). Then, Ag-Primer and S-Primer added into the extracted DS-DNA (Patient Sample). All of oligonucleotides were heated at 95°C for denaturation. After that, it was cooled, and annealed with primers during extension. Finally, the model analyte provided from patient sample was washed with the help of magnet to remove remaining from the environment for accurate detection. The method also has been tested via bonding DS-DNA and biotin labelled primer followed by magnetic micro bead modification before bonding Ag-Primer with DNA. Optimal primer and DNA concentrations have been determined right along with confirmation of this method. Thermo Scientific NanoDrop, ND-2000c UV-vis spectrometer has been used for confirmation experiments. Electrochemical measurements for yield calculations and confirmations were performed by using a 700E, CH Instruments biopotentiostat.

#### **4.2.5 Anodic stripping voltammetry measurements using the conventional electrochemical setup**

A background ASV in the presence of 125.0  $\mu\text{L}$  of PBCl, 50.0  $\mu\text{L}$  of 187.0  $\mu\text{M}$   $\text{KMnO}_4$ , and 50.0  $\mu\text{L}$  of deionized water was always performed between measurements to assure the surface of the glassy carbon electrode (GCE) was clean. After each background experiment and before each test run, the GCE was polished with micro-cut paper for 1 min, rinsed with deionized water, and dried with Kim-wipes. The surface of reference electrode also should be cleaned before each test run because of its porous membrane catches the AgNPs which is hard to be removed from the surface. An alkaline pH 10 medium solution was used to completely remove the AgNPs from the surface of the reference electrode followed rinsing deionized water.

### **4.3 Result and Discussion**

After the optimization of all the extraction steps are finished, we have worked on optimization and characterization of electrochemical detection before the fabrication of produced paper-based analytical microfluidic device. Prof. Crooks from Texas

provided a paper analytical device which detects concentrations of DNA as low as approximately 700 FM. Our aim is to improve the device sensitivity, and features in order to provide a new type for combined HPV16 and 18 DNA via non enzymatic amplification.

Herein, both magnetic microbeads and AgNPs were used to improve the amplification of the target DNA. The main idea of analytical detection relies on oxidation and reduction of AgNPs, and pre-concentration of sample on the surface of the working electrode via magnet and voltage. Thus, all the detection parameters were optimized by considering the working electrode surface, amount of  $\text{KMnO}_4$ , preconditioning time, and voltage optimization, reference electrode specialty as well as electrolyte solution properties. Borate Chloride and Phosphate Buffer Chloride Solution can be examples on conventional cell in order to adjust it in with more convenient properties for the real paper based detection device.

It has also been enhanced the properties of model analyte to be make proper the usage of patient samples as labeling primers. Therefore, different labeling methods had been developed and tested for HPV 16 and 18 in order to decrease detection limits and make applicable on the patient samples. The confirmation results of model analyte also presented in this section.

The electrochemical detection method, which is a key feature of the device, consists of three steps. Oxidation of AgNPs using  $\text{MnO}_4^-$ , reduction of the resulting  $\text{Ag}^+$  onto an electrode surface, and ASV to quantitate the number of AgNP labels originally present were each steps of detection procedure. It has been tested the basic principles using a conventional electrochemical cell prior to translating the approach to the paper microfluidic chip to ensure the viability of this method, and to ensure optimized performance. The electrochemical cell used for these experiments is shown in Figure 4.

The experiment was carried out as follows. First, the electrolyte, consisting of 125.0  $\mu\text{L}$  of 100.0 mM phosphate buffer (pH 7.4) containing 100.0 mM NaCl (this buffer is referred to hereafter as PBCl) and 50.0  $\mu\text{L}$  of 187.0  $\mu\text{M}$   $\text{KMnO}_4$ , were added to the test cell. Second, 50.0  $\mu\text{L}$  of an aqueous solution containing citrate-capped AgNPs were added. Under these conditions,  $\text{MnO}_4^-$  ( $E^\circ = 1.18 \text{ V vs NHE at pH 7.4}$ )<sup>149</sup> should be

oxidized the AgNPs to Ag<sup>+</sup> ( $E^\circ = 0.16 \text{ V vs NHE}$  in the presence of 100 mM Cl<sup>-</sup>).<sup>150</sup> Importantly, there are 250,000 Ag atoms in one AgNP, which results in 250,000 equivalents of charge for every AgNP. Third, after 30 s, the working electrode was held at constant temperature for a while to electrodeposit Ag. Finally, the potential was held at 0 V for 10 s, and then it was swept from  $E_i = 0$  to convenient  $E_f$  at  $v = 10 \text{ mV/s}$  to electrochemically oxidize Ag to Ag<sup>+</sup>.

### 4.3.1 Choosing proper reference electrode

First, the electrode medium voltages are optimized for arranging proper working potential range. A Glassy Carbon Electrode is used as a working electrode. A Platinum electrode is used as a counter electrode. It has been tried 3 different reference electrodes to achieve the best result for electrochemical detection of AgNP modified DNA. All optimization steps have been done in the conventional electrochemical cell (Figure 4.8)

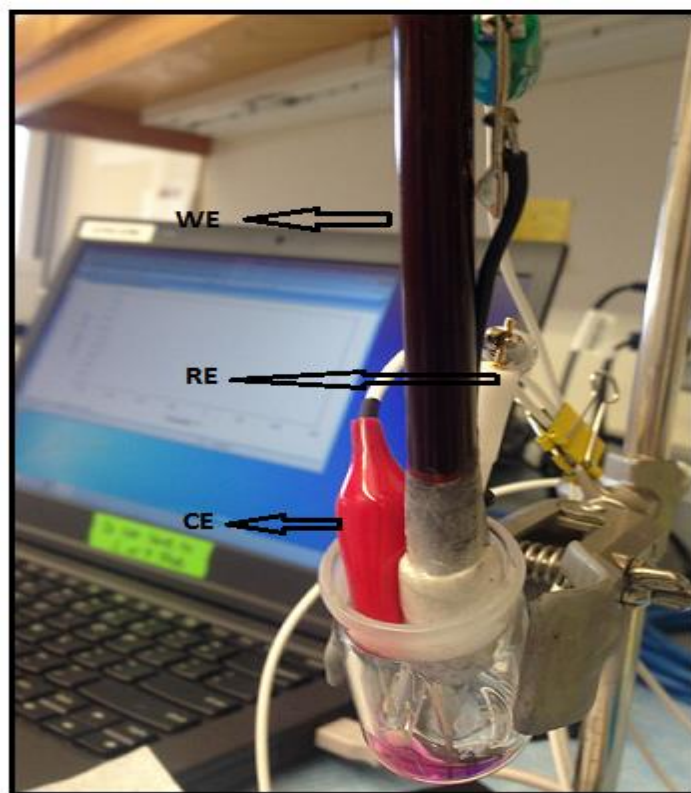


**Figure 4.8 :** Conventional Electrochemical Cell Setup. 3 different reference electrodes have been used during experiments such as Mercury, Wire Ag and Ag/AgCl. It has also used different working electrodes such as Graphite Pencil, Glassy Carbon and Graphene electrode.

Ag wire, Ag/AgCl and Mercury electrodes are used as a reference electrode. According to the results, Ag wire electrode is not proper for the detection. It gave additional peak in the working potential range. Mercury electrode results also didn't give a proper peak for the AgNPs compare to Ag/AgCl reference electrode.

The entire processes were done according to the parameters below;

Initial Potential (V)	-0.3
High Potential (V)	0.4
Low Potential (V)	-0.3
Scan Rate (V/s)	0.1

**Table 4.3.** Potential Range of the Processes

Electrochemical cell includes 125  $\mu\text{L}$  electrolyte solutions, 50  $\mu\text{L}$  deionize free water, 50  $\mu\text{L}$   $\text{KMnO}_4$  and various concentration of AgNPs. Additional to these parameters changing preconditioning time and voltage also applied for Anodic Stripping Voltammetry Detections. The electrolyte solution is also tested for achieving the highest charge capacity. AgCl electrode is used as a reference electrode.

#### 4.3.2 Electrochemical characterization of AgNPs detection with conventional cell

Electrochemical results are obtained from using a conventional electrochemical cell. It demonstrated the viability of the detection strategy used in the paper microchip platform. ASV is corresponding to samples containing 0 to 2.64 pM citrate-capped AgNPs (nominally 20 nm). The data was corrected for a sloping baseline. The working electrode was glassy carbon (1.0 mm diameter), and the electrolyte is consisted of 125.0  $\mu\text{L}$  of PBCl.  $v = 10$  mV/s. Calibration curve is showed the relationship between the charge and under the ASV peaks. After that, the AgNP concentration is introduced to the cell. The black dashed-line is the best linear fit of the experimental data. The error bars for each data point are represented with the standard deviation for three different measurements.

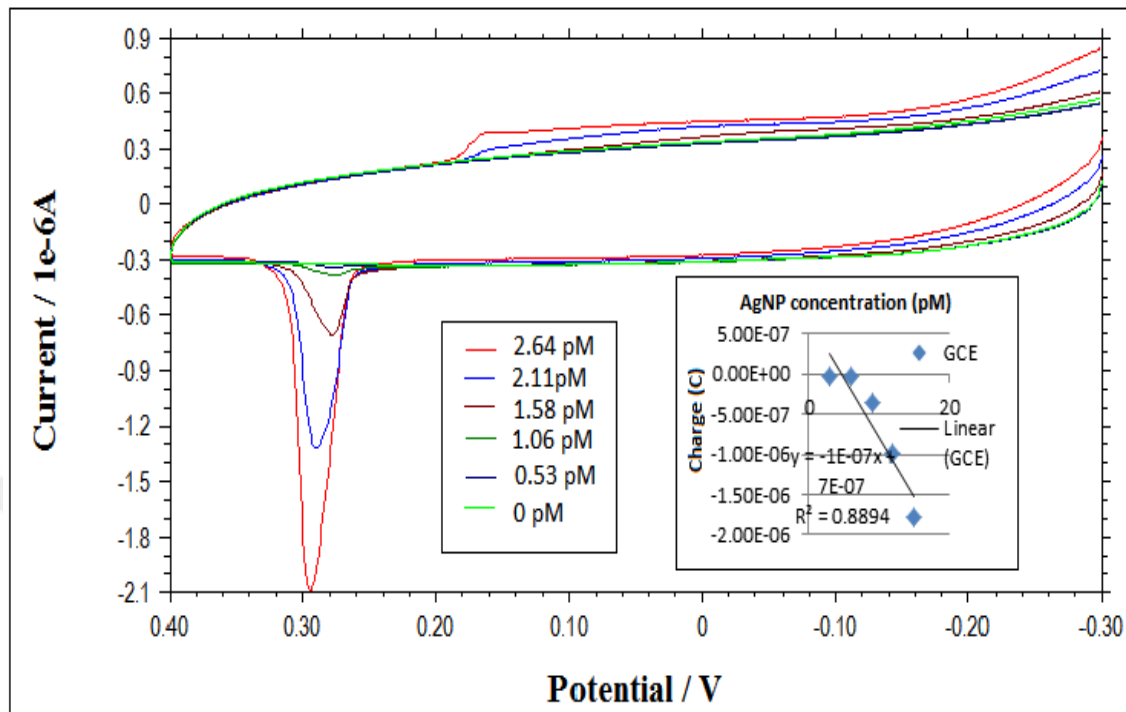


**Figure 4.9 :** Electrochemical results, obtained using a conventional electrochemical cell

The anodic stripping voltammetry resulting from the foregoing experiment are shown in Figure 4.9. There are two important observations. Figure 4.9 shows that electrodeposition of Ag followed by anodic stripping results in an easily detectable signal even at concentrations as low as 3.3 pM. Second, the calibration curve inside graphic reveals a linear correlation between the charge measured under the ASV peaks and the concentration of AgNPs over the range from 3.3 to 25 pM. The nonlinear part of the curve probably arises from the use of a fixed (and for the two data points at high AgNP concentration, substoichiometric) concentration of the  $\text{MnO}_4^-$  oxidant.

#### 4.3.3 Ag/AgCl reference electrode for different concentrations of $\text{KMnO}_4$

HPV electrochemical detection tool is first optimized with conventional electrochemical cell as changing different parameters for achieving the best detection limit of it. First the proper reference electrode has been chosen and the voltage range set for detection of AgNPs modified HPV16 and 18 DNA.



The entire detection process is occurred in the presence of 50uL  $\text{KMnO}_4$ , 47uL water. It is added in to the cell for each experiment for arrange the several dilutions of AgNPs. PBSCl buffer is used as electrolyte solution. 62.5 uL 100mM PBS and 62.5 uL 100mM NaCl are used to achieve the appropriate PBSCl buffer.

The  $\text{KMnO}_4$  concentration is very important for oxidation of AgNPs spontaneously. Figure 4.10 shows the result of  $\text{KMnO}_4$  optimization.

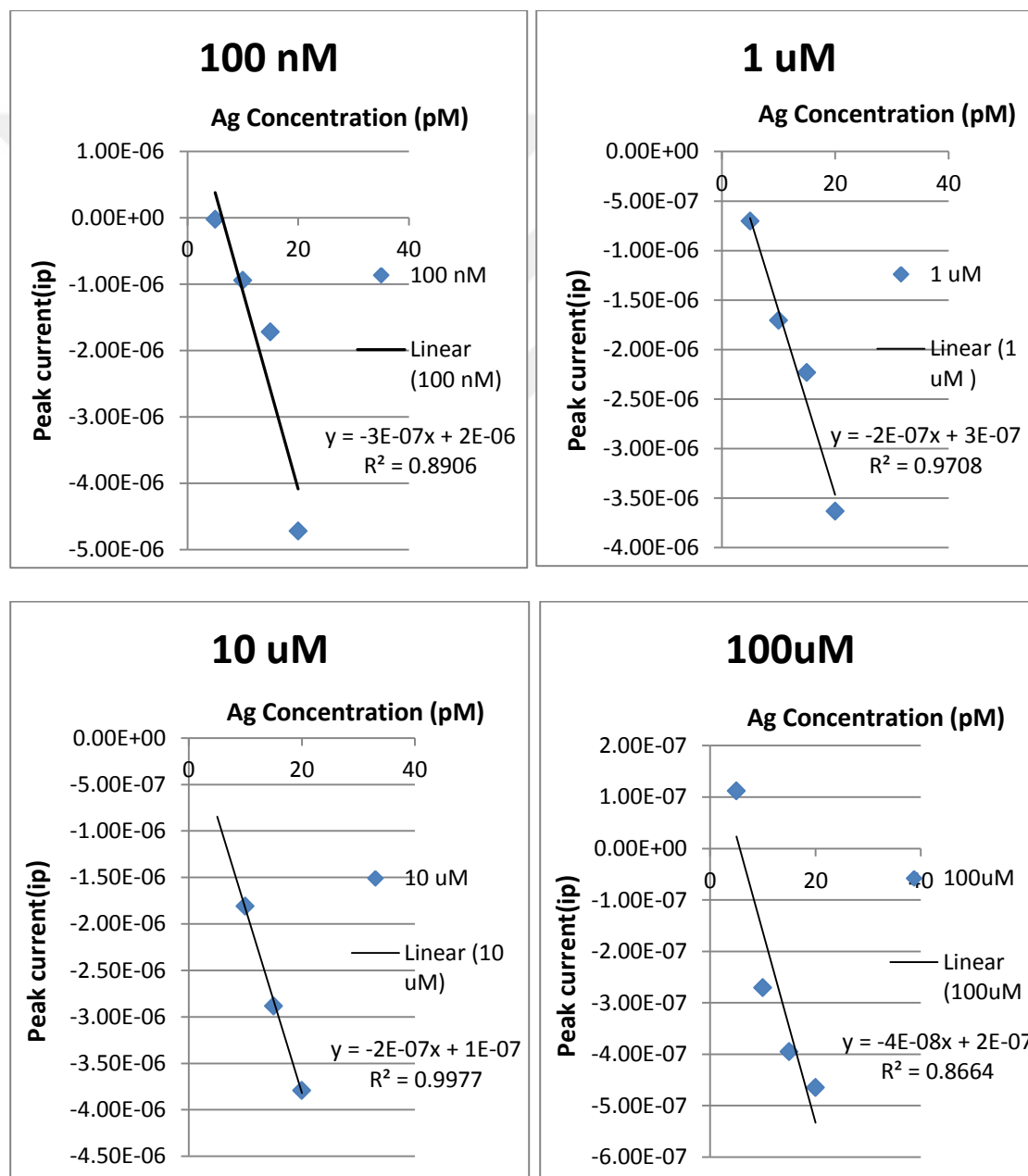


**Figure 4.10 :**  $\text{KMnO}_4$  Concentrations sensitivity results

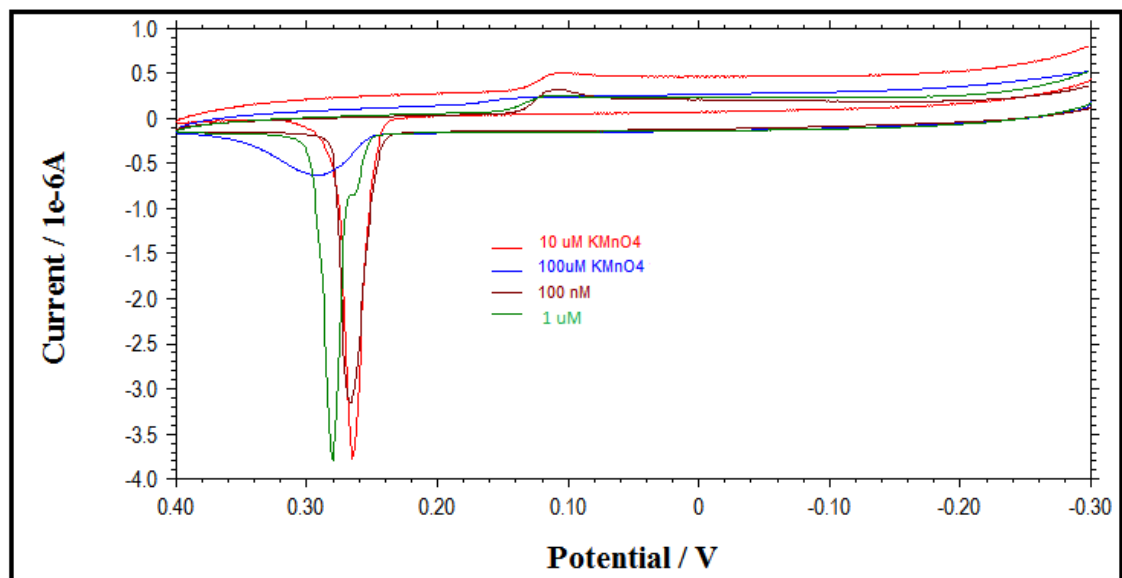


**Figure 4.11 :** The peak current results of  $\text{KMnO}_4$  concentrations for 3.53pM AgNPs

The 5 uL amount of AgNPs is detected as we expected. The surface of all electrodes cleaned also with alkaline solution to remove AgNPs. The maximum dilutions of  $\text{KMnO}_4$  resulted with huge capacitive current. It also reduced the peak current. 10uM  $\text{KMnO}_4$  has good repeatability then the others. 10 uM also has the highest current.

100 nM, 100  $\mu\text{M}$ , 10  $\mu\text{M}$  and 1  $\mu\text{M}$   $\text{KMnO}_4$  concentrations are tested for understanding the effect of it to the electrochemical detection of AgNps. 50  $\mu\text{L}$  solution of  $\text{KMnO}_4$  added for each experiment. The results are calculated. According to the graphics, it has been decided to use 10  $\mu\text{M}$   $\text{KMnO}_4$ .

100 nM	1 uM	10 uM	100uM	AgNPs
-2.30E-08	-7.05E-07		1.12E-07	5
-9.45E-07	-1.71E-06	-1.81E-06	-2.71E-07	10
-1.72E-06	-2.23E-06	-2.88E-06	-3.95E-07	15
-4.72E-06	-3.63E-06	-3.79E-06	-4.65E-07	20

**Table 4.4.**  $\text{KMnO}_4$  Concentrations for 100 nM, 100  $\mu\text{M}$ , 10  $\mu\text{M}$  and 1  $\mu\text{M}$

#### 4.3.4 Preconditioning time optimization

The preconditioning time and potential are optimized after the optimization of  $\text{KMnO}_4$  concentration. 9  $\mu\text{L}$  AgNPs are used for time optimization in the presence of 50  $\mu\text{L}$  10  $\mu\text{M}$   $\text{KMnO}_4$ . 47  $\mu\text{L}$  water is added in to the cell for each experiment for dilution of AgNPs. PBSCl buffer is used as electrolyte solution. 62.5  $\mu\text{L}$  100  $\text{mM}$  PBS and 62.5  $\mu\text{L}$  100  $\text{mM}$  NaCl are used to achieve the appropriate PBSCl buffer.

These are the preconditioning times that is worked on for optimal time; 30s, 60s, 90s, 120s, 150s, 180s, 210s, 240s, 260s, 290s, 320s. 11 different preconditioning time is applied for achieving the best one.

The results are shown below for different preconditioning times. We can see from the results that the preconditioning time after 260s shifted the voltage to the positives. The results are also shown that the increasing time always increases with the peak current. It will be a POC device, so we should set the time average.

Time Optimization	Time
4.52E-08	30
2.60E-08	60
8.63E-08	90
1.26E-07	120
2.91E-07	150
<b>2.30E-07</b>	180
<b>3.07E-07</b>	210
3.78E-07	240
8.44E-07	260
7.04E-07	290
1.69E-06	320

**Table 4.5.** Preconditioning time peak current results

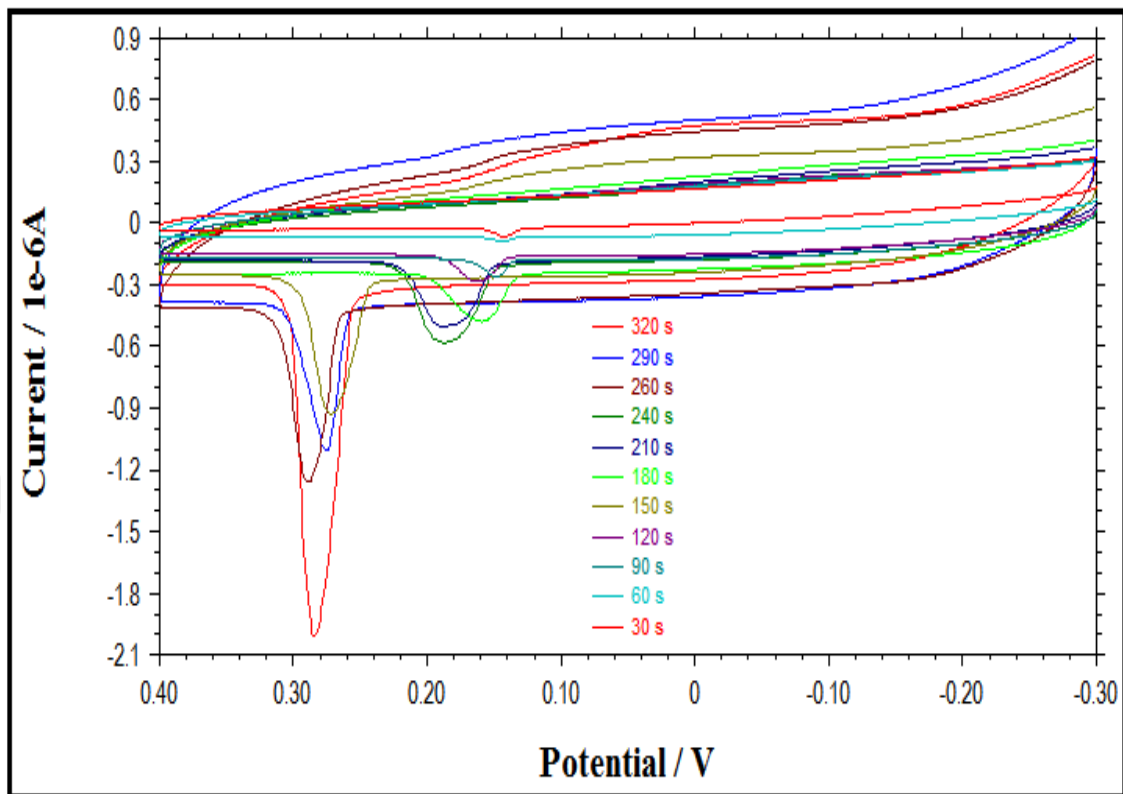


Figure 4.12 : Time optimization peak current results

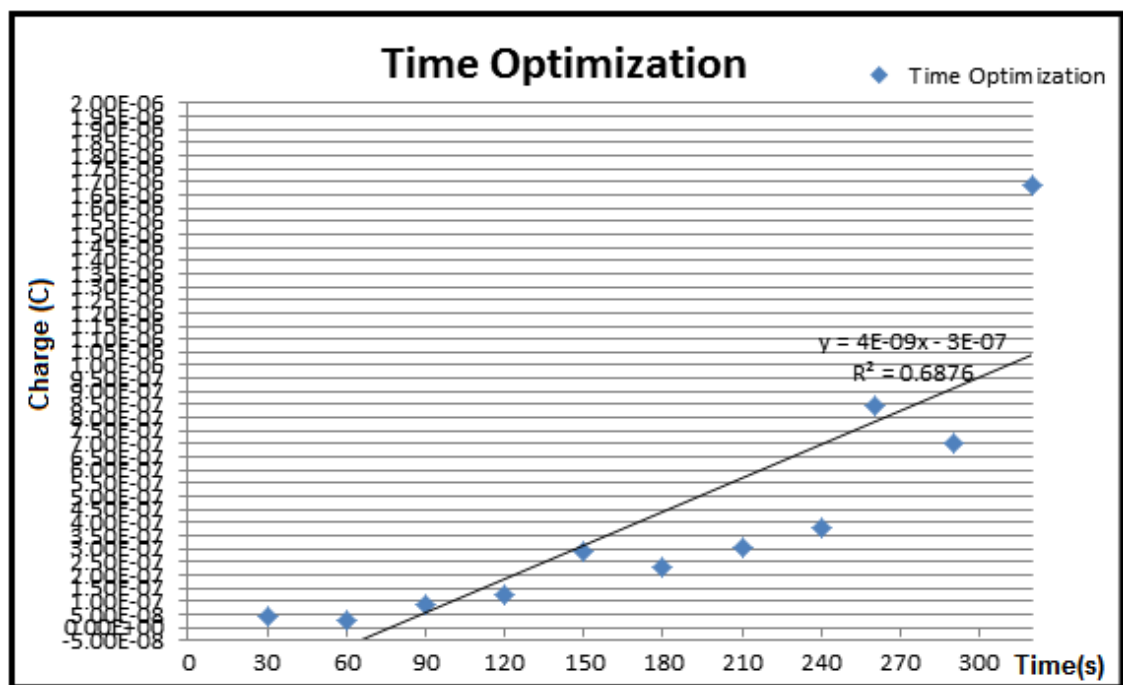


Figure 4.13 : Sensitivity results of time optimization

The plots show that preconditioning time increases with the AgNPs's current. The plots also show that increasing the preconditioning time is shifted the plots to the positive voltages. The red plot which has been taken for 150s gave much more efficiency than 210s and 240s. We can also see from the results that there is not an effective increase between 210s curve and 240s curve. Increasing effect is decreased, while the time is increased from 150s to 240s.

#### 4.3.5 Preconditioning voltage optimization

Increasing concentrations of AgNPs are detected for the voltages which changes from -0.4, -0.3, -0.2, -0.1 to 0. The electrolyte is same as with the preconditioning time experiment. These results show that -0.3 and -0.4 are good preconditioning voltages. Positive voltages are not proper for preconditioning.

For -0.4 V	For -0.3 V	AgNPs
-5.91E-07	-4.83E-07	3 $\mu$ L
-9.98E-07	-9.98E-07	6 $\mu$ L
-1.26E-06	-1.14E-06	9 $\mu$ L

**Table 4.6.** AgNPs voltage optimization for -0.4V and -0.3V

Increasing concentrations of AgNPs are detected for the voltages which changes from -0.4, -0.3, -0.2, -0.1 to 0. The electrolyte is same as with the preconditioning time experiment. These results are showed the optimal preconditioning voltage and sensitivity of it.

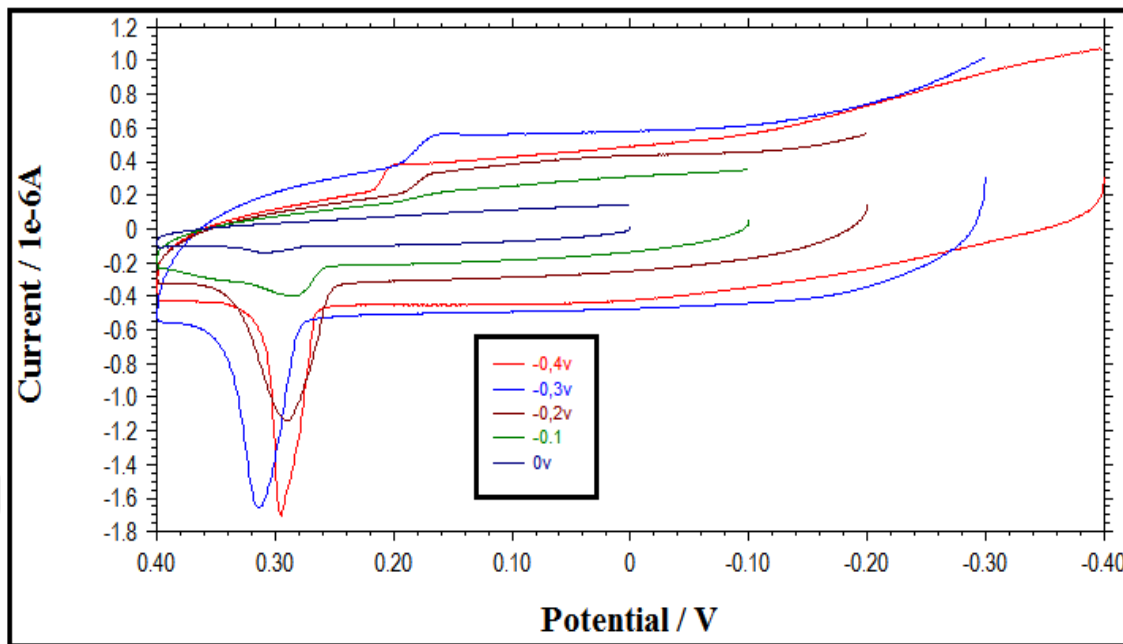


**Figure 4.14 :** Peak Current results of voltage changes

These results show that -0.3 and -0.4 are good preconditioning voltages. Positive voltages are not proper for preconditioning.

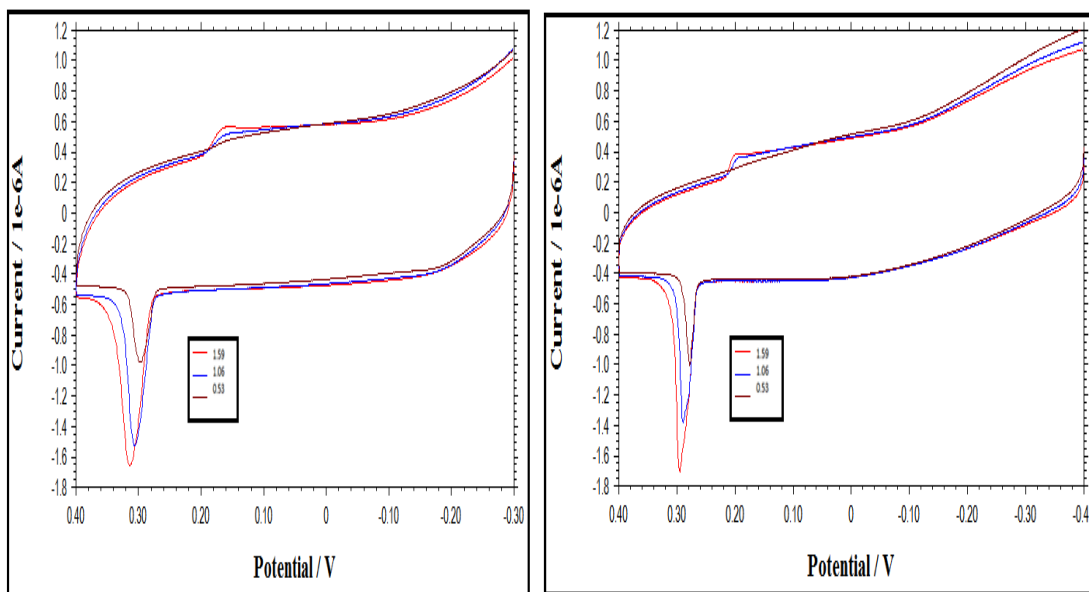


**Figure 4.15 :** Comparing -0.4 V and -0.3V preconditioning voltage

These results shows that -0.4 V preconditioning voltage has better sensitivity then -0.3.

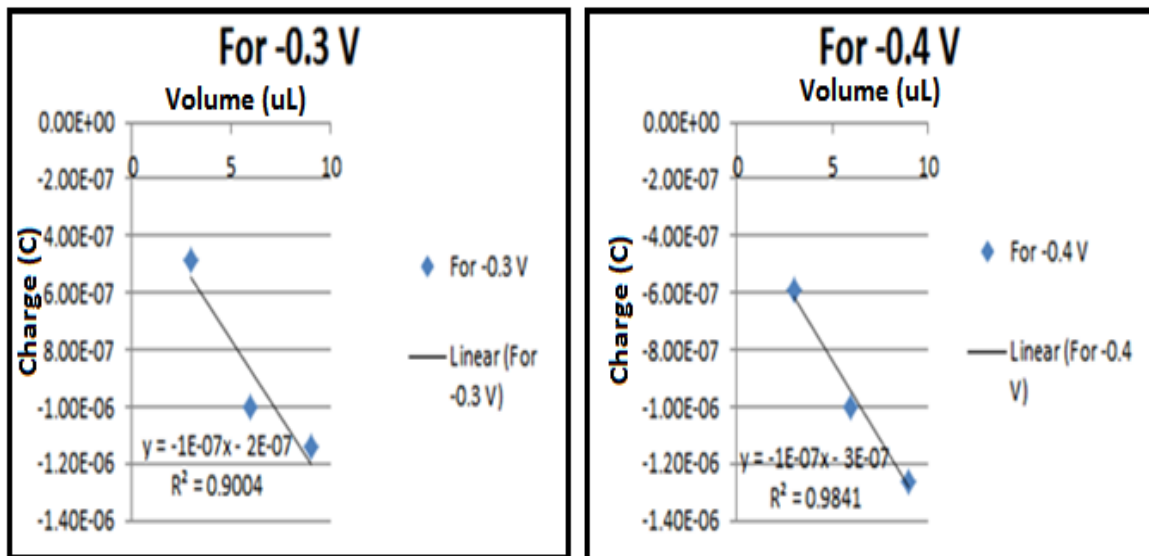


**Figure 4.16 :** Sensitivity results of -0.4 V and -0.3V preconditioning voltage

#### 4.3.6 Detection of AgNPs in the presence of borate chloride

The Borate Chloride medium increased the yield approximately 10 times more than PBSCl medium. Although the amount of AgNPs were decreased by adding more water, Borate solution is more sensitive and detection limit is better than PBSCl

Borate with 47 uL water	PBSCl	AgNPs
2.79E-06	1.78E-06	15
2.07E-06	9.90E-07	12
1.96E-06	3.62E-07	9
1.40E-06	3.98E-08	6
8.64E-07	2.26E-08	3

**Table 4.7.** Borate and PBSCl medium peak current results

The electrolyte solution buffer is also effected to the detection limit. The Borate Chloride medium increased the yield approximately 10 times more than PBSCl medium. It has been added 47 uL water for decreasing the molarity of AgNPs because

of the results. Borate Chloride electrolyte solution should use for achieving the 10 time better detection limits.

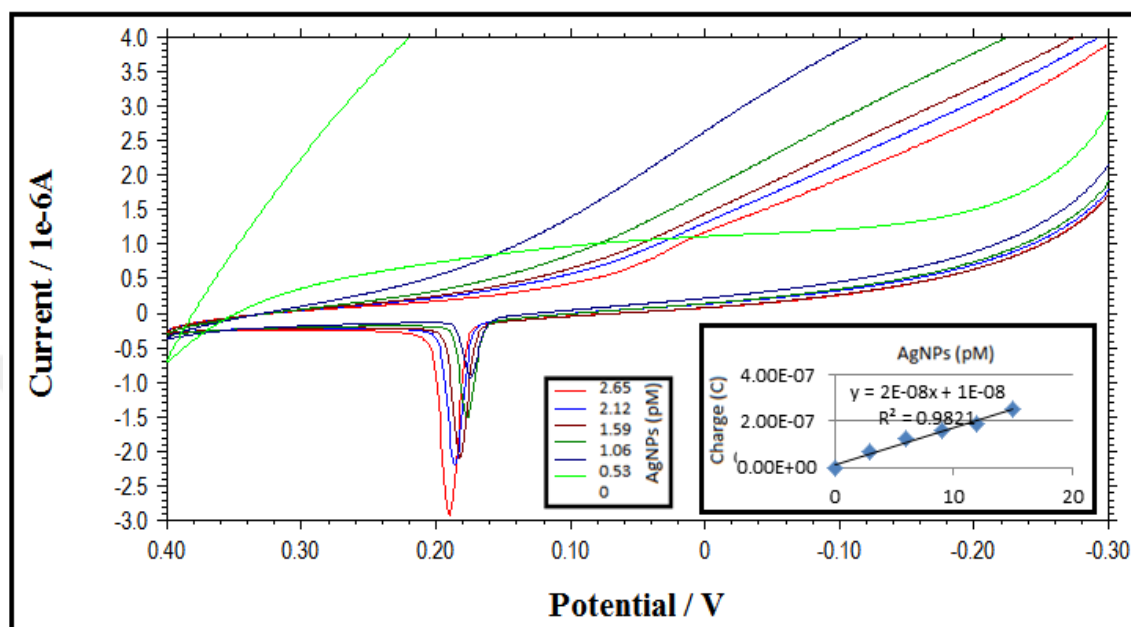


Figure 4.17 : Borate medium peak current results

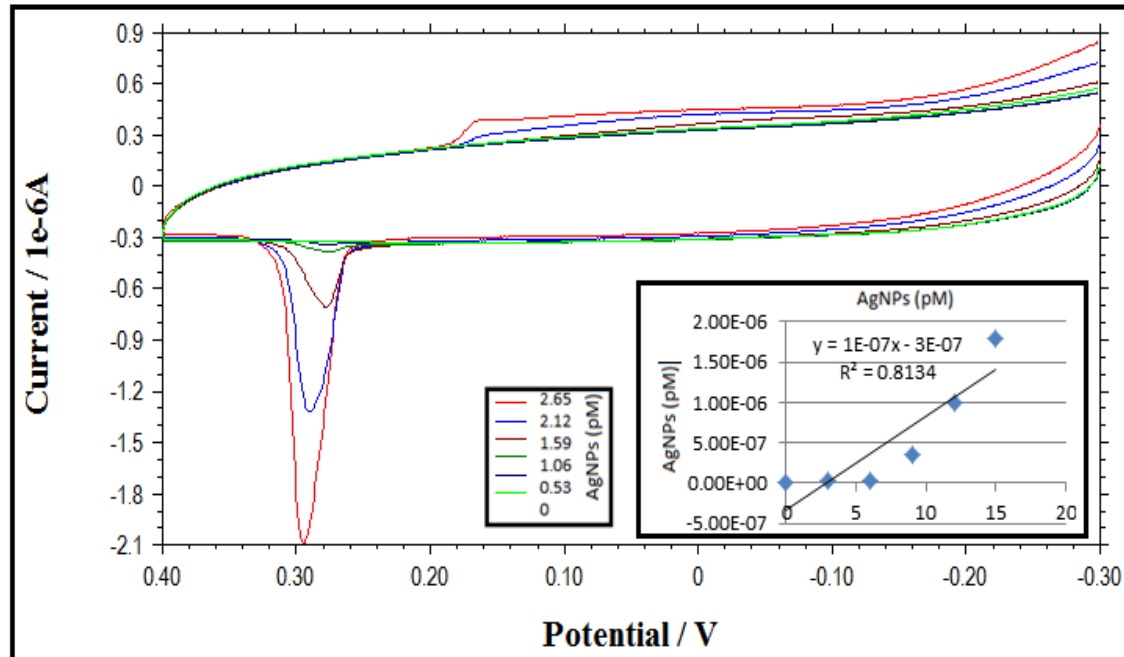


Figure 4.18 : Sensitivity results PBSCl medium



#### 4.3.7 Confirmation of model analyte and analyzes result of silver nanoparticles

Modification of HPV DNA with citrate capped AgNPs, and streptavidin coated magnetic micro beads have been confirmed with Thermo Scientific NanoDrop ND-2000c UV-vis spectrometer. The list of the modified primers and standard DNA which were labeled with biotin and thiol has also been showed below in Table ... . The analyze results of AgNPs and magnetic micro beads which were used during modification steps also have been given in this part.

The citrate-capped AgNPs was characterized, and its diameter, size statistic, mass concentration, and spectral properties are presented in Figure 4.19 and 4.20.

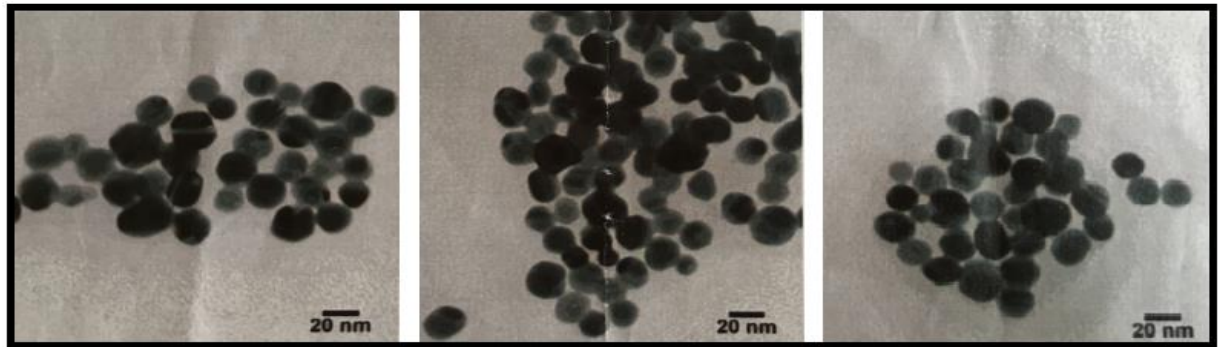


**Figure 4.19 :** Electron Microscope analyze results of AgNPs which were purchased from from Ted Pella (Redding, CA)

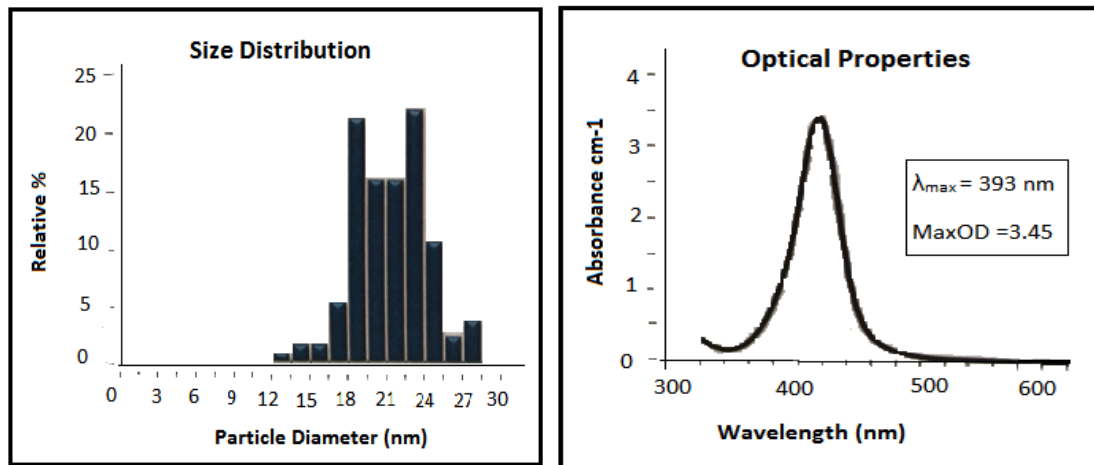


**Figure 4.20 :** UV-Visible Spectrometer and mass concentration results of AgNPs which were purchased from from Ted Pella (Redding, CA)

According to results Citrate-capped AgNPs, nominally 20 nm in diameter measured size is 19.9N+/-2.9 nm.

Figure 4.20 shows the UV-Vis spectra of the supernatant after removing the magnetic microbeads via magnetic separation before and after incubation with streptavidin-coated magnetic microbeads. The red trace corresponds to the biotinylated AgNP absorbance before incubation with streptavidin-coated magnetic microbeads. The brown trace corresponds to the supernatant absorbance after incubating biotinylated AgNPs with streptavidin-coated magnetic microbeads.

The peaks at 400 and 510 nm on the red trace are attributed to the plasmon excitation of individual and agglomerated AgNPs, respectively. The band at 200 and 220 nm corresponds to the absorption of the DNA coating the AgNPs. The large (Cate et al., 2013) absorbance decrease at 400 and 510 nm indicates the successful attachment of the AgNPs to the magnetic microbeads(Fridley et al., 2012).

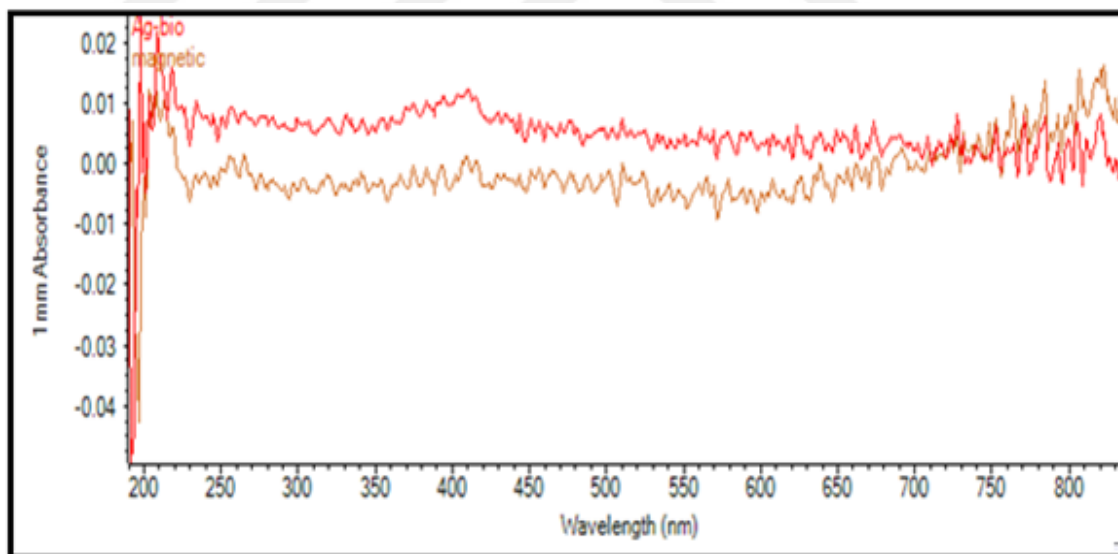


**Figure 4.21 :** UV -Vis spectra showing the formation of the AgNP/biotin/streptavidin/magnetic microbead model analyte.

This result is for showing the decrease of DNA presence after binding to the streptavidin coated beads. The red one is after binding to the trace.

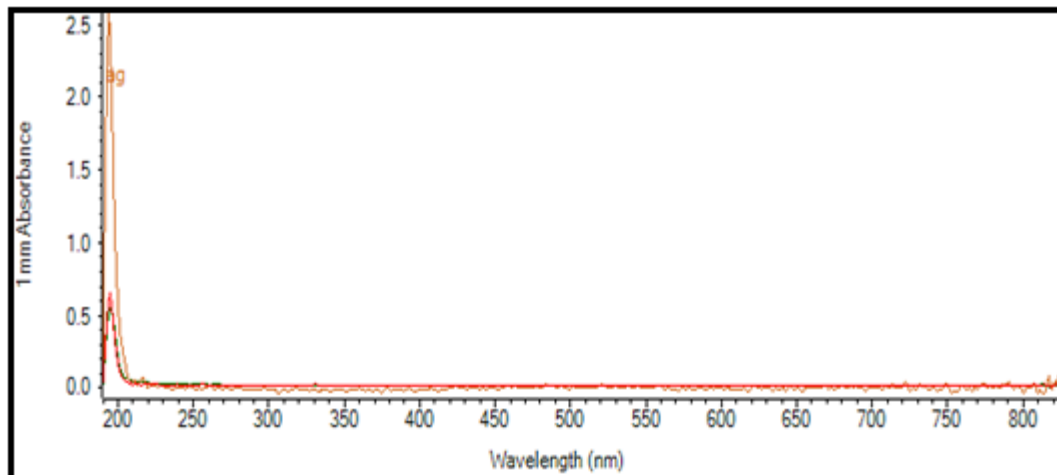


**Figure 4.22 :** Confirmation of AgNPs bonded DNA decrease adsorption of DNA coated AgNPs

Figure 4.23 is for comparing the model liquid (red trace) and its magnetic bead suspension analyte (yellow trace) differences. The blue trace is belongs to AgNPs-DNA combination and all experiments were occurred in borate medium.

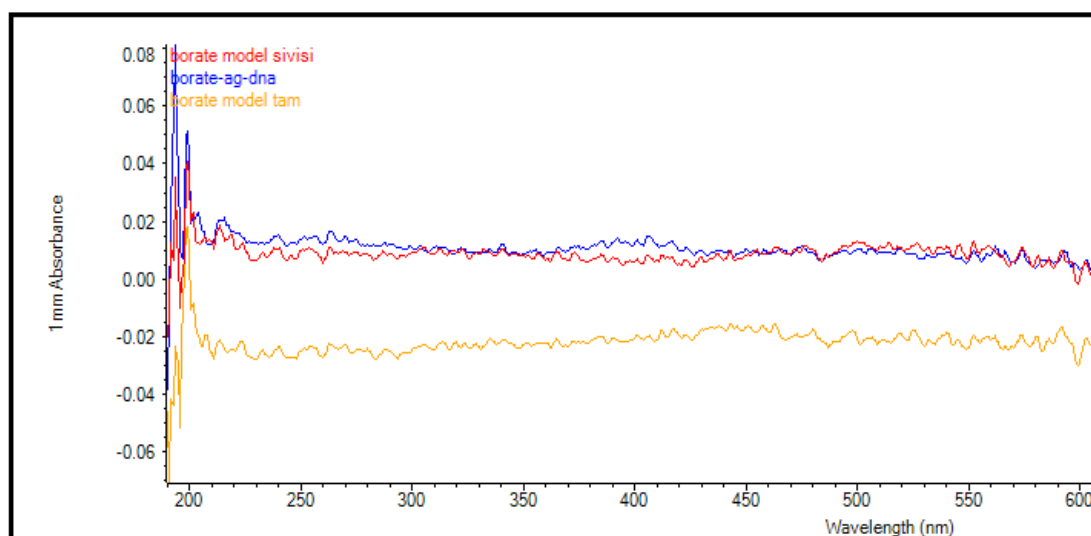


**Figure 4.23 :** Comparing the model liquid and its magnetic bead suspension analyte differences

The results of Uv-vis spectrometer in Figure 4.24 and 4.25 have been measured after modification of AgNPs-DNA-biotin with streptavidin coated magnetic microbeads. First, the supernatant of these modification resulted sample has been removed by

holding a magnet to the side part of tube and kept for running UV-vis test. Then, the resulted solid is washed as previously described in part 4.2.4. Finally, same buffer is added on last product. And, it is named as model analyte. All residual buffer of washing process has been collected into tubes to proof removing non-bonded AgNPs from magnetic beads.

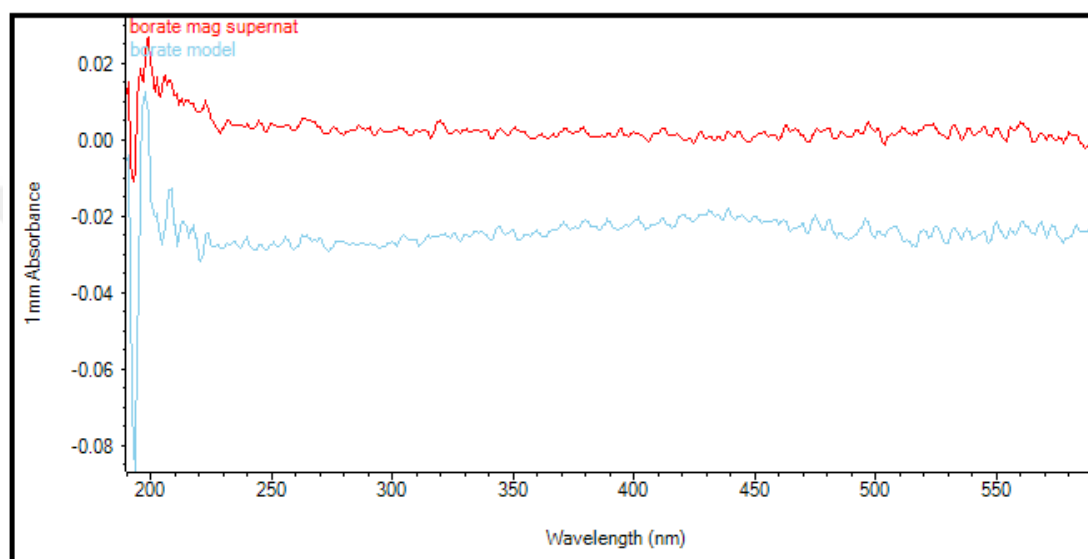


**Figure 4.24 :** Supernatant of model analyte model analyte in borate medium

Red trace in Figure 4.24 belongs to the supernatant of model analyte and the blue trace belongs to model analyte in borate medium. The result of supernatant shows that AgNPs modified biotinylated DNA have successfully bonded to streptavidin coated magnetic micro beads. In addition to this, Figure 4.25 promotes the conclusion as proof of AgNPs removing from the environment via washing utterly. The brownish trace, 1<sup>st</sup> washing residual UV-vis result shows a notable peak at 400 nm which demonstrate removal of non-bonded AgNPs amount. The decrease of peaks at approximately 200-210 nm is an evidence of DNA bonded AgNPs presence going down during washing of non-modified biotin-DNA-AgNPs. Wash 2 (green trace) and Wash 3 (red trace) do not have significant absorption peak at 400nm to show all AgNPs-DNA-biotin has already been bonded to streptavidin coated magnetic microbeads. Also, the residual non-bonded AgNPs has already been removed from the environment of resulted model analyte.

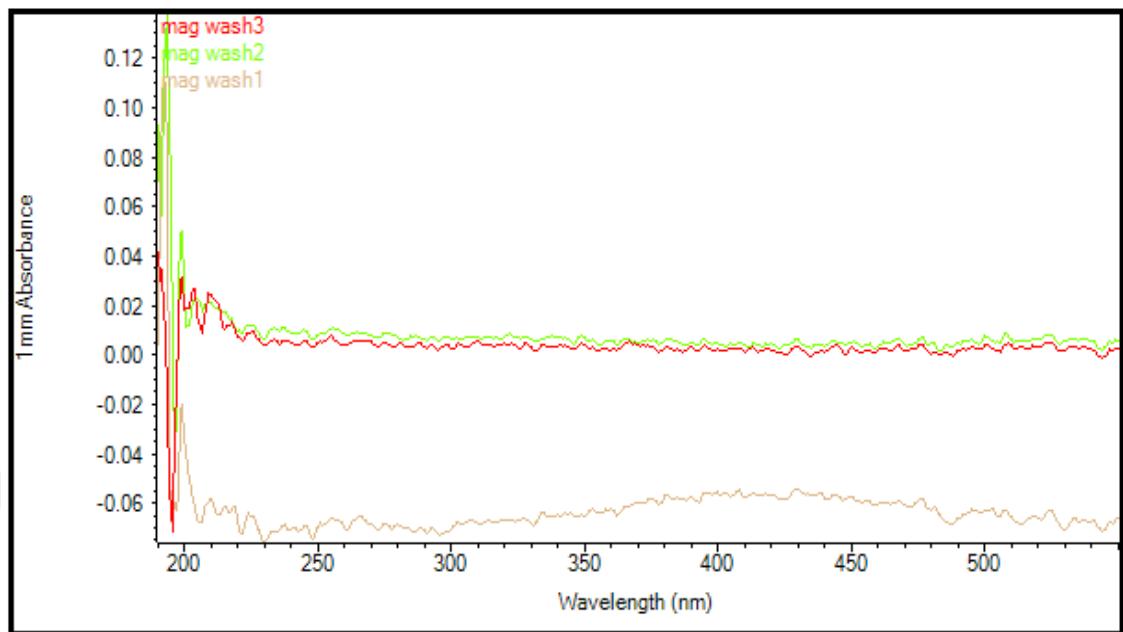


**Figure 4.25 :** Confirmation of AgNPs removing from the environment via washing. After the proof of removing residual, non-bonded AgNPs has been analyzed with UV-Vis spectra the formation of the AgNP/biotin/streptavidin/magnetic microbeads model analyte presented in the presence of borate buffer solution in Figure 4.26.

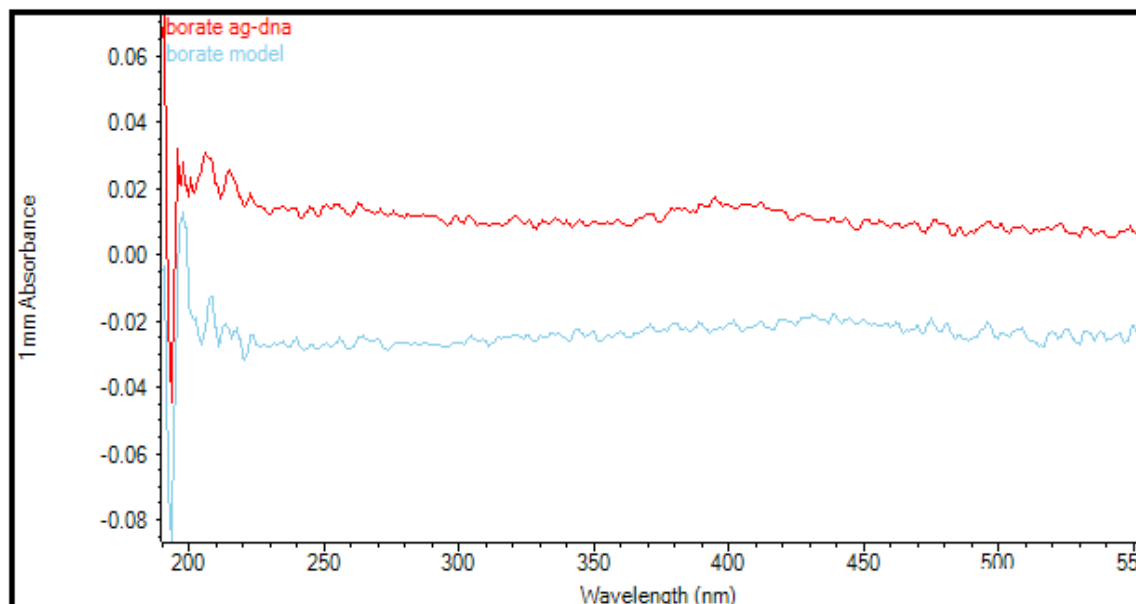


**Figure 4.26 :** Model analyte formation compared to Ag-DNA solution

The Bio-DNA-S-Ag was previously confirmed by Alexa Flour Streptavidin Conjugate fluorescence 4.2.3. Herein, pure AgNPs UV-vis absorbance spectral traces are compared with prepared Bio-DNA-S-Ag residual supernatant and Strep-MagBead-Bio-DNA-S-Ag residual supernatant as a proof of Ag-DNA modification (Figure 4.27).

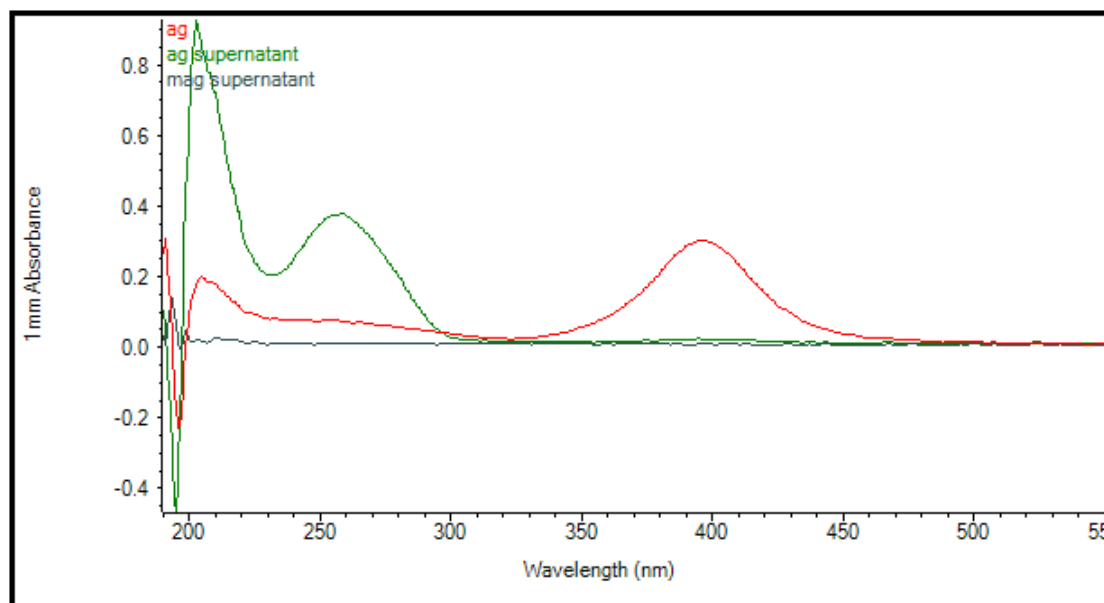


**Figure 4.27 :** DNA modification with reagents

AgNPs has a huge absorbance peak at 400nm before modification of Bio-DNA-S as shown in red trace. After modification with Bio-DNA-S, AgNPs peak at 400nm decreased significantly. Residual AgNPs supernatant also has huge peaks at 260 and 210 nm wavelengths which are belong to DNA and AgNPs labeled DNA. When Bio-DNA-S-AgNPs is bonded with streptavidin coated magnetic microbeads, absorbance peaks were decreased significantly for DNA, AgNPs-DNA and AgNPs as expected. Consequently, formation of Bio-DNA-S-AgNPs has been proven not only via Alexa Flour Streptavidin Conjugate fluorescence method but also with UV-vis spectrometer.

Although, borate has 10 times better efficiency during electrochemical detection as an electrolyte solution it is not a proper medium for preparation of model analyte as expected. Figure 4.28 compares absorbance peaks of both PBS model analyte, and Borate model analyte in order to maintain proper modification medium. Especially, using PBS for AgNPs modification with DNA-S gives higher absorbance peaks than

borate buffer solution medium (Figure 4.29, 4.30). Figure 4.28 also shows same results for different medium factors in model analyte comparison.

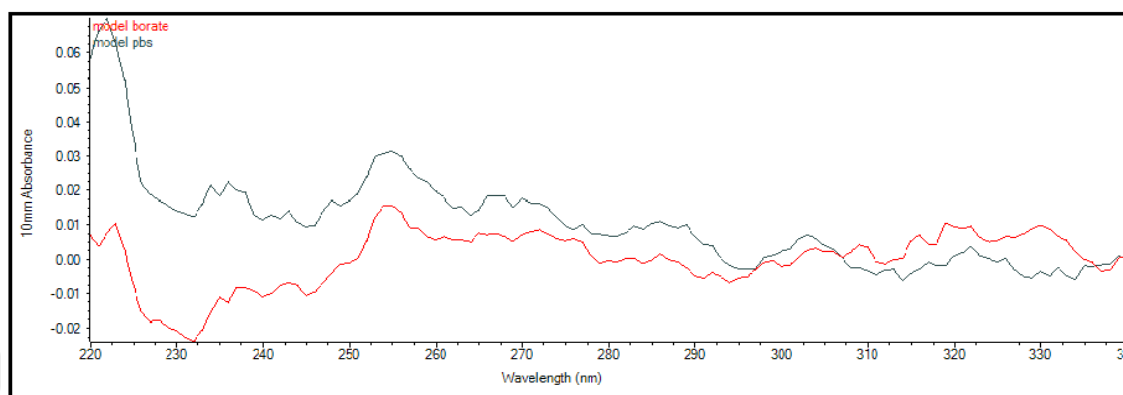


**Figure 4.28 :** Borate effect in preparation of model analyte

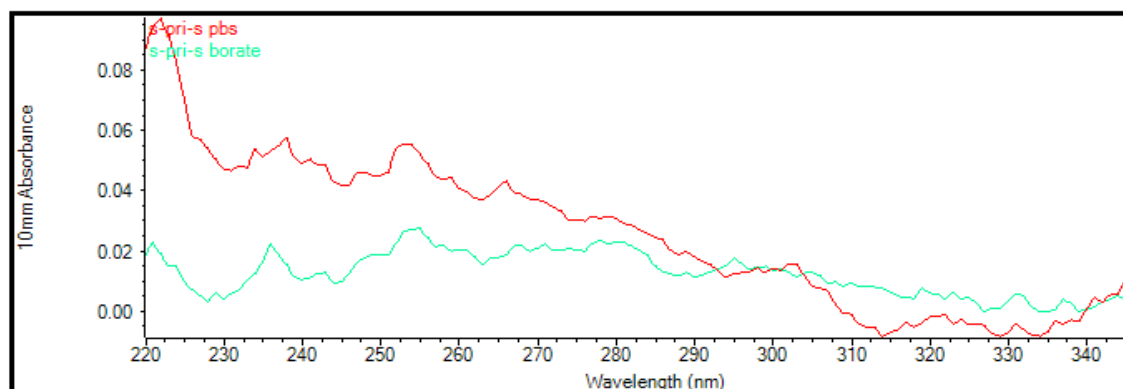


**Figure 4.29 :** PBS medium effect in AgNPs modification with DNA

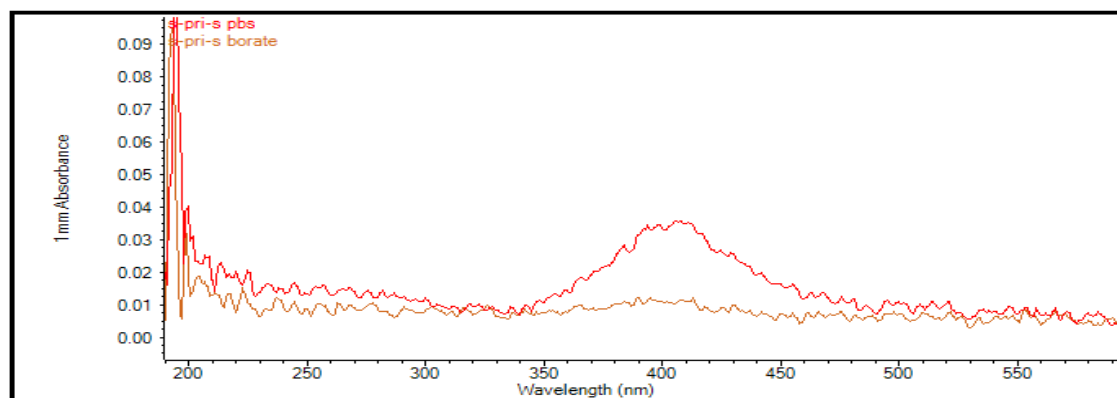


**Figure 4.30 :** Two thiol included DNA modification with AgNPS in PBS medium

#### 4.3.8 Confirmation results of DNA modified with magnetic bead and Ag bonded primers for detection of patient samples

Herein, our novel modification method which is explained in part 4.2.5 was confirmed. Optimization results of various concentrations of DNA, and primers are also presented in this part. Also, S-Primer-S and S-Primer oligonucleotides amounts were tested to increase the yield of detection. In addition to that, UV-visible confirmation results were supported with electrochemical confirmations as a proof. Presence of DNA also has been controlled after and before modification of DNA and its primers.

Figure 4.31 shows the comparison of biotinylated primer, magnetic bead bonded form of biotinylated primer, thiol labeled primer, Ag bonded form of thiol ended primer, double stranded DNA and model analyte which were developed from combined form of all these components. The purple absorbance peak is for thiol-primer-AgNPs. It shows a significant absorbance at approximately 400nm which is caused from AgNPs. Green peak is belong to magnetic bead modified primer and red peak shows wholly modified sample. Red trace has evidence of new DNA form which is apparently proved with the peak at 220nm and increase at 200nm compared to the previous state of each component.

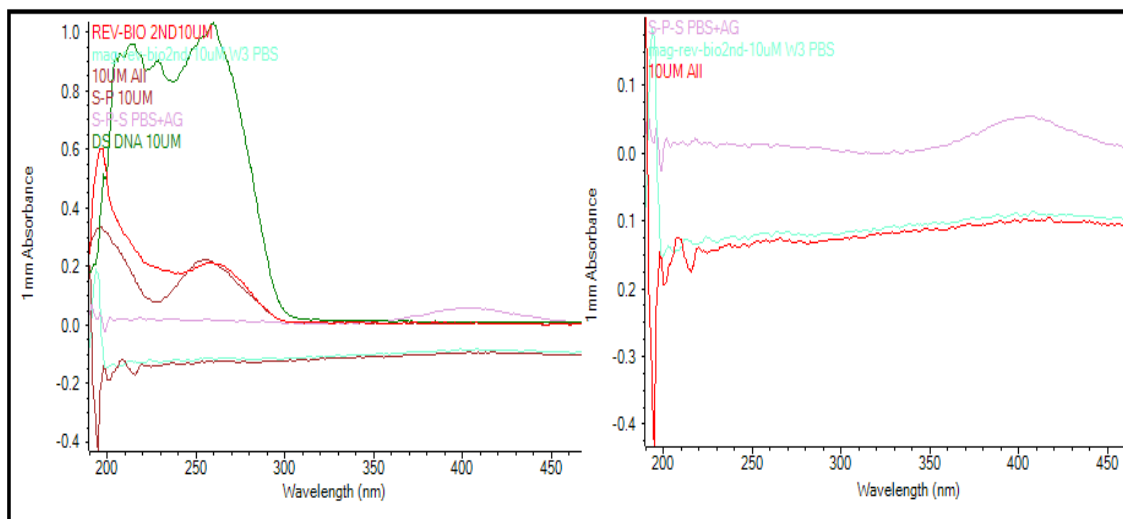


**Figure 4.31 :** DNA hybridization confirmation with reagents labeled primers

DNA modifications with the primers have been also proved with Nano-Drop DNA analyser. The red trace in Figure 4.32 consists of double stranded DNA (dsDNS) which



has a large peak at 260nm before hybridization with rev-biotin. On the contrary, dark red trace, belongs to biotinylated primer, has a lower peak at 260nm compared to new form DNA-bio-primer which shows via green peak. Red dsDNA peak decrease as a result of hybridization and the new green trace occurs as a result of this hybridization. Thiol primer attachment to HPV DNA also have been showed with yellow trace which has an increased peak at about 260nm and another lower peak at approximately 225nm. These plots provide a confirmation for hybridization of labeled primers with the target DNA.

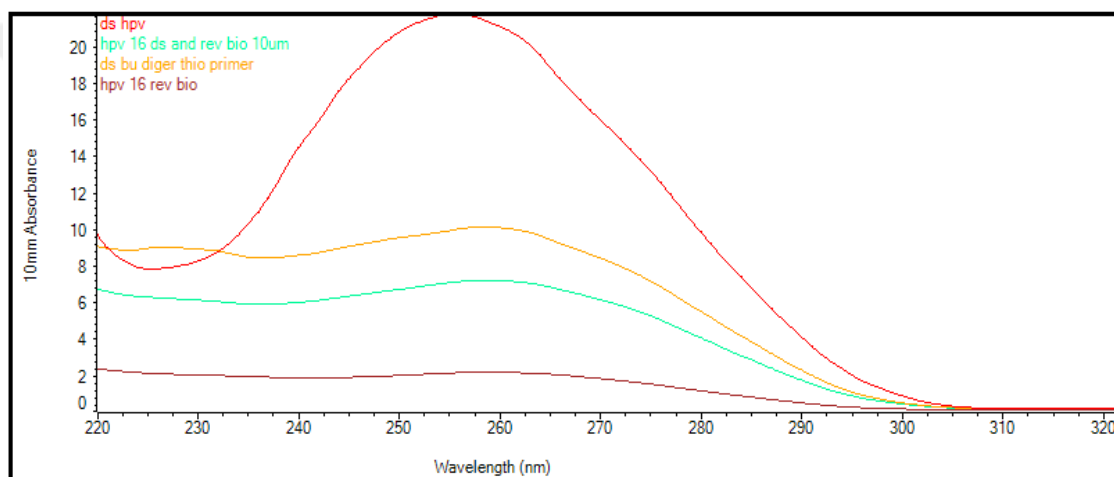


**Figure 4.32 :** DNA modifications with the primers have also been proved with Nano-Drop DNA analyser

Figure 4.33 absorbance measurements have been done in the DNA detection range as a proof of hybridization of AgNPs-Primer with DS-DNA which is modified with primer-magnetic beads. Green plot belongs to Ag modified primer, the red plot belongs to wholly hybridized DNA with modified primers and brownish plot belongs to magnetic micro bead modified primers. The decreases and increases of the peaks at 235 and 260nm show successfully hybridization of the modified primer types with DNA. The confirmation results of hybridization of DNA with modified primer types have also been tested with gel method in Figure A-3. All UV visible analysis results significantly indicate hybridization with the novel method is successfully done.

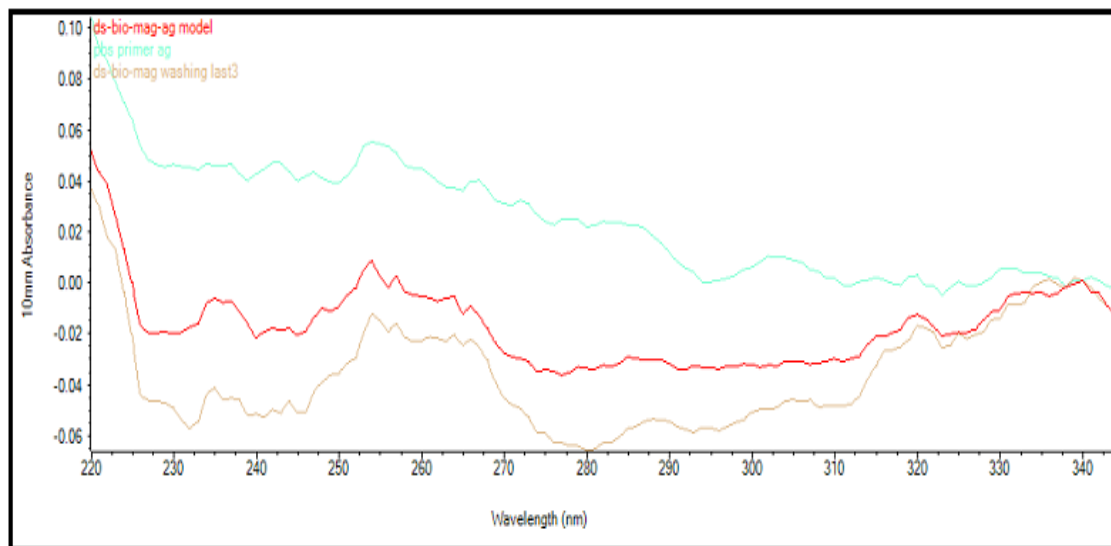


**Figure 4.33 :** Absorbance measurements have been done in the DNA detection range as a proof of hybridization of AgNPs-Primer with DS-DNA

#### 4.3.9 Optimization types of labeled primers modification for detection of patient samples

Two different hybridization methods have been tried for more efficient attachment of modified primers with DNA. AgNPs yield in electrochemical detection analysed and compared for each hybridization type. AgNPs peak results were small because modification of primers with Ag nanoparticles have been applied by using only 10uM nucleotides and half amount of reagents such as AgNPs and magnetic microbeads.

First, magnetic micro bead bonded primer hybridized with DNA and washed followed by hybridization of Ag modified primer as putting first 95 degree together and cooling it for annealing. First modification type which has been done with two step hybridization resulted analyte has been analyzed with electrochemical detection as shown in Figure 4.34 Several dilutions from 6.36pM to 11.3pM of AgNPs reagent included analyte have been detected and their charges have been calculated. This hybridization resulted target analyte did not give a peak for lower amounts as we expected. The minimum detection limit should be lower than it although 10uM nucleotides and small amounts reagents have been used to obtain model analyte.

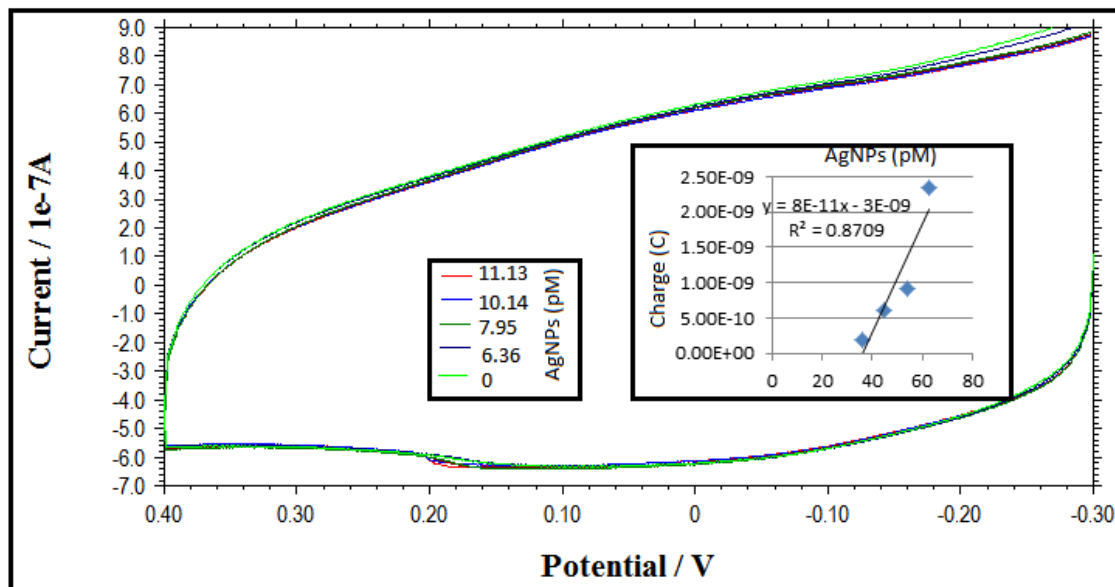


**Figure 4.34 :** ASV result of first modification type which has been done with two step hybridization resulted analyte

Second method has been also carried out with same amounts of primers and reagents as the first method. The point is here that hybridization of primers have been done only in one step. AgNPs and magnetic bead modified primers mixed with DS-DNA before applying denaturation temperature. Washing step is applied after this single step procedure with help of the magnet.

The anodic stripping voltammetry results are obtained using second method hybridization of model analyte. Various concentrations of AgNPs from 1.59pm to 11.59pm have been detected and their charge measurements have been calculated as shown in inserted graphic in Figure 4.35. This hybridization method has a peak for lower AgNPs amount than the first method. Second method gave a peak for 1.59pm amount of model analyte but first method gave its first detection peak at 6.36pm. The sensitivity of second method is also higher than the first hybridization method. In addition to these predominance features of second method, preparation of model analyte easiest make this method is preferable. Single step hybridization which is not requires additional washing and annealing step also provides time and energy saving.

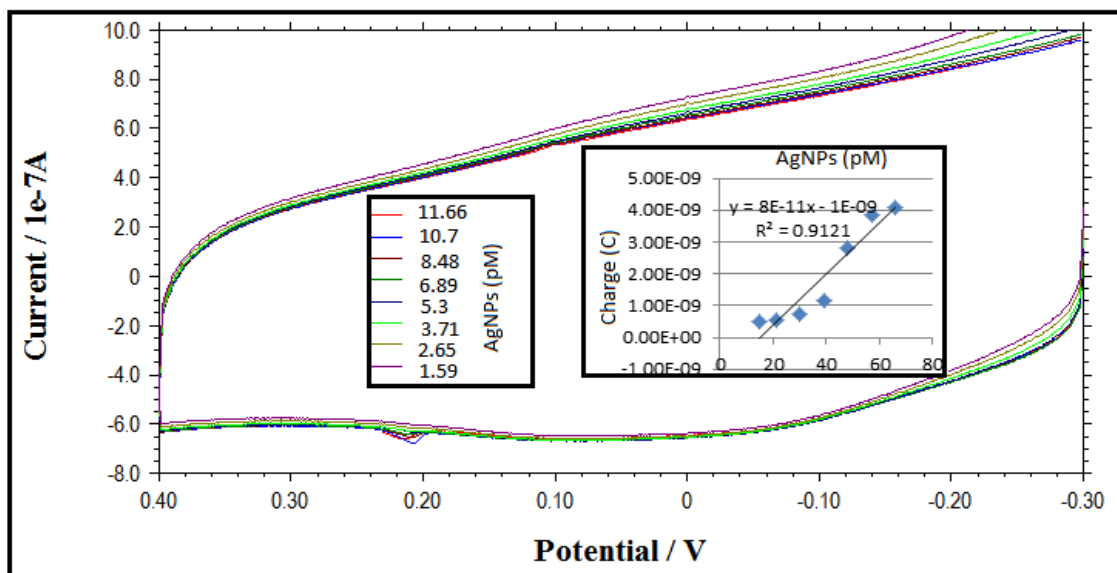


**Figure 4.35 :** ASV result of one step hybridization used model analyte

It is recognized that the peak current is very low if DNA. The primers concentrations are used at 10 $\mu$ M level while producing the model analyte. Thus, 10  $\mu$ M and 100  $\mu$ M amounts of ds-DNA have been used for single-step hybridization of model analyte to increase detection peak current. Several dilutions of these model analytes were tested and compared in order to choose proper DNA and primer concentrations. The results in Figures 4.36 and 4.37 show that using 100  $\mu$ M primers and ds-DNA were increased the peaks and charge values as expected.

10 $\mu$ M ds-DNA Charge	Concentrations(pM)	100 $\mu$ M ds-DNA Charge	Concentrations (pM)
1.07E-09	6.36	2.13E-08	4.42
8.39E-10	4.59	9.04E-09	3.53
3.10E-10	2.82	9.64E-09	2.65
1.21E-10	1.06	5.07E-09	1.77
0.00E+00	0.53	2.86E-09	0.88
0.00E+00	0	0.00E+00	0

**Table 4.8.** 10  $\mu$ M and 100  $\mu$ M amounts of ds-DNA have been used for various concentrations of single-step hybridization of model analyte

Table 4.8 shows apparently that 0.88pM concentrations of 100μM ds-DNA used model analyte charge result is calculated as 2.86E-09 C which is more than 10μM ds-DNA used model analyte. The 10μM ds-DNA hybridized model analyte has no peak for 0.53pM concentration. It has also 1.21E-10 C for 1.06pM model analyte.

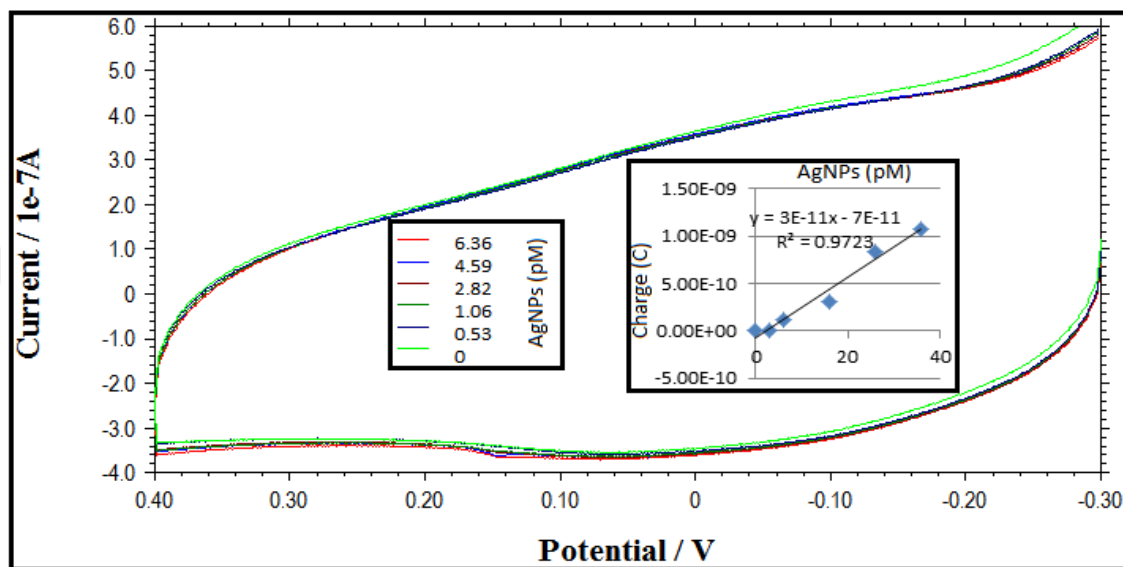


**Figure 4.36 :** 10μM ds-DNA hybridized model analyte

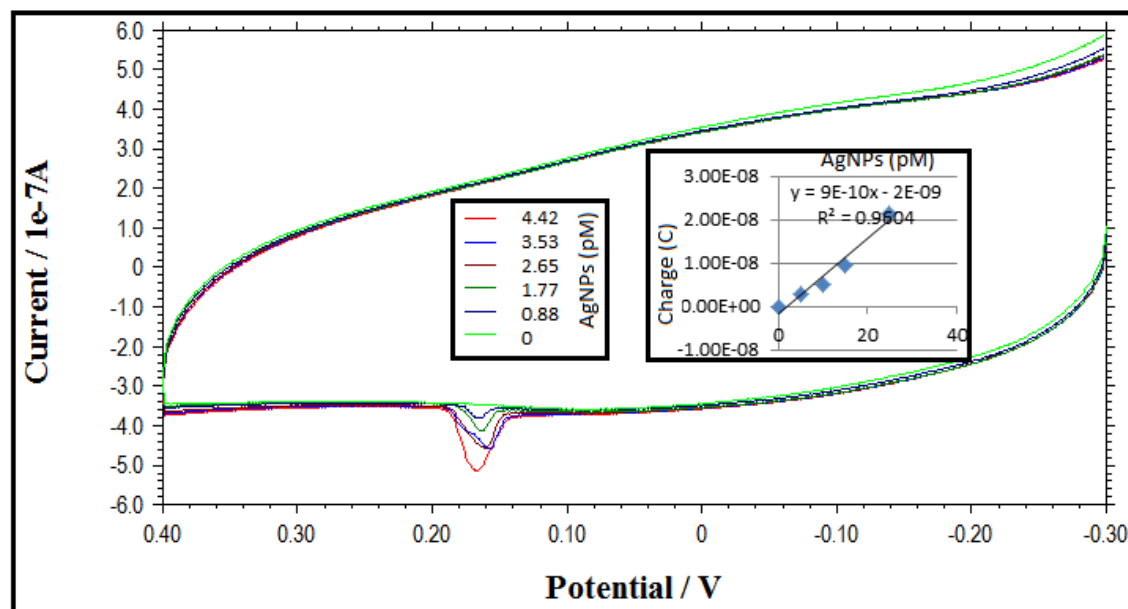


**Figure 4.37 :** 100μM ds-DNA used model analyte

Although, using 100μM ds-DNA increased the peak current to achieve low detection limits of Ag-primer and magnetic bead-primer modified model analyte, it did not give

enough charge value for lower concentrations. Thus, AgNPs volume which was added into the hybridization medium has been increased from 100 $\mu$ L to 200 $\mu$ L for each 10 $\mu$ M to 100 $\mu$ M dilution. The volume of DNA and primers were added equal during modification process.

The graphic at Figure 4.38 belongs to 100 $\mu$ M model analyte which is prepared as using 200  $\mu$ L AgNPs-primer. Citrate capped silver nanoparticles have been prepared according to the procedure described before at part 4.2.3 as adding 100  $\mu$ M primer. The point is here using 100  $\mu$ L AgNPs-Primer in modification did not gave a peak lower than 0.88pM. In addition to this it has 2.86E-09C charge value for 0.88pM although 200 $\mu$ L AgNPs-primer used model analyte gives 2.64E-07C charge value for the same concentrations. Increased AgNPs-primer amount during modification also gave a significant peak for lower concentrations of model analyte as low as 530fM. Consequently, hybridization of DNA with reagent labeled primers have been decided to modify with 200 $\mu$ L 100  $\mu$ M AgNPs-primer for detection of lower model analyte concentrations. The decided amounts gave 10<sup>2</sup> fold yield compared to 100 $\mu$ L 100  $\mu$ M AgNPs-primer modification.

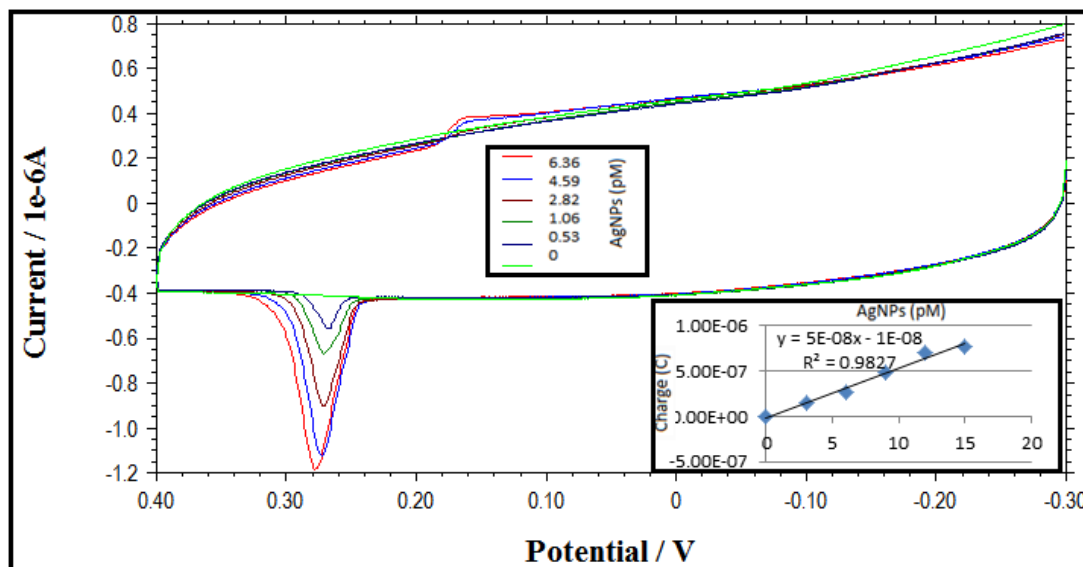


**Figure 4.38 :** 100 $\mu$ M model analyte which is prepared as using 200  $\mu$ L AgNPs-primer

The comparison is also confirmed, and presented with Figure 4.39 below. Constant 2.65pM model analyte were used to detect various concentrations included components.

The red curve is for 100 $\mu$ M DNA &Primer used 200 $\mu$ L AgNPs-Primer, the blue plot is for 100 $\mu$ M DNA &Primer used 100 $\mu$ L AgNPs-Primer, the brown plot is for 10 $\mu$ M DNA &Primer used 200 $\mu$ L AgNPs-Primer and the green plot is for 10 $\mu$ M DNA &Primer used 100 $\mu$ L AgNPs-Primer.

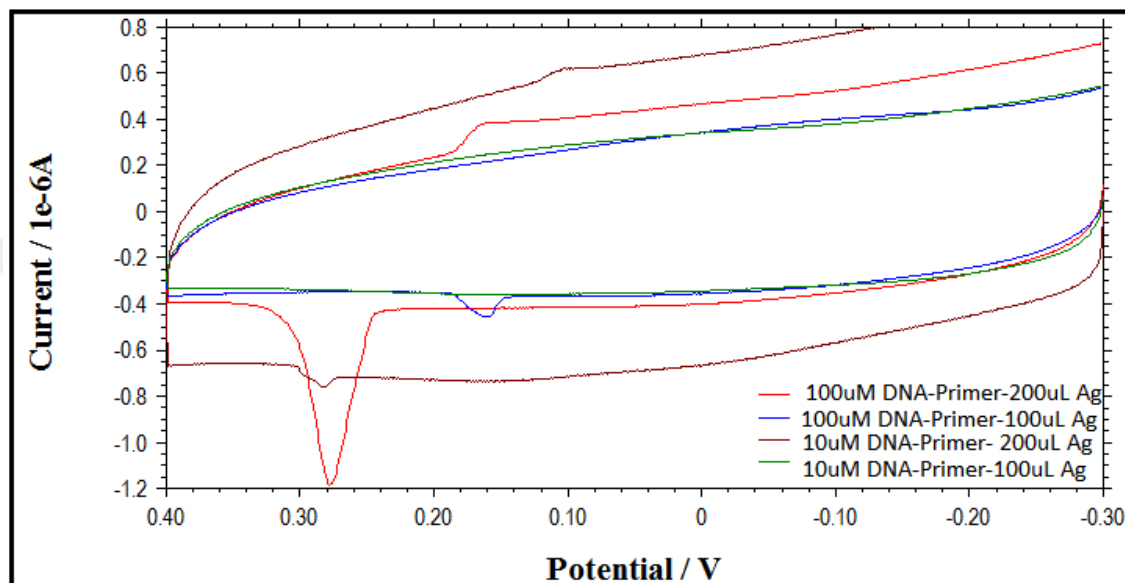


**Figure 4.39 :** Comparison of 100 $\mu$ M 200 $\mu$ L AgNPs-Primer, 100 $\mu$ M 100 $\mu$ L AgNPs-Primer, 10 $\mu$ M 200 $\mu$ L AgNPs-Primer and 10 $\mu$ M 100 $\mu$ L AgNPs-Primer for 2.65pM model analyte

Lowest detection limit is very important for getting maximum efficiency from the electrochemical detection. Thus, it has been decided to test primers which were ended from both ends with thiol. The previous experiments were done with S-primer. After all of this S-primer-S special primers purchased and modified with the same optimized amounts of DNA and reagents. 100 $\mu$ M and 60  $\mu$ M S-primer-S had been modified with citrate capped AgNPs and compared with only one thiol bonded S-primer results. Figure 4.40 shows that there is not a significant changes at peak charge values after using double S bonded primers during modification. When Figure 4.37 and 4.41 are compared with each other's, it has been noticed that the sensitivity of S-Primer used model analyte is better than S-primer-S modified.

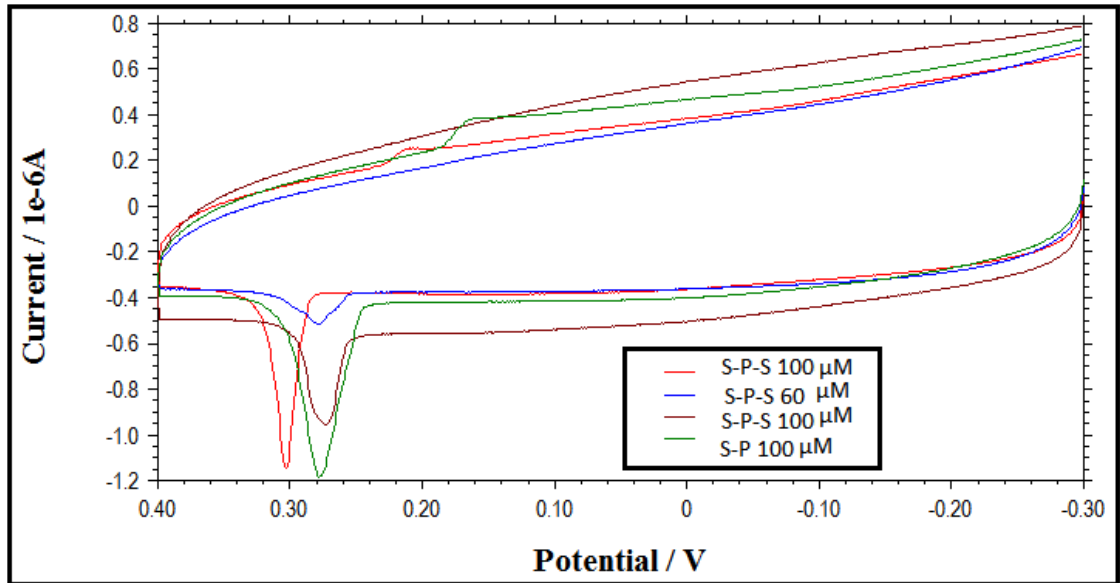


**Figure 4.40 :** Comparison of using double side and one side thiol labeled primers and their several concentration values in 636fM model analyte

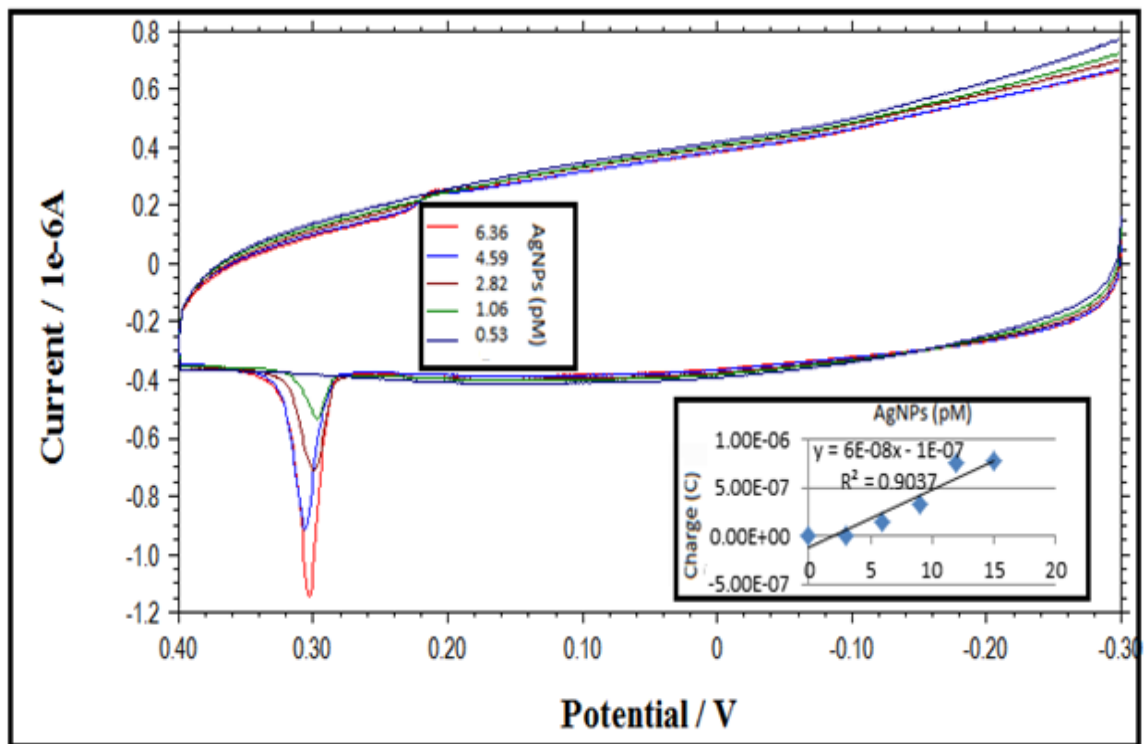


**Figure 4.41 :** 100uM S-primer-S used model analyte sensitivity and ASV result



#### 4.4 Summary and Future Works

The optimizations of the electrochemical detection have been done in the conventional electrochemical cell previously study on paper analytical device in order to achieve proper conditions for detection limits of target model analyte. There were significant parameters which should be optimized, and examined efficiency of them such as choosing electrodes, electrodes working conditions, surface properties and effects of working and reference electrode to the signal, electrolyte includes buffer features, voltage range and preconditioning voltage and times were only a part of them. The effects of  $\text{KMnO}_4$  and target molecule hybridization are another important effects which should be examined for lowest LOD.

Sample preparation which is mentioned before is only for extraction of DNA. The confirmation experiments of them were carried out in this part for use of detection device. As mentioned before, herein non-enzymatic amplification method was used to detect target HPV DNA analytically in paper device. Therefore, magnetic micro beads and AgNPs which were used to bond two opposite ends of DNA which were labeled with biotin and thiol. The labeling process of standard DNA by metal and magnetic reagents have also been applied to the patient sample DNA as a novel primer hybridization method. It was carried out successfully and specifically.

Several concentrations of AgNPs are used for optimization in the presence of 50 $\mu\text{L}$  10 $\mu\text{M}$   $\text{KMnO}_4$ . 47 $\mu\text{L}$  water is added in to the cell for each experiment for dilution of AgNPs. PBSCl or Borate buffer are used as electrolyte solution. 62.5  $\mu\text{L}$  100mM PBS and 62.5  $\mu\text{L}$  100mM NaCl are used to achieve the appropriate PBSCl buffer. Detection voltage range are arranged between -0.3 to 0.4V. 200s preconditioning time is applied for -0.3V in the presence of  $\text{KMnO}_4$  and PBSCl solution for detection of AgNPs. Consequently, hybridization of DNA with reagent labeled primers has been decided to modify with 200 $\mu\text{L}$  100  $\mu\text{M}$  AgNPs-primer for detection of lower model analyte concentrations. At least, 530fM of HPV model analyte was detected by using these optimized conditions in conventional cell.

## **5. CHAPTER: PAPER ANALYTICAL MICROFLUIDIC CHIP FABRICATION**

### **5.1 Introduction**

#### **5.1.1 Paper device introduction**

Human papilloma virus early detection needs quickly detection to allow analytical tools for chemical and biological weapons. Herein, a low cost, 3D (three-dimensional) point of care paper based analytical microfluidic chip is presented for sensitive and quantitative detection of HPV 16 and 18 types in order to diagnose Cervical Cancer. The paper based device allows to non-enzymatic amplification by using streptavidin coated magnetic micro beads and citrate capped silver nanoparticles. Primary detection relies on AgNPs detection which is modified with DNA. This fluidic platform has lower detection limit at femtomolar level, robust and faster than regular enzymatic amplifications.

Biological reagents are generally detected with PCR or mass spectrometer in a laboratory setting (Fitch et al., 2003). However, point of care devices provide unique features and advantages for rapid detection in only generally 30 minutes. There were several studies which is related to point of care detection strategies in the literature such as calorimetry (Bahadır and Sezgintürk, 2015), electrochemiluminescence (Higgins et al., 1999; Liljestrand et al., 2004), and fluorescence (Narang et al., 1997).

Whitesides and colleagues were first reported 3D paper fluidic devices which have great advances at the point of care platforms. These devices have been used, and improved for specific detection platforms as maintaining their features such as simplicity and low cost. 3D paper devices largely used for colorimeter detection, flow-time measurements and electrochemical detection. Various small molecules (Chen et al., 2012; Dungchai et al., 2013; Renault et al., 2013), such as bacteria (Jin et al., 2015), viruses (Larsson et al., 2013), proteins (Liu and Crooks, 2011; Renault et al., 2013; Sechi et al., 2013) and metals (Rattanarat et al., 2014; Wang et al., 2014), in natural waters (Wang et al., 2014), urine (Sechi et al., 2013), and serum (Chen et al., 2012). Resulted detection limits of these molecules are approximately at low micromolar level (Dungchai et al., 2013; Liu and Crooks, 2011; Wang et al., 2014). Quantitative detection of enzymes and

molecules had been applied using flow time by Philips group with analyte-specific hydrophobic to hydrophilic fluidic switches (Lewis et al., 2013; Noh and Phillips, 2010). It gave in femtomolar range detection limits for active enzymes.

Low power requirements and simplicity is provided advantages in electrochemical quantitative detection for low limits of analytes such as metals (Nie et al., 2010; Rattanarat et al., 2014), molecules (Ge et al., 2013c; Liu et al., 2012b; Santhiago et al., 2014), biomarkers (Ge et al., 2012; Wang et al., 2012) ions (Lan et al., 2014; Novell et al., 2012), proteins (Li et al., 2014; Zang et al., 2012), DNA (Cunningham et al., 2014; Lu et al., 2012) and gases (Dossi et al., 2012), as low as picomolar range (Lu et al., 2012). Electrochemical detection medium have generally been prepared from buffer except some cases which are requires water or serum (Santhiago et al., 2014; Wang et al., 2012).

Plasmonic (Zhang et al., 2013), electrochemistry (Chen et al., 2007; Luo et al., 2008) and colorimetry<sup>36</sup> detection methods have also been used detection of metal nanoparticles labeled assays for recent years. Limoges and colleagues gold nanoparticles oxidation based immunoassay with Br<sub>2</sub> in the medium of acidic bromine–bromide solution (Dequaire et al., 2000). Anodic stripping voltammetry has been used for oxidation of electrodeposited gold ions to achieve charge results correlated to the concentration of analyte on the surface of screen printed electrode. Szymanski and his friends were used silver nanoparticles instead of gold nanoparticles to label immunoassay as similar to Limoges (Szymanski et al., 2011; Szymanski et al., 2010). The main idea of this study is the formation of sandwich followed by adding ammonium thiocyanate for aggregation. Then, a positive potential was applied to provide electrostatically attraction of negatively charged AgNP aggregates to the electrode for oxidation of AgNPs. Crooks group was also produced a paper electrochemical detection platform which contains chemical oxidant to oxidize AgNPs followed by electrodeposition and anodic stripping voltammetry (Gubala et al., 2011; Scida et al., 2014).

In this study, HPV virus 16 and 18 types detectable microfluidic paper analytical device is presented as drawing inspiration of previous work and combining previously

findings. Another point of limitation at the Point of care has been demonstrated a novel modification method for DNA hybridization with AgNPs and magnetic beads reagents. Thiol and biotin ended nucleic acid primers were used instead of standard DNA which has same reagents. This is an outstanding idea to make the device usable for patient samples via non enzymatic amplification. Electrochemical detection is carried out at approximately femtomolar levels for both HPV types specifically after paper based single step extraction of analyte.

### **5.1.2 Wax patterning of paper microfluidic devices**

A porous, nitrocellulose layer is used to produce a lateral flow assay which has nonporous polyester polymer backing support material (Gubala et al., 2011). Lateral Flow detection tools provide readout of a localized line of color that forms due to binding of a target species. Nowadays, the common measurement systems eliminate human judgment in contrast to lateral flow device and provide quantitative outputs.

Paper based analytical microfluidic devices has recently been provided as an alternative to lateral flow strips to improve paper diagnostic tool technology (Parolo and Merkoçi, 2013; Yetisen et al., 2013). This new platforms eliminates the need of nitrocellulose and polymer supports and employs ordinary cellulose paper using. New device consist of wax printed hydrophobic flow paths and microchaneels which were printed onto hydrophilic cellulose paper<sup>4</sup>. Microfluidic paper can be folded as origami paper to maintain different strategies included fluidics (Maejima et al., 2013; Schilling et al., 2012). Capillary action as same in lateral flow assay provides liquids move through channels to analysis of reagents on the desired dried location. Resulted analytical signal were recognized when the sample containing the analyte contacts a particular reagent.

Whitesides and his friends were fabricated a paper analytical device as impregnating photoresist to chromatography paper followed by patterning channels by photolithography (Martinez et al., 2007). It has also been used several methods for patterning hydrophilic channels such as inkjet etching (Abe et al., 2008), plasma etching(Li et al., 2008), cutting and wax patterning (Fenton et al., 2008; Lu et al., 2009).

From all these wax patterning fabrication methods have advantages in production. Also, it is rapid in comparison to lateral flow assay, because several hundred devices can be produced in less than 1h. Lateral flow assay has been made a million per day via roll-to-roll processing system. This production method prevents the risk of contamination. However, the paper microchannel is not exposed to polymers or solvents during patterning in addition to low cost production (Dungchai et al., 2011). The easy usage of wax patterning technique which consist of printing wax onto the paper with a wax printer followed by applying low temperature (110–130 °C) in order to melt the wax and form the hydrophobic channel walls within the paper.

Open channels are the most common design for paper analytical devices but there were another types exist in the literature. Hemichannels (half-closed) channels were fabricated by Olkkonen and his friends using exographically printing which has a thin layer of polystyrene at one side of paper device (Olkkonen et al., 2010). A fully enclosed channels have been fabricated by Schilling et al. which includes both wax and tonner printing for fabrication (Schilling et al., 2012). They sealed on both sides of channels by printing several layers after patterning channels with wax for fabrication open channels. Inkjet printer which has UV-curable ink were also used to fabricate hemi-channels by Maejima and his colleague (Maejima et al., 2013).

An alternative method has been used for 3D microfluidic paper device preparation in this study based on origami folding (Liu and Crooks, 2011; Liu et al., 2012b). Prof Klapperich has collaborations with Prof. Crooks from Texas University. They have previously produced a device which can detect standard DNA. We improve the device and provide a new type for detection of HPV16 and 18. In addition to this paper extraction part were added to achieve a wholly included kit. Designed pattern of microchip first was printed onto chromatography paper. Then target empty areas have been removed as cutting them with laser cutter. Finally, paper device is folded as aligning hollows channel and hydrophilic surfaces. The simplicity of device eliminates the needs such as photo patterning and filling cut vias with cellulose powder.

3D specialty of this device provides more advantages such as flexibility in addition to principal wax patterned device's simplicity and speed. Number of required layers were

reduced with the usage of hemi channels in 3D origami paper device. The channels are fully enclosed with this method which decreases contamination risk and evaporation of solvent. In addition to these features, this fabrication technique enables to the lower detection limits, and improves the performance of separation.

### **5.1.3 Hollow channels of paper microfluidic devices**

Hollow channels previously are fabricated by Prof. Crooks Lab to allow simplicity in paper devices and electrochemical detections similar to traditional plastic and glass microchips (Renault et al., 2013). Electrochemistry is one of the best quantitative detection method for low detection limits at the POC technology (Maxwell et al., 2013). The amazing specialty of paper based device opens up new possibilities in paper analytical devices for future applications.

Individual sheets of paper were patterned, and taped together for fabrication of original 3D paper analytical device (Martinez et al., 2008). Simplification of multidimensional fabrication have been provide as folding paper to assemble desired configuration as taking advantage of paper flexibility (Liu and Crooks, 2011). Cellulose based devices also provide spontaneously flows through of solvent with capillary actions which eliminates the need of pump (Yetisen et al., 2013). Capillary driven flows have so many advantages despite some difficulties such as a size restriction on the mobility of objects within the cellulose matrix due to the size-exclusion properties of paper, low rates of convective mass transfer and significant nonspecific adsorption due to the high surface area of the cellulose fibers.

An outstanding idea has been prevented the non-expected shortcomings which are caused of the nature of paper device as removing the some parts of cellulose to run analytes directly empty spaces (Renault et al., 2013). The mentioned hollow channels have previously studied only in two group. Glavan and his friends fabricated hollow channels to achieve fast and laminar flow as engraving a trench in a cardstock paper followed by fluoroalkyl silane infusion and sealind (Glavan et al., 2013). The disadvantages of Glavan's paper device were hydrophobic channels limitation at capillary flow which was resulted syringe pump usage. Another study were carried out in Prof. Crooks group to fabricate hollow channels via cutting out the channels of wax

patterned chromatography paper and assembling final configuration by folding it (Renault et al., 2013). This device has non coated cellulose part at the bottom of the device which provides fast pressure-driven flow causes of hydrophilicity. Flow control in device has been controlled with paper barriers, and hydrophobic weirs.

In this study, HPV patient samples flows rate and quantitative electrochemical detection has been carried out for low detection limits. Anodic stripping voltammetry was applied on to the silver. Magnetic bead modified analytes and its flow transfer are presented in the hollow channel included wax patterned paper device to provide highly quantitative electrochemical properties of POC device.

#### **5.1.4 Electrodes of paper microfluidic devices**

Since cellulosic paper based fluidic devices have been built in 3D and 2D form by Whitesides group, a renovated interest growth in paper based point of care applications of because of its easy fabrication, low cost, and simple disposal features (Fanjul-Bolado et al., 2008; Li et al., 2012; Wang et al., 1998; Yetisen et al., 2013). Several detection techniques were presented in paper analytical device such as fluorescence (Carrilho et al., 2009b; Scida et al., 2013), naked-eye observable color changes (Dungchai et al., 2010; Mentele et al., 2012) and electrochemical methods (Ge et al., 2012; Noiphung et al., 2013; Wu et al., 2014) which allow low LOD quantitative and simple diagnose (Maxwell et al., 2013; Nie et al., 2010). The popularity of this, it was first increased after Henry's electrochemical study on paper device (Carvalho et al., 2010; Dungchai et al., 2009; Nie et al., 2010; Wang et al., 2012). Using smaller dimensions of electrodes at millimeter scales shows numerous advantages such as higher rates of mass transfer, lower overall currents and lower capacitances (Bard, 1980; Kissinger and Heineman, 1996). Henry and co-workers have already been demonstrated some of these advantages by placing microelectrode on a PAD which were produced by creating a hole in a plastic transparency film to use as stencil and filling the resulting hole with C paste (Santhiago et al., 2013).

There were still unmet needs in the paper fluidic area in the development of better electrode producing method in usage of low detection limits. Screen printed carbon electrodes are common electrodes of paper analytic devices as mentioned previously.

These electrodes are fabricated filling stencil vias with carbon paste or by pushing carbon suspended ink in a polymer matrix through a patterned mesh screen. Although, they were popular electrode systems, and they have poor electrical properties. Thus, it has been also used another electrode system while fabricating paper based device to achieve low detection limits of analytes. We propose to the use of graphite lead electrodes as an alternative.

In different application areas variety of micro wires have been used. Henry and his friends were produced postseparation amperometric detection using microwire in capillary electrophoresis (Liu et al., 2004). Osteryoung and his colleagues detected n-acetylpenicillamine behavior electrochemically using C fibers (Nuwer and Osteryoung, 1989). Micro wires have also been used in anodic stripping voltammetry (Alves et al., 2013; Salaün et al., 2011). This type electrodes employ flexibility to choose electrode material according to need of easy fabrication and rapid prototyping. It also provides modification ability prior to assemble of device (Liu et al., 2012b; Yu et al., 2012).

## **5.2 Experimental**

### **5.2.1 Chemicals, materials and instruments**

A 1/2 in. × 1/16 in. neodymium cylindrical magnet (N48) was purchased from Apex Magnets (Petersburg, WV). Conductive copper tape (6.3 mm wide) was from Ted Pella. Clear nail polish was purchased from Electron Microscopy Sciences (Hatfield, PA). Copper epoxy (EPO-TEK 430) was 81 acquired from Epoxy Technology (Billerica, MA). Acrylic plates (0.6 cm-thick) were obtained from Evonik Industries (AcryliteFF). Phosphate buffer solution was prepared by dissolving the appropriate amount of sodium phosphate monobasic and sodium phosphate dibasic in deionized water and adjusting to the desired pH with NaOH. Sodium phosphate monobasic, sodium phosphate dibasic, and  $\text{KMnO}_4$  were purchased from Sigma-Aldrich (St. Louis, MO). Erioglaurine disodium salt (blue dye) was obtained from Acros Organics (Pittsburgh, PA). NaOH, Whatman grade 1 chromatography paper (180  $\mu\text{m}$  thick, 20 cm × 20 cm, linear flow rate (water) of 13 cm/30 min), two-part 5 min epoxy were purchased from Fisher Scientific (Pittsburgh, PA). All solutions were prepared with deionized water (<18.0  $\text{M}\Omega\cdot\text{cm}$ ,



Milli-Q Gradient System, Millipore, Bedford, MA). Conductive carbon paste (CI-2042) was purchased from Engineered Conductive Materials (Delaware, OH).

All electrochemical measurements were performed by using a bipotentiostat (700E, CH Instruments). The stencil was cut by using an Epilog laser engraving system (Zing 16). Wax printing was carried out with a Xerox ColorQube 8570DN inkjet printer. An iPhone 6 was used to take the photographs.

### **5.2.2 Paper electrochemical device fabrication**

Paper based analytical device was designed proper to the target usage for both wax printer and laser cutter. SolidWorks 2014 software was used to design the target paper image to cut out inlet and hollow channels. The designed pattern was also colored with the same software for using in wax printer. First colored patterns wax printed on Whatman grade 1 chromatography paper (Carrilho et al., 2009a; Lu et al., 2009). Then, wax was impregnated as applying 120 °C about 30s on the heater (Gubala et al., 2011) to achieve three dimensional hydrophobic surfaces. Two different colors were largely effect the working principle of the device. Black wax provides hydrophobic features and the yellow wax provides hydrophilic features to paper device. 60% yellow wax has been applied to achieve hydrophilic part (Renault et al., 2013). Some parts of device were let non-waxed proper to aim. Subsequently, paper was cooled to room temperatures followed by cutting out red lines surrounded white sections with laser cutter to obtain hollow channels.

It has been also used stencil for printing the electrodes. The electrodes designs were prepared on SolidWork and transparent polymer sheet cut with laser cutter to achieve desired stencil. Then, stencil was used to spread on thickened carbon paste to paper device as aligning it. The scrapped carbon paste was dried in the room temperature for 1h. After that, electrical contacts of electrodes were added on it. Finally,  $\text{KMnO}_4$ , and blue dye were impregnated onto target locations of paper device as described later.

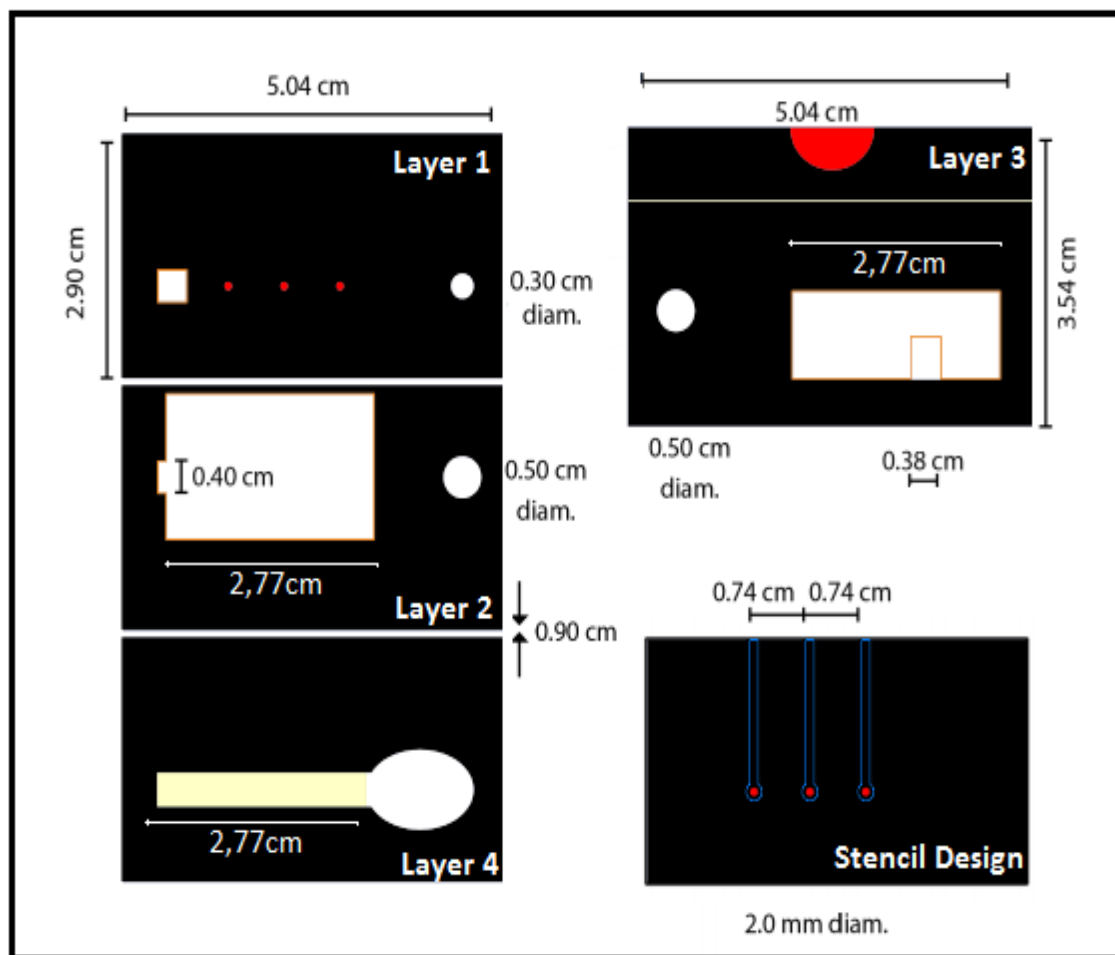


**Figure 5.1 :** Paper wax pattern and stencil design and dimensions Prof Crooks Lab collaborative work for HPV detection

Figure 5.1 was illustrated wax pattern, stencil design, and the dimensions of paper device. Layer 1-2-4 and 3 were wax printed on chromatography paper. The red dots at Layer 1 were for aligning stencil to printed carbon paste electrodes as shown at the right bottom side of Figure. 2mm diameter sized circular areas were designed as end point of 1mm width of the rectangular leads. The blue lines were presents the outline of the cut stencil. The black area between the blue lines was cut using laser engraving system. A non-colored design was designed in SolidWorks to apply laser cutting for removing target areas of wax printed chromatography paper (orange lined parts), and stencil (Figure 5.2).

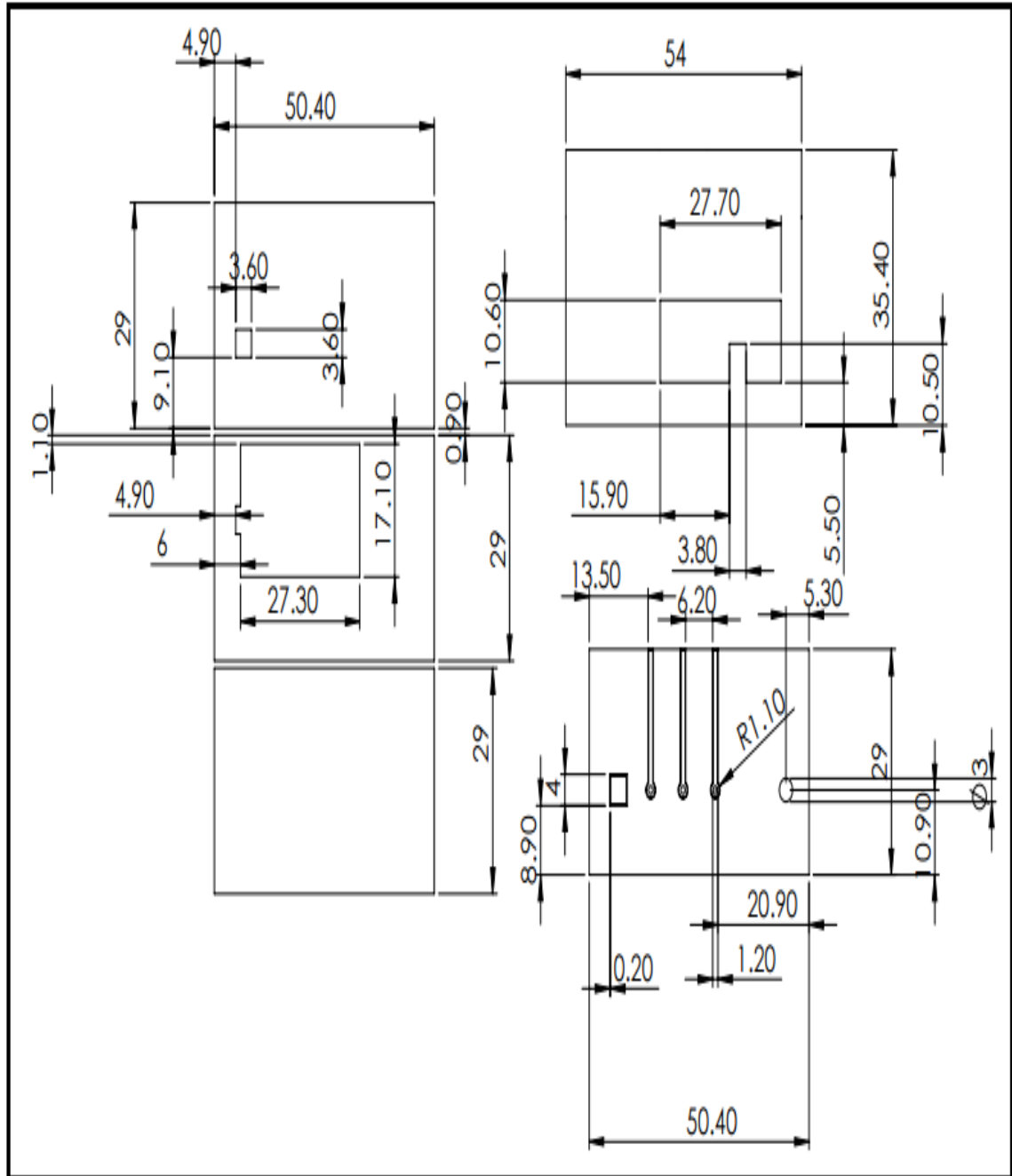


**Figure 5.2 :** SolidWorks detailed design of paper device and stencil for using in laser cutter system. This figure includes only target cutting areas of paper, polymer sheet and plate.

### 5.2.3 Carbon ink preparation for stencil printing

Carbon paste was prepared placing enough amounts into a glass vial at 65 °C temperature oven for 30 minutes. After that, glass vial is removed from the oven and

mixed with a glass road and placed more 5 minutes at 65 °C temperature. This procedure was applied for two times. Finally, thickened paste was cooled to room temperature and printed with stencil onto paper device as electrodes as scraping. 85 Herein, carbon paste was used for 3 electrode system. The reference, counter and working electrodes were both made from carbon paste.

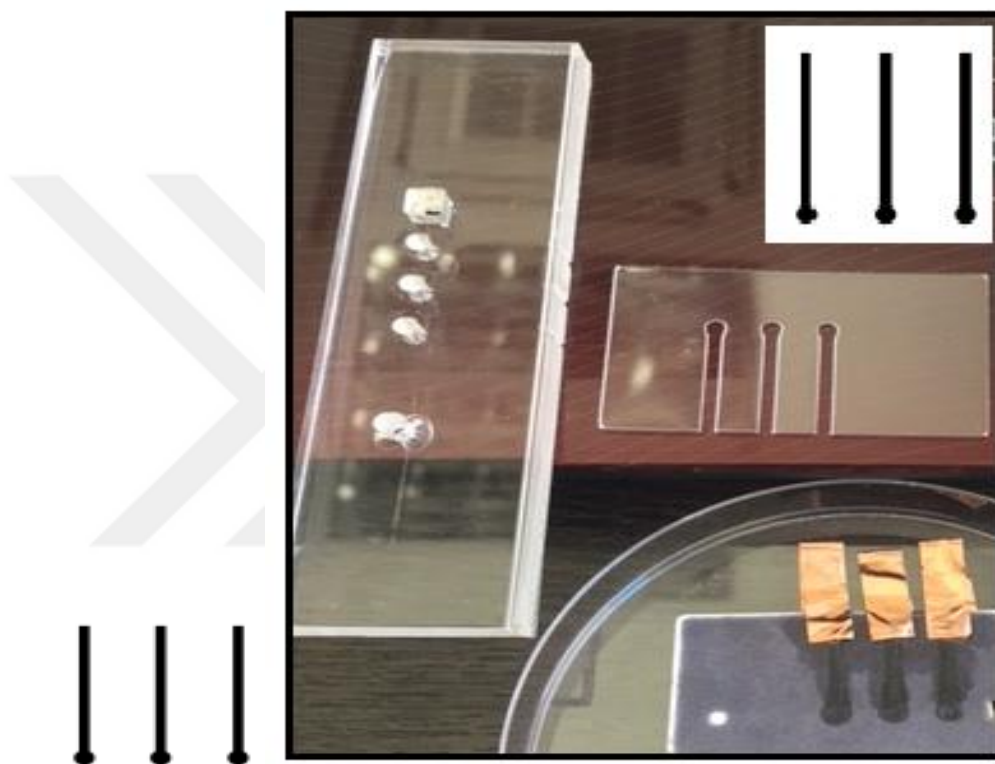


**Figure 5.3 :** Stencil placing onto device and printed line

The stencil printed carbon paste electrodes' circular areas were covered from top on with parafilm. A strip of copper taped at the end of each electrode by applying copper epoxy under the tape.

Then electrical contacts added paper device was placed into 60 °C oven followed by removing parafilm from the surface. Copper epoxy was cured and electrical properties of carbon paste electrodes were enhanced with this process during 1 hour. Because circular parts of electrodes are used for detection of target analyte, the areas except in the circular areas were insulated via applying a thin layer of epoxy. Epoxy were let dry for 30 minutes at room temperature.

Finally, hydrophobic specialty of epoxy applied surfaces was enhanced by putting on a thin layer of nail polish over it subsequently 30 minutes drying in room temperature.



**Figure 5.4 :** Electrical contacts of carbon paste printed electrode

#### **5.2.4 KMnO<sub>4</sub> and blue dye loading onto the paper device**

After that, electrodes were stencil printed, and electrical contacts were added. The wax printed, and subsequently hollow channels were cut out paper device production. It was completed by dispensing the KMnO<sub>4</sub>, and blue dye onto the target reservoirs of paper device followed by evaporation under nitrogen and in air flow respectively.



**Figure 5.5 :** Dispensing on Blue dye and KMnO<sub>4</sub> onto the paper device locations

#### **5.2.5 Preperation of patient sample for detection onto paper device**

The swabbed Human Papilloma Virus coming from patient samples were provided from Beth Israel Deaconess Medical Center which is Harvard Medical School Teaching Hospital. They were collected all the samples with patient consent and waived for the usage in researches. Methanol-water solution, a methanol based, buffered preservative

solution calls PreservCyt® solution was used as a preservative solution to support cells during transport and slide preparation. They were transferred to our laboratory without any patient health identifying information as labeled only simple number, and their positive or negative information. They have been tested using Invader Chemistry for high-risk types of HPV 16, 18, 31, 33, 35, 39, 45, 51, 52, 56, 58, 59, 66, and 68.

The patient samples were required several centrifugation steps which were described here. Normally, a dried or fresh swab sample were placed directly to lysis buffer which were provided for single step extraction of HPV in POC application in previous sections in order to eliminate these centrifuge steps in real world. Patient samples were received in large volumes of ethanol containing solution from medical center therefore these centrifugation steps were required here because unsuitable for direct use in a POC device. 50 mL conical tubes were used to centrifuge samples at 4000 RPM for 10 minutes followed by removing supernatant and washing them with 3mL PBS for two times. Next, pellets were resuspended in 3 mL PBS and divided by 1mL aliquots. It has also been prepared to use in DNeasy Blood & Tissue Kit (QIAGEN) extraction for comparison experiments.

## **5.3 Result and Discussion**

### **5.3.1 Assembling paper device to achieve final product**

The produced paper analytical device for HPV nucleic acid detection was designed, and fabricated as described in experimental section with its details. Illustration 5.1, 5.2 The paper based analytical microfluidic chip is composed of four layers. Layer 1, 2, and 3 have paper reservoirs which are circular. The layer 3 has one more reservoir which is square. Layer 2 and 3 consist of a large rectangular paper section to obtain hollow channels which was removed by laser engraving system previously. Layer 4 has a yellow rectangle with continued an oval Sink pad which were hydrophilic layers of paper device.

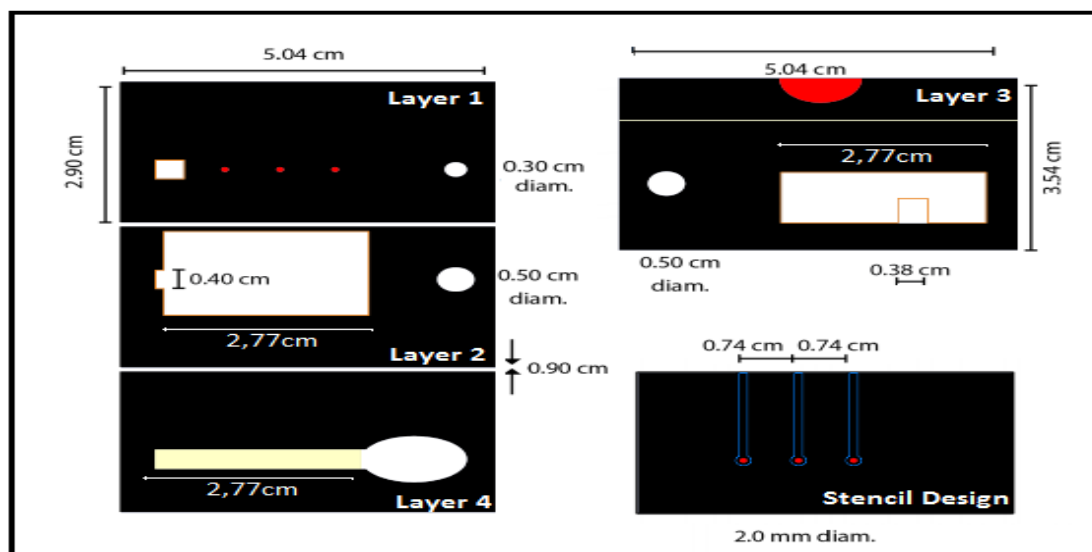


**Figure 5.6 :** Layer by layer composition of paper device and formed last production images from top

The Inlet, and the large rectangular sections of Layer 1, 2 and 3 were removed using a laser engraving system after wax printed. Then, carbon electrodes which were stencil printed as described before in part 5.2.3 and 5.2.4 refer to working, reference, and counter electrodes in Figure 5.4. Finally, 4.0  $\mu\text{L}$  of aqueous solution of  $\text{KMnO}_4$  and 3.0  $\mu\text{L}$  of a concentrated aqueous solution of a blue dye were dropped cast onto the target locations of paper device. At this point the device assembled by folding layer 1, 2 and 4. Layer 4 and the electrodes surfaces of layer 1 will contact with the opposite faces of layer 2 as zigzag. Then layer 3 is placed between 2 and 4 as aligning the circular areas.

A single hollow channel was formed with together assembly of empty spaces, and hydrophilic section which were presented in Layers 1, 2, 3 and 4. Layer 4 is very

important for device usage because of its hydrophilic part. It provides a mixture of capillary and low-pressure flow through the hollow channel which allows flow control of device. Figure 5.7 shows alignment of layers in order to obtain proper configuration getting expected flowing and detection result from paper analytic chip. Finally, the folded paper device is placed inside acrylic plates as holder to compress the device. The top surface of acrylic plate was previously engraved by using laser cutter to place a small magnet into hole which is aligned with working electrode. The acrylic plate also has additional holes on the target areas of inlet and outlet for sending sample through channel.

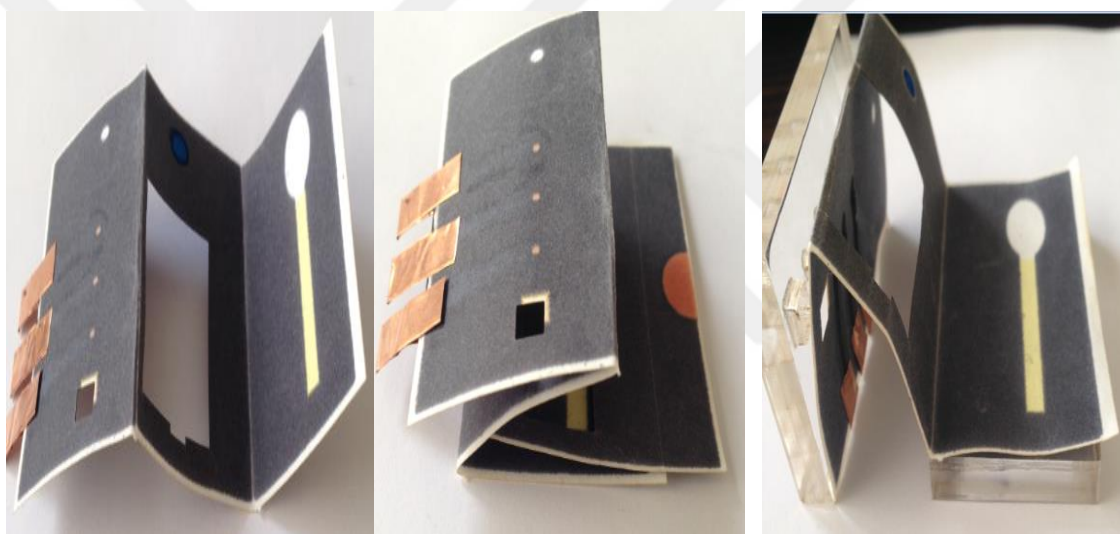


**Figure 5.7 :** Folding of the device for assembling in 3D form as aligning hollow channels, electrode surfaces and movable slip layer

### 5.3.2 Working principle of the device

The electrochemical detection method, which is a key feature of the paper device, involves different kinds of pre-concentration steps which is described in here. This is the working principle of paper based platform. Herein, we have 3 different kinds of electrodes. As you can see in the configuration, the red one is working electrode, the green one is reference electrode, and the orange one is counter electrode. We will detect the model analyte on the surface of working electrode with the help of a magnet.



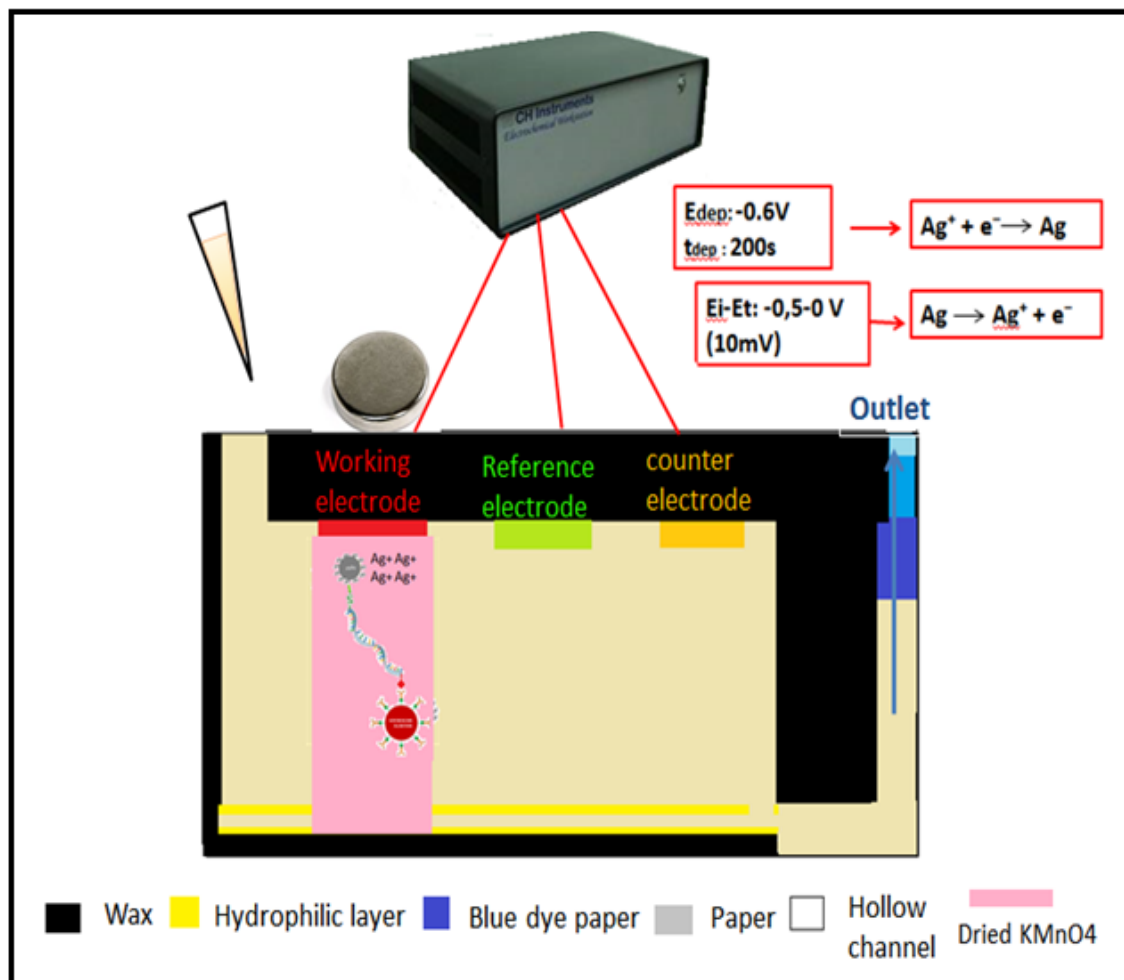


**Figure 5.8 :** Working principle of paper device from lateral section display for describing electrodes, hollow channel and preconcentration steps

First, the buffer containing model analyte is added to the inlet. The sample flows horizontally across the hollow channel and the model analyte is concentrated at the working electrode by the magnetic field. When the Sink becomes saturated with buffer, the preloaded blue dye turns the outlet to blue. At this point, a moveable piece of paper that is part of the device which contains dried KMnO<sub>4</sub> is simply slipped under the working electrode. The dissolved MnO<sub>4</sub><sup>-</sup> spontaneously oxidizes AgNps to Ag<sup>+</sup> ions. After that, -0.6 V potential is applied on to the working electrode to electrodeposit Ag<sup>+</sup> as zero valent. Finally, the electrode potential is swept from -0.5V to 0V. Then a current occurs as a result of oxidation.

### 5.3.3 Novel modification method for patient sample detection on paper device

Here, we explain the modification of patient sample with AgNPs and Magnetic microbeads. First, patient sample is extracted as described before via paper extraction support material. Then, DNA is denatured by boiling. For modification of HPV DNA, first of all, the Magnetic beads and Silver Nano particles are bonded to the HPV primers which are ended with thiol and biotin. Citrate capped AgNPs are added into the thiol labeled primers and streptavidin coated magnetic microbeads into biotin labeled primers.

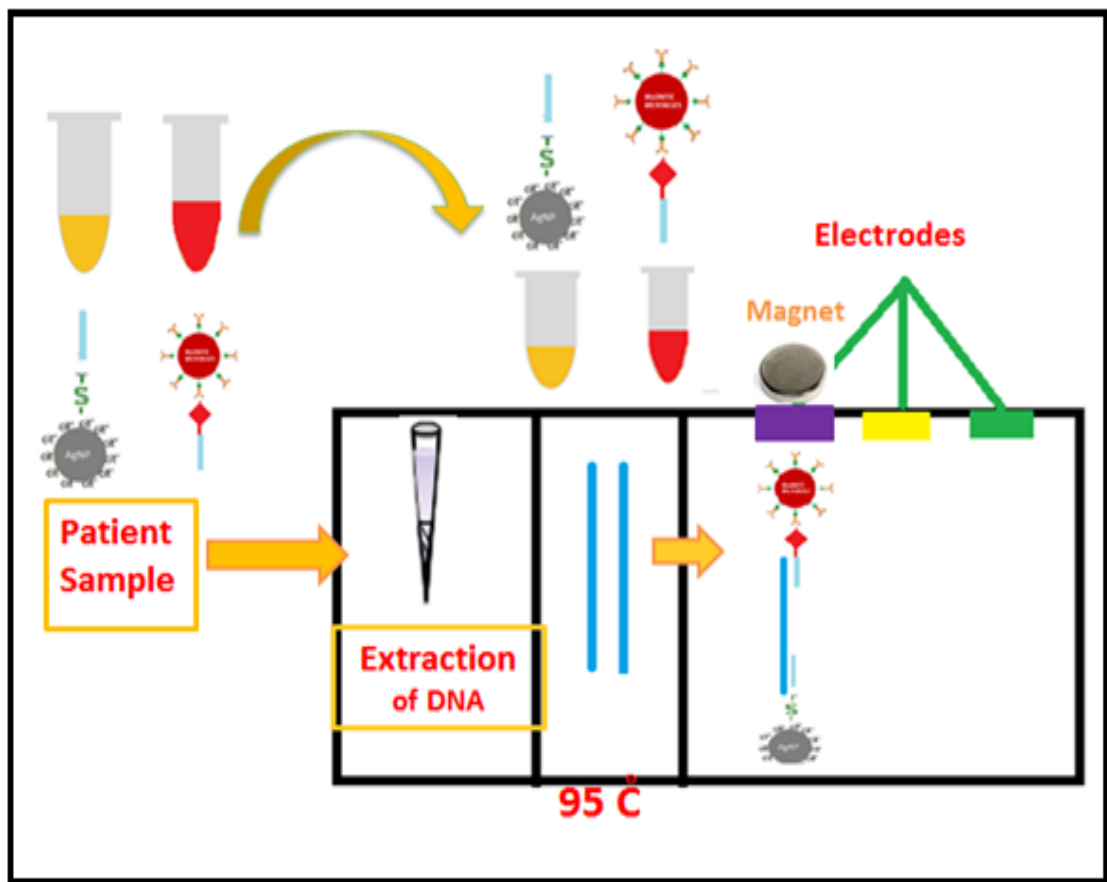


**Figure 5.9 :** Preperation of the model anlyte with novel method

After these steps, silver bonded primers and magnetic micro-bead bonded primers are poured into the denatured DNA for obtaining model analyte. Then, it is I detected on the part of the device that includes electrodes.

### 5.3.4 Testing the efficiency of designed paper analytical device

Analysis of different concentrations of the model analyte was presented in Figure 5.10 as anodic stripping voltammetry peaks. Total charges resulting from AgNP oxidation were presented with the area under these peaks which were correlated to the concentration of the model analyte detected on the paper device electrode surface. This correlation is linear as expected for both device platform and electrochemical detection method. The analytical sensitivity of paper device detection results was good as shown in Table 5.1 The lowest limit of detection which belongs to AgNPs label is shown with dark blue line inserted in Figures is 530 fM.

No anodic stripping signal was observed in the absence of  $\text{MnO}_4^-$  when performing the paper chip experiment even at higher AgNP concentrations because of AgNP labels and electrode surface has poor detection sensitivity. The detection was completed in paper device only in 5 minutes included electrodeposition of Ag about 200s.

Herein, patient sample concentration was compared with their electroanalytical detection resulted plots were presented. We have already showed standard DNA used data in chapter 4. The modification amounts of HPV DNA according to copies per mL amounts were studied in this part for both standard and patient sample into the paper device platform detection. Figure 5.10 is for comparing the standard DNA signal with patient sample DNA for  $10^4$ cp/mL.

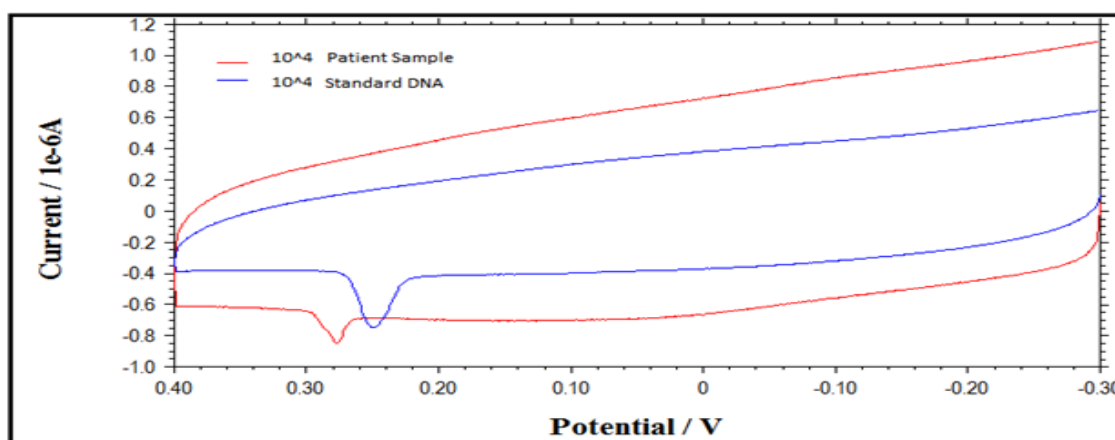


**Figure 5.10 :** Standard and patient sample DNA ASV peak for same concentration and copies.

The data indicates the patient samples modification compared to standard DNA has lower efficiency. And, it gave a capacitive current. The total charge amounts were for standard one is  $5.583 \times 10^{-8} \text{C}$  and  $1.541 \times 10^{-8} \text{C}$  for patient samples for same AgNPs concentrations.

Standard  $10^4 \text{cp/mL}$  DNA detection plots were also showed in Figure 5.11 from 0 to 2.65 pM linear range. The calibration curve which is inserted into the plot was also showed as a function of AgNPs concentrations.

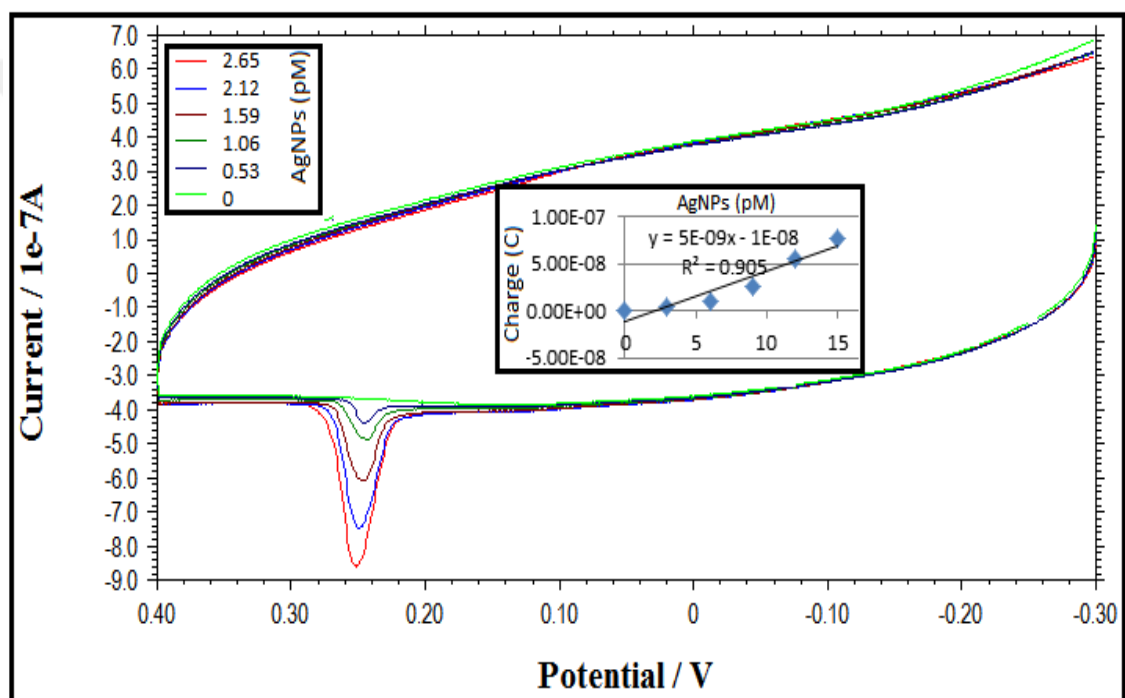


**Figure 5.11 :**  $10^4 \text{cp/mL}$  standard DNA ASV graphic and calibration curve compared to several dilutions of AgNPs

Several concentrations of HPV patient DNA for  $10^4 \text{cp/mL}$  which is the lowest detection limit of HPV DNA in the literature,  $10^5 \text{cp/mL}$  and  $10^6 \text{cp/mL}$  were modified with the same decided amounts of AgNPs-primer. Magnetic micro bead bonded to primers previously which is presented in Chapter 4. Figure 5.12, 5.13 and 5.14 are related to ASV determination of these patient samples, respectively.

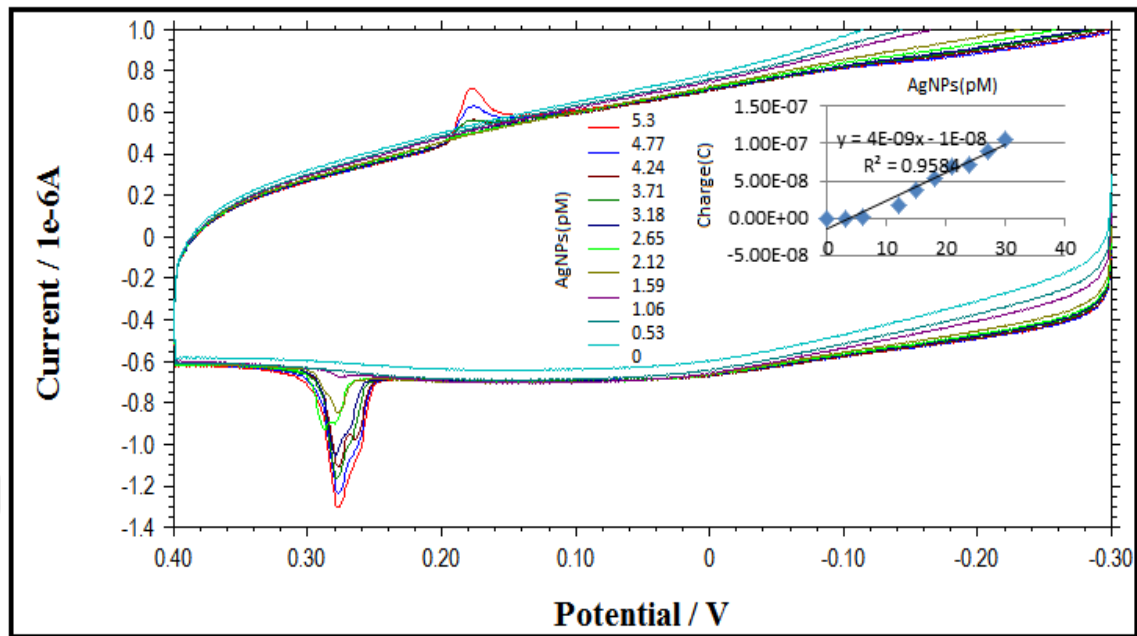


**Figure 5.12 :**  $10^4$  cp/mL patient sample DNA ASV graphic and calibration curve compared to several dilutions of AgNPs

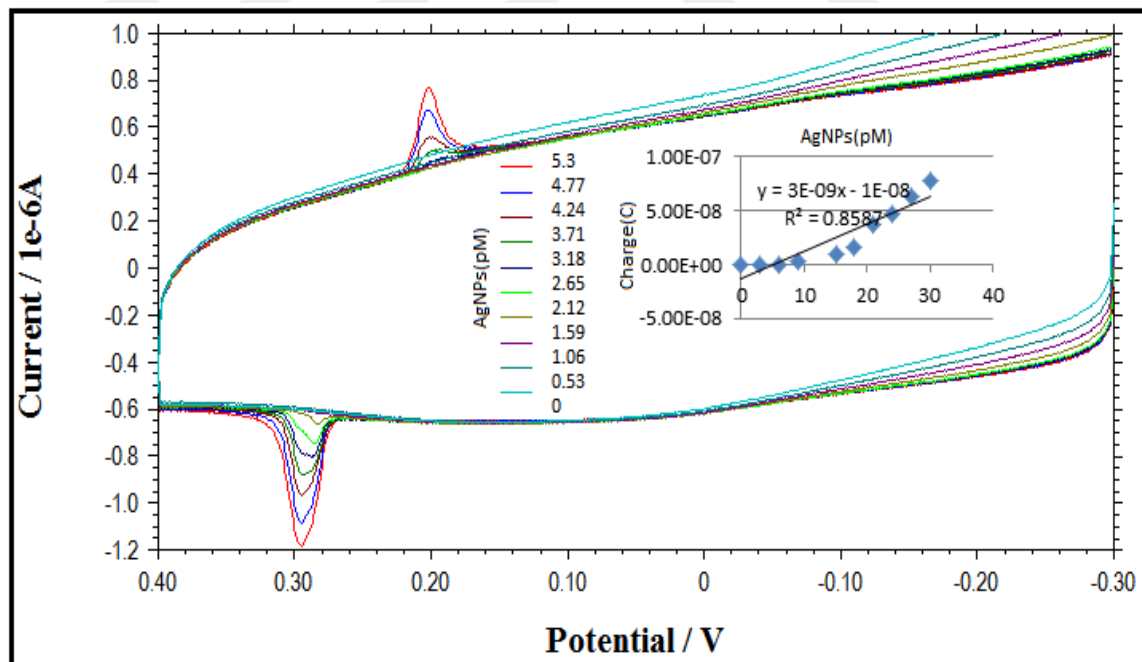


**Figure 5.13 :**  $10^6$  cp/mL patient sample DNA ASV graphic and calibration curve compared to several dilutions of AgNPs

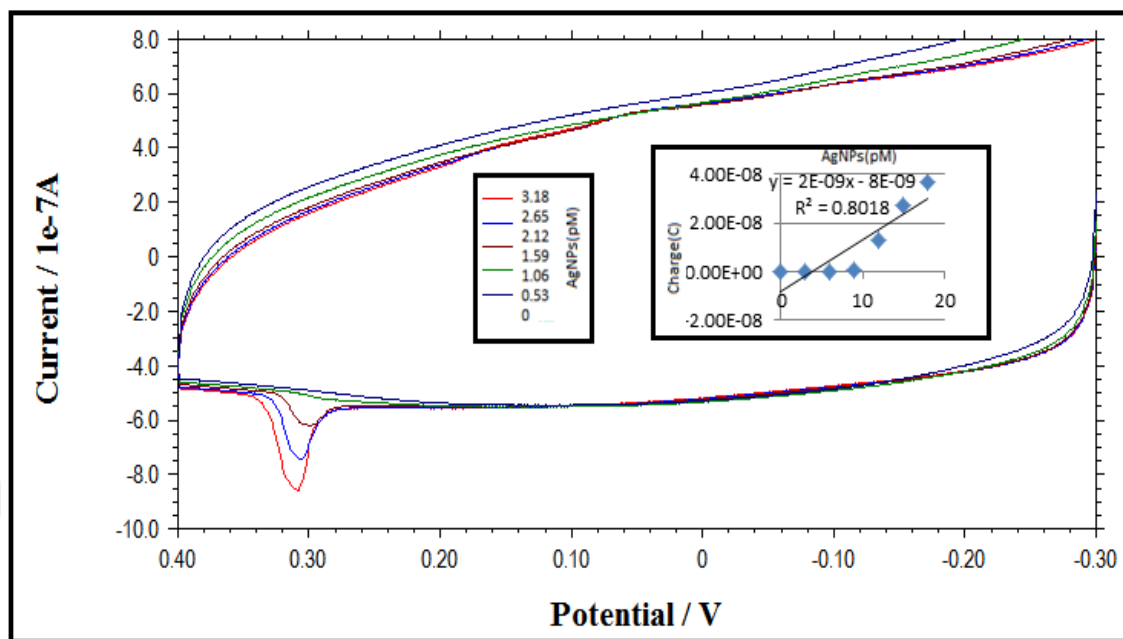


**Figure 5.14 :**  $10^5$  cp/mL patient sample DNA ASV graphic and calibration curve compared to several dilutions of AgNPs

Table 5.1 shows the patient samples detection results to figure out exact charge values which has not been notice from inserted calibration curve of analytes.

AgNPs (pM)	Patient $10^6$ cp/mL	Patient $10^5$ cp/mL	Patient $10^4$ cp/mL
2.65	1.53E-08C	3.71E-08C	5.42E-08C
2.12	9.74E-09C	2.75E-08C	3.83E-08C
1.59		1.28E-08C	1.66E-08C
1.06	3.02E-09C	5.06E-10C	
0.53	1.42E-10C	1.59E-10C	1.60E-09C

**Table 5.1.** Charge values of patient samples for  $10^4$ ,  $10^5$  and  $10^6$  cp/mL DNA amounts compared to concentrations of AgNPs from 530fM to 2.65pM

These electrochemical results are obtained as running the modified HPV samples onto paper device for electroanalytical anodic stripping determination at low detection limits. The plots show the ASV peaks as a function of the concentration of AgNPs 530fM to

2.65 Pm. The calibration curve is related to total measured charge to the concentration of AgNP labels.

Herein, saturation point of HPV patient DNA which are modified with reagents were showed as comparison of  $10^4$ ,  $10^5$  and  $10^6$  cp/mL dilutions. The red curve is the result of  $10^4$  cp/ $\mu$ L patient sample, blue one is for  $10^5$  cp/ $\mu$ L patient sample, and the Green one is for  $10^6$  cp/ $\mu$ L patient sample (Figure 5.15).

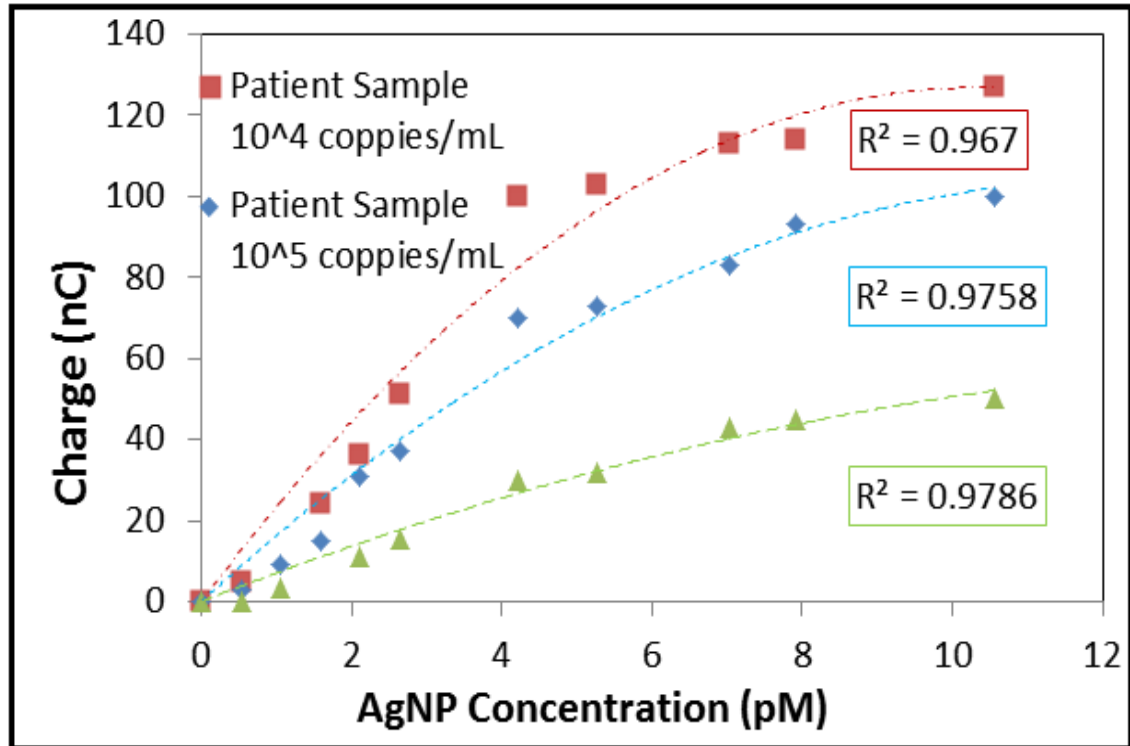


**Figure 5.15 :** Saturation of the model analyte for  $10^4$ ,  $10^5$  and  $10^6$  cp/MI DNA

The results show that the minimum copies of DNA have the max efficiency which is approximately after 7 pM. The linear range is demonstrated deviation from linearity at high Ag Np concentration.

This curve for HPV16 DNA that is modified with Ag bonded HPV 18 primer. It didn't give any peak as we expected to proof of modifying. As it can be seen, there is no peak occurred.

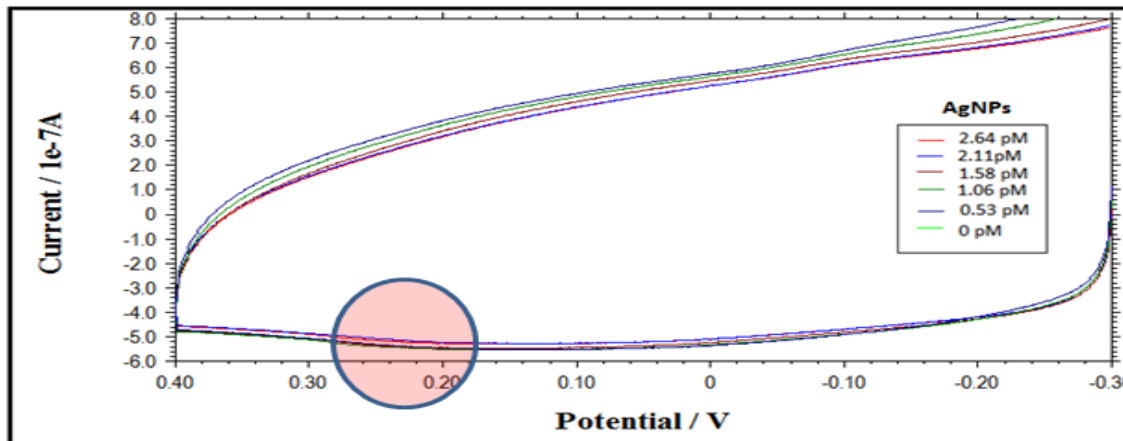


**Figure 5.16 :** AgNPs labeled HPV 18 primer hybridization with HPV 16 DNA resulted model analyte ASV plots.

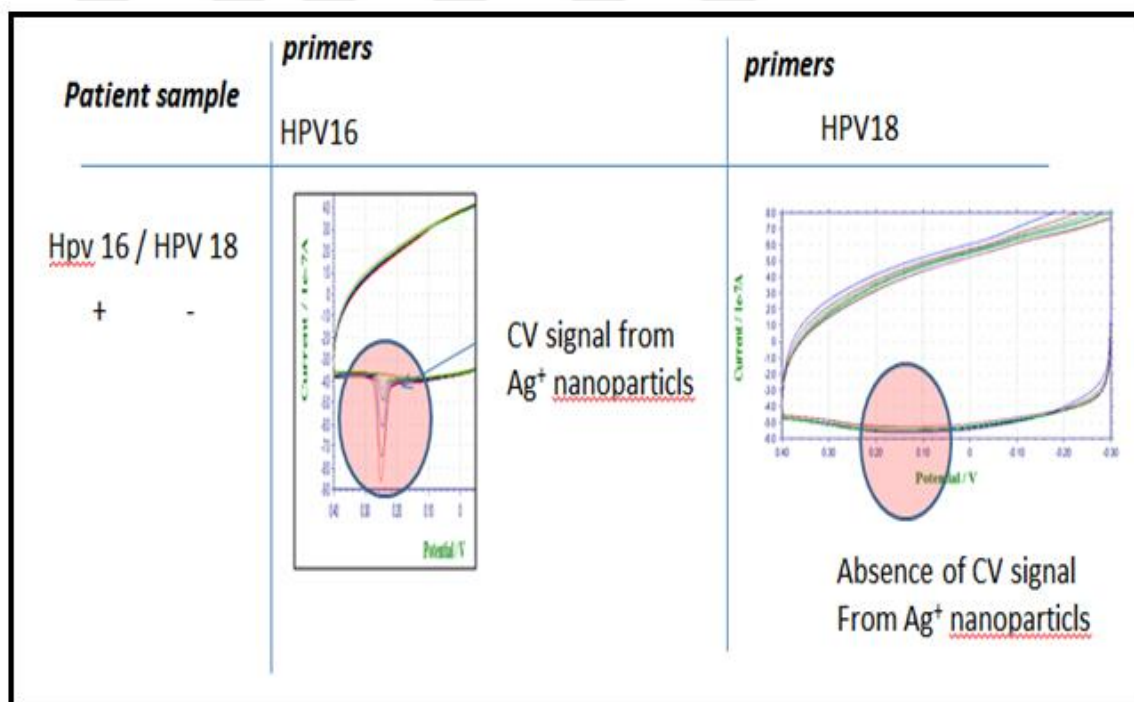


**Figure 5.17 :** Specificity conformation of model analyte as comparing different primers hybridized patient DNA

It means that we obtained a novel method for modifying the DNA with its Ag and Magnetic bead bonded primers specifically. After that, we can always use this modification process for detection of HPV via paper based analytical microchip.



#### 5.4 Summary and Future Works

It has been demonstrated a novel modification method included, new paper based device for point of care applications of Human Papilloma Virus in order to earlier diagnosis of cervical cancer. This analytical device was fabricated simply with rapid prototyping method. It is user friendly, inexpensive, robust, portable, sensitive and user friendly. It employs non enzymatic amplification and quantitative detection for low label concentrations as low as 530fM. These mentioned outstanding features were the result of novel modification technique of HPV patient sample DNA as well as its thoughtful integration of recent innovative studies such as wax printed chromatography paper surface specialties, hollow channels and analytical amplification technologies. The single step extraction by using a chemistry based non centrifuge requirement paper based platform also procure a wholly detectable paper kit for sample preparation detection of HPV. The device simplicity can be explain with its required actions by user which is rely on sending the sample onto device followed by slipping movable layer when get the signal.

The specificity of device and its simplicity provides in the use of POC application. Changing the primer which were AgNPs are labeled during hybridization process of target patient DNA. It was provided a desired specificity to detection of different types of HPV in human samples. The novel modification method which was presented in this study for labeling target DNA with silver nanoparticles, and magnetic micro beads previously labeling its primers is a consequence of this study to use in patient sample DNA directly. This process significantly provides time saving as preventing bonding AgNPs and magnetic microbeds to directly biotin and thiolated DNA.

All this desirable attributes in the proposed platform will make the device choosable for HPV POC detections. The solution conditions in electroanalytical detection assay in paper device were carried out in neutral pH and a NaCl concentration of 100 mM which provides a proper buffer medium for many bioassay (de La Escosura-Muñiz et al., 2011; Putnam, 1971; Yang et al., 2012).

In the future, the detection limit of model analyte will be decreased as using different electrode surfaces. Chapter 6 includes preliminary studies on this area.

## **6. CHAPTER: PENCIL LEAD GRAPHITE ELECTRODE AND GRAPHENE ELECTRODE BASED PAPER DEVICE IN HPV DETECTION**

### **6.1 Introduction**

Conductive wires electrodes based paper micro analytical devices are the main idea of this chapter. Conductive wire used electrodes can be prepared specific to an electrochemical assay proper its needs which makes this electrodes useful in paper device. This specific feature of wire electrodes increases the sophistication of paper analytic device compared to screen printed versions of it. Screen printed carbon electrodes only partially conductive even they have high surface areas and also surface modification is difficult with any kind of materials and receptors (Fanjul-Bolado et al., 2008; Ge et al., 2012; Tobjörk and Österbacka, 2011; Wang et al., 1998; Wu et al., 2014). In addition to these feature differences, using micro wire electrode instead of screen printed electrode in the fabrication of paper analytic device is significantly easier. It allows the electrode to be placed at any location within the device.

In the present report, we show that pencil lead graphite electrode and graphene, graphene oxide modified types can be used as electrodes in PADs based on the same principle. Besides, these electrodes can be placed within open channels cellulosic paper device as aligning target proper area. Pretreatments and modifications of these electrodes can be done externally prior to incorporation into the paper analytical device. In conclusion, this approach provides a changeable location of electrodes into device in addition to integration and immobilization.

#### **6.1.1 Graphene synthesis to use in electrochemistry**

Graphene is  $sp^2$  hybridized carbon atoms which formed of carbon allotropes as arranging in a two-dimensional planar structure (Geim and Novoselov, 2007). It is a common material for various applications because of its outstanding physical features such as large surface area and higher carrier mobility which is approximately 200 000  $cm^2 V$  per 1 s for a single layer (Bolotin et al., 2008; Geim and Novoselov, 2007; Zhu et al., 2010). The unique features of Graphene are not limited with these, it also has a huge thermal and mechanical resistance rely on two dimensional rigid structure of it.

Therefore, many special studies were done in polymer composite materials (Stankovich et al., 2006), energy storage (Yin et al., 2010), nanoelectronics (Li et al., 2010) and sensor (He et al., 2011) applications.

Graphene can be formed by one or more monolayers. It includes all C forms in its structure (Geim and Novoselov, 2007). Chemistry based method is the most common used method in the preparation of graphene which is reliable, and simple. Chemical synthesis of graphene consists of two steps. First, graphene oxide is synthesized from graphite via various methods such as Hoff- man (Hofmann and Holst, 1939; Hofmann and König, 1937), Hummers (Hummers Jr and Offeman, 1958), and Staudenmaier (Staudenmaier, 1898). Then, hydrazine and its derivatives such as hydro-iodic acid (Pei et al., 2010), sulfur containing compounds (Chen et al., 2010), chitosan (Liu et al., 2011), oxalic acid (Song et al., 2012), urea (Park et al., 2011; Wakeland et al., 2010), sodium borohyride (Shin et al., 2009; Si and Samulski, 2008), aminoacids (Gao et al., 2010), L-glutathione (Er and Çelikkan, 2014), ascorbic acid (Dai et al., 2011), metal salts (Zhuo et al., 2013), and sulfuric acid (Kim et al., 2012) based reduction agent were used to reduce graphene oxide to graphene. Reduction of graphene can also be procure by electrochemically (Shao et al., 2010). Even chemistry based graphene production method is simple and common used method, its reduction with reagents causes deterioration which effects its electronic properties (Dreyer et al., 2010). Remaining agents and oxygen groups were also affected the graphene typical honeycomb structure appearance (Pei and Cheng, 2012).

Hydrochloric acid, and hydrobromic acid which are halo acids were used by nucleophilic substitution reactions for dehydration. Dehydration is a green method that is a function of temperature in hydrothermal reduction (Zhou et al., 2009). Sulfate groups have previously been used by Dai et al. to obtain a sulfated graphene oxide structure in order to water elimination and temperature decreases effects of it (Liu et al., 2012c). There were another study carried out by Tien et al. to obtain more conductive graphene consist on a high C/O ratio as using DMF (N,Ndimethylformamide) and DMSO (dimethyl sulfoxide) mixed sulfuric acid solvents (Tien et al., 2012). Epoxy and hydroxyl groups have also been decreased in the resulted GO in Kim et al. reduction process which was carried out in the medium of sulfuric acid (Kim et al., 2012). It has

also studied reduction of graphene oxide with  $\text{NaBH}_4$  and  $\text{H}_2\text{SO}_4$  and hydroiodic acid by Pei et al. which is resulted much higher conductivity with hydroiodic acid (Pei et al., 2010).

As considering all these studies in the literature Celikkan and his group, who synthesized the graphene in our previous studies, were produced high quality graphene as using phosphoric acids and sulfuric acids because of the fact that the reaction of aliphatic or aromatic alcohols with strong acids at elevated temperatures gives alkenes with the elimination of water molecules. The graphene has been synthesized according to this method. It is used to modify pencil graphite lead in order to detect HPV target DNA in paper analytic device.

### **6.1.2 Pencil lead electrodes in electrochemical detection**

Molecular biology, and biotechnology studies on nucleic acids needs highly sensitive methods for quantitative detection. One of the most common and useful method in the analysis of DNA and RNA is electroanalytical technique (Paleček, 1996). DNA and RNA detection with adsorptive stripping voltammetry is the resulted development of the interfacial accumulation and reduction of the nucleobases at mercury electrodes (Palecek and Fojta, 1994). Micro fabricated carbon film and carbon paste electrodes also can be used in anodic stripping voltammetric assay to measure nucleic acids as using both constant-current potentiometric stripping operation and electrooxidation of the guanine moiety with the surface activity of nucleic acids (Wang et al., 1996; Wang et al., 1995). The role of electroanalysis in modern DNA diagnostics and nucleic-acid research is increased by replacement of the classical mercury drop electrode with solid-state electrochemical devices.

Using pencil lead (graphite) electrodes for adsorptive stripping measurements provides advantages in the detection of nucleic acids. Pencil electrodes have previously been used for anodic stripping voltammetric determination of metals as well as transducers successfully for electrochemical immunosensors (Engel and Baumann, 1993; Nagunuma et al., 1995; Wang et al., 2000).

Pencil electrode material has numerous advantages such as sensitive potentiometric measurements of nucleic acid inexpensively compared to the commonly used carbon paste electrode. The usage of this electrode also simpler and faster because its replacement provides a fresh surface which is not requires polishing procedures and results in good reproducibility for the individual surfaces.

### **6.1.3 Graphene interaction with DNA in electrochemistry**

Graphene is largely used in electrochemical applications because of its one atom thick honeycomb structure provides unique optical, electronic and mechanical properties in electrochemistry (Shao et al., 2010). The large area of graphene and its unique electrical conductivity make it a suitable platform to use as electrochemical biosensors (Brownson and Banks, 2010). It has numerous advantages compared to carbon nanotubes (CNTs) such as low cost various production methods and free metallic impurities provides decreases at the electrochemical signal (Shao et al., 2010). Several reagents such as nucleic acid (Bonanni et al., 2012; Yin et al., 2012), lysozyme (Bai et al., 2013), hydrogen peroxide (Kung et al., 2014) and glucose (Liu et al., 2013b) have been detected via electrochemical biosensors based on graphene and graphene oxides surfaces.

DNA in single stranded and double stranded forms. It is interacted with Graphene via hydrophobic adsorption,  $\pi$ - $\pi$  stacking and van der Waals attraction (Lei et al., 2011). Nucleobases of nucleic acids can be adsorbed to graphene via hydrophobic  $\pi$ -stacking effects. The nucleobases indicates different interactions strengths on graphene by physisorbed. DNA nucleobases interaction energy with graphene was identified with density functional theory method (Tang et al., 2010). The lowest stability of double stranded DNA on graphene has been increased by using high salt concentrations to solve the problem which is from also steric hindrance, and hydrophobic interaction (Lei et al., 2011).

In this study, AgNP labeled HPV DNA is detected with designed electrochemical assay for rapid and sensitive detection by graphene (GRP) modified pencil graphite electrode. It is an importantly first study in the literature that can detect HPV DNA in paper based

analytical platform with fabricated graphene modified, and non-modified forms of pencil graphite lead electrode for low detection limits.

## **6.2 Experimental**

### **6.2.1 Chemicals and instruments**

Anodic stripping measurements were carried out with using a bipotentiostat (700E, CH Instruments). These experiments were performed using a glassy carbon working electrode (1.0 mm diameter), Ag/AgCl reference electrode (KCl = 1 M), Ag wire reference electrode, Hg mercury reference electrode and Pt wire counter electrode (CH Instruments, Austin, TX). A Noki pencil model 2000 (Japan) was used as a holder for the pencil lead (Tombo, Japan), and a metallic wire was soldered between metallic parts of pencil to provide electrical contact. Only 3 mm of pencil lead was immersed into the solution while 4mm of pencil lead exposed outside.

Phosphoric acid ( $\text{H}_3\text{PO}_4$ ), hydrogen peroxide ( $\text{H}_2\text{O}_2$ ), nafionon, graphite powder and analytical-grade potassium permanganate ( $\text{KMnO}_4$ ), sulfuric acid ( $\text{H}_2\text{SO}_4$ ), , HCl,  $\text{NaBH}_4$  and DMF were purchased from Sigma-Aldrich. RNase free water was used which is purchased from Fisher to prepare all solutions.

The chemicals which were used during electrochemical detection as buffer and electrolyte solution and in preparation of model analyte have been previously given in art 4 and 5.

### **6.2.2 Synthesis of graphene**

Graphene oxide was produced with classical Hummers method and phosphoric acid based synthesis of graphene oxide to eliminate water also produced with Hummers method (Hummers Jr and Offeman, 1958). After GO synthesis it has been prepared to removing moisture from thin ground as keeping in vacuum oven. After that 100 mg of GO was added into a flask with 25 mL of concentrated  $\text{H}_3\text{PO}_4$  to boil the mixture at  $130^\circ\text{C}$  under the condenser during 2 hours.

The mixture was cooled down in a water ice bath after reaction was completed. The synthesized product then was taken to a beaker to wash with deionized water until

achieve desired pH level. Graphene was prepared to characterization after the product was kept in vacuum oven at 60°C during two days period. Finally, graphene solution has been prepared as adjusting it 1 mg/ mL for electrochemical measurements. Graphene was also prepared as using NaBH<sub>4</sub> (Shin et al., 2009; Si and Samulski, 2008) and H<sub>2</sub>SO<sub>4</sub> (Kim et al., 2012), for comparison in the usage of model analyte detection.

### **6.2.3 Preparation of the graphene-nafion and modification on glassy carbon electrode**

First, GO was synthesized from graphite powder using Hummers' method before preparation of Graphene-Nafion (Rahman et al., 2013). 0.25% m/v containing 25mL graphene solution was formed to (Er et al., 2016) obtain GR/NFN nanocomposite to use in electrochemical measurements as an electrode surface modification material. 1 mg/ mL graphene solution was used in this process. Graphene has oxygen functional groups on its surface which allows interaction between nafion which provides stability of Graphene.

A special polishing pad and diluted alumina solution were used to clean GCE surface followed by a base included and ultra-pure water used washing steps. Uniform dispersed solution of GR/NFN was dropped onto the surface of GCE and dried at room temperature.

### **6.2.4 Modification of pencil lead electrode with graphene, graphene-nafion, graphene oxide and graphite**

0.2 M, pH 5.0 acetate puffer solution is used for pretreatment of pencil lead electrodes before using and modifying with another material at +1.40 V for 30s followed by accumulation at +0.50 V for 60s. Each measurement was carried out using a new pencil surface.

Graphene solution was diluted ten times with in pH 5 acetate buffer solution which includes 20mM NaCl. Then pretreated pencil lead electrodes were immersed into ABS contains graphene solution for 30 minutes and washed again with ABS followed by drying step before using in electrochemical detection.

## 6.3 Result and Discussion

### 6.3.1 Characterization of synthesized graphene

Highly effective graphene synthesis was carried out according to experimental section which was previously mentioned in introduction part with Celikkan group in Gazi University, Ankara. It has the best heterogeneous electron transfer rate on the detection of HPV model analyte as expected. IR-Affinity 1 with ATR attachment (Shimadzu Corp) was used for getting FT-IR spectra. DTG-60H Thermogravimetric/Differential Thermal Analyzer(Shimadzu Corp.) was used for thermal measurements. Jeol JEM1400 instrument at 120 kV was used for TEM images recording.

Graphene oxide, and resulted synthesized graphene was characterized to figure out the functional groups investigation in their structure via FTIR spectroscopy as shown in Figure 6.1, 6.2 and 6.3. The sharp peak at  $1737\text{ cm}^{-1}$  and the broadband at  $3350\text{ cm}^{-1}$  in the graphene oxide spectrum are because of stretching of the -OH and C-O groups which are situated at the edges of GO sheets. The un-oxidized graphitic domain (C=C) consist on graphene oxide has skeletal vibrations which is appeared in the FTIR band at  $1590\text{ cm}^{-1}$ . Graphene oxide also has specific bands appears at 1215 and  $1035\text{ cm}^{-1}$  which are the characteristic bands of stretching of C-O-C (epoxy group) and C-O group in carboxylic acid.

Graphene oxide reduction has been largely effect the FTIR results of graphene as seen in Figure 6.1 Graphene spectrum apparently shows that the oxygen containing groups ( -OH, C-O and C-O-C) completely disappeared from the GO structure. There is a small band observed at  $1721\text{ cm}^{-1}$  which belongs to graphene carbonyl groups. Reduction step resulted graphene material has sharp aromatic C=C band observed at  $1547\text{ cm}^{-1}$ . This band was significantly increased as a result of the restoration of the highly conjugated graphitic structure.



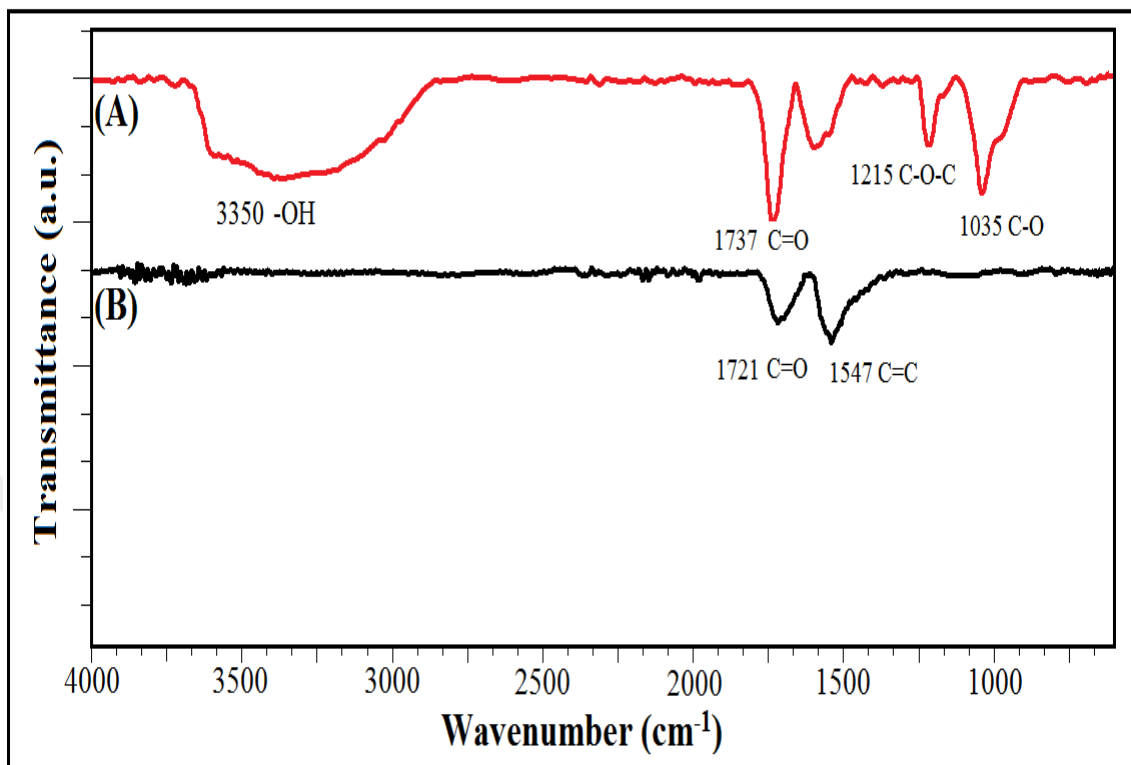


**Figure 6.1 : GO (A) and GR (B) FTIR**

Figure 6.2 represents thermal stability of graphene, and graphene oxide materials which is determined as using Thermal Gravimetric Analyzer. The red trace belongs to graphene oxide which shows a weight loss apparently up to 120° C caused the removal of adsorbed water in the sample as a result of reduction. The pyrolysis of the labile oxygen-containing functional groups in GO have been proved with the major weight loss occurred around at 200° C. Graphene oxide was totally lost 92% weight when the temperature reached 800° C.

Graphene has a superior thermal stability compared to graphene oxide according to the traces in Figure 6.2. The black trace which indicates graphene demonstrates that oxygen-containing functional groups in its structure had been removed during the chemical reduction process. The reduction of the GO with the proposed chemical reduction method have been confirmed with the total weight loss of GR was found to be 52% at 800° C.

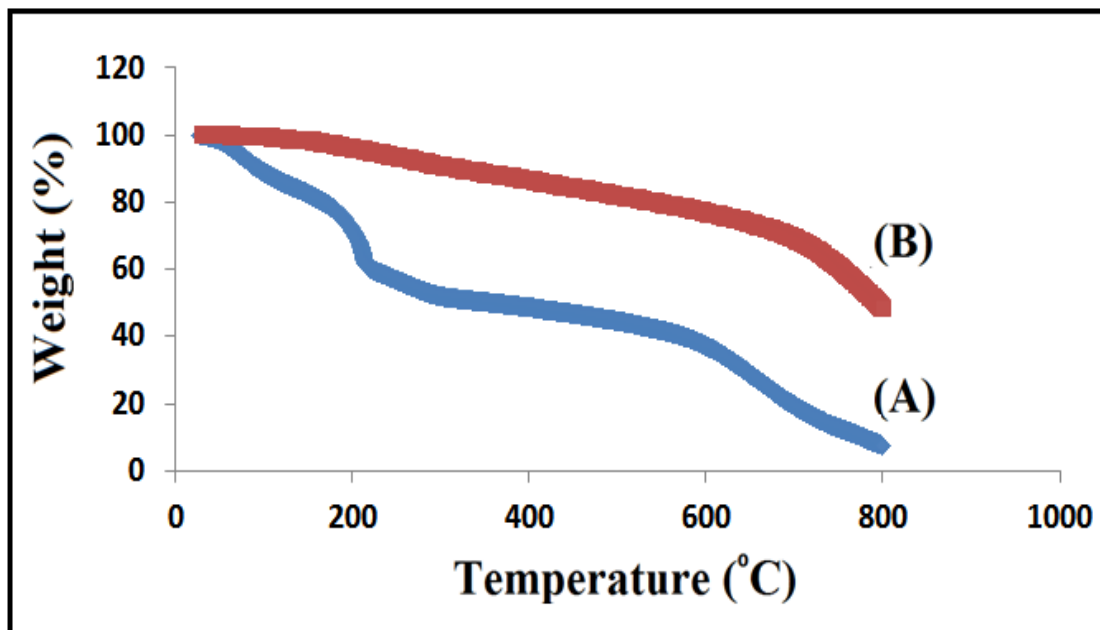


**Figure 6.2 :** Thermal Gravimetric Analyse curves of GO (A) and GR (B).

The holey carbon grids of graphene and surface morphologies of graphene oxide were characterized as using Transmission Electron Microscopy in Figure 6.3. The successful reduction of GO was occurred by phosphoric acid according to the large GR sheets with a few layers. The typical wrinkled large sheets indicate graphene oxide in the TEM (Transmission electron microscope) image.

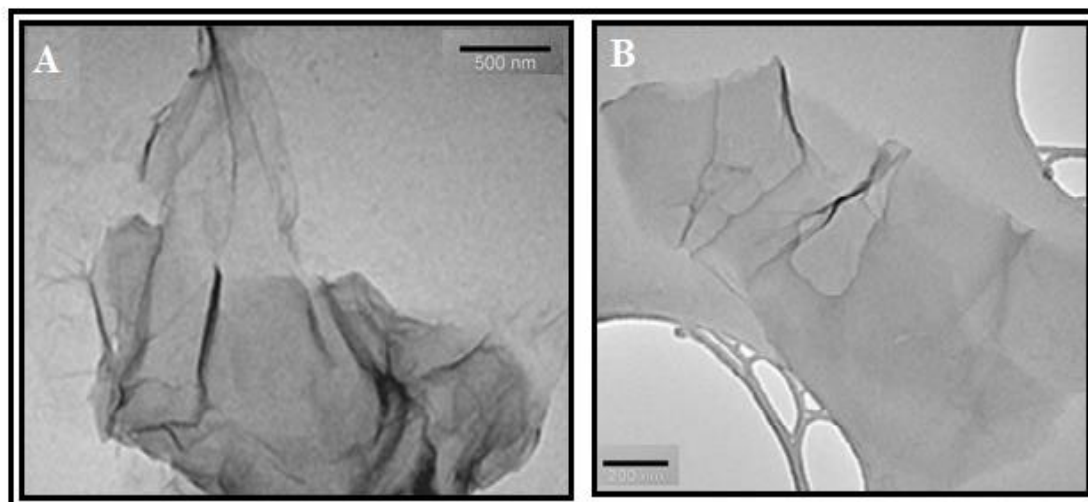


**Figure 6.3 :** TEM images of GO (A) and GR (B) nanosheets.

### 6.3.2 Pencil lead electrode included paper device fabrication

Paper leads were cut in two cm length and aligned onto the locations of wax printed, laser engraved and all dyes and reagents dispensed cellulose paper analytical device followed by attachment using epoxy. The epoxy was also put on to the pencil lead except 3mm area let on the top end of electrodes. A nail polish was also applied to obtain more hydrophobicity on the residual part of the electrode. Only the 3 mm area was used for analytical detection as optimized and studied prior in conventional cell.

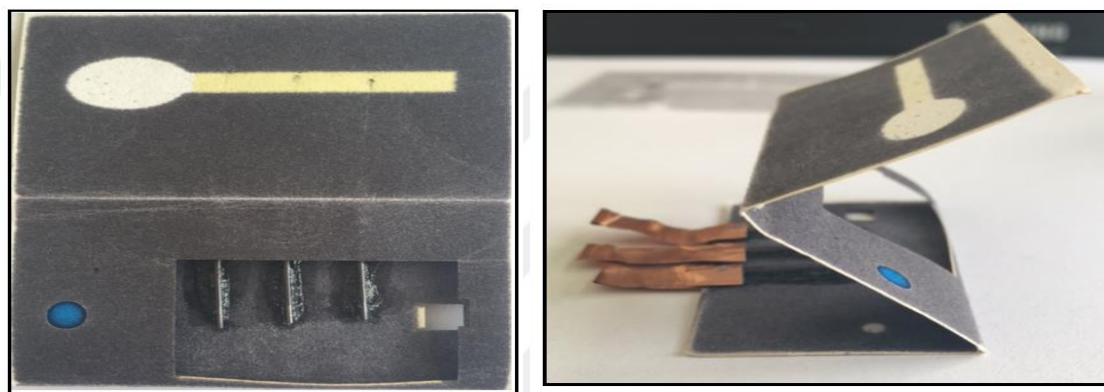


**Figure 6.4 :** Pencil Lead electrode in paper microfluidic chip fabrication

After fabrication of paper device with pencil lead electrodes, the cellulose paper was fold as shown in Figure 6.4 and 6.5 in a zigzag position. The assembled device has the 3mm detection targeted lead electrodes adjusted in hollow channels.

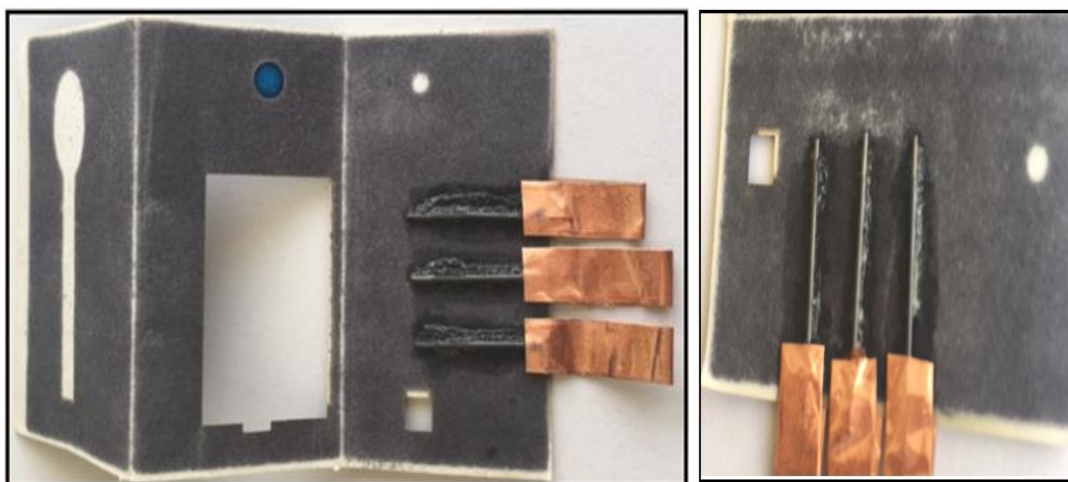


**Figure 6.5 :** Electrical contacts of pencil lead electrodes

The contacts of pencil lead electrodes were added before epoxy and nail polish painting process. A copper epoxy was used to attached copper tape on to the electrodes. The pencil lead electrode also used with its modified forms. Graphene, Graphene- Nafion and Graphene Oxide were previously synthesized and characterized which were presented in this chapter. The preparation of modification materials before adsorbance onto the pencil lead electrodes were also presented in details at experimental section.

The paper based analytical device which were fabricated with bare graphite pencil lead electrode and graphene, graphene oxide, graphene-nafion , graphite modified pencil electrodes have been used and compared in the detection of AgNPs and Magnetic microbeads labeled Human Papilloma Virus' DNA. The results were also compared with carbon printed electrodes in order to choose proper high yield electrode surface for earlier diagnosis of cervical cancer at the point of care technology.

### 6.3.3 Electrochemical results comparison of HPV model analyte on the surface of pencil lead, graphene, graphene oxide, graphene-nafion and graphite

Electrochemical studies of pencil lead electrodes were first carried out in conventional cell prior to use in paper analytical device. 530 fM model analyte which is labeled AgNPs were tested as using glassy carbon electrode, pencil lead electrode and graphene electrode and their anodic stripping results were compared according to charge values Figure 6.6.

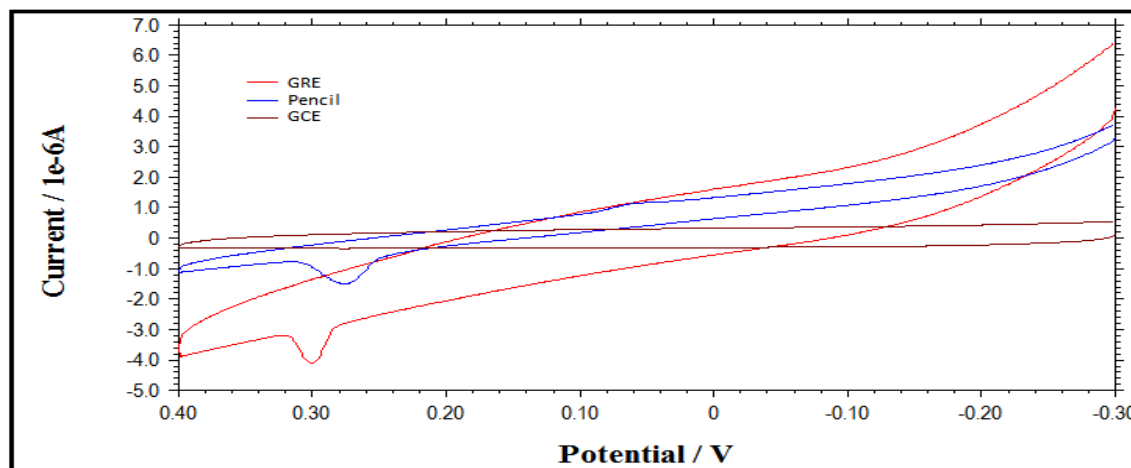


**Figure 6.6 :** Comparison of Glassy Carbon electrode, Pencil electrode and Graphene electrode

The red trace in Figure 6.6 belongs to graphene modified pencil electrode, the blue trace consists of bare pencil lead electrode and the brown trace belongs to glassy carbon electrode. Anodic stripping charge results were calculated  $4.78 \times 10^{-7}$ ,  $2.14 \times 10^{-7}$  and  $2.27 \times 10^{-8}$  coulomb respectively. The charge results were indicate that pencil electrode charge value is 10 times higher than glassy carbon electrode charge value for same concentrations of model analyte. Graphene modification also increased the charge value of AgNPs labels approximately 2 times. GCE results were compared with pencil electrode results according to their molarity in Table 6.1.

GCE	Pencil Electrode	AgNPs
-2.27E-08	-9.38E-07	3
-3.98E-08	-2.49E-06	6
-3.62E-07	-5.99E-06	9
-9.90E-07	-9.33E-06	12
-1.78E-06	-1.09E-05	15

**Table 6.1.** GCE and Pencil Electrode results for AgNPs

Graphene was synthesized with several methods to increase detection capacity as mentioned in experimental and introduction part of this chapter. Graphene oxide, two different graphene (1.21 and 1.9), and graphene-nafion solutions were used to modify pencil lead electrode. These electrodes were used for anodic stripping voltammetric determination of several dilutions of AgNPs labeled model analyte from 530fM to 2.65pM. The calibration curve which is related to total measured charge to the concentration of AgNP labels were presented inside the ASV graphics for each electrode types ( Figure 6.7,6.8.,6.9,6.10)

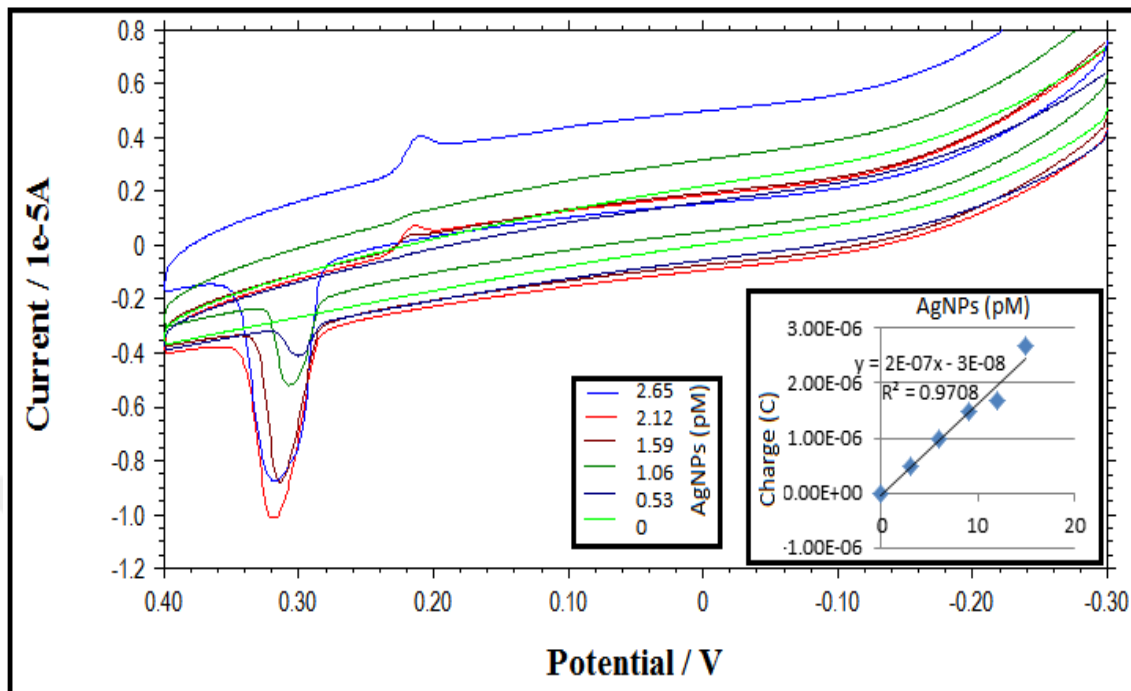


**Figure 6.7 :** GRE 1.21 modified pencil lead electrode ASV result and calibration curve

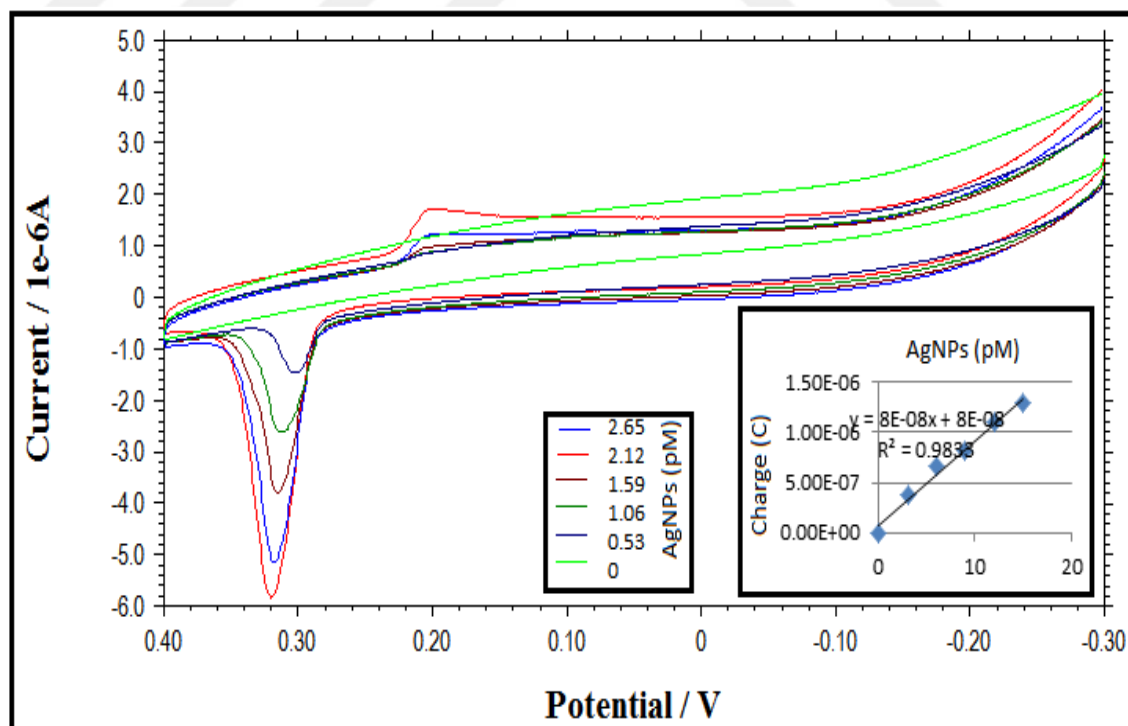


**Figure 6.8 :** GRE 1.9 modified pencil lead electrode ASV result and calibration curve

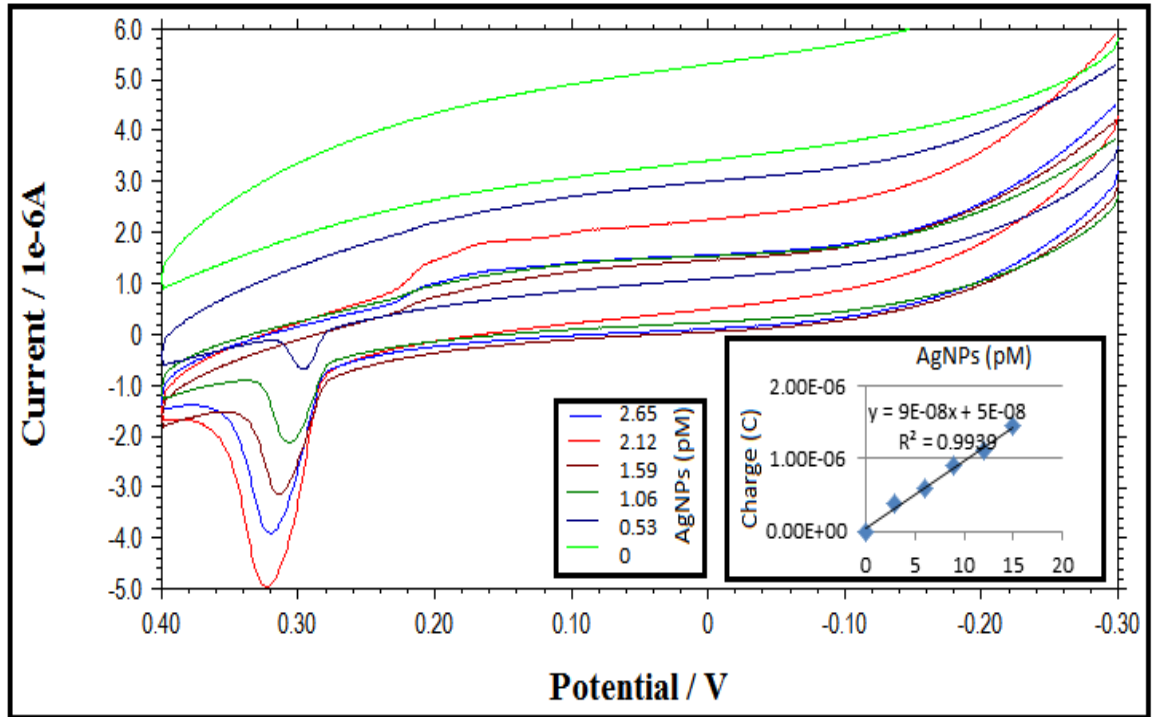


Figure 6.9 : GRO modified pencil lead electrode ASV result and calibration curve

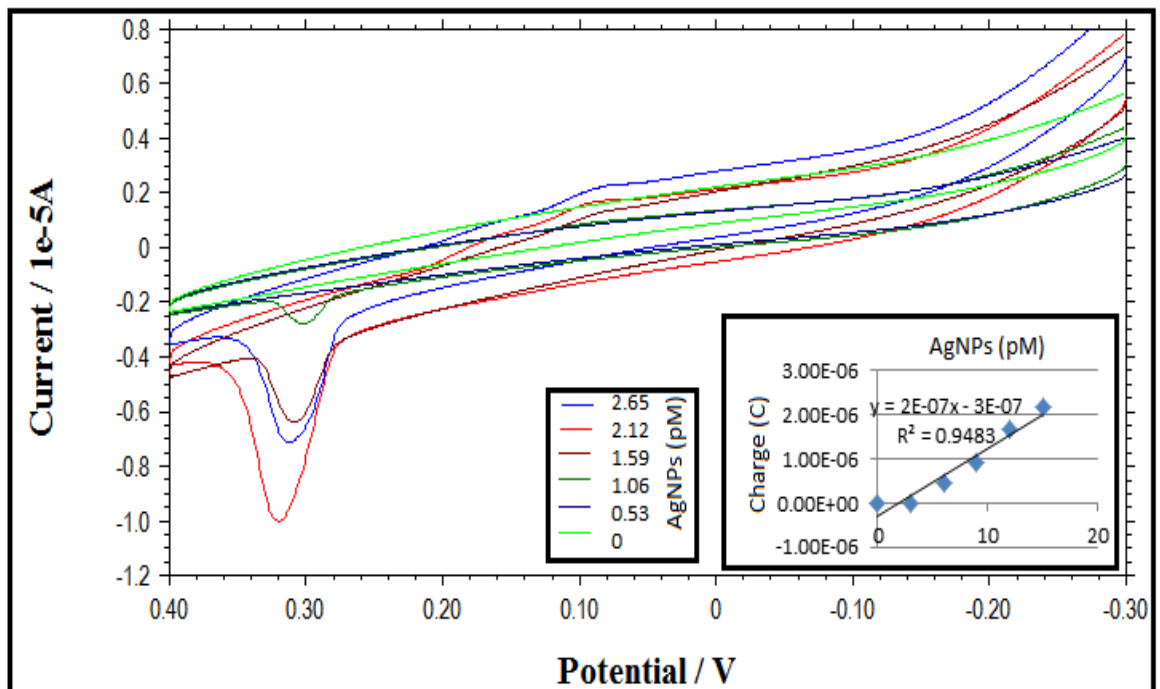


Figure 6.10 : Graphene-Nafion modified pencil lead electrode ASV result and calibration curve

The calibration curve of each modification material was compared and the sensitivity values have been found very close to each other. However, graphene-nafion modified electrode did not give a peak for LOD. There is no peak curve occurred at 530 fM.

In addition to this nafion-graphene material has a non-specific peak in the presence of solution without adding AgNPs which causes treatment of surface. As considering charge values resulted from peak currents were presented in Table 6.2 according to their molarities.

<b>Ag(pM)</b>	<b>GRO</b>	<b>gre 1.9</b>	<b>nfn</b>	<b>gre 1.21</b>
<b>2.65</b>	1.45E-06	1.29E-06	2.16E-06	2.67E-06
<b>2.12</b>	1.13E-06	1.10E-06	1.65E-06	1.67E-06
<b>1.59</b>	9.09E-07	8.20E-07	9.27E-07	1.48E-06
<b>1.06</b>	5.91E-07	6.72E-07	4.46E-07	9.67E-07
<b>0.53</b>	3.88E-07	3.72E-07	0.00E+00	4.78E-07

**Table 6.2.** Charge values of each type modified pencil electrodes for comparison

Table 6.2 apparently shows that graphene 1.21 modified electrode result for several dilutions of AgNPs labeled model analyte from 530fM to 2.65pM have a high sensitivity, and high yield charge values. Especially minimum amounts of analyte even not exactly has a huge difference for high values of analyte compared to other modification materials.



## 6.4 Summary and Future Works

As a result of this chapter, the detection limit of HPV DNA model analyte has been decreased by using different electrode surfaces. Pencil Lead Graphite electrode, graphene electrode, and graphene oxide electrode surfaces has been used in order to achieve LOD for analytical detection. Their ASV detection results were calculated as considering their charge results for each electrode surface compared to the stencil printed electrode results.

The anodic stripping charge results of pencil lead electrode and glassy carbon electrode were calculated as  $2.14 \times 10^{-7}$  and  $2.27 \times 10^{-8}$  C, respectively. The charge results were indicate that pencil electrode charge value is 10 times higher than glassy carbon electrode charge value for 530fM model analyte.

Herein, three different graphene types and graphene oxide were used in the modification of pencil lead electrode to obtain low detection limits of model analyte. Graphene has been synthesized with enhanced hummers method via phosphoric acid. It has been also synthesized nafion reinforced graphene to use in modification of pencil lead electrode.

Graphene modification also increased the charge value of AgNPs labels approximately two times. All types of graphene were modified onto the pencil lead electrode and their anodic stripping voltammetric charge results have been compared. Graphene 1.21 modified electrode result for several dilutions of AgNPs labeled as a model analyte from 530fM to 2.65pM demonstrated a high sensitivity, and high yield charge values.

Our analytical paper device is fabricated with graphene modified and unmodified pencil lead electrodes instead of stencil printed electrodes. Preparation of the electrode part of paper device with pencil lead electrodes are easier than stencil printing on the paper device. It also provides equal and wide detection area due to the 3D shape of the electrode. Graphene modification is increased the yield of detection with its 2D surface area particularly.

## 7. CONCLUSIONS AND RECOMMENDATIONS

In this thesis work, a paper based, disposable point-of-care microfluidic device has been developed that can isolate, amplify, and detect HPV 16 and 18 (the etiological agent of cervical cancer).

The adjustment of positive control of workouts via PCR has an undeniable role during these study. Thus, HPV DNA cloning steps and optimization parameters of their combined form amplifications have been studied in Chapter 2. Combined HPV types 16, 18 have been optimized with different concentration of primers, reagents ( $MgCl_2$ , dNTPs), reaction time, and temperature in order to use in confirmation steps. Before the optimization step, HPV DNA stocks have been prepared via cloning the E7 genes for HPV 18 and 16, and confirmed by using GeneWiz. These stocks are used for the optimization of efficiency and specificity of the TaqMan reaction.

The proper conditions for maximum amplification have been arranged by testing different dilutions of the reagents. The performance of the amplification has been done in different temperatures, and the reaction time on the qPCR machine. The concentration of HPV 16 and RNaseP primers have been adjusted to  $0.25 \mu M$  as shown on Table 2. The amount of HPV 18 primers was also  $10 \mu M$  in a combined tube. The optimal concentration of dNTPs reagent is  $10 mM$ . The dilution of  $MgCl_2$  is  $50 mM$  as an other reagent. The temperature and reaction time for maximum amplification have been demonstrated in Table 3.  $55 \text{ }^\circ C$ , extension temperature for 30 seconds, and  $60 \text{ }^\circ C$  reading time for 1.5 minutes gave the maximum performance (Figure 4).

Chapter 3 indicates sample preparation stepn which is very important for microfluidic chip fabrication. Traditional methods require some expensive instrumentations as centrifugation, extraction and concentration of DNA to achieve proper low detection limits. The rapid prototype must include an on-chip extraction part. The Klapperich Laboratory has a method for lysis, extraction, and precipitation of DNA in a single step. The combined solution has been optimized for HPV DNA, and tested on a paper pipet tip column. The fabrication of special paper tips had been done as the protocol that was shown previously before the solution is flowed through the column.

Cervical cells have been lysed to release HPV DNA for downstream amplification, and detection. The optimal amount of chemical lysis, extraction, and precipitation matrix has been arranged as 5.5 M guanidinium thiocyanate, 5 M sodium chloride, 15.8  $\mu\text{g}/\mu\text{l}$  glycogen, and 50% isopropanol. For capturing max DNA, it has been used the paper tips which have nearly 2-3 minutes extraction time. Lysis & extraction buffer efficiency had been quantified by PCR. The plots of each types of HPV DNA are drawn in order to reach more precipitation for minimum detection limit of the nucleic acids.

LOD study and optimal cell medium of the electrochemical detection have been done in the conventional electrochemical cell which is prior to use in the fabricated paper microfluidic chip, in Chapter 4. Several concentrations of AgNPs are used for optimization in the presence of 50  $\mu\text{L}$  10  $\mu\text{M}$   $\text{KMnO}_4$ . 47  $\mu\text{L}$  water is added into the cell for each experiment for dilution of AgNPs. PBSCl or Borate buffer are used as an electrolyte solution. 62.5  $\mu\text{L}$  100mM PBS, and 62.5  $\mu\text{L}$  100mM NaCl are used to achieve the appropriate PBSCl buffer. Detection voltage range is arranged between -0.7 to 0V. Also, the preconditioning time is adjusted to 200s. It is applied for -0.3V in the presence of  $\text{KMnO}_4$  and PBSCl solution for detection of AgNPs.

The paper based analytical microfluidic chip has been fabricated in chapter 5, after finishing optimization of PCR amplification in chapter 2, production of paper extraction support material and its single step chemical buffer in chapter 3, and adjusting proper optimal analytical cell conditions for low detection limits of combined HPV in chapter 4. Paper device is demonstrated on a chromatography paper, and designed device shape wax printed on it. The  $\text{KMnO}_4$  and blue dye dispense on to the paper cut off after the reservoirs. The electrodes are also stencil printed on to the target area of the device to obtain last folded 3D composition of paper microchip.

The detection limit of HPV DNA model analyte in paper device has been increased as using graphene modified pencil lead electrodes instead of stencil printed electrodes in chapter 6. Special high yield graphene has been synthesized to modify it on to the pencil lead electrodes. Their charge values have been calculated in order to compare with stencil printed electrode and bare pencil lead electrode. Charge value of the pencil lead electrode is ten times higher which makes it better than the carbon electrode. In addition

to this, graphene modification increased the charge value additional two more times than bare pencil lead electrode.

These new electrodes have been used in fabrication of the device. Pencil leads electrodes were provided simplicity in electrode addition onto the paper device. Surface of these electrodes also expanded the detection area due to their 3D equal structures. The special properties of graphene also effected the detection yield values depends on its 2D structure, and phosphoric acid based synthesis.

In conclusion, we have reported a paper extraction support material, and a new paper based electrochemical detection device which includes novel modification method for HPV 16 and 18 DNA at POC applications. We also applied the method to the patient samples which are provided from Beth Israel Hospital. It can extract at least 10 copies per  $\mu\text{L}$  DNA from patient samples approximately in 10 minutes, and detect low label concentrations as low as 530 fM in only 4.6 min. This device is inexpensive, user friendly, sensitive to HPV detection, quantitative, robust, and compatible to simple and rapid fabrication techniques.

## APPENDIX 1

Save all plates and DNA Mixtures (ligation, digestion, etc) UNTIL all cloning has been completed, confirmed, and sequenced.

Klapperich Lab Protocols Helpful links:

[http://www.addgene.org/plasmid\\_protocols/PCR\\_cloning/](http://www.addgene.org/plasmid_protocols/PCR_cloning/)

### Day 1

#### 1) PCR with Stock DNA; This step replicates the DNA!

PCR Protocol: PCR Protocol for Phusion HighFidelity

DNA Polymerase ;

Use the 50 µl reaction template, Run PCR on Thermocycler with proper settings based on protocol. Test conditions with varied DNA, MgCl<sub>2</sub>, and DMSO. Save 5 µl of the final reaction to run in a gel.

#### 2) Validate PCR Reaction with Agarose Gel

Check to see if the PCR worked! Note: >1KB 1% gel, <1KB .5% gel, <300KB .1% gel

Make 1.5% agarose gel

1. Set up gel box in 720. Wet rubber gasket before putting gel tray in. Add comb (16well).
2. Take out EtBr waste container.
3. Prepare gel solution in designated gel flask.
4. For a larger agarose gel,
  - a. 1.5 g of ultrapure agarose
  - b. 100 mL of 1x TAE buffer
5. Microwave ~1.52 min until solution is clear.
6. Let cool in water bath until flask is cool to touch.
7. Add 5 µL Ethidium Bromide (put tip in EtBr waste container!) directly into flask

8. Pour gel into gel tray, avoiding bubbles. Move bubbles to bottom of tray with a pipette tip.
9. Let polymerize at room temperature for 30 min.
10. Clean flask with hot water and make sure there is no residue.

### **Run the gel**

1. Flip gel tray so samples will run vertically
2. Thaw appropriate ladders for gel. We used the NEB 100 bp ladder.
3. Add Blue DNA loading Dye with Ficoll at a 1:5 ratio to sample. (1  $\mu$ l of dye for 5  $\mu$ l of pcr sample). Flick tubes gently to mix.
4. Fill box with 1x TAE buffer until gel is covered.
5. Take out comb and make map of samples.
6. Add 5  $\mu$ l for each ladder you will run in your gel.
7. Add your samples with dye into the appropriate lane.
8. Make sure the black lead is next to the lanes when running the gel.
9. Attach the leads and cap and connect to power supply. Set power supply to 100V and run for approximately 1 hr.
10. Image the gel with Quantity One system

Check the bands against the ladder to make sure you have the appropriate DNA.

Pick the lanes that have the darkest/most concentrated DNA based on the image.  
(consider the options below)

If all of the lanes have similar concentrations pick lanes without DMSO for the next step. If the lanes are light and not dark in color use all four PCR lanes

### **3) Phenol Chloroform Extraction**

This step cleans up all the PCR junk from the DNA!

For Phenol Chloroform Extractions, the key thing to note is the final concentration of your mixture has to have a 0.3 M concentration of sodium acetate.

For each DNA type being cloned, the below reaction must be done. For example, HPV16 and HPV18 will need its own 500 µl reaction.

For a 500 µL reaction,

Reaction Component Final Concentration Volume

DNA 1X 45 µl \* (# of lanes are good from agarose gel) 3 M Sodium Acetate, pH 5.2  
0.3 M 50 µl Buffer TE 500 [DNA + 3M Sodium Acetate Volume]

1. Add equal reaction volume (500 µl) of neutral pH Phenol:Chloroform (in 720 left fridge the unlabeled bottle) to the reactions.
2. Vortex for 20 sec. This will dissolve all proteins and bring them into the organic phase, while leaving DNA in the aqueous phase.
3. Centrifuge @13,000 rpm for 10 min. This will separate the aqueous phase (top) from the organic phase (bottom).
4. Remove top chloroform phase to a new 1.5 ml tube, and discard lower phenol phase to waste. (Do not remove any of the lower phenol phase!)
5. Add 2 µl of white glycogen and 500 µl of isopropanol to the tubes.
  - a. White glycogen packs more DNA than blue glycogen but is harder to see.
  - b. Can use 1 aqueous solution of isopropanol OR 3 aqueous solutions of 95% ethanol.
  - c. If using glycogen, all the next steps can be done with room temperature solutions. If not using glycogen, the solutions must be icecold.
6. Vortex for 15 sec, and centrifuge @13,000 rpm for 10 min
7. Decant tubes and add 600 µl of 70% ethanol to tubes.
8. Vortex 15 sec, and centrifuge @13,000 rpm for 5 min
9. Decant tubes and remove remaining liquid with 20 µl pipette tip
10. Dry tubes for 10 min @ room temperature
11. Add 25 µl of Buffer TE to resuspend the DNA/glycogen pellet for each tube

#### 4) Digest the PCR Product

This step will cut the DNA at the locations that will stick to the plasmid and remove excess DNA.

Reaction Component Volume

DNA 25  $\mu$ l, SPEI 2  $\mu$ l, AATII 2  $\mu$ l ,BSA (1 mg/ml) 4  $\mu$ l, NEB Buffer 4 4  $\mu$ l, RNase free DNase free water 3  $\mu$ l= Total Volume 40  $\mu$ l

Leave overnight in 37°C incubator or at least 3 hours.

Day 2

1) Run gel for digest products Isolate the DNA that you want!

Note: Make sure you have LB, LB + AMP, and LB + AMP plates.

1. Prepare gel (follow protocol from Day 1)
2. Thaw ladders appropriate for this gel
3. Add 8  $\mu$ l loading dye to 40  $\mu$ L digest product
4. Try to load all of the digest product + dye if possible otherwise load as much as you can!
5. Run gel for 1 hr @ 100 V
6. Image gel according to the protocol in Day 1

2) Gel extraction (preheat 50°C heat block!)

Extracts your DNA!

1. Pick the lanes you would like to extract.
2. Label tubes before cutting the gel.
3. Retrieve the UV light and protective eye wear and lab coat to cut out the bands from the gel.
4. Use a clean blade for each lane (be sure not to contaminate!)
5. Follow instructions for Qiagen Gel Extraction Kit



6. Elute in 30  $\mu$ l Buffer EB @ center of column

### 3) Ligation

Inserts your DNA into the plasmid! This step can be done at room temperature, but add the ligase last.

#### Reaction Component Volume

DNA 7  $\mu$ l, pGEM vector 1  $\mu$ l, 10x ligase buffer 1  $\mu$ l, T4 DNA ligase 1  $\mu$ l = Total 10  $\mu$ l

1. Using a p10 tip, pipette each mix up/down to mix; do not vortex!
2. Incubate on bench @ room temperature for 1 hr
3. Meanwhile, add water to heat block and set temperature to 42°C for transformation step
4. Retrieve ice bucket for the Top 10 Cells
5. When close to the 1hr mark, thaw one vial of Invitrogen Top 10 cells (for 2 samples) in ice bucket
6. When cells are thawed, split cells into 2 equal aliquots (~2530  $\mu$ l each)

### 4) Transformation

Inserts your DNA + plasmid into the cell!

Top 10 Cells must be kept on ice at all times, unless indicated otherwise.

1. Add 5  $\mu$ l of your ligate to the aliquoted Top 10 Cells. Tap gently to mix and place on ice for 5 minutes.
2. Heat shock in 42°C heat block for 45 seconds and return to ice bucket for 2 minutes.
3. Take the cells off ice and add 250  $\mu$ l of LB (no drugs) to each tube (use burner to sterilize)
4. Place in 37°C shaker for 1 hr recovery
5. To minimize the volume, before plating spin down the cells 13,000 rpm, 30 sec, and decant media. Leave ~ 100  $\mu$ l of liquid in the tube. Vortex to resuspend.

6. Plate cells on LB + AMP plates and wrap with parafilm. Flame glass stick and streak until all of the liquid is dried. Grow overnight in 37° incubator.

Day 3

1) Restreak

To ensure you have individual colonies for Mini Prep!

1. Warm LB + Amp plates in 37°C incubator

2. Divide the plate into 4 quadrants and label each quadrant

3. Restreak 1 colony per quadrant following the pattern below:

a. Orange mark: Using a clean flat toothpick, pick a colony from Day 2 plate and smear vigorously back and forth a few times at the edge of the plate. Discard toothpick.

b. Blue mark: With another toothpick, make 1 smear through the orange mark. Discard toothpick.

c. Magenta mark: With another toothpick, make a continuous smear squiggle toward the center of the plate. Discard toothpick.

4. Wrap plates with Parafilm and let grow overnight @ 37°C.

5. If doing Mini Prep in 2 days, grow up liquid cultures. If not, can store plate in fridge until ready to do Mini Prep in 2 days.

Day 4

Grow up liquid cultures for Mini Prep and Frozen Stocks.

1) Grow Liquid Culture

Put 3 ml LB + Amp media in each 15 ml tube Pick 1 colony from each quadrant and vigorously stir into media Place tubes diagonally in 37°C shaker and let grow overnight

Day 5

Make frozen stocks and extract plasmids from bacteria!

1) Mini Prep and Frozen Stocks

1. Freeze 1.25 ml cells with 0.75 ml of 40% glycerol in the orange 2 ml tubes.
2. Use the rest of the cells (~1.75 ml) for Mini Prep
3. Follow Qiagen Mini Prep protocol
4. Elute in 30  $\mu$ l Buffer EB.
5. Measure DNA concentration with Nanodrop using Buffer EB as the blank. This determines how much DNA to use in the test digest.

## 2) Test Digest

If DNA concentration is  $>200$  ng/ $\mu$ l, dilute by 1/10 with Buffer EB and use 1  $\mu$ l for test digest. If DNA concentration is  $<200$  ng/ $\mu$ l, use 1  $\mu$ l directly.

Mix all reaction components and add enzymes last (SpeI and AatII).

### Reaction Component Volume

DNA 1  $\mu$ l, SPEI 1  $\mu$ l, AATII 1  $\mu$ l, BSA (1 mg/ml) 2  $\mu$ l, NEB Buffer 4 2  $\mu$ l, RNase free DNase free water 33  $\mu$ l = Total Volume 40  $\mu$ l

Leave overnight in 37°C incubator or at least 3 hours.

## Day 6

- 1) Run gel for test digest Double check your DNA!

Run another gel based on Day 1 to check to see if your DNA is the correct one that you would like in your final product! If it looks correct, pick the samples that have the most promising results and prepare to send out for sequencing. Refer to post it on bench next to Blackbird. Sent DNA to control to GeneWiz.

## Day 7

- 1) Midiprep Grow up all of the colonies from the quadrants to get a bajillion DNA!

## REFERENCES

- Abe, K., K. Suzuki, and D. Citterio. 2008. Inkjet-printed microfluidic multianalyte chemical sensing paper. *Analytical chemistry*. 80:6928-6934.
- Alves, G., J.M. Magalhães, R. Tauler, and H.M. Soares. 2013. Simultaneous anodic stripping voltammetric determination of Pb and Cd, using a vibrating gold microwire electrode, assisted by chemometric techniques. *Electroanalysis*. 25:1895-1906.
- Amatatongchai, M., O. Hofmann, D. Nacapricha, and O. Chailapakul. 2007. A microfluidic system for evaluation of antioxidant capacity based on a peroxyoxalate chemiluminescence assay. *Analytical and bioanalytical chemistry*. 387:277-285.
- Anand, R.K., E. Sheridan, K.N. Knust, and R.M. Crooks. 2011. Bipolar Electrode Focusing: Faradaic Ion Concentration Polarization. *Analytical chemistry*. 83:2351-2358.
- Anderson, J.R., D.T. Chiu, H. Wu, O. Schueller, and G.M. Whitesides. 2000. Fabrication of microfluidic systems in poly (dimethylsiloxane). *Electrophoresis*. 21:27-40.
- Arney, A., and K.M. Bennett. 2010. Molecular diagnostics of human papillomavirus. *Laboratory Medicine*. 41:523-530.
- Bahadır, E.B., and M.K. Sezgintürk. 2015. Applications of commercial biosensors in clinical, food, environmental, and biothreat/biowarfare analyses. *Analytical biochemistry*. 478:107-120.
- Bai, L., B. Yan, Y. Chai, R. Yuan, Y. Yuan, S. Xie, L. Jiang, and Y. He. 2013. An electrochemical aptasensor for thrombin detection based on direct electrochemistry of glucose oxidase using a functionalized graphene hybrid for amplification. *Analyst*. 138:6595-6599.
- Bard, A.E.F. 1980. LR Electrochemical Methods. *Fundamentals and applications*.
- Barden, C.B., K.W. Shister, B. Zhu, G. Guiter, D.Y. Greenblatt, M.A. Zeiger, and T.J. Fahey. 2003. Classification of follicular thyroid tumors by molecular signature results of gene profiling. *Clinical Cancer Research*. 9:1792-1800.
- Bartholomeusz, D.A., R.W. Boutté, and J.D. Andrade. 2005. Xurography: rapid prototyping of microstructures using a cutting plotter. *Microelectromechanical Systems, Journal of*. 14:1364-1374.
- Baseman, J.G., and L.A. Koutsky. 2005. The epidemiology of human papillomavirus infections. *Journal of clinical virology*. 32:16-24.
- Bedford, S. 2009. Cervical cancer: physiology, risk factors, vaccination and treatment. *British journal of nursing*. 18.
- Berg, J.M., J.L. Tymoczko, and L. Stryer. 2002. Biochemistry. 5th. New York: WH Freeman.
- Bertsch, A., S. Jiguet, and P. Renaud. 2003. Microfabrication of ceramic components by microstereolithography. *Journal of micromechanics and microengineering*. 14:197.
- Bhattacharyya, A., and C.M. Klapperich. 2006. Thermoplastic microfluidic device for on-chip purification of nucleic acids for disposable diagnostics. *Analytical Chemistry*. 78:788-792.

- Bhattacharyya, A., and C.M. Klapperich. 2008. Microfluidics-based extraction of viral RNA from infected mammalian cells for disposable molecular diagnostics. *Sensors and Actuators B: Chemical*. 129:693-698.
- Bienvenue, J.M., N. Duncalf, D. Marchiarullo, J.P. Ferrance, and J.P. Landers. 2006. Microchip-Based Cell Lysis and DNA Extraction from Sperm Cells for Application to Forensic Analysis. *Journal of forensic sciences*. 51:266-273.
- Bierman, R., L. Beardsley, C. Chang, and R. Burk. 1998. Natural History of Cervicovaginal Papillomavirus Infection in Young Women GYF Ho. *Journal of Lower Genital Tract Disease*. 2:235.
- Boel, C., C. Van Herk, P. Berretty, G.W. Onland, and A. Van Den Brule. 2005. Evaluation of conventional and real-time PCR assays using two targets for confirmation of results of the COBAS AMPLICOR Chlamydia trachomatis/Neisseria gonorrhoeae test for detection of Neisseria gonorrhoeae in clinical samples. *Journal of clinical microbiology*. 43:2231-2235.
- Bohunicky, B., and S.A. Mousa. 2011. Biosensors: the new wave in cancer diagnosis. *Nanotechnology, science and applications*. 4:1-10.
- Bolotin, K.I., K. Sikes, Z. Jiang, M. Klima, G. Fudenberg, J. Hone, P. Kim, and H. Stormer. 2008. Ultrahigh electron mobility in suspended graphene. *Solid State Communications*. 146:351-355.
- Bonanni, A., A. Ambrosi, and M. Pumera. 2012. Nucleic acid functionalized graphene for biosensing. *Chemistry—A European Journal*. 18:1668-1673.
- Boom, R., C. Sol, M. Salimans, C. Jansen, P. Wertheim-van Dillen, and J. Van der Noordaa. 1990. Rapid and simple method for purification of nucleic acids. *Journal of clinical microbiology*. 28:495-503.
- Bosch, F.X., M.M. Manos, N. Muñoz, M. Sherman, A.M. Jansen, J. Peto, M.H. Schiffman, V. Moreno, R. Kurman, and K.V. Shan. 1995. Prevalence of human papillomavirus in cervical cancer: a worldwide perspective. *Journal of the National Cancer Institute*. 87:796-802.
- Breadmore, M.C., K.A. Wolfe, I.G. Arcibal, W.K. Leung, D. Dickson, B.C. Giordano, M.E. Power, J.P. Ferrance, S.H. Feldman, and P.M. Norris. 2003. Microchip-based purification of DNA from biological samples. *Analytical chemistry*. 75:1880-1886.
- Brinkmann, B. 1998. Overview of PCR-based systems in identity testing. *METHODS IN MOLECULAR BIOLOGY-CLIFTON THEN TOTOWA-*. 98:105-120.
- Brivio, M., R.H. Fokkens, W. Verboom, D.N. Reinhoudt, N.R. Tas, M. Goedbloed, and A. van den Berg. 2002. Integrated microfluidic system enabling (bio) chemical reactions with on-line MALDI-TOF mass spectrometry. *Analytical chemistry*. 74:3972-3976.
- Brody, J.R., and S.E. Kern. 2004. History and principles of conductive media for standard DNA electrophoresis. *Analytical biochemistry*. 333:1-13.
- Brownson, D.A., and C.E. Banks. 2010. Graphene electrochemistry: an overview of potential applications. *Analyst*. 135:2768-2778.
- Bruni, L., L. Barrionuevo-Rosas, G. Albero, M. Aldea, B. Serrano, S. Valencia, M. Brotons, M. Mena, R. Cosano, and J. Mu-oz. 2014. ICO information centre on HPV and cancer (HPV information centre). *Human Papillomavirus and Related Diseases in Ethiopia. Summary Report*. 12:18.

- Bunyakul, N., C. Promptmas, and A.J. Baeumner. 2015. Microfluidic biosensor for cholera toxin detection in fecal samples. *Analytical and bioanalytical chemistry*. 407:727-736.
- Byrnes, S., A. Fan, J. Trueb, F. Jareczek, M. Mazzochette, A. Sharon, A.F. Sauer-Budge, and C.M. Klapperich. 2013. A portable, pressure driven, room temperature nucleic acid extraction and storage system for point of care molecular diagnostics. *Analytical Methods*. 5:3177-3184.
- Cady, N.C., S. Stelick, and C.A. Batt. 2003. Nucleic acid purification using microfabricated silicon structures. *Biosensors and Bioelectronics*. 19:59-66.
- Campos-Ferreira, D.S., G.A. Nascimento, E.V. Souza, M.A. Souto-Maior, M.S. Arruda, D.M. Zanforlin, M.H. Ekert, D. Brunaska, and J.L. Lima-Filho. 2013. Electrochemical DNA biosensor for human papillomavirus 16 detection in real samples. *Analytica chimica acta*. 804:258-263.
- Cao, Q., M. Mahalanabis, J. Chang, B. Carey, C. Hsieh, A. Stanley, C.A. Odell, P. Mitchell, J. Feldman, and N.R. Pollock. 2012. Microfluidic chip for molecular amplification of influenza A RNA in human respiratory specimens. *PLoS One*. 7:e33176.
- Cao, W., C.J. Easley, J.P. Ferrance, and J.P. Landers. 2006. Chitosan as a polymer for pH-induced DNA capture in a totally aqueous system. *Analytical chemistry*. 78:7222-7228.
- Carrilho, E., A.W. Martinez, and G.M. Whitesides. 2009a. Understanding wax printing: a simple micropatterning process for paper-based microfluidics. *Analytical chemistry*. 81:7091-7095.
- Carrilho, E., S.T. Phillips, S.J. Vella, A.W. Martinez, and G.M. Whitesides. 2009b. Paper microzone plates. *Analytical chemistry*. 81:5990-5998.
- Carvalho, R.F., M. Simão Kfour, M.H. de Oliveira Piazzetta, A.L. Gobbi, and L.T. Kubota. 2010. Electrochemical detection in a paper-based separation device. *Analytical chemistry*. 82:1162-1165.
- Cate, D.M., W. Dungchai, J.C. Cunningham, J. Volckens, and C.S. Henry. 2013. Simple, distance-based measurement for paper analytical devices. *Lab on a Chip*. 13:2397-2404.
- Chakrabarti, R., and C.E. Schutt. 2001. The enhancement of PCR amplification by low molecular-weight sulfones. *Gene*. 274:293-298.
- Chatterjee, A., P.L. Mirer, E. Zaldivar Santamaria, C. Klapperich, A. Sharon, and A.F. Sauer-Budge. 2010. RNA isolation from mammalian cells using porous polymer monoliths: an approach for high-throughput automation. *Analytical chemistry*. 82:4344-4356.
- Chen, W., L. Yan, and P. Bangal. 2010. Chemical reduction of graphene oxide to graphene by sulfur-containing compounds. *The Journal of Physical Chemistry C*. 114:19885-19890.
- Chen, X., J. Chen, F. Wang, X. Xiang, M. Luo, X. Ji, and Z. He. 2012. Determination of glucose and uric acid with bienzyme colorimetry on microfluidic paper-based analysis devices. *Biosensors and Bioelectronics*. 35:363-368.
- Chen, Z.-P., Z.-F. Peng, Y. Luo, B. Qu, J.-H. Jiang, X.-B. Zhang, G.-L. Shen, and R.-Q. Yu. 2007. Successively amplified electrochemical immunoassay based on

- biocatalytic deposition of silver nanoparticles and silver enhancement. *Biosensors and Bioelectronics*. 23:485-491.
- Chin, C.D., S.Y. Chin, T. Laksanasopin, and S.K. Sia. 2013. Low-cost microdevices for point-of-care testing. *In Point-of-Care Diagnostics on a Chip*. Springer. 3-21.
- Chin, C.D., T. Laksanasopin, Y.K. Cheung, D. Steinmiller, V. Linder, H. Parsa, J. Wang, H. Moore, R. Rouse, and G. Umvilighozo. 2011. Microfluidics-based diagnostics of infectious diseases in the developing world. *Nature medicine*. 17:1015-1019.
- Chow, W.H.A., C. McCloskey, Y. Tong, L. Hu, Q. You, C.P. Kelly, H. Kong, Y.-W. Tang, and W. Tang. 2008. Application of isothermal helicase-dependent amplification with a disposable detection device in a simple sensitive stool test for toxigenic *Clostridium difficile*. *The Journal of Molecular Diagnostics*. 10:452-458.
- Chung, T.K., P. Van Hummelen, P.K. Chan, T.H. Cheung, S.F. Yim, M.Y. Yu, M.D. Ducar, A.R. Thorner, L.E. MacConaill, and G. Doran. 2015. Genomic aberrations in cervical adenocarcinomas in Hong Kong Chinese women. *International Journal of Cancer*. 137:776-783.
- Civit, L., A. Fragoso, S. Hölters, M. Dürst, and C.K. O'Sullivan. 2012. Electrochemical genosensor array for the simultaneous detection of multiple high-risk human papillomavirus sequences in clinical samples. *Analytica chimica acta*. 715:93-98.
- Clarke, S., and J. Foster. 2012. A history of blood glucose meters and their role in self-monitoring of diabetes mellitus. *British journal of biomedical science*. 69:83.
- Control, C.f.D., and Prevention. 2007. Prevention of genital HPV infection and sequelae: report of an external consultants' meeting.
- Crow, J.M. 2012. HPV: The global burden. *Nature*. 488:S2-S3.
- Cunningham, J.C., N.J. Brenes, and R.M. Crooks. 2014. Paper electrochemical device for detection of DNA and thrombin by target-induced conformational switching. *Analytical chemistry*. 86:6166-6170.
- Curtis, K.A., D.L. Rudolph, I. Nejad, J. Singleton, A. Beddoe, B. Weigl, P. LaBarre, and S.M. Owen. 2012. Isothermal amplification using a chemical heating device for point-of-care detection of HIV-1. *PloS one*. 7:e31432.
- Cuzick, J., M. Arbyn, R. Sankaranarayanan, V. Tsu, G. Ronco, M.-H. Mayrand, J. Dillner, and C.J. Meijer. 2008. Overview of human papillomavirus-based and other novel options for cervical cancer screening in developed and developing countries. *Vaccine*. 26:K29-K41.
- Cuzick, J., C. Bergeron, M. von Knebel Doeberitz, P. Gravitt, J. Jeronimo, A.T. Lorincz, C.J. Meijer, R. Sankaranarayanan, P.J. Snijders, and A. Szarewski. 2012. New technologies and procedures for cervical cancer screening. *Vaccine*. 30:F107-F116.
- Dai, C., X. Yang, and H. Xie. 2011. One-step synthesis of reduced graphite oxide-silver nanocomposite. *Materials Research Bulletin*. 46:2004-2008.
- Dai Tran, L., D.T. Nguyen, B.H. Nguyen, Q.P. Do, and H. Le Nguyen. 2011. Development of interdigitated arrays coated with functional polyaniline/MWCNT for electrochemical biodetection: Application for human papilloma virus. *Talanta*. 85:1560-1565.

- Davies, R., S. Eapen, and S. Carlisle. 2007. Lateral-Flow Immunochromatographic Assays. *Handbook of Biosensors and Biochips*.
- de La Escosura-Muñiz, A., C. Parolo, F. Maran, and A. Mekoçi. 2011. Size-dependent direct electrochemical detection of gold nanoparticles: application in magnetoimmunoassays. *Nanoscale*. 3:3350-3356.
- De Villiers, E.-M., C. Fauquet, T.R. Broker, H.-U. Bernard, and H. zur Hausen. 2004. Classification of papillomaviruses. *Virology*. 324:17-27.
- Dequaire, M., C. Degrand, and B. Limoges. 2000. An electrochemical metalloimmunoassay based on a colloidal gold label. *Analytical chemistry*. 72:5521-5528.
- Devegowda, D., P. Doddamani, and P. Vishwanath. 2014. Human papillomavirus screening: Time to add molecular methods with cytology. *International Journal of Health & Allied Sciences*. 3:145.
- Dieffenbach, C., T. Lowe, and G. Dveksler. 1993. General concepts for PCR primer design. *PCR Methods Appl*. 3:S30-S37.
- Dineva, M.A., L. Mahilum-Tapay, and H. Lee. 2007. Sample preparation: a challenge in the development of point-of-care nucleic acid-based assays for resource-limited settings. *Analyst*. 132:1193-1199.
- Dossi, N., R. Toniolo, A. Pizzariello, E. Carrilho, E. Piccin, S. Battiston, and G. Bontempelli. 2012. An electrochemical gas sensor based on paper supported room temperature ionic liquids. *Lab on a Chip*. 12:153-158.
- Dreyer, D.R., S. Park, C.W. Bielawski, and R.S. Ruoff. 2010. The chemistry of graphene oxide. *Chemical Society Reviews*. 39:228-240.
- Duffy, D.C., J.C. McDonald, O.J. Schueller, and G.M. Whitesides. 1998. Rapid prototyping of microfluidic systems in poly (dimethylsiloxane). *Analytical chemistry*. 70:4974-4984.
- Dungchai, W., O. Chailapakul, and C.S. Henry. 2009. Electrochemical detection for paper-based microfluidics. *Analytical chemistry*. 81:5821-5826.
- Dungchai, W., O. Chailapakul, and C.S. Henry. 2010. Use of multiple colorimetric indicators for paper-based microfluidic devices. *Analytica chimica acta*. 674:227-233.
- Dungchai, W., O. Chailapakul, and C.S. Henry. 2011. A low-cost, simple, and rapid fabrication method for paper-based microfluidics using wax screen-printing. *Analyst*. 136:77-82.
- Dungchai, W., Y. Sameenoi, O. Chailapakul, J. Volckens, and C.S. Henry. 2013. Determination of aerosol oxidative activity using silver nanoparticle aggregation on paper-based analytical devices. *Analyst*. 138:6766-6773.
- Ellerbee, A.K., S.T. Phillips, A.C. Siegel, K.A. Mirica, A.W. Martinez, P. Striehl, N. Jain, M. Prentiss, and G.M. Whitesides. 2009. Quantifying colorimetric assays in paper-based microfluidic devices by measuring the transmission of light through paper. *Analytical chemistry*. 81:8447-8452.
- Ellsworth, D., K. Rittenhouse, and R. Honeycutt. 1993. Artfactual variation in randomly amplified polymorphic DNA banding patterns. *Biotechniques*. 14:214-217.
- Engel, L., and W. Baumann. 1993. Direct potentiometric immunoelectrodes. *Fresenius' journal of analytical chemistry*. 346:745-751.



- Er, E., and H. Çelikkan. 2014. An efficient way to reduce graphene oxide by water elimination using phosphoric acid. *RSC Advances*. 4:29173-29179.
- Er, E., H. Çelikkan, and N. Erk. 2016. Highly sensitive and selective electrochemical sensor based on high-quality graphene/nafion nanocomposite for voltammetric determination of nebulolol. *Sensors and Actuators B: Chemical*. 224:170-177.
- Erlich, H.A., D. Gelfand, and J.J. Sninsky. 1991. Recent advances in the polymerase chain reaction. *Science*. 252:1643-1651.
- Fanjul-Bolado, P., D. Hernández-Santos, P.J. Lamas-Ardisana, A. Martín-Pernía, and A. Costa-García. 2008. Electrochemical characterization of screen-printed and conventional carbon paste electrodes. *Electrochimica Acta*. 53:3635-3642.
- Faulstich, K., R. Gruler, M. Eberhard, D. Lentzsch, and K. Haberstroh. 2009. Lateral Flow Immunoassay. N<sup>o</sup> w York.
- Fenton, E.M., M.R. Mascarenas, G.P. López, and S.S. Sibbett. 2008. Multiplex lateral-flow test strips fabricated by two-dimensional shaping. *ACS applied materials & interfaces*. 1:124-129.
- Ferlay, J., H.R. Shin, F. Bray, D. Forman, C. Mathers, and D.M. Parkin. 2010. Estimates of worldwide burden of cancer in 2008: GLOBOCAN 2008. *International journal of cancer*. 127:2893-2917.
- Ferlay, J., I. Soerjomataram, R. Dikshit, S. Eser, C. Mathers, M. Rebelo, D.M. Parkin, D. Forman, and F. Bray. 2015. Cancer incidence and mortality worldwide: sources, methods and major patterns in GLOBOCAN 2012. *International journal of cancer*. 136:E359-E386.
- Fitch, J.P., E. Raber, and D.R. Imbro. 2003. Technology challenges in responding to biological or chemical attacks in the civilian sector. *Science*. 302:1350-1354.
- Folch, A., A. Ayon, O. Hurtado, M. Schmidt, and M. Toner. 1999. Molding of deep polydimethylsiloxane microstructures for microfluidics and biological applications. *Journal of Biomechanical Engineering*. 121:28-34.
- Fridley, G.E., H.Q. Le, E. Fu, and P. Yager. 2012. Controlled release of dry reagents in porous media for tunable temporal and spatial distribution upon rehydration. *Lab on a Chip*. 12:4321-4327.
- Friedrich, C.R., and M.J. Vasile. 1996. Development of the micromilling process for high-aspect-ratio microstructures. *Microelectromechanical Systems, Journal of*. 5:33-38.
- Gao, J., F. Liu, Y. Liu, N. Ma, Z. Wang, and X. Zhang. 2010. Environment-friendly method to produce graphene that employs vitamin C and amino acid. *Chemistry of Materials*. 22:2213-2218.
- Ge, L., P. Wang, S. Ge, N. Li, J. Yu, M. Yan, and J. Huang. 2013a. Photoelectrochemical lab-on-paper device based on an integrated paper supercapacitor and internal light source. *Analytical chemistry*. 85:3961-3970.
- Ge, S., L. Ge, M. Yan, X. Song, J. Yu, and J. Huang. 2012. A disposable paper-based electrochemical sensor with an addressable electrode array for cancer screening. *Chemical Communications*. 48:9397-9399.
- Ge, S., L. Ge, M. Yan, X. Song, J. Yu, and S. Liu. 2013b. A disposable immunosensor device for point-of-care test of tumor marker based on copper-mediated amplification. *Biosensors and Bioelectronics*. 43:425-431.

- Ge, S., W. Liu, L. Ge, M. Yan, J. Yan, J. Huang, and J. Yu. 2013c. In situ assembly of porous Au-paper electrode and functionalization of magnetic silica nanoparticles with HRP via click chemistry for Microcystin-LR immunoassay. *Biosensors and Bioelectronics*. 49:111-117.
- Geim, A.K., and K.S. Novoselov. 2007. The rise of graphene. *Nature materials*. 6:183-191.
- Gerbers, R., W. Foellscher, H. Chen, C. Anagnostopoulos, and M. Faghri. 2014. A new paper-based platform technology for point-of-care diagnostics. *Lab on a Chip*. 14:4042-4049.
- Glavan, A.C., R.V. Martinez, E.J. Maxwell, A.B. Subramaniam, R.M. Nunes, S. Soh, and G.M. Whitesides. 2013. Rapid fabrication of pressure-driven open-channel microfluidic devices in omniphobic RF paper. *Lab on a chip*. 13:2922-2930.
- Goel, A., G. Gandhi, S. Batra, S. Bhambhani, V. Zutshi, and P. Sachdeva. 2005. Visual inspection of the cervix with acetic acid for cervical intraepithelial lesions. *International Journal of Gynecology & Obstetrics*. 88:25-30.
- Goldmeyer, J., H. Li, M. McCormac, S. Cook, C. Stratton, B. Lemieux, H. Kong, W. Tang, and Y.-W. Tang. 2008. Identification of *Staphylococcus aureus* and determination of methicillin resistance directly from positive blood cultures by isothermal amplification and a disposable detection device. *Journal of clinical microbiology*. 46:1534-1536.
- Govindarajan, A., S. Ramachandran, G. Vigil, P. Yager, and K. Böhringer. 2012. A low cost point-of-care viscous sample preparation device for molecular diagnosis in the developing world; an example of microfluidic origami. *Lab on a Chip*. 12:174-181.
- Green, M.R., and J. Sambrook. Molecular cloning: a laboratory manual. 2012. *Cold Spring Spring*. 264:66-68.
- Gruenwedel, D.W., and C.H. Hsu. 1969. Salt effects on the denaturation of DNA. *Biopolymers*. 7:557-570.
- Gubala, V., L.F. Harris, A.J. Ricco, M.X. Tan, and D.E. Williams. 2011. Point of care diagnostics: status and future. *Analytical chemistry*. 84:487-515.
- Hadidi, A., L. Levy, and E. Podleckis. 1995. Polymerase chain reaction technology in plant pathology. *Molecular methods in plant pathology*:167-187.
- Hagan, K.A., J.M. Bienvenue, C.A. Moskaluk, and J.P. Landers. 2008. Microchip-based solid-phase purification of RNA from biological samples. *Analytical chemistry*. 80:8453-8460.
- Hagan, K.A., W.L. Meier, J.P. Ferrance, and J.P. Landers. 2009. Chitosan-coated silica as a solid phase for RNA purification in a microfluidic device. *Analytical chemistry*. 81:5249-5256.
- He, Q., S. Wu, S. Gao, X. Cao, Z. Yin, H. Li, P. Chen, and H. Zhang. 2011. Transparent, flexible, all-reduced graphene oxide thin film transistors. *ACS nano*. 5:5038-5044.
- Hegde, D., H. Shetty, P.K. Shetty, S. Rai, L. Manjeera, N. Vyas, A. Hegde, H. Mallya, and A. Rajesh. 2015. Diagnostic value of VIA comparing with conventional Pap smear in the detection of colposcopic biopsy proved CIN. *Nepal Journal of Obstetrics and Gynaecology*. 6:7-12.

- Henson, J.M., and R.C. French. 1993. The polymerase chain reaction and plant disease diagnosis. *Papers in Plant Pathology*:2.
- Higgins, J., M. Ibrahim, F. Knauert, G. Ludwig, T. Kijek, J. Ezzell, B. Courtney, and E. Henchal. 1999. Sensitive and rapid identification of biological threat agents. *Annals of the New York Academy of Sciences*. 894:130-148.
- Hofmann, O., G. Voirin, P. Niedermann, and A. Manz. 2002. Three-dimensional microfluidic confinement for efficient sample delivery to biosensor surfaces. Application to immunoassays on planar optical waveguides. *Analytical chemistry*. 74:5243-5250.
- Hofmann, U., and R. Holst. 1939. Ber. Dtsch. ber die S urenatur und die Methylierung von Graphitoxyd. *Chem. Ges. B*. 72:754-771.
- Hofmann, U., and E. König. 1937. Untersuchungen über graphitoxyd. *Zeitschrift für anorganische und allgemeine Chemie*. 234:311-336.
- Hoory, T., A. Monie, P. Gravitt, and T.-C. Wu. 2008. Molecular epidemiology of human papillomavirus. *Journal of the Formosan Medical Association*. 107:198-217.
- Hu, J., S. Wang, L. Wang, F. Li, B. Pingguan-Murphy, T.J. Lu, and F. Xu. 2014. Advances in paper-based point-of-care diagnostics. *Biosensors and Bioelectronics*. 54:585-597.
- Huang, L.-W., S.-L. Chao, P.-H. Chen, and H.-P. Chou. 2004. Multiple HPV genotypes in cervical carcinomas: improved DNA detection and typing in archival tissues. *Journal of Clinical Virology*. 29:271-276.
- Huang, S., J. Do, M. Mahalanabis, A. Fan, L. Zhao, L. Jepeal, S.K. Singh, and C.M. Klapperich. 2013. Low cost extraction and isothermal amplification of DNA for infectious diarrhea diagnosis. *PLoS One*. 8:e60059.
- Hummers Jr, W.S., and R.E. Offeman. 1958. Preparation of graphitic oxide. *Journal of the American Chemical Society*. 80:1339-1339.
- Hwang, S.J., and K.R. Shroyer. 2011. Biomarkers of cervical dysplasia and carcinoma. *Journal of oncology*. 2012.
- Innis, M.A., D.H. Gelfand, J.J. Sninsky, and T.J. White. 2012. PCR protocols: a guide to methods and applications. Academic press.
- Jampasa, S., W. Wonsawat, N. Rodthongkum, W. Siangproh, P. Yanatatsaneejit, T. Vilaivan, and O. Chailapakul. 2014. Electrochemical detection of human papillomavirus DNA type 16 using a pyrrolidinyl peptide nucleic acid probe immobilized on screen-printed carbon electrodes. *Biosensors and Bioelectronics*. 54:428-434.
- Ji, J., L. Nie, Y. Li, P. Yang, and B. Liu. 2013. Simultaneous online enrichment and identification of trace species based on microfluidic droplets. *Analytical chemistry*. 85:9617-9622.
- Jin, S.-Q., S.-M. Guo, P. Zuo, and B.-C. Ye. 2015. A cost-effective Z-folding controlled liquid handling microfluidic paper analysis device for pathogen detection via ATP quantification. *Biosensors and Bioelectronics*. 63:379-383.
- Jo, B.-H., L.M. Van Lerberghe, K.M. Motsegood, and D.J. Beebe. 2000. Three-dimensional micro-channel fabrication in polydimethylsiloxane (PDMS) elastomer. *Microelectromechanical Systems, Journal of*. 9:76-81.

- Kim, D., S.J. Yang, Y.S. Kim, H. Jung, and C.R. Park. 2012. Simple and cost-effective reduction of graphite oxide by sulfuric acid. *Carbon*. 50:3229-3232.
- Kissinger, P., and W.R. Heineman. 1996. Laboratory Techniques in Electroanalytical Chemistry, revised and expanded. CRC press.
- Komiyama, M., N. Takeda, and H. Shigekawa. 1999. Hydrolysis of DNA and RNA by lanthanide ions: mechanistic studies leading to new applications. *Chemical Communications*:1443-1451.
- Kryndushkin, D.S., I.M. Alexandrov, M.D. Ter-Avanesyan, and V.V. Kushnirov. 2003. Yeast [PSI+] prion aggregates are formed by small Sup35 polymers fragmented by Hsp104. *Journal of Biological Chemistry*. 278:49636-49643.
- Kulinski, M.D., M. Mahalanabis, S. Gillers, J.Y. Zhang, S. Singh, and C.M. Klapperich. 2009. Sample preparation module for bacterial lysis and isolation of DNA from human urine. *Biomedical microdevices*. 11:671-678.
- Kung, C.-C., P.-Y. Lin, F.J. Buse, Y. Xue, X. Yu, L. Dai, and C.-C. Liu. 2014. Preparation and characterization of three dimensional graphene foam supported platinum–ruthenium bimetallic nanocatalysts for hydrogen peroxide based electrochemical biosensors. *Biosensors and Bioelectronics*. 52:1-7.
- LaBarre, P., J. Gerlach, J. Wilmoth, A. Beddoe, J. Singleton, and B. Weigl. 2010. Non-instrumented nucleic acid amplification (NINA): instrument-free molecular malaria diagnostics for low-resource settings. In Engineering in Medicine and Biology Society (EMBC), 2010 annual international conference of the IEEE. IEEE. 1097-1099.
- LaBarre, P., K.R. Hawkins, J. Gerlach, J. Wilmoth, A. Beddoe, J. Singleton, D. Boyle, and B. Weigl. 2011. A simple, inexpensive device for nucleic acid amplification without electricity—toward instrument-free molecular diagnostics in low-resource settings. *PloS one*. 6:e19738.
- Lan, W.-J., X.U. Zou, M.M. Hamed, J. Hu, C. Parolo, E.J. Maxwell, P. Bühlmann, and G.M. Whitesides. 2014. Paper-based potentiometric ion sensing. *Analytical chemistry*. 86:9548-9553.
- Larsson, P.A., S.G. Puttaswamaiah, C. Ly, A. Vanerek, J.C. Hall, and F. Drolet. 2013. Filtration, adsorption and immunodetection of virus using polyelectrolyte multilayer-modified paper. *Colloids and Surfaces B: Biointerfaces*. 101:205-209.
- Lasky, L.A., M.S. Singer, D. Dowbenko, Y. Imai, W.J. Henzel, C. Grimley, C. Fennie, N. Gillett, S.R. Watson, and S.D. Rosent. 1992. An endothelial ligand for L-selectin is a novel mucin-like molecule. *Cell*. 69:927-938.
- Lee, S., J. Taylor, M. Innis, D. Gelfand, J. Sninsky, and T. White. 1990. PCR protocols: a guide to methods and applications. Academic Press New York.
- Lee, S.H., S.-W. Kim, J.Y. Kang, and C.H. Ahn. 2008. A polymer lab-on-a-chip for reverse transcription (RT)-PCR based point-of-care clinical diagnostics. *Lab on a Chip*. 8:2121-2127.
- Lei, H., L. Mi, X. Zhou, J. Chen, J. Hu, S. Guo, and Y. Zhang. 2011. Adsorption of double-stranded DNA to graphene oxide preventing enzymatic digestion. *Nanoscale*. 3:3888-3892.

- Leto, M.d.G.P., S. Júnior, A.M. Porro, and J. Tomimori. 2011. Human papillomavirus infection: etiopathogenesis, molecular biology and clinical manifestations. *Anais brasileiros de dermatologia*. 86:306-317.
- Lewis, G.G., J.S. Robbins, and S.T. Phillips. 2013. Point-of-care assay platform for quantifying active enzymes to femtomolar levels using measurements of time as the readout. *Analytical chemistry*. 85:10432-10439.
- Lewis, M. 2001. Agarose gel electrophoresis (basic method). *Biological protocols*. Liverpool: University of Liverpool.
- Li, B., X. Cao, H.G. Ong, J.W. Cheah, X. Zhou, Z. Yin, H. Li, J. Wang, F. Boey, and W. Huang. 2010. All-Carbon Electronic Devices Fabricated by Directly Grown Single-Walled Carbon Nanotubes on Reduced Graphene Oxide Electrodes. *Advanced Materials*. 22:3058-3061.
- Li, L., J. Xu, X. Zheng, C. Ma, X. Song, S. Ge, J. Yu, and M. Yan. 2014. Growth of gold-manganese oxide nanostructures on a 3D origami device for glucose-oxidase label based electrochemical immunosensor. *Biosensors and Bioelectronics*. 61:76-82.
- Li, X., D.R. Ballerini, and W. Shen. 2012. A perspective on paper-based microfluidics: current status and future trends. *Biomicrofluidics*. 6:011301.
- Li, X., J. Tian, T. Nguyen, and W. Shen. 2008. Paper-based microfluidic devices by plasma treatment. *Analytical chemistry*. 80:9131-9134.
- Liepold, P., T. Kratzmüller, N. Persike, M. Bandilla, M. Hinz, H. Wieder, H. Hillebrandt, E. Ferrer, and G. Hartwich. 2008. Electrically detected displacement assay (EDDA): a practical approach to nucleic acid testing in clinical or medical diagnosis. *Analytical and bioanalytical chemistry*. 391:1759-1772.
- Liljestrand, J.E., Y. Naoi, J. Kapec, Y. Matsuda, K. Tanaka, C.J. Turk, and G.W. Egerton. 2004. Detection device. Google Patents.
- Linnes, J.C., A. Fan, N.M. Rodriguez, B. Lemieux, H. Kong, and C.M. Klapperich. 2014. Paper-based molecular diagnostic for Chlamydia trachomatis. *RSC Adv*. 4:42245-42251.
- Liu, C., Y. Luo, E.J. Maxwell, N. Fang, and D.D. Chen. 2010. Reverse of Mixing Process with a Two-Dimensional Electro-Fluid-Dynamic Device. *Analytical chemistry*. 82:2182-2185.
- Liu, C., M.G. Mauk, R. Hart, M. Bonizzoni, G. Yan, and H.H. Bau. 2012a. A low-cost microfluidic chip for rapid genotyping of malaria-transmitting mosquitoes. *PloS one*. 7:e42222.
- Liu, G., Y.-Y. Lin, J. Wang, H. Wu, C.M. Wai, and Y. Lin. 2007. Disposable electrochemical immunosensor diagnosis device based on nanoparticle probe and immunochromatographic strip. *Analytical Chemistry*. 79:7644-7653.
- Liu, H., and R.M. Crooks. 2011. Three-dimensional paper microfluidic devices assembled using the principles of origami. *Journal of the American Chemical Society*. 133:17564-17566.
- Liu, H., X. Li, and R.M. Crooks. 2013a. Paper-based SlipPAD for high-throughput chemical sensing. *Analytical chemistry*. 85:4263-4267.

- Liu, H., Y. Xiang, Y. Lu, and R.M. Crooks. 2012b. Aptamer-based origami paper analytical device for electrochemical detection of adenosine. *Angewandte Chemie*. 124:7031-7034.
- Liu, J., Y. Xue, and L. Dai. 2012c. Sulfated graphene oxide as a hole-extraction layer in high-performance polymer solar cells. *The journal of physical chemistry letters*. 3:1928-1933.
- Liu, M., R. Liu, and W. Chen. 2013b. Graphene wrapped Cu<sub>2</sub>O nanocubes: non-enzymatic electrochemical sensors for the detection of glucose and hydrogen peroxide with enhanced stability. *Biosensors and Bioelectronics*. 45:206-212.
- Liu, S., J. Tian, L. Wang, Y. Luo, W. Lu, and X. Sun. 2011. Self-assembled graphene platelet–glucose oxidase nanostructures for glucose biosensing. *Biosensors and bioelectronics*. 26:4491-4496.
- Liu, Y., J.A. Vickers, and C.S. Henry. 2004. Simple and sensitive electrode design for microchip electrophoresis/electrochemistry. *Analytical Chemistry*. 76:1513-1517.
- Lu, J., S. Ge, L. Ge, M. Yan, and J. Yu. 2012. Electrochemical DNA sensor based on three-dimensional folding paper device for specific and sensitive point-of-care testing. *Electrochimica Acta*. 80:334-341.
- Lu, Y., W. Shi, L. Jiang, J. Qin, and B. Lin. 2009. Rapid prototyping of paper-based microfluidics with wax for low-cost, portable bioassay. *Electrophoresis*. 30:1497-1500.
- Luo, Y., X. Mao, Z.-F. Peng, J.-H. Jiang, G.-L. Shen, and R.-Q. Yu. 2008. A new strategy for electrochemical immunoassay based on enzymatic silver deposition on agarose beads. *Talanta*. 74:1642-1648.
- Mabey, D., R.W. Peeling, A. Ustianowski, and M.D. Perkins. 2004. Tropical infectious diseases: diagnostics for the developing world. *Nature Reviews Microbiology*. 2:231-240.
- Maejima, K., S. Tomikawa, K. Suzuki, and D. Citterio. 2013. Inkjet printing: an integrated and green chemical approach to microfluidic paper-based analytical devices. *Rsc Advances*. 3:9258-9263.
- Magrath, I., E. Steliarova-Foucher, S. Epelman, R.C. Ribeiro, M. Harif, C.-K. Li, R. Kebudi, S.D. Macfarlane, and S.C. Howard. 2013. Paediatric cancer in low-income and middle-income countries. *The lancet oncology*. 14:e104-e116.
- Mahalanabis, M., H. Al-Muayad, M.D. Kulinski, D. Altman, and C.M. Klapperich. 2009. Cell lysis and DNA extraction of gram-positive and gram-negative bacteria from whole blood in a disposable microfluidic chip. *Lab on a Chip*. 9:2811-2817.
- Maniatis, T., E.F. Fritsch, and J. Sambrook. 1982. Molecular cloning: a laboratory manual. Cold Spring Harbor Laboratory Cold Spring Harbor, NY.
- Marie Dupuy, A., S. Lehmann, and J. Paul Cristol. 2005. Protein biochip systems for the clinical laboratory. *Clinical Chemical Laboratory Medicine*. 43:1291-1302.
- Markoulatos, P., N. Sifakas, and M. Moncany. 2002. Multiplex polymerase chain reaction: a practical approach. *Journal of clinical laboratory analysis*. 16:47-51.
- Martinez, A.W., S.T. Phillips, M.J. Butte, and G.M. Whitesides. 2007. Patterned paper as a platform for inexpensive, low-volume, portable bioassays. *Angewandte Chemie International Edition*. 46:1318-1320.

- Martinez, A.W., S.T. Phillips, and G.M. Whitesides. 2008. Three-dimensional microfluidic devices fabricated in layered paper and tape. *Proceedings of the National Academy of Sciences*. 105:19606-19611.
- Martinez, A.W., S.T. Phillips, G.M. Whitesides, and E. Carrilho. 2009. Diagnostics for the developing world: microfluidic paper-based analytical devices. *Analytical chemistry*. 82:3-10.
- Mason, P., G. Neilson, C. Dempsey, A. Barnes, and J. Cruickshank. 2003. The hydration structure of guanidinium and thiocyanate ions: implications for protein stability in aqueous solution. *Proceedings of the National Academy of Sciences*. 100:4557-4561.
- Maxwell, E.J., A.D. Mazzeo, and G.M. Whitesides. 2013. Paper-based electroanalytical devices for accessible diagnostic testing. *MRS bulletin*. 38:309-314.
- McCalla, S.E., C. Ong, A. Sarma, S.M. Opal, A.W. Arntstein, and A. Tripathi. 2012. A simple method for amplifying RNA targets (SMART). *The Journal of Molecular Diagnostics*. 14:328-335.
- McNeely, M.R., M.K. Sputea, N.A. Tusneem, and A.R. Oliphant. 1999. Sample processing with hydrophobic microfluidics. *Journal of the Association for Laboratory Automation*. 4:30-33.
- Mentele, M.M., J. Cunningham, K. Koehler, J. Volckens, and C.S. Henry. 2012. Microfluidic paper-based analytical device for particulate metals. *Analytical chemistry*. 84:4474-4480.
- Miller, S. 2012. The effect of insurance on emergency room visits: an analysis of the 2006 Massachusetts health reform. *Journal of Public Economics*. 96:893-908.
- Mirasoli, M., F. Bonvicini, L.S. Dolci, M. Zangheri, G. Gallinella, and A. Roda. 2013. Portable chemiluminescence multiplex biosensor for quantitative detection of three B19 DNA genotypes. *Analytical and bioanalytical chemistry*. 405:1139-1143.
- Mullis, K.B., H.A. Erlich, D.H. Gelfand, G. Horn, and R.K. Saiki. 1990. Reacting nucleic acid with oligonucleotide primer in presence of catalytic enzyme dna polymerase; polymerase chain reaction patent. Google Patents.
- Munoz, N., F. Bosch, S. De Sanjose, L. Tafur, I. Izarzugaza, M. Gili, P. Viladiu, C. Navarro, C. Martos, and N. Ascunce. 1992. The causal link between human papillomavirus and invasive cervical cancer: A population-based case-control study in colombia and spain. *International Journal of Cancer*. 52:743-749.
- Nagunuma, T., F. Anuda, and J. Jin. 1995. Aichi Kyoiku Daigaku Kenkyu Hokoku. *Shizen Kagaku*. 44:25.
- Narang, U., G. Anderson, F.S. Ligler, and J. Burans. 1997. Fiber optic-based biosensor for ricin. *Biosensors and Bioelectronics*. 12:937-945.
- Nasirizadeh, N., H.R. Zare, M.H. Pournaghi-Azar, and M.S. Hejazi. 2011. Introduction of hematoxylin as an electroactive label for DNA biosensors and its employment in detection of target DNA sequence and single-base mismatch in human papilloma virus corresponding to oligonucleotide. *Biosensors and Bioelectronics*. 26:2638-2644.
- Nie, Z., C.A. Nijhuis, J. Gong, X. Chen, A. Kumachev, A.W. Martinez, M. Narovlyansky, and G.M. Whitesides. 2010. Electrochemical sensing in paper-based microfluidic devices. *Lab on a Chip*. 10:477-483.

- Niemz, A., T.M. Ferguson, and D.S. Boyle. 2011. Point-of-care nucleic acid testing for infectious diseases. *Trends in biotechnology*. 29:240-250.
- Noh, H., and S.T. Phillips. 2010. Fluidic timers for time-dependent, point-of-care assays on paper. *Analytical chemistry*. 82:8071-8078.
- Noiphung, J., T. Songjaroen, W. Dungchai, C.S. Henry, O. Chailapakul, and W. Laiwattanapaisal. 2013. Electrochemical detection of glucose from whole blood using paper-based microfluidic devices. *Analytica chimica acta*. 788:39-45.
- Novell, M., M. Parrilla, G.n.A. Crespo, F.X. Rius, and F.J. Andrade. 2012. Paper-based ion-selective potentiometric sensors. *Analytical chemistry*. 84:4695-4702.
- Nuwer, M.J., and J. Osteryoung. 1989. Electrochemical behavior of N-acetylpenicillamine thionitrite at glassy carbon and carbon fiber electrodes. *Analytical Chemistry*. 61:1954-1959.
- Ohno, K.i., K. Tachikawa, and A. Manz. 2008. Microfluidics: applications for analytical purposes in chemistry and biochemistry. *Electrophoresis*. 29:4443-4453.
- Olkkonen, J., K. Lehtinen, and T. Erho. 2010. Flexographically printed fluidic structures in paper. *Analytical chemistry*. 82:10246-10250.
- Ostrowska, K.M., A. Malkin, A. Meade, J. O'Leary, C. Martin, C. Spillane, H.J. Byrne, and F.M. Lyng. 2010. Investigation of the influence of high-risk human papillomavirus on the biochemical composition of cervical cancer cells using vibrational spectroscopy. *Analyst*. 135:3087-3093.
- Pai, N.P., C. Vadnais, C. Denking, N. Engel, and M. Pai. 2012. Point-of-care testing for infectious diseases: diversity, complexity, and barriers in low-and middle-income countries. *PLoS Med*. 9:e1001306.
- Paleček, E. 1996. From polarography of DNA to microanalysis with nucleic acid-modified electrodes. *Electroanalysis*. 8:7-14.
- Palecek, E., and M. Fojta. 1994. Differential pulsed voltammetric determination of RNA at the picomole level in the presence of DNA and nucleic acid components. *Analytical Chemistry*. 66:1566-1571.
- Park, S., J. An, J.R. Potts, A. Velamakanni, S. Murali, and R.S. Ruoff. 2011. Hydrazine-reduction of graphite-and graphene oxide. *Carbon*. 49:3019-3023.
- Parkin, D.M., and F. Bray. 2006. The burden of HPV-related cancers. *Vaccine*. 24:S11-S25.
- Parolo, C., and A. Merkoçi. 2013. Paper-based nanobiosensors for diagnostics. *Chemical Society Reviews*. 42:450-457.
- Peeters, S., T. Stakenborg, F. Colle, C. Liu, L. Lagae, and M. Van Ranst. 2012. Specific magnetic isolation for direct detection of HPV16. *European journal of clinical microbiology & infectious diseases*. 31:539-546.
- Pei, S., and H.-M. Cheng. 2012. The reduction of graphene oxide. *Carbon*. 50:3210-3228.
- Pei, S., J. Zhao, J. Du, W. Ren, and H.-M. Cheng. 2010. Direct reduction of graphene oxide films into highly conductive and flexible graphene films by hydrohalic acids. *Carbon*. 48:4466-4474.
- Piro, B., A. Kapella, V. Le, G. Anquetin, Q. Zhang, S. Reisberg, V. Noel, L. Tran, H. Duc, and M. Pham. 2011. Towards the detection of human papillomavirus infection by a reagentless electrochemical peptide biosensor. *Electrochimica Acta*. 56:10688-10693.



- Poletti, P.-A., A. Halfon, and M.-C. Marti. 1998. Papillomavirus and anal carcinoma. *International journal of colorectal disease*. 13:108-111.
- Pollock, N.R., J.P. Rolland, S. Kumar, P.D. Beattie, S. Jain, F. Noubary, V.L. Wong, R.A. Pohlmann, U.S. Ryan, and G.M. Whitesides. 2012. A paper-based multiplexed transaminase test for low-cost, point-of-care liver function testing. *Science translational medicine*. 4:152ra129-152ra129.
- Powledge, T.M. 2004. The polymerase chain reaction. *Advances in physiology education*. 28:44-50.
- Psyrrri, A., and D. DiMaio. 2008. Human papillomavirus in cervical and head-and-neck cancer. *Nature Clinical Practice Oncology*. 5:24-31.
- Puren, A., J.L. Gerlach, B.H. Weigl, D.M. Kelso, and G.J. Domingo. 2010. Laboratory operations, specimen processing, and handling for viral load testing and surveillance. *Journal of Infectious Diseases*. 201:S27-S36.
- Putnam, D. 1971. Composition and Concentrative Properties of Human Urine. In NASA Contractor Report.
- Qiao, Y.-l., J.W. Sellors, P.S. Eder, Y.-p. Bao, J.M. Lim, F.-h. Zhao, B. Weigl, W.-h. Zhang, R.B. Peck, and L. Li. 2008. A new HPV-DNA test for cervical-cancer screening in developing regions: a cross-sectional study of clinical accuracy in rural China. *The lancet oncology*. 9:929-936.
- Rahman, M.M., S.B. Khan, A.M. Asiri, K.A. Alamry, and A.O. Al-Youbi. 2013. Detection of nebivolol drug based on as-grown un-doped silver oxide nanoparticles prepared by a wet-chemical method. *Int J Electrochem Sci*. 8:323-335.
- Ramachandran, S., E. Fu, B. Lutz, and P. Yager. 2014. Long-term dry storage of an enzyme-based reagent system for ELISA in point-of-care devices. *Analyst*. 139:1456-1462.
- Rattanarat, P., W. Dungchai, D. Cate, J. Volckens, O. Chailapakul, and C.S. Henry. 2014. Multilayer paper-based device for colorimetric and electrochemical quantification of metals. *Analytical chemistry*. 86:3555-3562.
- Renault, C., M.J. Anderson, and R.M. Crooks. 2014. Electrochemistry in hollow-channel paper analytical devices. *Journal of the American Chemical Society*. 136:4616-4623.
- Renault, C., X. Li, S.E. Fosdick, and R.M. Crooks. 2013. Hollow-channel paper analytical devices. *Analytical chemistry*. 85:7976-7979.
- Rife, J., M. Miller, P. Sheehan, C. Tamanaha, M. Tondra, and L. Whitman. 2003. Design and performance of GMR sensors for the detection of magnetic microbeads in biosensors. *Sensors and Actuators A: Physical*. 107:209-218.
- Robyt, J.F., and B.J. White. 1990. Biochemical techniques: theory and practice. Waveland Press ChicagoUSA.
- Rohrman, B.A., V. Leautaud, E. Molyneux, and R.R. Richards-Kortum. 2012. A lateral flow assay for quantitative detection of amplified HIV-1 RNA. *PLoS One*. 7:e45611.
- Rohrman, B.A., and R.R. Richards-Kortum. 2012. A paper and plastic device for performing recombinase polymerase amplification of HIV DNA. *Lab on a chip*. 12:3082-3088.

- Rosen, J., M. He, C. Umbricht, H.R. Alexander, A.P. Dackiw, M.A. Zeiger, and S.K. Libutti. 2005. A six-gene model for differentiating benign from malignant thyroid tumors on the basis of gene expression. *Surgery*. 138:1050-1057.
- Rosen, J.E., and M.D. Stone. 2006. Contemporary diagnostic approach to the thyroid nodule. *Journal of surgical oncology*. 94:649-661.
- Ruecha, N., R. Rangkupan, N. Rodthongkum, and O. Chailapakul. 2014. Novel paper-based cholesterol biosensor using graphene/polyvinylpyrrolidone/polyaniline nanocomposite. *Biosensors and Bioelectronics*. 52:13-19.
- Salaün, P., K. Gibbon-Walsh, and C.M. van den Berg. 2011. Beyond the hydrogen wave: new frontier in the detection of trace elements by stripping voltammetry. *Analytical chemistry*. 83:3848-3856.
- Sambrook, J., E.F. Fritsch, and T. Maniatis. 1989. Molecular cloning. Cold spring harbor laboratory press New York.
- Sankaranarayanan, R., B.M. Nene, S.S. Shastri, K. Jayant, R. Muwonge, A.M. Budukh, S. Hingmire, S.G. Malvi, R. Thorat, and A. Kothari. 2009. HPV screening for cervical cancer in rural India. *New England Journal of Medicine*. 360:1385-1394.
- Santhiago, M., C.S. Henry, and L.T. Kubota. 2014. Low cost, simple three dimensional electrochemical paper-based analytical device for determination of p-nitrophenol. *Electrochimica Acta*. 130:771-777.
- Santhiago, M., J.B. Wydallis, L.T. Kubota, and C.S. Henry. 2013. Construction and electrochemical characterization of microelectrodes for improved sensitivity in paper-based analytical devices. *Analytical chemistry*. 85:5233-5239.
- Saslow, D., D. Solomon, H.W. Lawson, M. Killackey, S.L. Kulasingam, J. Cain, F.A. Garcia, A.T. Moriarty, A.G. Waxman, and D.C. Wilbur. 2012. American Cancer Society, American Society for Colposcopy and Cervical Pathology, and American Society for Clinical Pathology screening guidelines for the prevention and early detection of cervical cancer. *CA: a cancer journal for clinicians*. 62:147-172.
- Schägger, H. 2006. Tricine–SDS–PAGE. *Nature Protocols*. 1:16-22.
- Schiffman, M., and P.E. Castle. 2005. The promise of global cervical-cancer prevention. *New England Journal of Medicine*. 353:2101-2104.
- Schiffman, M., P.E. Castle, J. Jeronimo, A.C. Rodriguez, and S. Wacholder. 2007. Human papillomavirus and cervical cancer. *The Lancet*. 370:890-907.
- Schilling, K.M., A.L. Lepore, J.A. Kurian, and A.W. Martinez. 2012. Fully enclosed microfluidic paper-based analytical devices. *Analytical chemistry*. 84:1579-1585.
- Scida, K., J.C. Cunningham, C. Renault, I. Richards, and R.M. Crooks. 2014. Simple, sensitive, and quantitative electrochemical detection method for paper analytical devices. *Analytical chemistry*. 86:6501-6507.
- Scida, K., B. Li, A.D. Ellington, and R.M. Crooks. 2013. DNA detection using origami paper analytical devices. *Analytical chemistry*. 85:9713-9720.
- Scorza, R., L. Levy, V. Damsteegt, L.M. Yepes, J. Cordts, A. Hadidi, J. Slightom, and D. Gonsalves. 1995. Transformation of plum with the papaya ringspot virus coat protein gene and reaction of transgenic plants to plum pox virus. *Journal of the American Society for Horticultural Science*. 120:943-952.

- Sechi, D., B. Greer, J. Johnson, and N. Hashemi. 2013. Three-dimensional paper-based microfluidic device for assays of protein and glucose in urine. *Analytical chemistry*. 85:10733-10737.
- Shao, Y., J. Wang, M. Engelhard, C. Wang, and Y. Lin. 2010. Facile and controllable electrochemical reduction of graphene oxide and its applications. *Journal of Materials Chemistry*. 20:743-748.
- Sharma, H., D. Nguyen, A. Chen, V. Lew, and M. Khine. 2011. Unconventional low-cost fabrication and patterning techniques for point of care diagnostics. *Annals of biomedical engineering*. 39:1313-1327.
- Shimomura, O., T. Masugi, F.H. Johnson, and Y. Haneda. 1978. Properties and reaction mechanism of the bioluminescence system of the deep-sea shrimp *Oplophorus gracilorostris*. *Biochemistry*. 17:994-998.
- Shin, H.J., K.K. Kim, A. Benayad, S.M. Yoon, H.K. Park, I.S. Jung, M.H. Jin, H.K. Jeong, J.M. Kim, and J.Y. Choi. 2009. Efficient reduction of graphite oxide by sodium borohydride and its effect on electrical conductance. *Advanced Functional Materials*. 19:1987-1992.
- Si, Y., and E.T. Samulski. 2008. Synthesis of water soluble graphene. *Nano letters*. 8:1679-1682.
- Sia, S.K., and L.J. Kricka. 2008. Microfluidics and point-of-care testing. *Lab on a Chip*. 8:1982-1983.
- Sidransky, D. 1997. Nucleic acid-based methods for the detection of cancer. *Science*. 278:1054-1058.
- Simon, L.S., L.M. Grierson, Z. Naseer, A.A. Bookman, and J.Z. Shainhouse. 2009. Efficacy and safety of topical diclofenac containing dimethyl sulfoxide (DMSO) compared with those of topical placebo, DMSO vehicle and oral diclofenac for knee osteoarthritis. *PAIN®*. 143:238-245.
- Smisek, D.L., and D.A. Hoagland. 1989. Agarose gel electrophoresis of high molecular weight, synthetic polyelectrolytes. *Macromolecules*. 22:2270-2277.
- Snyder, A., V. Makarov, T. Merghoub, J. Yuan, J.M. Zaretsky, A. Desrichard, L.A. Walsh, M.A. Postow, P. Wong, and T.S. Ho. 2014. Genetic basis for clinical response to CTLA-4 blockade in melanoma. *New England Journal of Medicine*. 371:2189-2199.
- Song, P., X. Zhang, M. Sun, X. Cui, and Y. Lin. 2012. Synthesis of graphene nanosheets via oxalic acid-induced chemical reduction of exfoliated graphite oxide. *Rsc Advances*. 2:1168-1173.
- Sönnichsen, C., B.M. Reinhard, J. Liphardt, and A.P. Alivisatos. 2005. A molecular ruler based on plasmon coupling of single gold and silver nanoparticles. *Nature biotechnology*. 23:741-745.
- Stankovich, S., D.A. Dikin, G.H. Dommett, K.M. Kohlhaas, E.J. Zimney, E.A. Stach, R.D. Piner, S.T. Nguyen, and R.S. Ruoff. 2006. Graphene-based composite materials. *nature*. 442:282-286.
- Staudenmaier, L. 1898. Verfahren zur darstellung der graphitsäure. *Berichte der deutschen chemischen Gesellschaft*. 31:1481-1487.
- Suh, Y.S., M. Kamruzzaman, A.M. Alam, S.H. Lee, Y.H. Kim, G.M. Kim, and T.D. Dang. 2014. Chemiluminescence determination of moxifloxacin in pharmaceutical and biological samples based on its enhancing effect of the

- luminol–ferricyanide system using a microfluidic chip. *Luminescence*. 29:248-253.
- Szymanski, M., R. Porter, G.V. Dep, Y. Wang, and B.G. Haggett. 2011. Silver nanoparticles and magnetic beads with electrochemical measurement as a platform for immunosensing devices. *Physical Chemistry Chemical Physics*. 13:5383-5387.
- Szymanski, M., A.P. Turner, and R. Porter. 2010. Electrochemical dissolution of silver nanoparticles and its application in metalloimmunoassay. *Electroanalysis*. 22:191-198.
- Tan, A., K. Rodgers, J.P. Murrhly, C. O’Mathuna, and J.D. Glennon. 2001. Rapid fabrication of microfluidic devices in poly (dimethylsiloxane) by photocopying Presented at the 14th International Symposium on Microscale Separations and Analysis, Boston, January 13–18, 2001. *Lab on a Chip*. 1:7-9.
- Tang, Z., H. Wu, J.R. Cort, G.W. Buchko, Y. Zhang, Y. Shao, I.A. Aksay, J. Liu, and Y. Lin. 2010. Constraint of DNA on functionalized graphene improves its biostability and specificity. *Small*. 6:1205-1209.
- Tasoglu, S., H. Cumhur Tekin, F. Inci, S. Knowlton, S.Q. Wang, F. Wang-Johanning, G. Johanning, D. Colevas, and U. Demirci. 2015. Advances in Nanotechnology and Microfluidics for Human Papillomavirus Diagnostics. *Proceedings of the IEEE*. 103:161-178.
- Then, W.L., and G. Garnier. 2013. Paper diagnostics in biomedicine. *Reviews in Analytical Chemistry*. 32:269-294.
- Thorsen, T., S.J. Maerkl, and S.R. Quake. 2002. Microfluidic large-scale integration. *Science*. 298:580-584.
- Tian, H., A.F. Hühmer, and J.P. Landers. 2000. Evaluation of silica resins for direct and efficient extraction of DNA from complex biological matrices in a miniaturized format. *Analytical biochemistry*. 283:175-191.
- Tien, H.N., T.K. Lee, B.-S. Kong, J.S. Chung, E.J. Kim, and S.H. Hur. 2012. Enhanced solvothermal reduction of graphene oxide in a mixed solution of sulfuric acid and organic solvent. *Chemical engineering journal*. 211:97-103.
- Tobjörk, D., and R. Österbacka. 2011. Paper electronics. *Advanced Materials*. 23:1935-1961.
- Toner, M., and D. Irimia. 2005. Blood-on-a-chip. *Annual review of biomedical engineering*. 7:77.
- Tothill, I.E. 2009. Biosensors for cancer markers diagnosis. In *Seminars in cell & developmental biology*. Vol. 20. Elsevier. 55-62.
- Wakeland, S., R. Martinez, J.K. Grey, and C.C. Luhrs. 2010. Production of graphene from graphite oxide using urea as expansion–reduction agent. *Carbon*. 48:3463-3470.
- Wang, H., Y.-j. Li, J.-f. Wei, J.-r. Xu, Y.-h. Wang, and G.-x. Zheng. 2014. Paper-based three-dimensional microfluidic device for monitoring of heavy metals with a camera cell phone. *Analytical and bioanalytical chemistry*. 406:2799-2807.
- Wang, J., X. Cai, B. Tian, and H. Shiraishi. 1996. Microfabricated thick-film electrochemical sensor for nucleic acid determination. *Analyst*. 121:965-969.

- Wang, J., X. Cai, J. Wang, C. Jonsson, and E. Palecek. 1995. Trace measurements of RNA by potentiometric stripping analysis at carbon paste electrodes. *Analytical Chemistry*. 67:4065-4070.
- Wang, J., A.-N. Kawde, and E. Sahlin. 2000. Renewable pencil electrodes for highly sensitive stripping potentiometric measurements of DNA and RNA. *Analyst*. 125:5-7.
- Wang, J., B. Tian, V.B. Nascimento, and L. Angnes. 1998. Performance of screen-printed carbon electrodes fabricated from different carbon inks. *Electrochimica Acta*. 43:3459-3465.
- Wang, P., L. Ge, M. Yan, X. Song, S. Ge, and J. Yu. 2012. Paper-based three-dimensional electrochemical immunodevice based on multi-walled carbon nanotubes functionalized paper for sensitive point-of-care testing. *Biosensors and Bioelectronics*. 32:238-243.
- Weaver, W., H. Kittur, M. Dhar, and D. Di Carlo. 2014. Research highlights: microfluidic point-of-care diagnostics. *Lab on a Chip*. 14:1962-1965.
- Weising, K., H. Nybom, M. Pfenninger, K. Wolff, and W. Meyer. 1994. DNA fingerprinting in plants and fungi. CRC press.
- Wen, J., C. Guillo, J.P. Ferrance, and J.P. Landers. 2006. DNA extraction using a tetramethyl orthosilicate-grafted photopolymerized monolithic solid phase. *Analytical chemistry*. 78:1673-1681.
- Wen, J., C. Guillo, J.P. Ferrance, and J.P. Landers. 2007. Microfluidic-based DNA purification in a two-stage, dual-phase microchip containing a reversed-phase and a photopolymerized monolith. *Analytical chemistry*. 79:6135-6142.
- Whitesides, G.M. 2006. The origins and the future of microfluidics. *Nature*. 442:368-373.
- Williams, J.F. 1988. Optimization strategies for the polymerase chain reaction. *Biotechniques*. 7:762-769.
- Wolfe, K.A., M.C. Breadmore, J.P. Ferrance, M.E. Power, J.F. Conroy, P.M. Norris, and J.P. Landers. 2002. Toward a microchip-based solid-phase extraction method for isolation of nucleic acids. *Electrophoresis*. 23:727-733.
- Wong, A.P., M. Gupta, S.S. Shevkoplyas, and G.M. Whitesides. 2008. Egg beater as centrifuge: isolating human blood plasma from whole blood in resource-poor settings. *Lab on a Chip*. 8:2032-2037.
- Wu, Q., J.M. Bienvenue, B.J. Hassan, Y.C. Kwok, B.C. Giordano, P.M. Norris, J.P. Landers, and J.P. Ferrance. 2006. Microchip-based macroporous silica sol-gel monolith for efficient isolation of DNA from clinical samples. *Analytical chemistry*. 78:5704-5710.
- Wu, Y., P. Xue, K.M. Hui, and Y. Kang. 2014. A paper-based microfluidic electrochemical immunodevice integrated with amplification-by-polymerization for the ultrasensitive multiplexed detection of cancer biomarkers. *Biosensors and Bioelectronics*. 52:180-187.
- Xia, Y., and G.M. Whitesides. 1998. Soft lithography. *Annual review of materials science*. 28:153-184.
- Xu, L., H. Yu, M.S. Akhras, S.-J. Han, S. Osterfeld, R.L. White, N. Pourmand, and S.X. Wang. 2008. Giant magnetoresistive biochip for DNA detection and HPV genotyping. *Biosensors and Bioelectronics*. 24:99-103.

- Xu, Y., Y. Liu, Y. Wu, X. Xia, Y. Liao, and Q. Li. 2014. Fluorescent probe-based lateral flow assay for multiplex nucleic acid detection. *Analytical chemistry*. 86:5611-5614.
- Yager, P., G.J. Domingo, and J. Gerdes. 2008. Point-of-care diagnostics for global health. *Annu. Rev. Biomed. Eng.* 10:107-144.
- Yager, P., T. Edwards, E. Fu, K. Helton, K. Nelson, M.R. Tam, and B.H. Weigl. 2006. Microfluidic diagnostic technologies for global public health. *Nature*. 442:412-418.
- Yang, H., L. Chen, C. Lei, J. Zhang, D. Li, Z.-M. Zhou, C.-C. Bao, H.-Y. Hu, X. Chen, and F. Cui. 2010. Giant magnetoimpedance-based microchannel system for quick and parallel genotyping of human papilloma virus type 16/18. *Applied Physics Letters*. 97:043702.
- Yang, X., O. Forouzan, T.P. Brown, and S.S. Shevkoplyas. 2012. Integrated separation of blood plasma from whole blood for microfluidic paper-based analytical devices. *Lab on a Chip*. 12:274-280.
- Yang, X., A. Hadidi, and S. Garnsey. 1992. Enzymatic cDNA amplification of citrus exocortis and cachexia viroids from infected citrus hosts. *Phytopathology*. 82:279-285.
- Yetisen, A.K., M.S. Akram, and C.R. Lowe. 2013. Paper-based microfluidic point-of-care diagnostic devices. *Lab on a Chip*. 13:2210-2251.
- Yin, H., Y. Zhou, H. Zhang, X. Meng, and S. Ai. 2012. Electrochemical determination of microRNA-21 based on graphene, LNA integrated molecular beacon, AuNPs and biotin multifunctional bio bar codes and enzymatic assay system. *Biosensors and Bioelectronics*. 33:247-253.
- Yin, Z., S. Sun, T. Salim, S. Wu, X. Huang, Q. He, Y.M. Lam, and H. Zhang. 2010. Organic photovoltaic devices using highly flexible reduced graphene oxide films as transparent electrodes. *ACS nano*. 4:5263-5268.
- Ying, H., F. Jing, Z. Fanghui, Q. Youlin, and H. Yali. 2014. High-risk HPV nucleic acid detection kit-the careHPV test-a new detection method for screening. *Scientific reports*. 4.
- Yu, A., J. Shang, F. Cheng, B.A. Paik, J.M. Kaplan, R.B. Andrade, and D.M. Ratner. 2012. Biofunctional Paper via the Covalent Modification of Cellulose†. *Langmuir*. 28:11265-11273.
- Yuen, P.K., and V.N. Goral. 2010. Low-cost rapid prototyping of flexible microfluidic devices using a desktop digital craft cutter. *Lab on a Chip*. 10:384-387.
- Zang, D., L. Ge, M. Yan, X. Song, and J. Yu. 2012. Electrochemical immunoassay on a 3D microfluidic paper-based device. *Chemical Communications*. 48:4683-4685.
- Zhang, C.-Y., H.-C. Yeh, M.T. Kuroki, and T.-H. Wang. 2005. Single-quantum-dot-based DNA nanosensor. *Nature materials*. 4:826-831.
- Zhang, F., N. Turgeon, M.-J. Toulouse, C. Duchaine, and D. Li. 2012. A simple and rapid fluorescent neuraminidase enzymatic assay on a microfluidic chip. *Diagnostic microbiology and infectious disease*. 74:263-266.
- Zhang, H., D. Song, S. Gao, J. Zhang, H. Zhang, and Y. Sun. 2013. Novel SPR biosensors based on metal nanoparticles decorated with graphene for immunoassay. *Sensors and Actuators B: Chemical*. 188:548-554.

- Zhou, Y., Q. Bao, L.A.L. Tang, Y. Zhong, and K.P. Loh. 2009. Hydrothermal dehydration for the “green” reduction of exfoliated graphene oxide to graphene and demonstration of tunable optical limiting properties. *Chemistry of Materials*. 21:2950-2956.
- Zhu, Y., S. Murali, W. Cai, X. Li, J.W. Suk, J.R. Potts, and R.S. Ruoff. 2010. Graphene and graphene oxide: synthesis, properties, and applications. *Advanced materials*. 22:3906-3924.
- Zhuo, Q., J. Gao, M. Peng, L. Bai, J. Deng, Y. Xia, Y. Ma, J. Zhong, and X. Sun. 2013. Large-scale synthesis of graphene by the reduction of graphene oxide at room temperature using metal nanoparticles as catalyst. *Carbon*. 52:559-564.



## **CURRICULUM VITAE**

**Name Surname:** Melike KARAKAYA

**Place of Birth:** Ankara

**Address:** Izmir, TURKEY

**E-Mail:** melike.karakaya.tr@gmail.com

**B.Sc.:** Gazi University

**M.Sc.:** Gazi University

**Ph.D.:** Izmir Katip Celebi University & Gediz University

### **Professional Experience and Rewards:**

**Boston University, Biomedical Engineering, Boston, MA, USA  
2014- 2015** Visiting Researcher in Prof. Klapperich Lab, Center for Future Technologies in Cancer Care, NIH, TUBITAK\* **Research Topic:** Paper Lysis, Extraction Support Material and Detection tool for HPV the Etiologic Agent of Cervical Cancer

**Izmir Katip Celebi University- Gediz University, Izmir, Turkey  
PhD in Nanotechnology 2012 - 2016**

**Gazi University, Graduate School of Natural and Applied Sciences, Ankara, Turkey 2013** M.Sc. in Chemistry /Analytical Chemistry- Electroanalytical Chemistry \*  
**M. Sc. Thesis:** Anodic and Cathodic Stripping Voltammetric Determination of Gold Using Graphene Modified Glassy Carbon Electrode

**Gazi University, Institute of Education Sciences, Ankara, Turkey  
2009** M.Sc. in Chemistry Secondary School Teacher Education Program (Pedagogical Proficiency in Chemistry) \* Without Thesis

**Gazi University, Faculty of Science, Ankara, Turkey  
2007** U.Sc. in Chemistry

### **Projects**



- **TUBITAK Project (The Scientific and Technological Research Council of Turkey):** Characterization and Synthesis of Nano-scale Ag and Pt Metallic Powder Bound Carbon Support (2011)
- **BAP Project:** Electrochemical determination of gold by using graphene electrode. Research conducted at Gazi University.(2012-2013)
- **TUBITAK 2214-A:** 3D Portable Microfluidic Device Fabrication for Earlier Detection of Cervical Cancer via extraction of HPV (2014-2015)
- **BAP Project:** Enhancing opto-electronic circuit performances via modification of chemical structures of transmission materials (2013-2016 )
- **BAP Project:** Servik Kanserinin Erken Teşhisi için 3D Portatif Mikroakışkan Cihazların Üretimi 2014-1-TEZ-48 2014-2016 (Continue)

### **Publications**

- M. Karakaya , S. Gürsoy ve H. Çelikkan , ‘Preparation of Ag Load Carbon Material with Pyrolysis Method from PVA-Ag NO<sub>3</sub> Hybrid Polymer’ Poster presented at the 25. International Participation National Chemistry Congress-Ataturk University-Erzurum (2011)
- M.Karakaya , H. Çelikkan , ‘Electrochemical Behaviour of Gold(III) on The surface of GCE Modified with Graphene’26. National Chemistry Congress, Muğla (2012)
- Yavuz Asci, Koray Kara, Melike Karakaya et. All. , ‘Modification of ITO Surface Using Anorganic Self Assembly Small Molecules on The Performance of OLEDs Applications’ Poster presented at International Workshop on Flexible Bio-and Organic Printed Electronics-Konya (2014)
- Abdullah Bayram, Melike Karakaya, Seçil Kurtalan, Salih Okur, ‘Effect of Nanoparticle doping on CO sensing of ferrocene conjugated polypyrrole conducting polymers’, 10th Nanoscience and Nanotechnology Conference (2014)- Istanbul

### **List of Publications and Presentation:**

- Melike Karakaya, Jacqueline C. Linnes, Salih Okur, Catherine M. Klapperich, ‘Paper Lysis, Extraction Support Material and Detection tool for HPV the Etiologic Agent of Cervical Cancer’, 25<sup>th</sup> Biomedical Engineering Society Annual Meeting-Tampa-Florida (2015)
- Melike Karakaya, ‘Paper Based Molecular Diagnosis of Human Papillomavirus at the POC’, Poster Presented at 1st International Cell Death Research Congress-Izmir- 2016